

THE SEDIMENTOLOGY OF THE  
BLOOMINGTON FAN COMPLEX:  
AN ELEMENT OF THE OAK RIDGES MORaine, SOUTHERN ONTARIO

by

JENS TORE PATERSON

A thesis submitted to the Department of Earth Sciences

Brock University

in partial fulfillment of the requirements for the degree of  
Master of Science

© Jens Tore Paterson, 1995

Dr. R. J. Cheel

Supervisor

## ABSTRACT

The Oak Ridges Moraine is a major physiographic feature of south-central Ontario, extending from Rice Lake westward to the Niagara Escarpment. While much previous work has largely postulated a relatively simple the origin of the moraine, recent investigations have concentrated on delineating the discernible glacial deposits (or landform architectural elements) which comprise the complex mosaic of the Oak Ridges Moraine. This study investigates the sedimentology of the Bloomington fan complex, one of the oldest elements of the Oak Ridges Moraine.

The main sediment body of the Bloomington fan complex was deposited during early stages of the formation of the Oak Ridges Moraine, when the ice subdivided, and formed a confined, interlobate lake basin between the northern and southern lobes. Deposition from several conduits produced a fan complex characterized by multiple, laterally overlapping, fan bodies.

It appears that the fans were active sequentially in an eastward direction, until the formation of the Bloomington fan complex was dominated by the largest fan fed by a conduit near the northeastern margin of the deposit. Following deposition of the fan complex, the northern and southern ice margins continued to retreat, opening drainage outlets to the west and causing water levels to drop in the lake basin. Glaciofluvial sediment was deposited at this time, cutting into the underlying fan complex. Re-advancing northern ice then closed westerly outlets, and caused water levels to increase, initiating the re-advance of the southern ice. As the southern ice approached the Bloomington fan, it deposited an ice-marginal sediment complex consisting of glacial sediment gravity flows, and glaciolacustrine and glaciofluvial sediments exhibiting north and northwesterly paleocurrents. Continued advance of the southern ice, overriding the fan complex,

produced large-scale glaciotectonic deformation structures, and deposited the Halton Till.

The subaqueous fan depositional model that is postulated for the Bloomington fan complex differs from published models due to the complex facies associations produced by the multiple conduit sources of sediment feeding the fans. The fluctuating northern and southern ice margins, which moved across the study area in opposite directions, controlled the water level in the interlobate basin and caused major changes in depositional environments. The influence of these two lobes also caused deposition from two distinct source directions. Finally, erosion, deposition, and deformation of the deposit with the readvance of the southern ice contributed further to the complexity of the Bloomington fan complex.

## ACKNOWLEDGEMENTS

First and foremost I would like to thank my supervisor, Dr. R.J. Cheel, for encouragement, suggestions in the field, critical reviews of this thesis, and particularly for his patience. His help went beyond this thesis, and I would like to thank him for his encouragement and understanding during my involvement with graduate student affairs at Brock.

I would also like to thank Dr. J. Menzies for stimulating discussions, both in the office and the field, and to Mr. E.C. Little for his companionship and assistance in the field that dreadfully hot summer. Thanks to Dr. P.J. Barnett of the Ontario Geological Survey for getting me involved with this project. His help and discussion in the field, and his willingness to provide unpublished figures are greatly appreciated.

I would also like to thank the pit managers and operators of the two aggregate companies, specifically Mike Roxborough of Standard Aggregates and Rodney Lee of Lee Sand and Gravel, for granting access to the pits. Appreciation is also expressed to Mike Lozon for putting up with numerous questions regarding the generation of the illustrations included in this thesis.

Thanks to friends who provided the, at times, much needed support during the final push to get things complete, and for making life in St. Catharines much more enjoyable. Thanks to my dad for the use of his darkroom, and his expertise and help with developing the numerous photographs. Thanks to my mom for constant encouragement and support.

Financial support was provided by an NSERC PGS A scholarship to the author, and by an NSERC Research Grant to Dr. R.J. Cheel.



## TABLE OF CONTENTS

ABSTRACT .....	ii
ACKNOWLEDGEMENTS.....	iv
TABLE OF CONTENTS .....	v
LIST OF TABLES .....	viii
LIST OF FIGURES .....	ix
1.0 INTRODUCTION .....	1
1.1 SITE LOCATION.....	3
1.2 PREVIOUS WORK ON THE OAK RIDGES MORaine .....	3
1.3 BEDROCK GEOLOGY .....	7
1.4 QUATERNARY GEOLOGY OF THE OAK RIDGES MORaine.....	10
1.5 SUBAQUEOUS OUTWASH FANS.....	13
1.6 METHODS .....	18
2.0 FACIES DESCRIPTIONS AND INTERPRETATIONS .....	22
2.1 FACIES 1 COARSE PROXIMAL GRAVEL	
2.1.1 Description .....	25
2.1.2 Interpretations .....	30
2.2 FACIES 2 PROXIMAL INTERCHANNEL	
2.2.1 Description .....	34
2.2.2 Interpretations .....	35
2.3 FACIES 3 PROXIMAL TO MID-FAN CHANNELS	
2.3.1 Descriptions .....	38
2.3.2 Interpretations .....	40
2.4 FACIES 4 MID-FAN INTERCHANNEL	
2.4.1 Descriptions .....	43
2.4.2 Interpretations .....	48
2.5 FACIES 5 DISTAL CHANNEL-INTERCHANNEL	
2.5.1 Descriptions .....	53
2.5.2 Interpretations .....	55
2.6 FACIES 6 MASSIVE SAND CHANNELS	
2.6.1 Descriptions .....	57
2.6.2 Interpretations .....	59
2.7 FACIES 7 GLACIOLACUSTRINE DEPOSITS	
2.7.1 Descriptions .....	62
2.7.2 Interpretations .....	66
2.8 FACIES 8 ICE-MARGINAL COMPLEX	
2.8.1 Descriptions .....	67
2.8.2 Interpretations .....	69

2.9 FACIES 9 STRATIFIED SAND AND GRAVEL	
2.9.1 Descriptions .....	73
2.9.2 Interpretations .....	81
2.10 FACIES 10 DIAMICT	
2.10.1 Descriptions .....	83
2.10.2 Interpretations .....	86
2.11 LARGE-SCALE DEFORMATION STRUCTURES	
2.11.1 Sections L10a and L10b	
2.11.1.1 Description .....	91
2.11.1.2 Interpretation .....	98
2.11.2 Section S5	
2.11.2.1 Description .....	100
2.11.2.2 Interpretation .....	100
2.11.3 Section S11	
2.11.3.1 Description .....	102
2.11.3.2 Interpretation .....	102
2.11.4 Summary .....	102
3.0 FACIES DISTRIBUTIONS AND ASSOCIATIONS .....	105
3.1 FACIES 1 COARSE PROXIMAL GRAVEL	
3.1.1 Description .....	106
3.1.2 Interpretation .....	106
3.2 FACIES 2 PROXIMAL INTERCHANNEL	
3.2.1 Description .....	110
3.2.2 Interpretation .....	113
3.3 FACIES 3 PROXIMAL TO MID-FAN CHANNELS	
3.3.1 Description .....	114
3.3.2 Interpretation .....	114
3.4 FACIES 4 MID-FAN INTERCHANNEL	
3.4.1 Description .....	117
3.4.2 Interpretation .....	119
3.5 FACIES 5 DISTAL CHANNEL-INTERCHANNEL	
3.5.1 Description .....	119
3.5.2 Interpretation .....	121
3.6 FACIES 6 MASSIVE SAND CHANNELS	
3.6.1 Description .....	121
3.6.2 Interpretation .....	122
3.7 FACIES 7 GLACIOLACUSTRINE DEPOSITS	
3.7.1 Description .....	122
3.7.2 Interpretation .....	122
3.8 FACIES 8 ICE-MARGINAL COMPLEX	
3.8.1 Description .....	124
3.8.2 Interpretation .....	124
3.9 FACIES 9 STRATIFIED SAND AND GRAVEL	
3.9.1 Description .....	126
3.9.2 Interpretation .....	128

3.10 FACIES 10 DIAMICT	
3.10.1 Description .....	128
3.10.2 Interpretation .....	130
3.11 SUMMARY OF FACIES DISTRIBUTIONS .....	130
4.0 DEPOSITIONAL MODEL .....	133
4.1 PHASE 1 .....	133
4.1.1 Subphase 1a .....	136
4.1.2 Subphase 1b .....	136
4.1.3 Subphase 1c .....	136
4.2 PHASE 2 .....	138
4.3 PHASE 3 .....	140
4.4 PHASE 4 .....	140
5.0 DISCUSSION .....	142
5.1 COMPARISON WITH OTHER SUBAQUEOUS FAN MODELS .....	142
5.2 CONTROLS OF WATER LEVEL CHANGES ON THE CREST OF THE OAK RIDGES MORaine .....	146
5.2.1 Elevations Of Depositional Model Phases 1 to 3 .....	146
5.2.2 Late Wisconsinan Glacial History Along the Niagara Escarpment, .....	149
Port Bruce Stade .....	149
Mackinaw Interstade .....	150
Port Huron Stade .....	151
5.2.3 Summary .....	152
6.0 CONCLUSIONS .....	154
7.0 REFERENCES .....	156
APPENDIX I: PALEOCURRENT DATA .....	171
APPENDIX II: GRAVEL FABRICS .....	175
APPENDIX III: SECTION LOGS .....	179
APPENDIX IV: FENCE DIAGRAMS .....	194

## LIST OF TABLES

Table 1.1. Summary of Subaqueous Outwash Fan Facies .....	14
Table 2.1. Summary of Bloomington Fan Complex Facies.....	23
Table 2.2. Summary lithologies of diamict clast samples .....	90

## LIST OF FIGURES

Fig. 1.1.	Location map of the study site. ....	2
Fig. 1.2.	Topographic map of region surrounding Bloomington Fan complex. ....	4
Fig. 1.3.	Various definitions of the Oak Ridges Moraine .....	6
Fig. 1.4.	Landform architecture of the Uxbridge Wedge.....	8
Fig. 1.5.	Tunnel channels leading into the Oak Ridges Moraine .....	9
Fig. 1.6.	Depositional history of the Uxbridge Wedge. ....	11
Fig. 1.7.	Paleocurrent measurement trial test.....	20
Fig. 2.1.	Section and fence diagram locations. ....	24
Fig. 2.2.	Coarse proximal deposits at S13. ....	26
Fig. 2.3.	Gravel "core" flanked by interbedded sands and gravels. ....	26
Fig. 2.4.	Normal grading within facies 1 gravel. ....	27
Fig. 2.5.	Cross-bedded, open and closed framework gravel. ....	27
Fig. 2.6.	Facies 1b gravel beneath S21 and S23.....	29
Fig. 2.7.	Laterally discontinuous, lenticular gravels. ....	31
Fig. 2.8.	Climbing gravel "dunes". ....	31
Fig. 2.9.	Section showing exposures of both facies 1b and overlying facies 9.....	32
Fig. 2.10.	Steeply dipping, thinly bedded sand and gravel.....	36
Fig. 2.11.	Large scale sand and pebbly sand cross-beds. ....	39
Fig. 2.12.	Normally graded gravel beds. ....	41
Fig. 2.13.	"Chaotic" channel gravels, marked by numerous scoured channels. .	41
Fig. 2.14.	Enigmatic exposure of contact between facies 3 and facies 4 at Section S1. ....	42
Fig. 2.15.	Topsets preserved in cross-bedded sands. ....	44
Fig. 2.16.	Inversely graded, pebbly sand tabular cross-beds truncated by horizontal beds. ....	46
Fig. 2.17.	Shallow dipping beds of slightly pebbly medium to coarse sand. ....	46
Fig. 2.18.	Vaguely bedded and massive pebbly sands.....	47
Fig. 2.19.	Thin horizontal beds and laminae of coarse sand and silts. ....	49
Fig. 2.20.	Gravel lens scoured into underlying sediments. ....	49
Fig. 2.21.	Faulting that affects sediments near S2. ....	50
Fig. 2.22.	Fining-upward sequence, from rippled sand, to silt, to clay laminae.....	54
Fig. 2.23.	Small, nested scoured channels filled with trough cross-beds. ....	54

Fig. 2.24. Soft-sediment deformation structures.....	56
Fig. 2.25. Scours filled with rippled sand sequences.....	58
Fig. 2.26. Large, steep-walled channels filled with massive sand.....	60
Fig. 2.27. Sandy channels truncated by stratified gravels. ....	60
Fig. 2.28. Downflow transition from steep-walled massive sand channels into subhorizontally laminated sediment.....	61
Fig. 2.29. Laminated silt and clay, containing dropstones. ....	64
Fig. 2.30. Basal contact of facies 7, overlying glaciofluvial gravels of facies 9. ..	64
Fig. 2.31. Laterally discontinuous exposure of facies 7.....	64
Fig. 2.32. Deformation of facies 7. ....	65
Fig. 2.33. Massive, pebbly sand diamict beds, interbedded with laminated sands.....	68
Fig. 2.34. Complex flame of silts within flow diamicts.....	68
Fig. 2.35. Fault-bounded block of diamict protruding into overlying sediments.....	70
Fig. 2.36. Erosional basal contact of facies 8. ....	70
Fig. 2.37. Trough-like isolated depression bounded by high-angle reverse faults .....	71
Fig. 2.38. Deformed sediments associated with facies 8.....	71
Fig. 2.39. Cross-bedded gravels. ....	75
Fig. 2.40. Sorting in gravels. ....	76
Fig. 2.41. Large scale gravel cross-beds.....	77
Fig. 2.42. Weakly stratified horizontally bedded gravel. ....	79
Fig. 2.43. Pebbly medium to coarse sand planar and trough cross-bedded sand. ....	79
Fig. 2.44. Characteristics of well-defined channels of facies 9.....	80
Fig. 2.45. Weak internal stratification in diamict.....	84
Fig. 2.46. Diamict clast fabric stereonets. ....	85
Fig. 2.47. Sharp, planar contact between diamict and thin, underlying rippled sand bed.....	87
Fig. 2.48. Small scale injection structures along basal Halton Till contact.....	87
Fig. 2.49. Plot of $S_1$ vs $S_3$ eigenvalues from diamict clast fabrics.....	89
Fig. 2.50. Imbricate thrust slices at L10b. ....	92
Fig. 2.51. High angle normal faults in upper portions of thrust slices. ....	94
Fig. 2.52. Bulbous noses of gravel at base of thrust slices where normal faulting occurs. ....	95
Fig. 2.53. Deformed unit, L10a. ....	96
Fig. 2.54. Deformed unit is attenuated towards the north. ....	97

Fig. 2.55. Deformed unit of at S11. ....	97
Fig. 2.56. Deformed sequence at S5. ....	101
Fig. 2.57. Complex deformation exhibiting both normal and reverse (thrust) faults at S5. ....	101
Fig. 2.58. Overturned sand beds re-oriented towards the north. ....	103
Fig. 3.1. Paleocurrent map, facies 1. ....	107
Fig. 3.2. Paleocurrent map, facies 2. ....	111
Fig. 3.3. Contact between facies 1 and facies 2, section L5. ....	112
Fig. 3.4. Paleocurrent map, facies 3. ....	115
Fig. 3.5. Paleocurrent map, facies 4. ....	118
Fig. 3.6. Paleocurrent map, facies 5 and 6. ....	120
Fig. 3.7. Paleocurrent map, facies 8. ....	125
Fig. 3.8. Geometry of facies 9 basal erosional channels. ....	127
Fig. 3.9. Paleocurrent map, facies 9. ....	129
Fig. 3.10. Schematic cross-section of Bloomington fan complex. ....	131
Fig. 4.1. Distribution of sections exhibiting facies 1, and locations of eskers feeding the Bloomington fan complex. ....	134
Fig. 4.2. Depositional model, phase 1. ....	135
Fig. 4.3. Depositional model, phase 2. ....	139
Fig. 4.4. Depositional model, phase 3. ....	141
Fig. 5.1. Lake levels elevations of selected glacial lakes in southern Ontario. Outlet elevations along the Niagara Escarpment. ....	147

## 1.0 INTRODUCTION

A large, fan-shaped deposit in the vicinity of Bloomington, Ontario, is an element of the Oak Ridges Moraine (ORM), a prominent ridge of sand and gravel extending from the eastern margin of Rice Lake westward to the Niagara Escarpment (Fig. 1.1). Although it is one of the most striking landforms of Southern Ontario, very few details are available concerning its origin. Early work has simply treated the ORM as a single sediment package. For example, Chapman and Putnam (1943, p.39) noted in their study that "No attempt was made to separate the component parts of the Oak Ridges, interlobate, moraine". However, Taylor (1913a,b) had earlier suggested that the ORM was composed of discernible sediment bodies. It was only recently that detailed surface mapping (Barnett, 1992a, 1993; Sharpe *et al.*, 1994) has begun to delineate the various landform architectural elements. This thesis investigates the detailed sedimentology of one of the largest and oldest discernible single elements of the Oak Ridges Moraine, the Bloomington fan complex.

The two sand and gravel pits described here expose sediments that were deposited from meltwater flowing southwards from the Simcoe ice lobe in an ice-bounded glaciolacustrine basin between the Simcoe and Ontario ice lobes (Barnett, 1992a, 1993). This basin, perched on the highland of the ORM, drained westward towards and along the Niagara Escarpment (Duckworth, 1975, 1979), and eventually emptied into Glacial Lakes Iroquois or Whittlesey (White, 1975; Barnett, 1979). The glaciofluvial and glaciolacustrine deposits of this basin are overlain by diamicts associated with the Ontario ice lobe which later readvanced northwards out of the Lake Ontario basin.

The primary objective of this study is to describe and interpret the sedimentology of the deposit in order to develop a depositional model. The



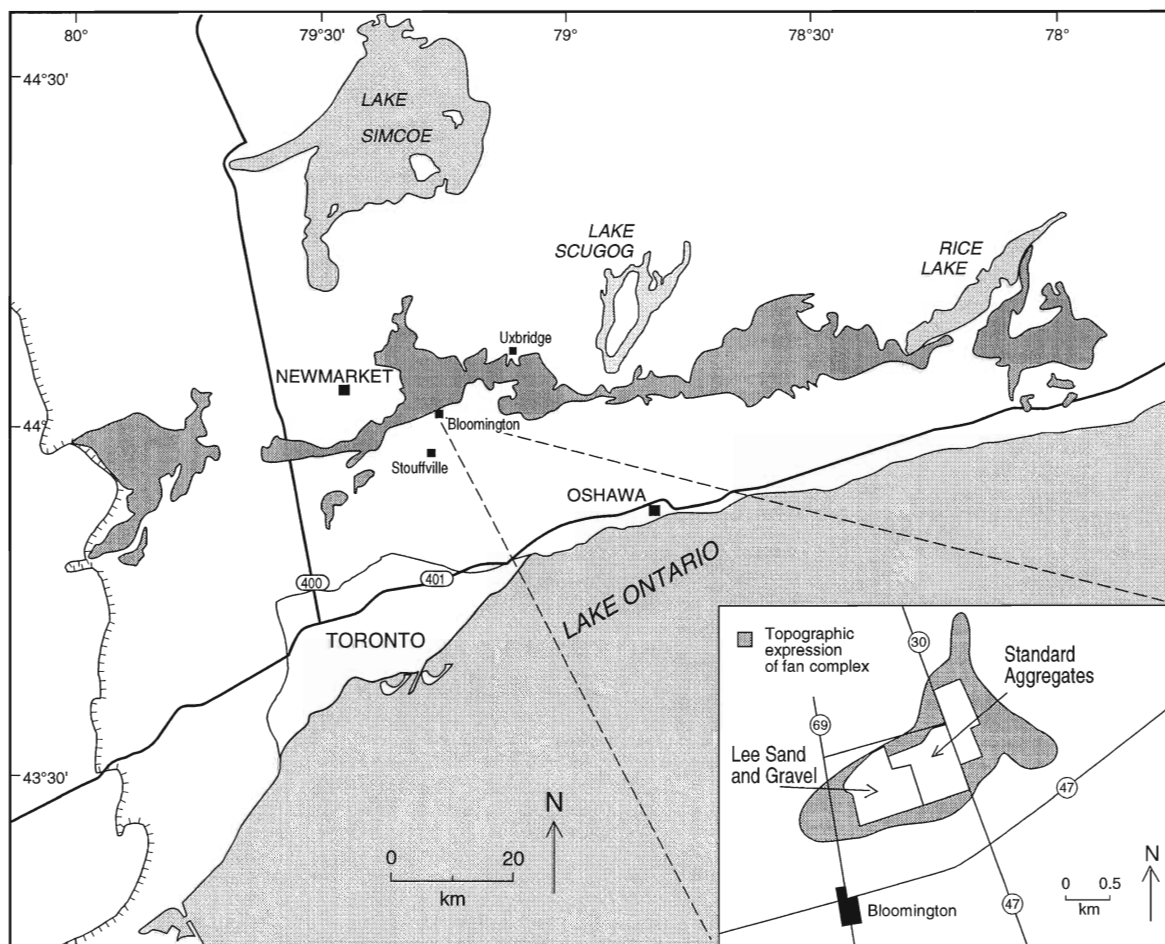


Fig. 1.1. Location map showing Bloomington fan complex along the southern margin of the Oak Ridges Moraine (dark grey; after Sharpe *et al.*, 1994). The deposit is presently being excavated by two aggregate companies; Standard Aggregates and Lee Sand and Gravel. Note the fan-shaped deposit which broadens towards the southwest.

development of the model is largely based on facies geometries, spatial distribution, and associations. It will be shown that the deposits reflect major changes in depositional environments due to water level fluctuations in the interlobate lake basin.

## **1.1 SITE LOCATION**

The two sand and gravel pits described in this study are located approximately two kilometres northeast of the town of Bloomington, Ontario (Fig. 1.1). The Standard Aggregates Pit is in Uxbridge Township, (Conc. 1, Lots 16 to 18) and Whitchurch Township (Conc. 10, Lots 12 to 15); the Lee Sand and Gravel Pit is in Whitchurch Township (Conc. 9, Lots 13 to 15). Regional access is from Bloomington Side Road, with direct access to the pits by Regional Roads 30 and 69, respectively.

The pits expose part of an approximately fan-shaped deposit, its apex pointing northward, broadening towards the south and southwest; the topographic expression of this deposit indicates a second fan lobe, just east of the main lobe which is directed towards the southeast (Figs. 1.1, 1.2). Exposure in the westerly lobe, on which this thesis is based, is almost continuous for approximately 2 km along the fan axis and 1 km across the axis.

## **1.2 PREVIOUS WORK ON THE OAK RIDGES MORaine**

As a major physiographic feature of Southern Ontario, the ORM has been discussed in the Canadian geologic literature for over a century (e.g., Bigsby, 1829; Logan, 1863). According to the most commonly used definition of Chapman and Putnam (1984), the ORM extends approximately 160 kilometres from Castleton, west to the Niagara Escarpment, and varies from 1 to 14 kilometres in width (Fig. 1.3a). Although it was first recognized as a moraine in 1899 (Coleman, 1899), Taylor

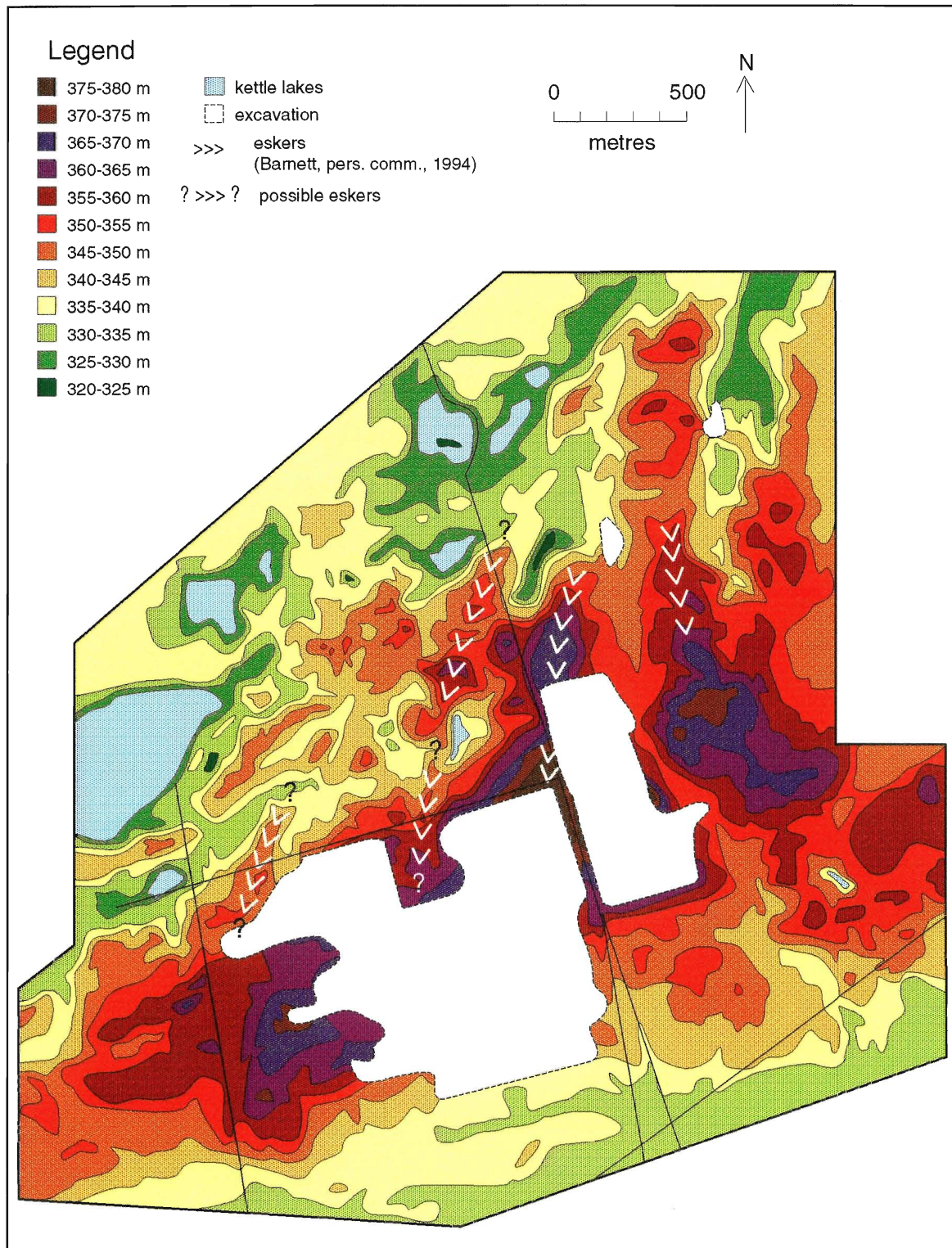


Fig. 1.2. Topographic map of region surrounding the Bloomington fan complex. Note the position of eskers feeding the western portion of the deposit, and the line of kettle lakes which lie just beyond the northern limit of the Halton Till as mapped at surface. Five metre elevation contours taken from Ontario Base Maps, Ministry of Natural Resources.

(1913a,b) was the first to identify the glacial significance of the deposits.

The Oak Ridges Moraine has not always been defined in the manner outlined above. Several definitions have been proposed in the past, based on geomorphologic expression and surface sediment distribution (Fig. 1.3). The earliest was proposed by Taylor (Fig. 1.3b; 1913a,b). His definitions were generally utilized by Duckworth (1975) and White (1975; Figs. 1.3c,d), who agreed that the Palgrave Moraine, marking the northern limit of the ice which deposited the Halton Till, and outwash along the Niagara Escarpment should not be considered part of the ORM. Chapman and Putnam combined these separate components in their definition of the ORM (Chapman and Putnam, 1943, 1951, 1966, 1984; Fig. 1.3a). However, all of these authors consider the ORM to have been deposited between ice lobes advancing out of the Lake Simcoe and Lake Ontario basins (hereafter termed the Simcoe (northern) and Ontario (southern) ice lobes, respectively).

The Oak Ridges Moraine is presently the object of a collaborative project between the Ontario Geological Survey and Geological Survey of Canada. Part of the mandate of this project is to define the extent of the Oak Ridges Moraine, as much for political planning purposes (Kanter, 1990) as for its geological interpretation. The southern boundary has been set at the 244 metre (above sea level) contour, which is physiographically part of the southern slope. The northern boundary is defined by the mapped extent of ice-contact stratified drift on the north slope of the Moraine (Kanter, 1990; Sharpe *et al.*, 1994).

Although it has been recognized as a complex system since the turn of the century (Taylor, 1913a,b), it was not until recently that the ORM was firmly established as a complex landform composed of numerous discernible glacial deposits (e.g., Barnett, 1992a, 1993; Sharpe *et al.*, 1994). Detailed mapping of the central portion of the ORM surrounding the study site ("Uxbridge Wedge"; Barnett,

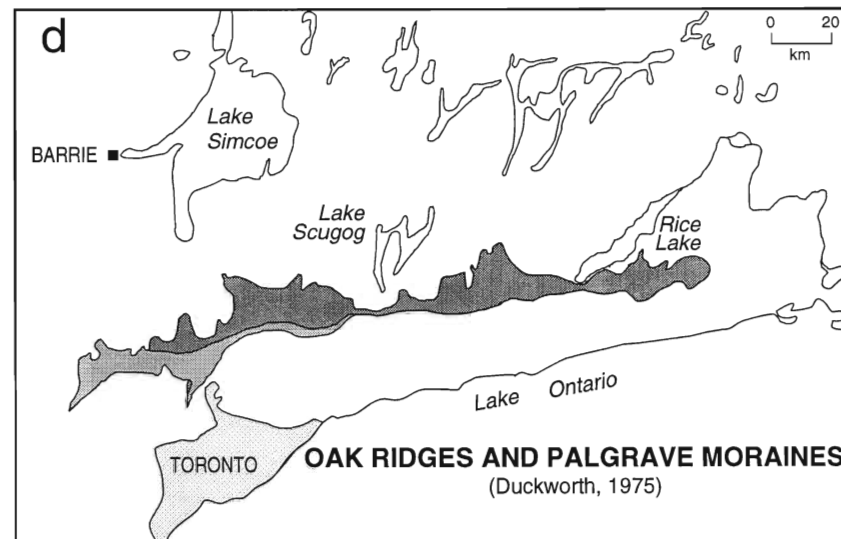
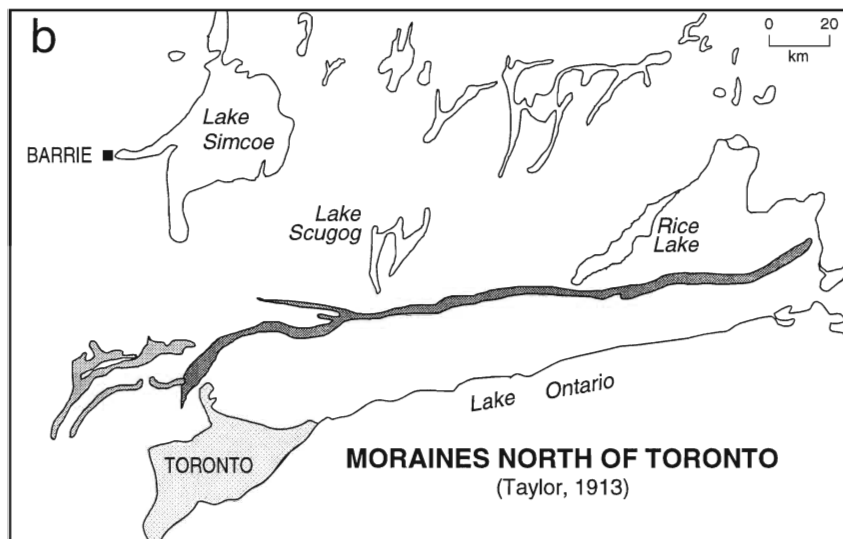
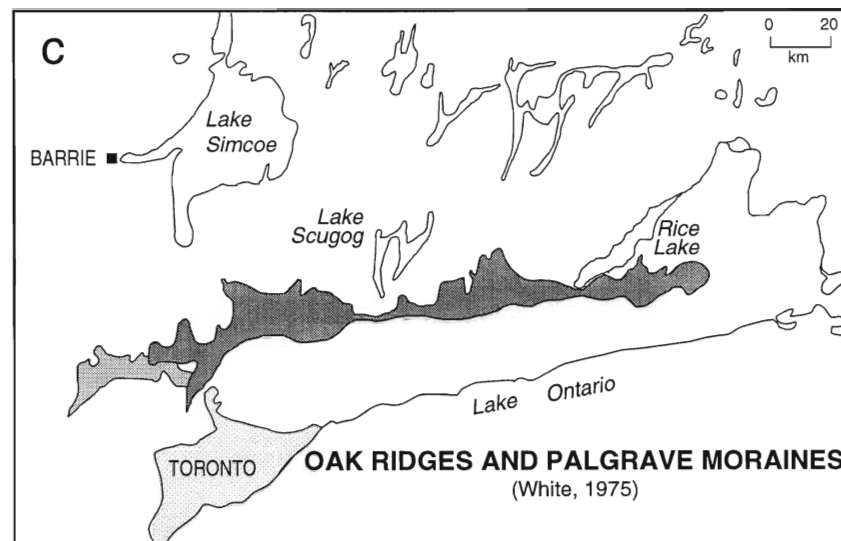
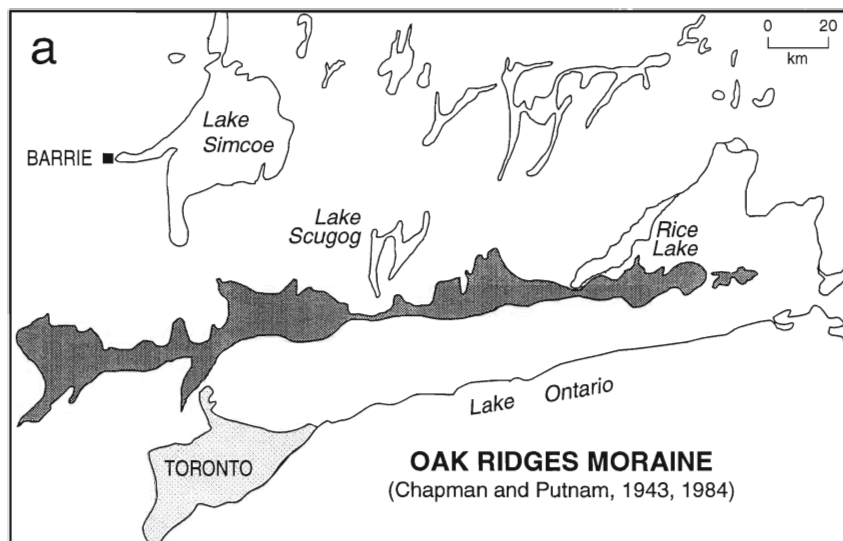


Fig. 1.3. Various definitions of the Oak Ridges Moraine (dark grey) and adjacent moraines (light grey).  
After Sharpe *et al.*, 1994.

1992a, pers. comm., 1994), has identified numerous landform architectural elements near the Bloomington fan complex (Fig. 1.4).

Subsurface data obtained by recent drilling programs of the OGS and GSC along with previous studies by other workers, has documented large channel networks which lead into, and pass beneath the core of the ORM (e.g., Barnett, 1990; Gorrell and Shaw, 1991; Brennand and Shaw, 1994; Sharpe *et al.*, 1994; Fig. 1.5). It is thought that tunnel channels were carved prior to the formation of the ORM (e.g., Barnett, 1993; Sharpe *et al.*, 1994). One of these tunnel channels is located directly north of the Bloomington fan complex (Fig. 1.4).

### 1.3 BEDROCK GEOLOGY

The Oak Ridges Moraine overlies Upper Ordovician shales and thinly-bedded limestones of the Georgian Bay and Blue Mountain formations (Liberty, 1969; Russell and Telford, 1983; Johnson *et al.*, 1992). These formations are composed mainly of blue, black and brown fissile shales. Hewitt and Karrow (1963) reported that 75% to 95% of the pebbles in pits in the Stouffville area are composed of limestones of the Lower to Middle Ordovician Gull River, Verulam and Lindsay Formations.

The bedrock topography generally slopes gently westward into the centre of the Michigan Basin. However, regional bedrock surfaces are dissected by valleys believed to be carved by pre- and post-glacial fluvial processes (Spencer, 1890; Flint and Lolcama, 1985). Most of these valleys are buried in southern Ontario. For example, the Laurentian River Valley, which drained the upper Great Lakes via Georgian Bay to Lake Ontario (Spencer, 1890, 1907; White and Karrow, 1971; Eyles *et al.*, 1985; Karrow, 1989; Barnett, 1992b) may have been eroded during an extensive period of subaerial exposure and weathering prior to the Quaternary Period. Glacial erosion would have widened and deepened the valleys along lowlands underlain by



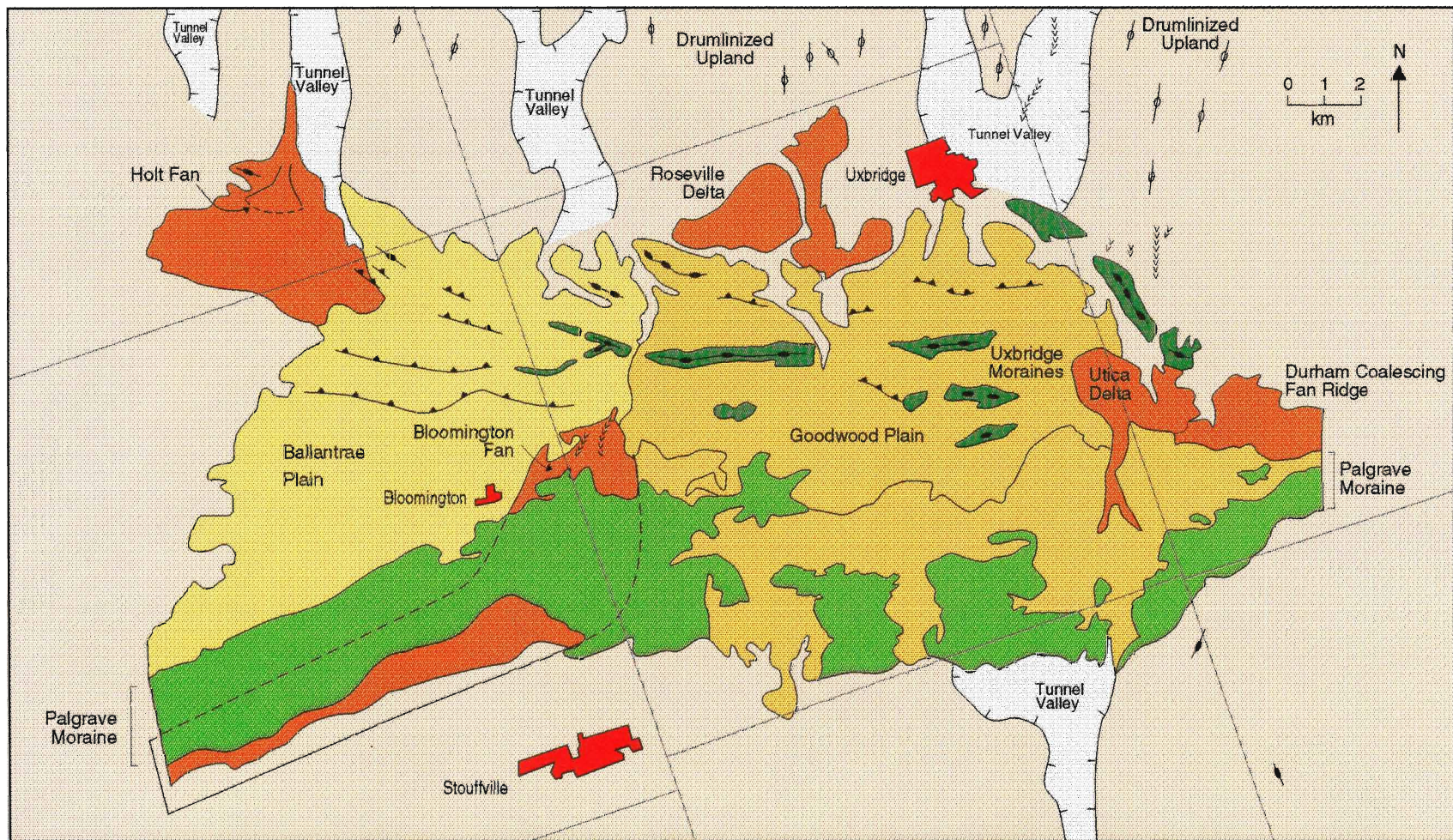


Fig. 1.4. Landform architectural elements of the Uxbridge Wedge, Oak Ridges Moraine. Unpublished map courtesy of P.J. Barnett, Ontario Geological Survey, 1994.



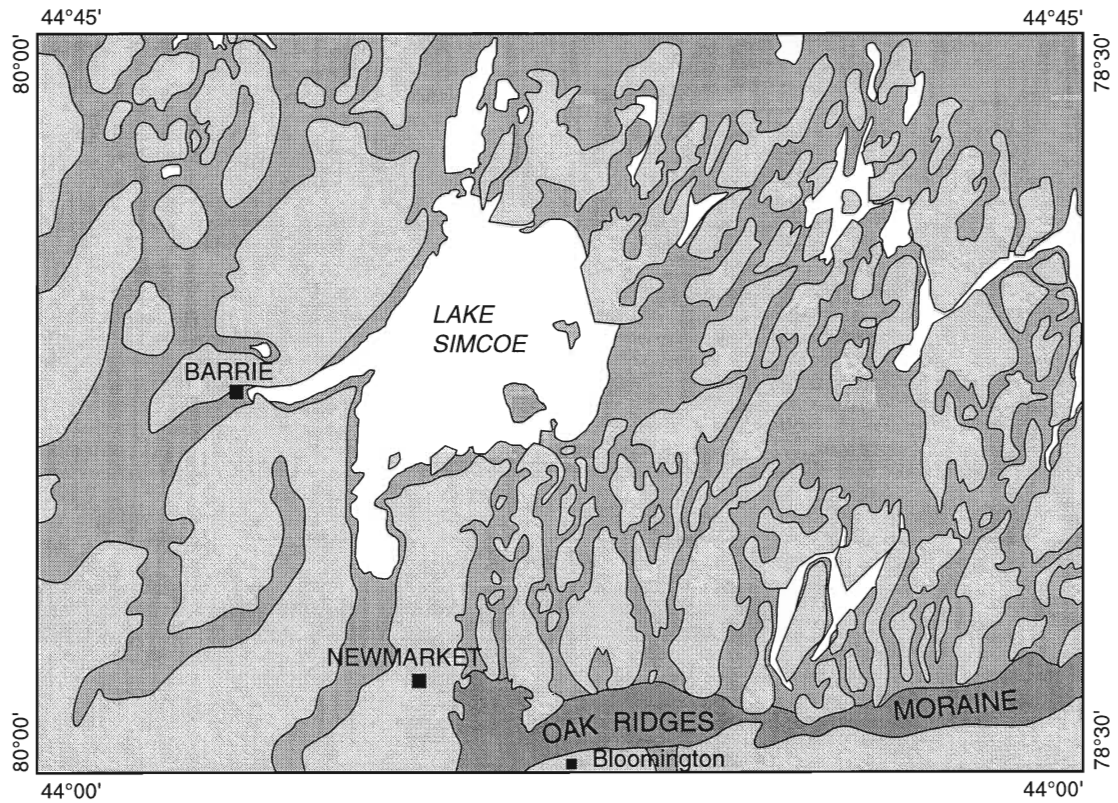


Fig. 1.5. Tunnel channels (medium grey) mapped relative to the Oak Ridges Moraine (dark grey); (after Barnett, 1990).



softer shales. As a result, where the Laurentian Valley passes under the ORM drift thickness exceeds 250 metres (Karrow, 1989) and the drift is stratigraphically complex.

#### 1.4 QUATERNARY GEOLOGY OF THE OAK RIDGES MORaine

It is generally accepted that the Oak Ridges Moraine is composed of deposits of the Late Wisconsinan Substage (e.g., Barnett, 1992b), although older glacial and non-glacial sediments have been found along the Lake Ontario bluffs (Karrow, 1967; Brookfield *et al.*, 1982) and may underlie the Moraine (Gravenor, 1957; Duckworth, 1979; Eyles *et al.*, 1985; Sharpe *et al.*, 1994). The last major ice advance was from the northeast, and deposited a regional till sheet which underlies the ORM. This till has been given various names (Sharpe *et al.*, 1994), but will be referred to here as the Newmarket Till, deposited during the late stages of the Port Bruce Stage by the Simcoe ice lobe (Gwyn, 1972; Duckworth, 1979; Karrow, 1984), and occurs to the north of the ORM (Gwyn and DiLabio, 1973). Recent subsurface data suggests that this till sheet was subsequently dissected by a number of channels (Barnett, 1990, 1992a, 1993; Sharpe *et al.*, 1994).

In south-central Ontario the Late Wisconsinan was characterized by rapid ice margin fluctuations of the Simcoe and Ontario ice lobes, making it difficult to determine the exact timing of the deposition of the sediments exposed in the study pits. However, regional correlations (Barnett, 1992a; 1993; Sharpe *et al.*, 1994) indicate that deposition may have been initiated during the Mackinaw Interstage, just before 13 ka (Karrow, 1989). The Bloomington fan complex comprises the oldest deposits of this portion of the ORM, and was deposited in an ice-bounded interlobate lake basin that formed where the northern ice subdivided into two lobes (Fig. 1.6a). Continued recession of both the northern and southern lobes increased the size of the lake basin, which has been termed Early Lake Schomberg at this stage



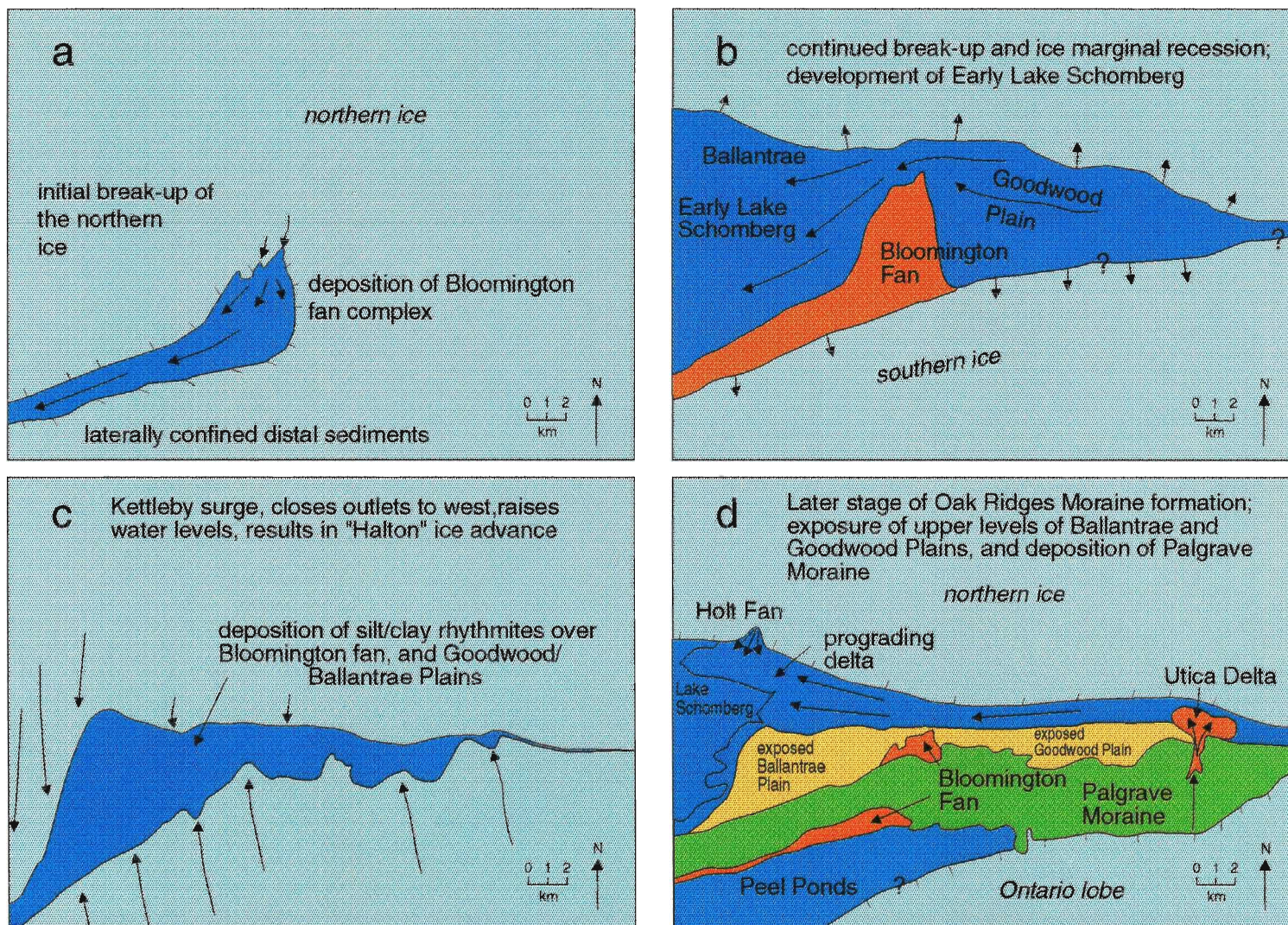


Fig. 1.6. Depositional history of the Uxbridge Wedge, Oak Ridges Moraine. Unpublished schematic diagrams courtesy of P.J. Barnett, Ontario Geological Survey, 1994.



(e.g., Duckworth, 1975, 1979; Barnett, pers. comm., 1994; Fig. 1.6b).

Ice-marginal environments characterized by stagnating conditions and numerous proglacial ponds and lakes produced generally rapid ice margin fluctuations of the Simcoe and Ontario ice lobes during the Port Huron Stade (maximum at 13 ka, Dreimanis and Goldthwait, 1973; Karrow, 1984). A re-advance (surge ?) by the Simcoe ice lobe to the west of the study site deposited the Kettleby Till (Hewitt, 1969; Gwyn, 1972;; Duckworth, 1975, 1979; Cowan, 1976; Gwyn and Cowan, 1978; Barnett, 1992a, 1993) and caused water levels to rise in the interlobate lake basin. This may have triggered the Ontario ice lobe to re-advance (P.J. Barnett, pers. comm., 1994; Fig. 1.6c), depositing the Halton Till and the Palgrave Moraine at its terminal position (e.g., Karrow, 1967; White, 1975; Barnett, 1992a, 1993, pers. comm., 1994; Fig. 1.6d).

Isolated pondings developed on the crest and flanks of the Oak Ridges Moraine during the recession of the Simcoe and Ontario ice lobes (e.g., Chapman and Putnam, 1943, 1951, 1966; Gwyn and DiLabio, 1973; White, 1975; Chapman, 1985; Barnett, 1992a, 1993). Water ponded between the Ontario ice lobe, the Niagara Escarpment and the Moraine formed Lake Peel. Similarly, water ponded between the Moraine, the Escarpment and the Simcoe ice lobe formed Lake Schomberg.

A recession of the Laurentide Ice Sheet margin from the study area had occurred by about 12 ka (Karrow, 1989; Barnett, 1992b) with the initiation of the Two Creeks Interstade. At that time, separate lakes formed in the Lake Ontario (glacial Lake Iroquois) and Lake Erie (Early Lake Erie) basins, and waters in the Lakes Huron and Michigan basins coalesced (glacial Lake Algonquin).

## 1.5 SUBAQUEOUS OUTWASH FANS

The overall form and reconnaissance-level field investigation led to the initial interpretation of the deposit as a subaqueous fan (Barnett, 1992a). The purpose of this study will be to document the detailed sedimentology of the deposit, and to facilitate the interpretation of the Bloomington fan complex. Therefore, it will be useful to briefly review and summarize the literature concerning subaqueous outwash fans.

The term "subaqueous outwash fan" was coined by Rust and Romanelli (1975) and has since been adopted by numerous workers in their description and interpretation of similar deposits (Rust, 1977; Cheel, 1982; Cheel and Rust, 1982; Shaw, 1985; Gorrel, 1986; Kaszycki, 1987; Diemer, 1988; Henderson, 1988; Spooner, 1988; Delorme, 1989). Subaqueous outwash fans are produced by the deposition of glaciofluvial sediment beneath a standing body of water (Rust and Romanelli, 1975). Suitable conditions for proglacial subaqueous outwash deposits are probably widespread during deglaciation since large-scale isostatic depression tends to pond water against the ice front (Rust and Romanelli, 1975). Subaqueous fan deposits have been described from both glaciomarine (Rust, 1977; Cheel, 1982; Burbidge and Rust, 1988; Rust, 1988) and glaciolacustrine environments (Gorrel, 1986; Kaszycki, 1987; Spooner, 1988; Delorme, 1989).

Sediment is transported onto the subaqueous fans by various meltwater density currents, which are controlled by the density contrast between the sediment-laden glacial meltwater and the proglacial water body. The main causes of the density variations are temperature, concentration of sediment and concentration of dissolved salts (Ashley *et al.*, 1985). In glaciomarine conditions, underflows occur when the concentration of sediments is sufficiently high to overcome the buoyancy effects of the denser marine waters. Glaciolacustrine conditions do not involve such

differences in salinity between the meltwater and the proglacial body of water, so that underflows are more common in this environment (Sharpe, 1988a).

Table 1.1 Summary of Subaqueous Fan Facies

FACIES	DESCRIPTION	INTERPRETATION
Proximal Gravel	1) Poorly sorted, matrix-supported gravel.  2) Clast-supported gravel, mainly a(p) b(i) imbrication, but rare a(t) b(i) orientation.	Deposited from high sediment concentration flows within, or near the mouth of a conduit.  Deposition in proximal proglacial channels.
Proximal to Mid-Fan Deposits	Laterally extensive gravel beds, interbedded with horizontally bedded sand, planar and trough cross-bedded sand, laterally extensive massive sand, and rippled cross-laminated sand.	Deposition in proximal interchannel zones, or very broad channels in mid-fan zones.
Mid to Distal Fan Deposits	Climbing ripple cross-laminated sands.	Deposition from suspension from rapidly waning, low-density turbidity currents in mid to distal channel zones of fans, in distal regions adjacent to main channels.
Laterally Extensive Massive Sands		Deposited from high sediment concentration flows that passed beyond channel termini or spilled over their banks
Channel Facies	Steep-sided channels which filled with massive to weakly-laminated sand.	Erosion and progressive infilling by high sediment concentration density underflows.
Distal Facies	Horizontally laminated sand, silt and clay.	Deposited from underflow and overflow/interflow combinations in distal zones.
Reworked Littoral Deposits	Ubiquitous cap gravel facies unconformably overlying deposits; consists of a moderately to well sorted planar stratified pebble gravels, with occasional lenses of horizontally stratified medium sands.	Wave reworking of previously-deposited sediments as water level dropped in proglacial water bodies.

### Proximal Gravel Facies

One of the two proximal gravel facies deposited at a subaqueous outwash fan apex is a massive, poorly sorted, matrix-supported gravel deposited from powerful, high sediment concentration flows at or near the mouth of a conduit (Table 1.1). The poorly sorted gravels generally grade upsection and downfan into clast-supported

gravels, dominantly with a-axes parallel to flow and a-b planes dipping upstream (Table 1.1); (Rust, 1975, 1977; Shaw, 1985). Weak subhorizontal bedding is normally exhibited (Banerjee and McDonald, 1975; Shaw, 1985; Cheel and Rust, 1986; Henderson, 1988) and is formed by vertical accretion within channels. Gravels exhibiting weak cross-bedding are deposited from migrating bedforms (Diemer, 1988).

#### Proximal to Mid-Fan Deposits

The gravel facies grades laterally and distally into several sand facies (Table 1.1). Rapid energy dissipation by turbulent mixing within standing water causes a downfan transition from horizontally bedded sands, planar and trough cross-bedded sands, laterally extensive massive sands, and rippled cross-stratified sands.

Laterally extensive units of horizontally-bedded, granular to pebbly sands have been documented by workers adjacent to the horizontally-bedded gravel facies (Shaw, 1985), and in some instances interbedded with planar-stratified pebble gravels and cross-bedded sands (Delorme, 1989). This facies is deposited in proximal interchannel areas (Cheel, 1982; Kaszycki, 1987) or very broad channels (Cheel, 1982) in mid-fan areas. These deposits normally grade downfan into planar and trough cross-bedded sands (Rust, 1977).

Planar-tabular and trough cross-bedded sands are deposited in moderate to low energy, proximal to mid-fan channel regions (Rust and Romanelli, 1975; Rust, 1977; Cheel, 1982; Kaszycki, 1987; Diemer, 1988), and normally grade upwards and downflow into massive and graded sands (Rust and Romanelli, 1975; Shaw, 1975; Rust, 1977; Postma *et al.*, 1983; Rust, 1988; Burbidge and Rust, 1988; Sharpe, 1988a). Sediments that display large scale cross-stratification (planar tabular and trough) are deposited from migrating dunes within in a zone of rapidly varying flow and diverging flow lines (Banerjee and McDonald, 1975).

## Mid to Distal Fan Deposits

Climbing ripple cross-laminated sands occur in mid to distal channel areas of the fans and in distal regions adjacent to main channels (Table 1.1), but may occur in more proximal regions of the fan during periods of low meltwater discharge (Kaszycki, 1987). All three types of climbing ripples (Jopling and Walker, 1968; Allen, 1970; Ashley *et al.*, 1982) are normally present, indicating rapid deposition rates and variable flow conditions, probably resulting from suspension deposition from rapidly waning, low-density turbidity currents (Jopling and Walker, 1968). Ripple units are usually laterally continuous; beds are often traceable for distances exceeding several tens of metres.

## Laterally Extensive Massive Sands

Laterally extensive massive sand units have been described by a some workers (Cheel, 1982; Diemer, 1988; Delorme, 1989), and may be deposited from high concentration sediment flows that passed beyond channel termini or spilled over their banks (Cheel, 1982; Diemer, 1988; Ashley *et al.*, 1985). Syndepositional fluidization may explain the predominance of dish structures in this facies (Cheel and Rust, 1986; Delorme, 1988; Rust, 1988).

## Channel Facies

Most of the various sand facies have been found to be truncated by large (up to 7 metres deep, 40 metres wide, and several hundred metres long), steep-sided (up to 37°) channels which normally contain massive to weakly-laminated sands (Table 1.1); (Rust and Romanelli, 1975; Rust, 1977; Cheel, 1982; Shaw, 1985; Diemer, 1988). Most workers have associated the erosion and progressive infilling of these channels by high sediment concentration density underflows (Rust and Romanelli, 1975; Rust, 1977; Shaw, 1985; Smith and Ashley, 1985; Diemer, 1988). High sediment

concentrations in the flow inhibits bedform development, and may allow the channel walls to be maintained due to dispersive pressure (Rust, 1988). Other workers suggest that the scour events are a local process beneath an extensive sheet flow and not a channelization process, based partially on the existence of laterally continuous massive sand units located directly overlying the channels (Gorrell and Shaw, 1991).

### Distal Facies

These facies are dominated by thinly-bedded to laminated silt and clay which is deposited from underflow and overflow/interflow combinations (Table 1.1); (e.g., Ashley *et al.*, 1985). In some locations rippled or normally graded sands are found interbedded with the silt and clay, usually with lenticular bedding.

### Reworked Littoral Deposits

Most documented subaqueous fan deposits are unconformably overlain by a ubiquitous cap of gravel which is usually found as a lag across the entire deposit (Table 1.1). These planar stratified pebble gravels tend to be well sorted, with occasional lenses of horizontally stratified medium sands. Most workers believe that these gravels represent wave reworking of abandoned fan surfaces as water levels drop in proglacial water bodies in response to isostatic rebound (e.g., Rust, 1977; Spooner, 1988).

### Typical Sequences

One of the distinguishing features of subaqueous outwash fans is their tendency to produce deposits that display fining upwards cycles, both overall and within beds. The larger cycles are due to source (glacier) retreat, so that progressively distal glaciomarine or glaciolacustrine sediments are deposited overlying coarser proximal sediments. The tendency to produce fining upward



cycles within beds is due to periodic sediment gravity flows.

The various facies documented by authors studying subaqueous outwash fan deposits normally exhibit an upward fining vertical sequence that reflects ice retreat and superposition of proximal through distal deposits. Such a sequence normally consists of proximal boulder gravels, overlain by parallel-bedded, cross-bedded and rippled sands, and perhaps lacustrine or glaciomarine sediments if deposition from the source continues to reach the original location from an increasingly distal position. Most deposits are unconformably overlain by well-sorted pebble-gravels which represent littoral zone reworking of the sediments as water levels in the glacial lakes drop following deglaciation.

The subaqueous outwash fan environment is extremely variable, with many factors controlling the complex distribution and spatial arrangement of the deposits. The main autocyclic control on the fans involves shifts in the orientation of the glacial conduit and sediment source can produce abrupt facies transitions associated with channel switching and depositional lobe development. These changes are overprinted by the larger scale allocyclic control of ice margin retreat. This tends to produce a fining-upward trend across the entire deposit. The dynamic nature of these deposits is also a reflection of other processes, including debris flows originating at the glacier margin, and post-depositional slumping and dewatering of the sediments.

## **1.6 METHODS**

Field work was completed in the two study pits during a six week period from mid May through to the end of June 1993 and two additional weeks in mid-August 1993. Although exposures were excellent, access in the two pits varied. Pit faces in the Standard Pit were particularly accessible, and twenty-four detailed vertical sections were logged (some sections were re-logged following further

excavation and two additional sections were documented in less detail). Access in the Lee Pit was limited as most sections had near vertical faces produced by ongoing excavation. Eighteen vertical sections were logged in this pit, and the bulk of the descriptions based on observations using binoculars. The elevation of each section was obtained by leveling from permanent fixtures in the pits. The elevations of the fixtures were then measured relative to nearby bench marks using an aneroid barometer.

The descriptions of vertical sections include grain size (determined in the field), sedimentary structures, and the vertical and lateral spatial relationships between units. Numerous directional structures (Appendix I) and pebble fabrics (Appendix II) were also measured to determine paleocurrent directions. Sample size for both the measurements of cross-stratification and pebble fabrics had to be considered. To obtain a valid sample size, a test unit was selected from which measurements were taken in increments of 25, and plotted as rose diagrams for  $N=25, 50, 75$  and  $100$  (Fig. 1.7). Rose diagrams were plotted using Vector Rose 1.0. Because the mean does not vary notably between the 50, 75 and 100 measurement plots, it was decided that a sample size of 50 measurements would be made at each site. Pebble fabric consisted of 25 measured clasts at each site, after Rust (1975) who determined that 20 clasts generally give a reasonably accurate preferred orientation. Pebble fabrics consisted of the measurement of the orientation of the a-b planes and a-axes of clasts, which are combined to produce the fabric diagrams in Appendix II. Diamict clast fabrics were measured using clasts with a minimum 2:1:1 a:b:c axial ratios (after Boulton, 1971; Lawson, 1979). Pebble fabrics and diamict clast fabrics were plotted using Stereonet 4.7.

In the Standard Pit, cross-strata were measured at 36 locations, and were supplemented by 42 pebble fabric measurements. In the Lee Pit, the lack of direct access in many faces allowed only 15 measurements of cross-stratification and 5

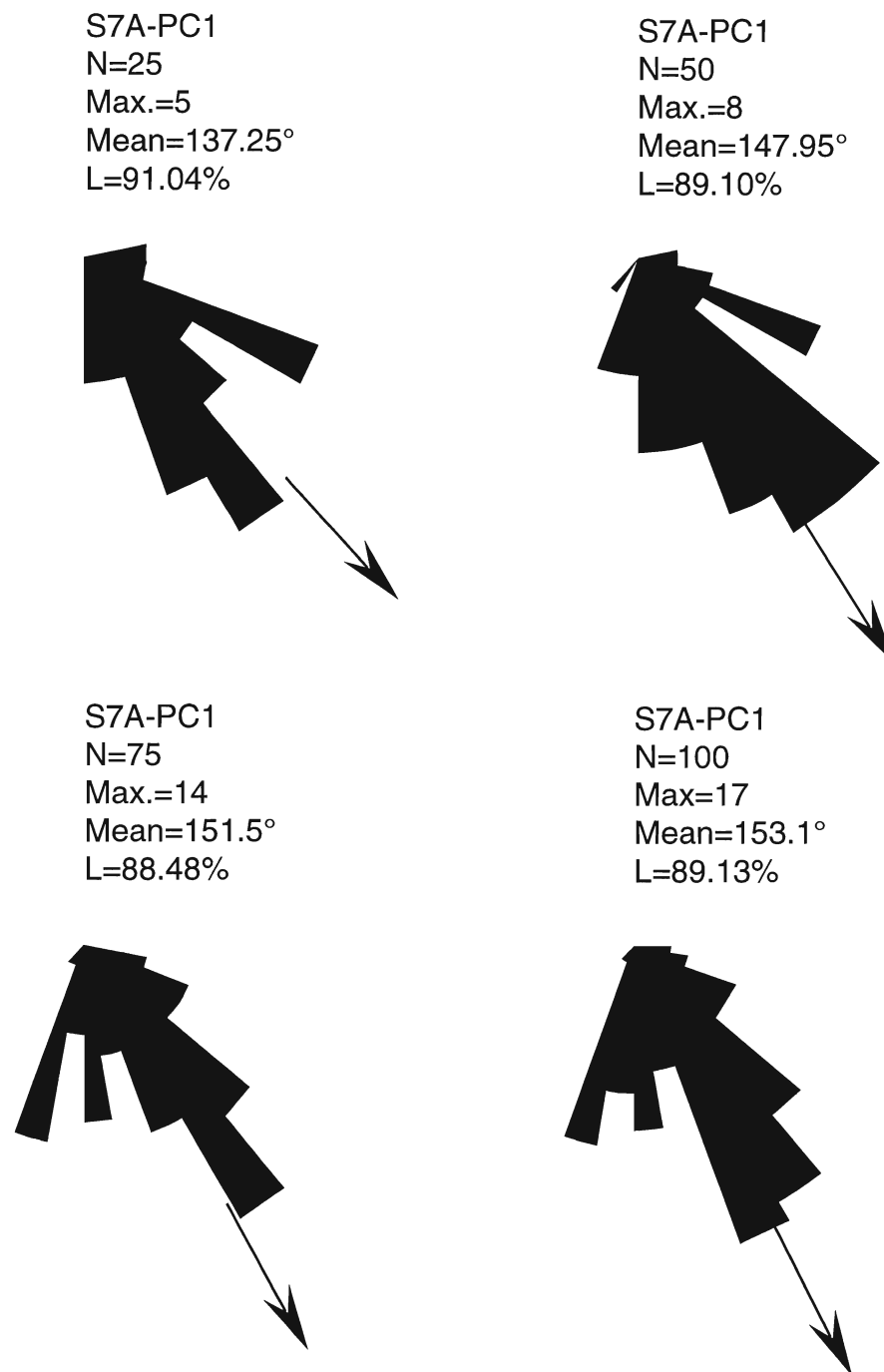


Fig. 1.7. Paleocurrent measurement trial test. Measurements were taken from the same unit, and statistics were calculated with N=25, 50, 75 and 100. Results indicate that N=50 is a valid sample size for this study, as mean directions do not differ drastically from N=50 to N=75 or 100.

pebble fabrics. Diamict clast fabrics were measured at nine sites.

The vertical sections were drawn as graphical logs, with patterns and symbols depicting the detailed sedimentology (Appendix III). Paleocurrent data are superimposed onto the graphical logs. Photo-mosaics taken in the field produced panoramic coverage of most exposures in the pits. The graphical logs were correlated with the photo-mosaics to produce fence diagrams (Appendix IV), where possible, to depict the spatial distribution and architecture of sediment facies. Photo-mosaics were an essential tool, especially where direct access was limited and the sediment body geometries and architecture could be determined from the photographs.

## 2.0 FACIES DESCRIPTIONS AND INTERPRETATIONS

This chapter will describe and interpret the sedimentology of the ten facies which comprise the Bloomington fan complex. Facies 1 to 6 (Table 2.1) are identified in terms of depositional sub-environments on a fan complex. Facies 7 to 10 include deposits formed in response to changes in major depositional environment due to water level fluctuations in the interlobate lake basin and the subsequent readvance of Ontario ice lobe.

It is thought that deposits of subglacial or englacial conduit origin were not exposed, although sediments exposed after initial field work was complete may have been deposited within subglacial conduits or in a proximal proglacial environment. The inferred locations of possible conduits are based on the distribution of proximal proglacial sediments (facies 1 and 2), in combination with mapped eskers (P.J. Barnett, pers. comm., 1994) and topographic ridges leading into the deposit (Fig. 1.2). Elongate gravel bodies were previously documented in the pits (Duckworth, 1975, 1979), but have been removed by subsequent excavation. Early stages of excavation were parallel to these gravel bodies; their orientation is still weakly mimicked by present exposures (Fig. 1.2).

A total of 44 sections were logged from both pits (Fig. 2.1), and provided good coverage of the lateral and vertical variation across the exposed portion of the deposit. Paleocurrents across the deposit are generally towards the southwest (see grand rose, Fig. 2.1). This chapter provides descriptions and interpretations of each of the ten facies and includes numerous references to the following supplementary data which are presented in the appendices:

Appendix I	Paleocurrent data from cross-stratified sand
Appendix II	Gravel fabrics
Appendix III	Graphical section logs (S1...S26; L1...L18)
Appendix IV	Fence diagrams

Table 2.1. Summary of Bloomington Fan Complex Facies

FACIES	DOMINANT SEDIMENTS
Facies 1 Coarse Proximal Gravel	Heterogeneous, unstratified to weakly stratified gravel.
Facies 2 Proximal Interchannel	Laterally continuous sheets of interbedded sand and gravel.
Facies 3 Proximal to Mid-Fan Channel	Well defined or vague channels infilled with large-scale tabular and trough cross-bedded pebbly sand.
Facies 4 Mid-Fan Interchannel	Horizontal to gently inclined medium to coarse sand beds, discontinuous sand cross-bed sets and rippled beds.
Facies 5 Distal Channel to Interchannel	Fining-upward sequences from basal horizontal and rare cross-bedded sand passing upwards into climbing ripple sequences.
Facies 6 Massive Sand Channels	Steep-walled channels filled with massive to vaguely bedded sand, and associated with shallow scours filled with climbing ripple sequences.
Facies 7 Glaciolacustrine Deposits	Horizontally laminated sand, silt and clay; units are rarely rhythmically laminated.
Facies 8 Ice-Marginal Complex	Interstratified glaciolacustrine deposits, thin beds of glaciofluvial sediments, and weakly stratified to massive diamicts.
Facies 9 Stratified Sand and Gravel	Dominated by horizontally bedded gravel, also large-scale cross-bedded gravel, tabular and trough cross-bedded pebbly sand, discontinuous lenses of rippled sand and laminated silt.
Facies 10 Diamict	Diamict which exhibits variable textures ranging from massive to weak internally stratification.

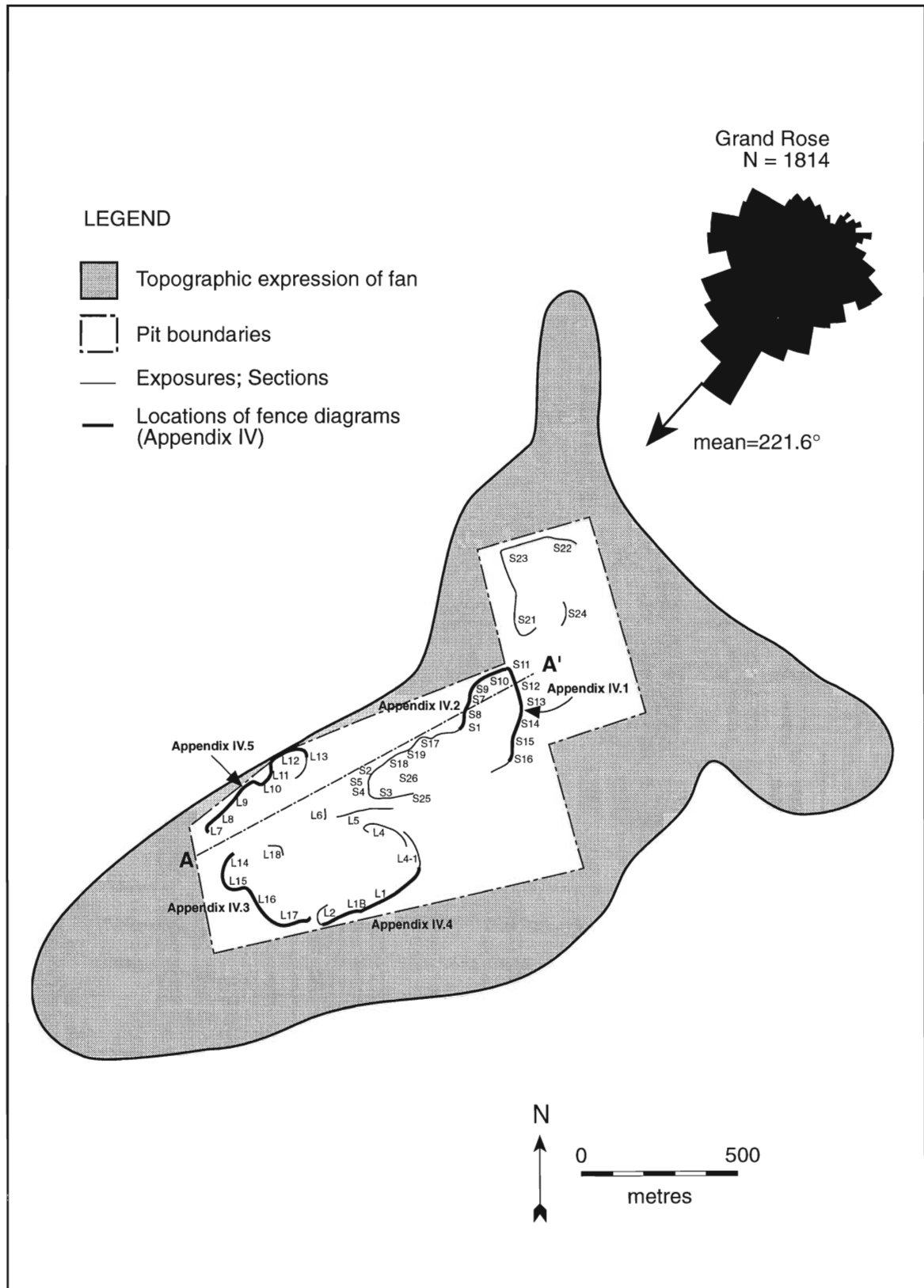


Fig. 2.1. Section and fence diagram locations. Section A-A' is shown in Fig. 3.10. Note the grand rose exhibiting general southwesterly paleoflows.

## 2.1 FACIES 1 COARSE PROXIMAL GRAVEL

### 2.1.1 Description

#### Facies 1a

This facies is characterized by poorly to moderately sorted, generally massive to weakly stratified gravel that is exposed in thick (up to 17 m) sequences at S13 (Fig. 2.2). Weak stratification, defined primarily by beds of sand and discontinuous cobble and boulder gravel concentrations (clusters?), dips gently (10-15°) to the south-southwest near sections S12 and S13. Facies 1a also occurs as gravel cores at the base of the deposit in the central and southwestern portion of the deposit; these gravels are normally flanked by interbedded sand and gravel of facies 2 and 4 (Fig. 2.3).

Exposures of this facies from S12 to S14 exhibit a slight downflow (towards the southwest; see Fig. 2.1) grading from coarse cobble to boulder gravel (maximum clast size 0.6 m) into pebble to cobble gravel. Gravel beds are dominantly clast-supported but are locally matrix-supported. Vertical grading is rare in proximal beds, but becomes more common downflow where beds are normally graded (Fig. 2.4), and less commonly inversely graded.

Individual gravel beds range in thickness from one to two metres in proximal exposures, thinning downflow to approximately 0.5 metres. Bedding within the gravel becomes better defined downflow as sand interbeds increase in thickness and number, and cobble and boulder clusters become more discernible. In this better-sorted zone, some open framework beds exhibit poorly defined internal cross-bedding (Fig. 2.5). Overall improved sorting and fining of facies 1a downflow is common to both the clasts and the matrix fraction of the gravel; grain size of the matrix ranges from fine to very coarse sand and granules.



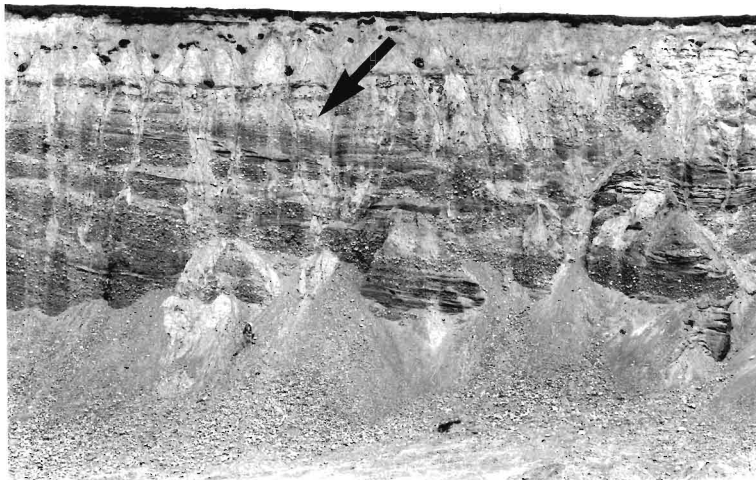


Fig. 2.2. Coarse gravel deposits at S13 that are inclined towards the south (to the right). Note the erosional surface which truncates the dipping gravels (arrow). The face is 25 to 30 m high.

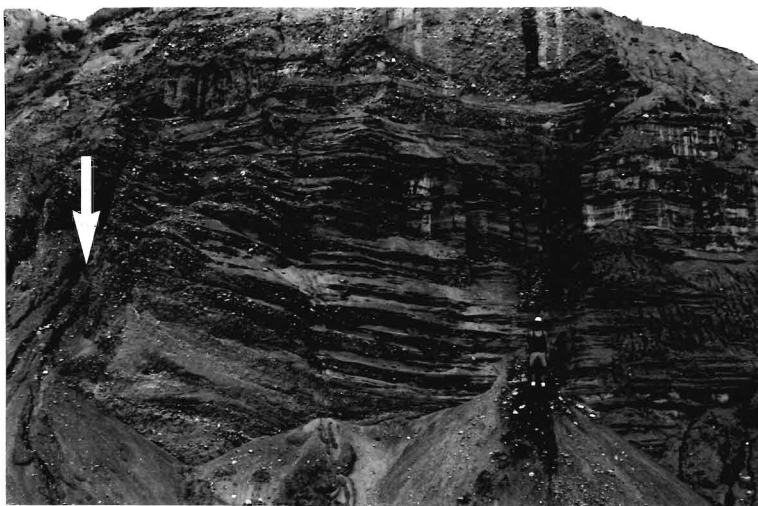


Fig. 2.3. Gravel "core" (arrow) flanked by interbedded sands and gravels; note the decreasing angle of dip upsection (L14). The person is 1.85 m high.

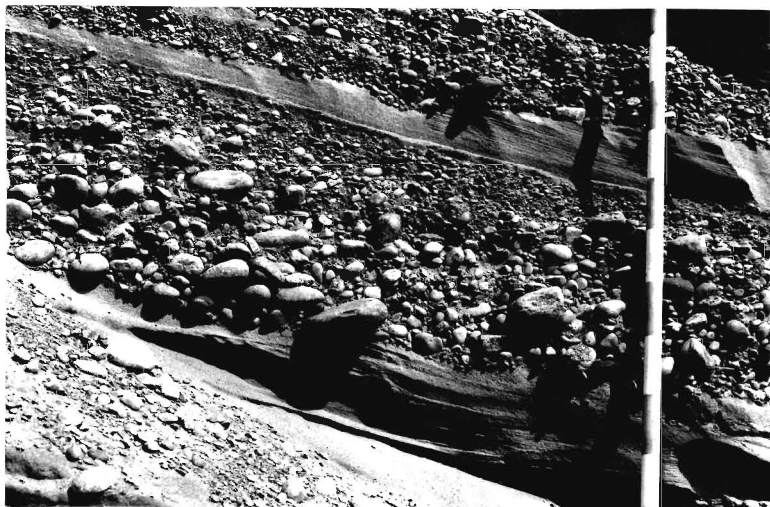


Fig. 2.4. Normal grading within gravels which are scoured into underlying sand beds; note the well-developed imbrication (S13). Flow from left to right. Scale bar has 10 cm increments.

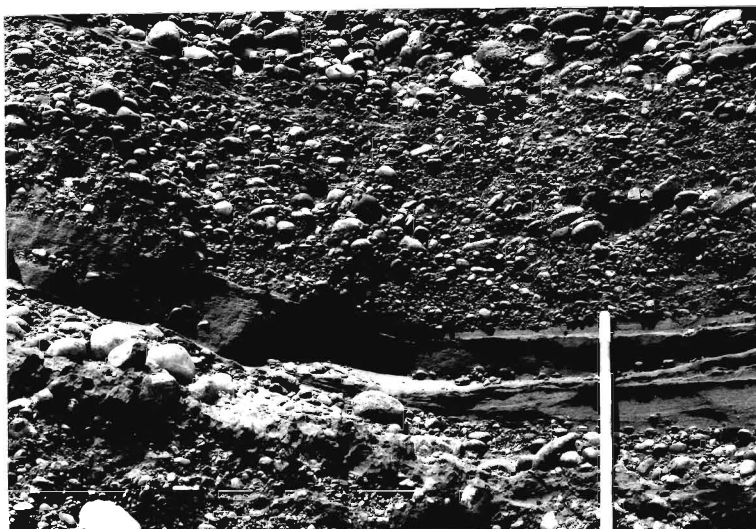


Fig. 2.5. Cross-bedded, open and closed framework gravel (S13). Scale bar has 10 cm increments.

In proximal and basal portions of facies 1a, clasts are dominantly gently inclined to weakly defined bedding planes. Measured clast fabrics are variable in strength and orientation, ranging from a-axes transverse and b-axes imbricate and dipping upflow (a(t) b(i)) to a-axes aligned parallel to flow and imbricate (a(p) a(i); Appendix II). The imbrication of clasts is better developed in sections downflow, where a-axes are dominantly transverse to flow (Fig. 2.4).

The sand interbeds increase in number and thickness downflow, where they are regularly spaced at approximately 2 metre intervals. They display a variety of structures, including pebbly trough cross-bedding, gently inclined parallel bedding marked by heavy mineral concentrations and weakly rippled and laminated fine sand to silt.

Facies 1a is also exposed at the base of sections in the central and southwestern portion of the deposit, as gravel cores that are flanked by interbedded sand and gravel (S23.2, L5, L14). Contacts between the two units commonly exhibit interdigitation along an otherwise sharp margin which tends to maintain its location upsection, or shows minimal lateral migration (Fig. 2.3). The flanking deposits appear to drape over the cores of gravel and the angle of dip of these beds normally decreases upsection. In some sections the relationship between the two facies is less clear, and the contact is sharp, with no interdigitation along its length (L5). At section L5 facies 1a attains a thickness of 10 metres, and appears to be faulted and deformed into convoluted strata.

#### Facies 1b

Excavations beneath S21 and S23 that took place following field work exposed some enigmatic sand and gravel structures. The most common structures are undeformed (Fig. 2.6a) and deformed (Fig. 2.6b) metre-scale gravel mounds draped by stratified sand. Numerous nested, small gravel channels marked by near-

a



b



Fig. 2.6. Exposures beneath S21 and S23: a) undeformed gravel anticlinal structure, draped by laminated sands; b) gravel mound which has been subsequently folded over towards the south. Scale bar has 10 cm increments.

vertical faults characterize other faces. Other lenticular gravels are interdigitated with flanking deposits, and associated with high angle-reverse faults (Fig. 2.7). The most remarkable structures are metre-scale climbing gravel dunes characterized by concentrations of clasts between the brink and the crest, and slightly pebbly sand in the troughs (Fig. 2.8).

These deposits occur at a similar stratigraphic position as facies 1a at other sections. This stratigraphic position is inferred in part by overlying facies 9 (Fig. 2.9), but the transition from facies 1b up into the facies 9 is unclear.

### 2.1.2 Interpretations

Heterogeneous, unstratified to weakly stratified gravel has been documented by numerous workers, including Walker (1975; disorganized gravel), Rust (1977; gravel deposited proximally in front of a conduit) and Saunderson (1977; sliding bed facies). Most workers agree that the poor sorting and lack of grading is indicative of rapid deposition from hyperconcentrated flows characterized by high internal shear stress which prevent effective grain interactions (Collinson and Thompson, 1989). Hyperconcentrated flows may be driven by momentum of the inflowing meltwater jet. Others attribute such deposits to rapid deposition from suspension due to flow expansion at the mouths of conduits (Shaw, 1985; Gorrell and Shaw, 1991), perhaps associated with an hydraulic jump at the transition from supercritical to subcritical flows (Shaw and Gorrell, 1991; McCabe and Ó Cofaigh, 1994).

Facies 1a generally lacks faulting and interbedded diamicts normally associated with conduit sedimentation (McDonald and Shilts, 1975; Thomas, 1984). This may suggest that deposition occurred rapidly at or directly in front of the conduit exit. Weakly defined bedding in proximal gravel suggests that flow was characterized by successive flow pulses, which varied either temporally or spatially (Postma, 1986). Other workers believe that similar gravels are deposited from

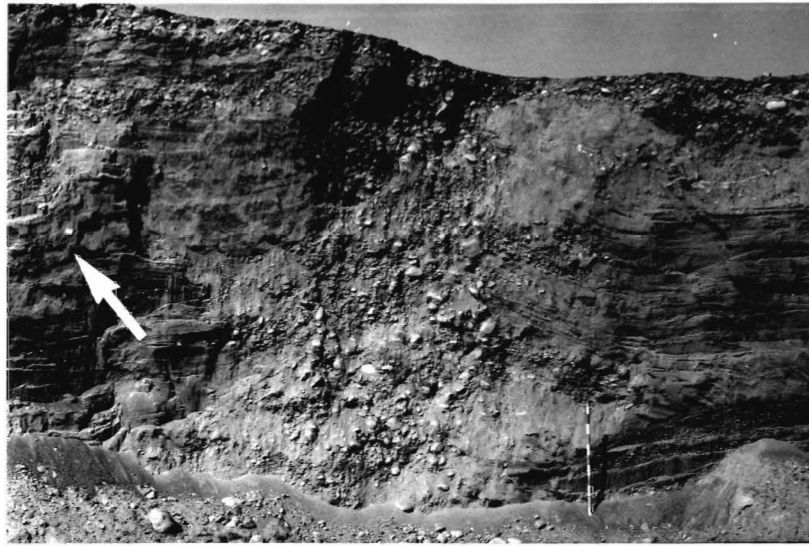


Fig. 2.7. Laterally discontinuous, lenticular gravels interdigitated with horizontally bedded sand beneath S23. Note the high-angle reverse faults to the left of the gravel channel (arrow). Scale bar has 10 cm increments.

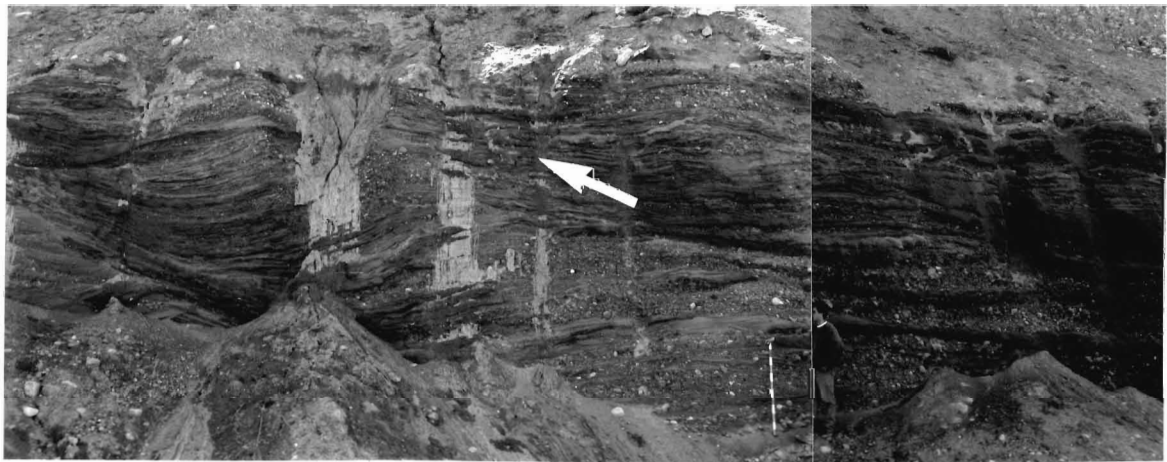


Fig. 2.8. Climbing gravel "dunes" exposed beneath S23; arrow indicates direction and angle of climb along dune crests. Flow was from right to left (towards the south). Scale bar has 10 cm increments.

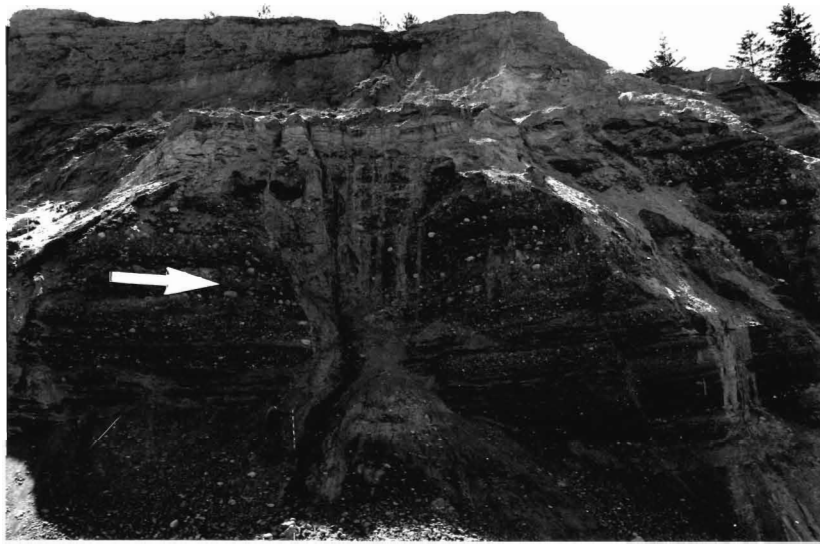


Fig. 2.9. Section showing exposures which were excavated following field work beneath S21. Facies 1 deposits are beneath facies 9 (horizontally bedded gravels; arrow above contact). Scale bar has 10 cm increments.



hyperconcentrated, cohesionless grain flows (Maizels, 1989, 1991). The relatively steep slope angles ( $\approx 10^\circ$ ) are produced by very rapid sedimentation of coarse gravels in a proximal location (Pharo and Carmack, 1979), which may enhance the susceptibility to slump failure and re-sedimentation (Postma *et al.*, 1983; Lash, 1984). Clast orientation within grain flows is maintained upon rapid deposition; as a result, only large clasts exhibit weak a-axis parallel to flow imbrication.

Within gravel beds clast size decreases and sorting increases in the downflow direction (S13, S14), suggesting rapid deceleration of flows into a standing body of water. Rapid deposition near the conduit reduces sediment concentration downflow (Maizels, 1989, 1991), resulting in better sorted deposits. Increased sorting and better definition of bedding could also result from related longitudinal sorting mechanisms (Iseya and Ikeda, 1987; Kuhnle and Southard, 1988; Whiting *et al.*, 1988). For example, a reduction of the concentration of sediment in transport results in increasingly turbulent flows that deposit normally graded beds during waning stages, and allow clast movement dominantly as traction load (Postma *et al.*, 1983; Postma, 1984). The combination of a(t) b(i) fabrics, typical of large clasts, with smaller clasts displaying a(p) b(i) fabrics, indicates a mixture of particles transported by rolling and suspension or saltation, respectively (Johansson, 1963; Rust, 1972, 1975). Inverse grading occurs largely at the base of beds, and is produced by dispersive pressures in grain flows (Middleton and Hampton, 1976; Lash, 1984). Dip angle of clasts decreases upwards in a given bed due the increased shear during late stages of flow, as pore-waters are expelled, and sediment concentrations rise (Postma *et al.*, 1983; Lindsay, 1968, Eyles and Kocsis, 1988).

Exposures of Facies 1b revealed after field work was completed exhibited a variety of complexly bedded and deformed gravel. Most of the gravel structures can be attributed to rapid rates of sedimentation. Their occurrence at a similar stratigraphic position as Facies 1a perhaps suggests contemporaneous deposition

with proximal facies 1a at S11, and therefore the sediments of Facies 1b below S21 and S23 may have been deposited either in a proglacial or subglacial conduit environment. The presence of high-angle reverse faults flanking gravel cores suggests subglacial conduit deposition; however, without further evidence, it is difficult to determine.

## **2.2 FACIES 2 PROXIMAL INTERCHANNEL**

### **2.2.1 Description**

This facies is characterized by laterally continuous interbedded sand and gravel located in positions adjacent to proximal gravel of facies 1a. Bed thickness is on average less than 0.5 metres, but ranges up to 2 metres.

Gravels are predominantly poorly sorted, and interbedded with horizontally bedded and cross-bedded sand. The gravels contain clasts ranging from pebbles to small cobbles, and are mainly matrix-supported, with local clast-supported lenses. The poorly sorted matrix ranges from fine to very coarse sand and granules. These gravels are generally massive, with rare beds showing weak normal grading. Gravel beds normally thin upsection, but locally coarsen (S9, L5) or fine (S18, L13) upsection. Contacts between the gravel beds and sand beds are commonly sharp, with little or no grading between them. Clasts in some beds lie parallel to bedding planes, whereas in others, clasts are imbricate and range from a(p) a(i) to a(t) b(i) alignment (Appendix II).

Sand beds exhibit a variety of structures, ranging from poorly defined cross-bedding to well-developed ripple cross-laminae. Horizontal lamination is predominant within fine to medium sand. Laminae are commonly defined by heavy mineral concentrations. Shallow scours are normally filled with horizontal to gently dipping beds and/or normally graded beds of massive coarse to medium sand. Both tabular and trough cross-bedding occur in pebbly fine to medium sand as sets

up to 0.4 m thick. Ripple cross-laminated beds are of fine to very fine sand, and vary in thickness from a few centimetres to greater than 1 metre. Some beds exhibit climbing ripple sequences from type A to type B ripple cross-laminae, overlain by sinusoidal ripples. Other beds include only type A ripple cross-laminae. Rare beds are draped by silt laminae. Many exposures of sand beds exhibit soft-sediment deformation (convolute laminae, flames), especially when overlain by thin beds of massive sand or pebbly sand. Like the gravel beds, most of the sand beds thin upsection.

Undeformed sequences of facies 2 generally have variable dip directions; beds to the southwest at S14, S15 and S17-S19, to the west at L5 and to the northwest at S1, S10, L6, L13. In some sections beds dip as steeply as 30°, in directions that differ markedly from surrounding sediments. Normal faulting commonly occurs in these oversteepened units. Paleocurrents in these sections generally parallel the dip directions. For example, in section S14 beds strike 155° and dip 25° towards the southwest; paleocurrents derived from ripple cross-laminated sand (mean 244°) and gravel fabrics (mean 253°) are similar to the dip direction of the beds (Appendix I and II). In these exposures, facies 2 is predominantly thinly bedded and varies from cobble gravel and poorly sorted gravel lenses to massive and laminated sand (Fig. 2.10). In many of the thicker gravel beds clast orientations are notably random, with many near-vertical clasts.

### 2.2.2 Interpretations

Laterally continuous sand and gravel beds are deposited by episodic unconfined sheet flows. The rhythmically interbedded sand and gravel may reflect cycles related to annual or seasonal discharge variations (e.g., Banerjee and McDonald, 1975; Ringrose, 1982), or episodic floods caused by lake (e.g., Nye, 1976) or subglacial cavity drainage (e.g., Kamb *et al.*, 1985; Kamb, 1987). The apparent lateral gradation from facies 1 gravel indicates contemporaneous deposition of facies



Fig. 2.10. Steeply dipping, thinly bedded sand and gravel (S15). Scale bar has 10 cm increments.

2 on proximal flanks of the fan lobes. The gravels are similar in texture to proximal gravels and deposition would have occurred from flows which passed laterally from the proximal proglacial flows, producing beds of massive, and rarely normally graded gravel. Normal grading was produced when flows waned.

Variations from a(t) b(i) to a(p) a(i) clast orientations (Appendix II) may be due to changes in sediment concentrations, and clast size (Johansson, 1963; Sedimentary Petrology Seminar, 1965; Rust, 1972, 1975). A(t) b(i) orientation is normally associated with deposition of rolling clasts from traction currents, which suggests relatively low sediment concentrations (Johansson, 1963; Rust, 1972, 1975). A(p) a(i) imbrication is normally associated with deposition from flows with high sediment concentrations and high shear stresses.

Sand beds were deposited during relatively low flow stages, or from lower energy flows that spread out from the source, and spilled out over the proximal regions of the deposit. Horizontally bedded sand predominates, and is produced by aggradation of plane beds. Shallow scours filled with low-angle migrating cross-stratified sand and normally graded massive sand suggests periodic flows which erode small, localized channels. Sets of tabular and trough cross-beds were deposited from migrating straight-crested and sinuous-crested dunes, respectively.

Rapid deposition of a variety of sediment sizes produces ideal conditions for the development of soft-sediment deformation structures. Density inversions and rapid deposition of sediment with supersaturated pore-waters contribute to the formation of a variety of load structures.

Beds that dip steeply towards a central point indicate post-and syn-depositional deformation that occurred during fan construction (e.g., S14 and S15). These sequences are interpreted as kettle fills (Hayward and French, 1980). Dominantly thin beds of poorly sorted sandy pebble gravel indicate a distinct

change in style of sedimentation, and are deposited from numerous, smaller scale sediment gravity flows. Variable distribution of sand beds may be due to flows which were deflected around ice blocks, and into depressions which formed when the ice blocks were moved by large flow events (Maizels, 1989, 1991), or from scouring by large flow events on the lee of the ice block. Variable paleocurrent directions (S14) probably indicate deflection of flows around these ice blocks, or into scoured depressions in the lee of the ice blocks or as the ice block slowly melted.

## **2.3 FACIES 3 PROXIMAL TO MID-FAN CHANNELS**

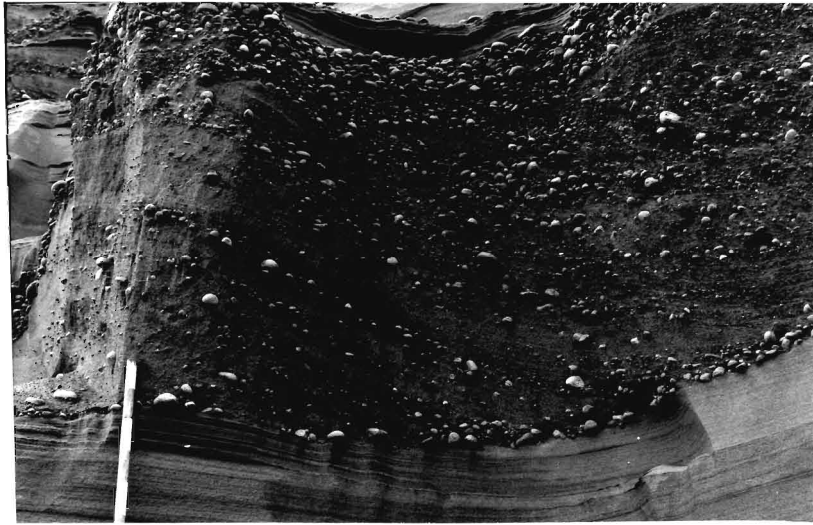
### **2.3.1 Descriptions**

This facies is characterized by stratified pebbly sand and gravel, and is distinct due to the large scale cross-bedding, and the association with mid-fan "channels". The channels range from metre-scale, steep-walled and well-defined, to others which are poorly defined, broad, shallow zones which contain facies 3 sediments.

Large-scale, (up to 2 metres) trough and tabular cross-beds in pebbly medium to coarse sand normally overlie broad scoured surfaces or occur as laterally continuous cross-bed sets (Fig. 2.11). Most sets are, in turn, overlain by horizontal beds, some of which have been scoured prior to deposition of subsequent cross-bed sets. These deposits dominate exposures near section L4 and L4-1, and occur at the same elevation as a large sand filled-channel with gently-dipping beds, which decrease in angle of dip upsection. Thin beds containing ripple cross-laminated sand are rare.

Stratified sandy gravel of this facies ranges from clast- to matrix-supported, and are locally normally graded (Fig. 2.12) with notable basal pebble and cobble lags. Clasts range from steeply imbricate (e.g., S1-CF2), to lying parallel to bedding planes (e.g., S16-BF1). Gravel lenses are generally discontinuous and lenticular

a



b

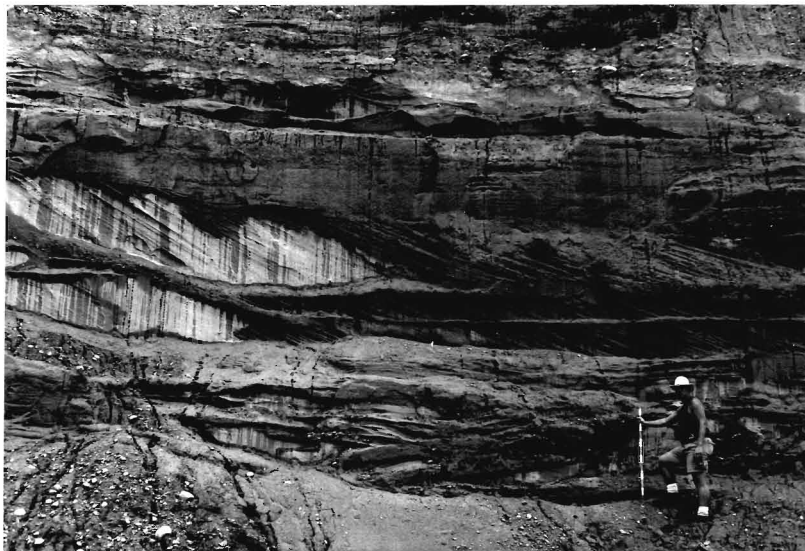


Fig. 2.11. a) Large pebbly sand tabular cross-beds within channel scour, truncating horizontal to gently inclined beds of fine to medium sand (L2). Note pebble lag at base of scour; b) Large scale cross-bed sets (L4-1). Scale bar has 10 cm increments.



within these units, and the dip direction of bedding is highly variable in some exposures (Fig. 2.13).

Facies 3 normally occupies vague channels in the mid-portion of the deposit; poor definition of channels may be due to exposures which parallel the channel trends. Other, more distal exposures exhibit facies 3 sediments filling broad, shallow scours (e.g., L17; Appendix IV.3). These sediments are included in facies 3 (rather than facies 4) because they are characterized by vertically and laterally continuous cross-bed sets, and are generally comprised of coarser grained sediment than facies 4 (i.e., pebbly medium to coarse sand of facies 3 compared to fine to medium sand of facies 4). Facies 4 is characterized by laterally discontinuous, isolated cross-bed sets which are normally associated with shallow, broad erosion surfaces.

Section S1 exhibits an unusual contact between facies 3 and adjacent facies 4. The contact is relatively sharp and very steep, but displays some minor interdigitation of the two facies (Fig. 2.14). A further curious characteristic of this contact is that the facies 3 sand and gravel display deformation by faulting and oversteepened beds (Fig. 2.14), but the adjacent facies 4 appears to be undisturbed. The deformation is also exposed directly behind section S1, where thick gravel displays a similar contact defined by a normal fault. Paleocurrent data collected from facies 4 in this section indicate westerly flow into the facies 3 "channel".

### 2.3.2 Interpretations

The large scale cross-beds in pebbly sand indicate powerful flows that caused the migration of large bedforms within these confined channels, which pass downflow into broad, poorly-defined channels in more distal locations. Interstratified sand and gravel is normally confined within mid-fan, scoured channels.



Fig. 2.12. Normally graded gravel beds (L4a). Scale bar has 10 cm increments.



Fig. 2.13. "Chaotic" channel gravels marked by numerous nested scoured channels (L15). Approximately 4 metres of exposure in photograph.

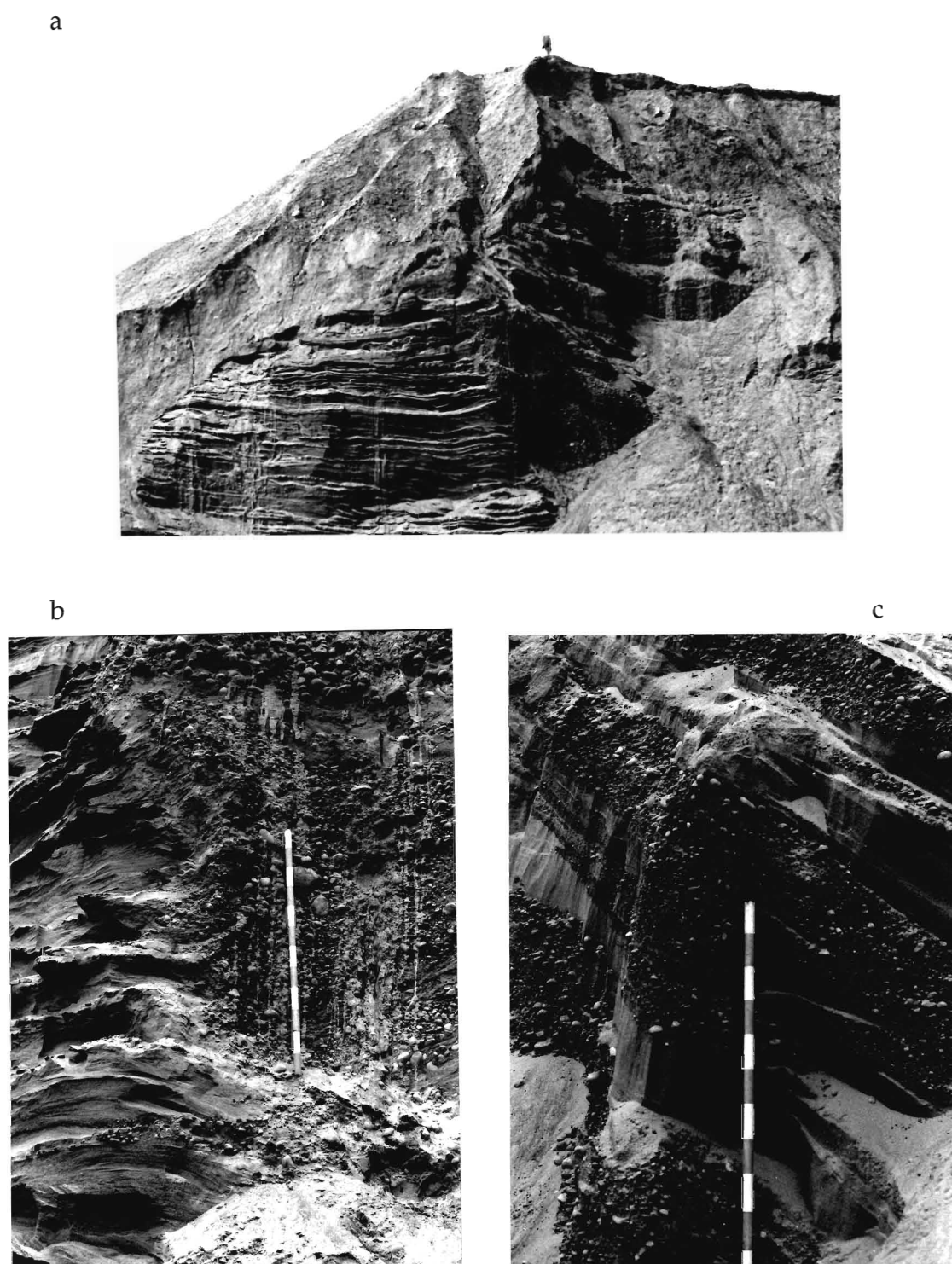


Fig. 2.14. Section S1 showing: a) sharp, steep contact between facies 3 and adjacent facies 4 sediments; note the increased interdigitation near the top of the exposure. Person standing on top of section is 1.85 m; b) close-up of the contact; minor interdigitation, upturned margins of both facies within the contact zone; c) oversteepened beds. Scale bar has 10 cm increments.

Massive, clast-supported imbricate gravel was deposited from episodic, high-energy flows that passed across the mid-fan regions, mainly within confined, scoured channels (e.g., S1-CF2). A(t) b(i) imbrication indicates deposition from traction currents (Johannson, 1963; Rust, 1972, 1975). Normal grading in some of these beds also reflects deposition from waning flows.

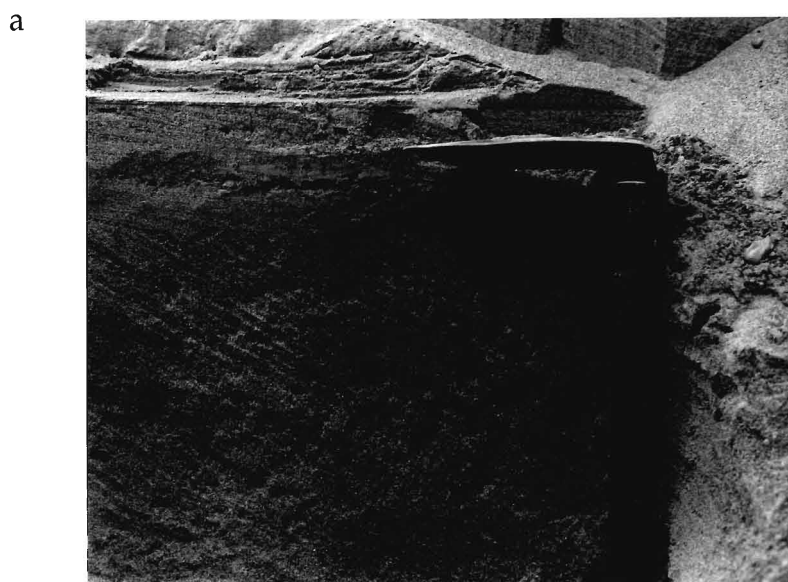
The large scale tabular cross-beds that lack evidence of channelization were deposited as large, dominantly straight-crested dunes, or as transverse bars within shallow scours. Grouped or solitary sets of trough cross-beds indicate zones dominated by sinuous-crested dunes. Sub-horizontal beds were deposited as low-angle lee-slopes and on inter-dune areas. These are partially scoured during subsequent dune migration. Interbedded rippled beds were deposited during waning flow stages, and are also scoured by subsequent dune migration.

## **2.4 FACIES 4 MID-FAN INTERCHANNEL**

### **2.4.1 Descriptions**

The characteristics of this facies varies and includes: 1) interbedded cross-bedded and horizontally bedded sand; 2) weakly bedded to massive pebbly medium to coarse sand; 3) metre-scale vertical successions of thin, horizontal beds of fine to medium sand and silt; and 4) ripple cross-laminated sand beds. Isolated, discontinuous gravel lenses occur sporadically.

Planar tabular cross-bedding, and to a lesser extent trough cross-bedding, occur in mid-fan deposits in sets up to 1 m thick and are normally interbedded with horizontal and low-angle dipping beds. Cross-laminae are commonly preserved on both the crest and lee slopes of bedforms (Fig. 2.15). In these examples, the bedforms would have grown in height as the substrate aggraded. Basal contacts are normally angular, with rare tangential to set contacts. Cross-beds are defined by



b

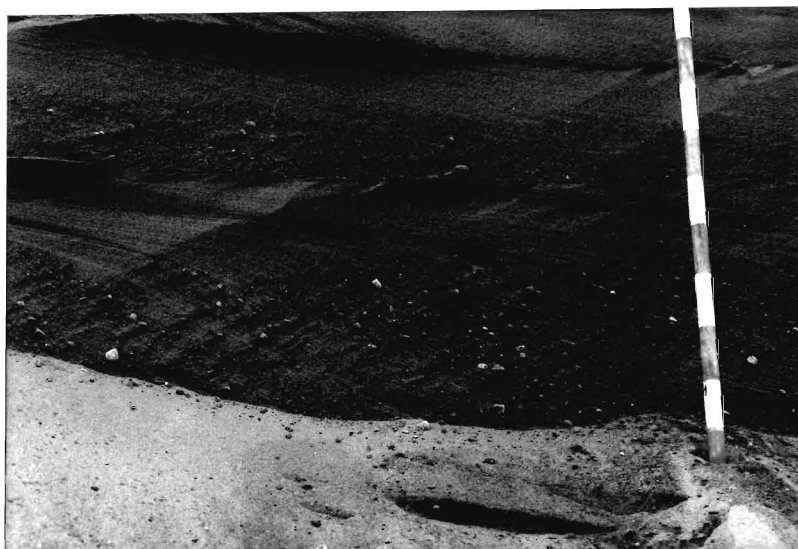


Fig. 2.15. Topsets preserved in cross-bedded sands. a) planar tabular cross-bed set; shovel blade is approximately 15 cm long (S3); b) cross-bed set with tangential internal cross-strata (L1). Scale bar has 10 cm increments.

layers of pebbly fine to medium sand, with pebble to coarse sand lags at the base of cross-beds so that sets appear to be normally graded. However, in some sets pebbles are concentrated near the crest so that sets appear to coarsen upwards (Fig. 2.16).

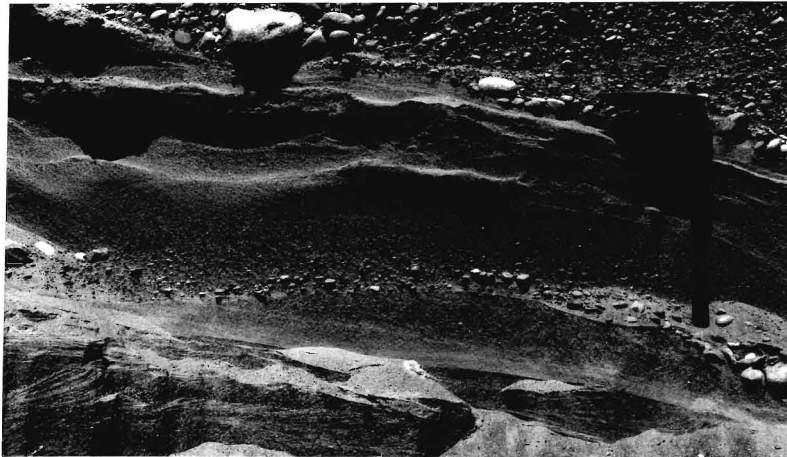
Sand beds with horizontal and low-angle dipping laminae are interbedded with cross-bedded sand and range in grain size from well sorted medium sand, to pebbly medium-to-coarse sand with pebble lags (Fig. 2.17). Bed thickness ranges from 0.1 m to 0.5 m and display either normal or inverse grading.

In sections adjacent to the fan apex (S9, S7) this facies is characterized by weakly defined fining-upward sequences. Basal portions of these sequences are commonly composed of low-angle dipping beds and/or cross-beds. Horizontal beds are often cut by shallow scours with pebble lags and are locally normally graded, and commonly truncate tabular cross-beds.

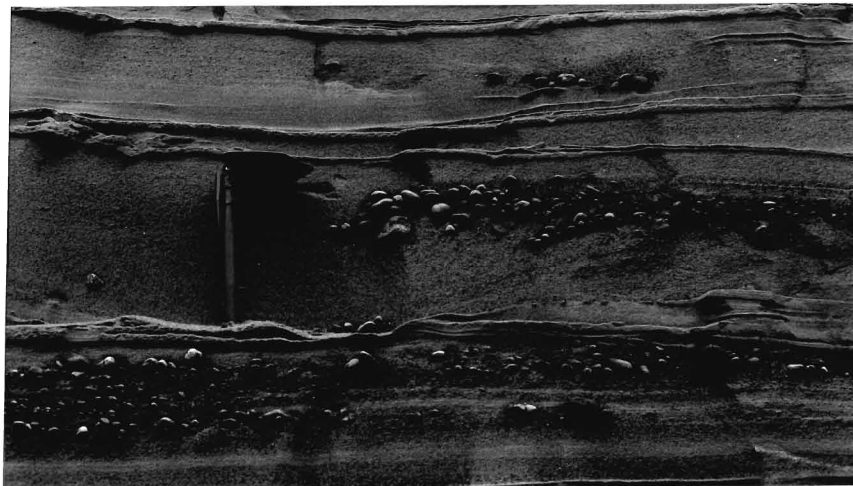
Some exposures exhibit cross-bedded sand overlain by vaguely bedded to massive beds of pebbly medium to coarse sand. Massive beds are commonly normally graded (Fig. 2.18a); only rare beds exhibit inverse grading. Clasts are aligned along vague cross-beds or horizontal beds (Fig. 2.18b), appear to float in massive sand (Fig. 2.18c), or form lenses of imbricate clasts at the base of beds. Thin beds of weakly ripple cross-laminated and horizontally laminated sand and silt overlie most beds (Fig. 2.18b,c). Sections that are dominated by these structures grade laterally into a several metre-thick unit of thin, horizontally bedded sand (S4-S2); grain size in these thin beds ranges from granules and very coarse sand, to pebbly fine-to-medium sand (Fig. 2.19). These beds exhibit normal or inverse grading, and are commonly interbedded with laminated very fine sand, silt and clay.

Most sequences of facies 4 also contain beds of ripple cross-laminated sand and silt, which increase in number and thickness in the downflow direction (e.g., in

a



b



c

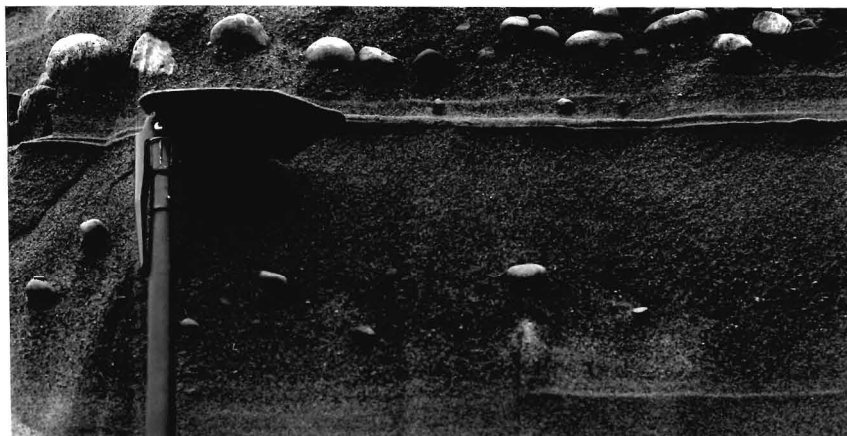


Fig. 2.18. Vaguely bedded and massive pebbly sands: a) normally graded, massive sand; b) clasts aligned along vague cross-beds; note also the thin silty very fine sand lenses which drape each vaguely bedded or massive bed; c) "floating" clasts in massive medium to coarse sand. Shovel blade approximately 15 cm long.



L1B). Most beds contain a variety of ripple cross-laminae, including type A, type B, sinusoidal and drape laminae. Ripple cross-laminated beds are normally interbedded with horizontally bedded fine to medium sand. These fine-grained beds occur at almost regularly spaced intervals every few metres.

Gravel in this facies is normally restricted to discontinuous isolated lenses up to 0.3 m thick, with clast a-axes up to 10 cm. Lenses are scoured into underlying sediment (Fig. 2.20), but also exhibit rare positive relief. Imbrication is generally better developed than in proximal interchannel zones (facies 2), with strong a(t) b(i) imbrication (e.g., S9-AF1.2). Poorly sorted gravel lenses with a(p) orientations are rare (S17-BF1).

Soft-sediment deformation is abundant where massive, coarse-grained sand beds overlie rippled sand. In some sections various styles of faulting are common, including low-angle reverse, high angle reverse and normal faults (Fig. 2.21). These faults do not penetrate the entire vertical exposure, as faults in facies 4 are truncated by facies 8. Fault planes strike predominantly north-northwest to south-southeast (Fig. 2.21c). This facies is similarly distorted at sections L10-L11, by large-scale imbricate thrust slices. These structures will be discussed in detail later in section 2.11.

#### 2.4.2 Interpretations

The inherent variability of this facies represents a variety of depositional sub-environments, all within the mid-fan region. The dominance of laterally continuous, gently inclined beds suggests deposition largely from unconfined sheet flows.

Some of the relatively high energy zones in the mid-fan region were characterized by migrating straight and sinuous-crested dunes that produced tabular and trough cross-beds, respectively. Sub-horizontal beds which normally



Fig. 2.19. Thin horizontal beds and laminae of coarse sand and silt (S2).

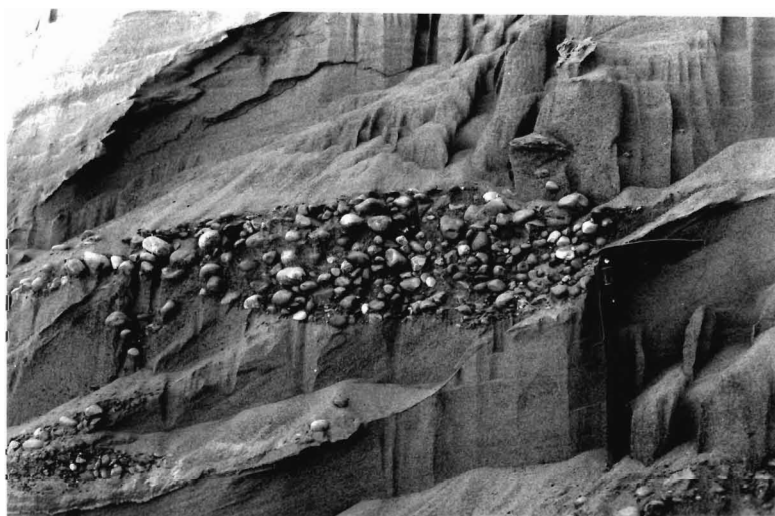


Fig. 2.20. Gravel lens scoured into underlying sand (S5.2). Shovel blade approximately 15 cm long.

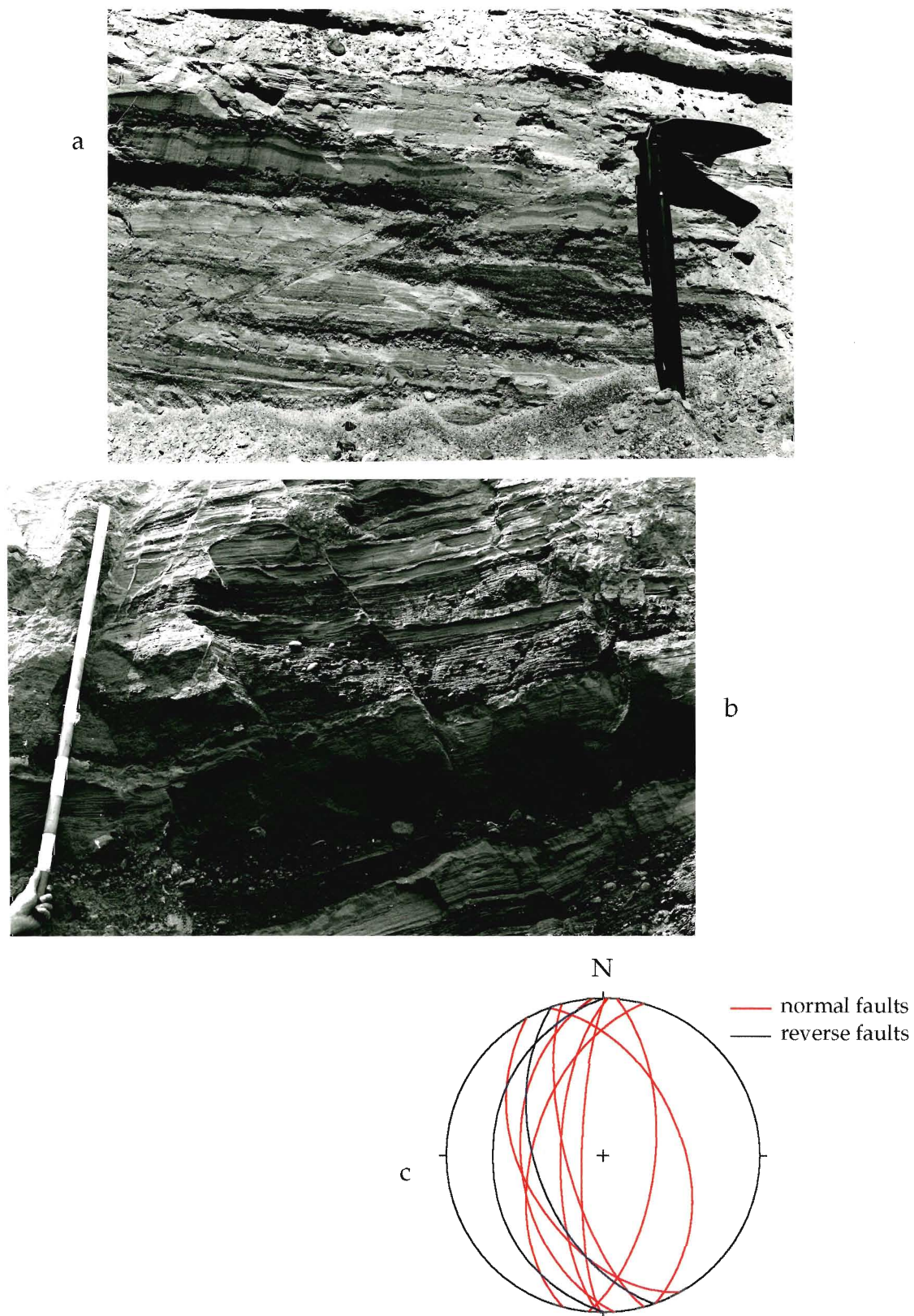


Fig. 2.21. Faulting of facies 4 near S2: a) low-angle reverse; b) high angle reverse and normal; c) stereonet plot of measured fault planes.

overlie tabular cross-beds were deposited on the low-angle stoss slopes of dunes. High rates of deposition from suspension on migrating dunes produced supercritically climbing tabular cross-bedded sets (Allen, 1982; Rubin and Hunter, 1982). Variable flow conditions are reflected by the presence of both angular and tangential toset contacts. Transitions from the angular to the tangential contacts reflects increasing flow strength, as return flow in the zone of separation increases (Collinson and Thompson, 1989, after Jopling, 1965). Normally graded cross-bed sets are common, and look very similar to cross-strata produced by humpback bars which cause pebbles to accumulate in the tosets by overpassing the crest of the bar (Allen, 1983).

Deposition of sheet flows on plane beds deposited mainly gently dipping and horizontal beds which dominate portions of the mid-fan region. Distal density underflows would have also affected this region, and produced local scours and shallow channels contained migrating dunes. Where scours were not present, thin, normally graded massive beds indicate deposition from waning flows. Distal margins of density underflows also deposited the rippled beds that are locally interbedded with horizontally bedded sand.

Vaguely bedded to massive sand and pebbly sand are rapidly deposited from high sediment concentration density underflows. Vaguely normally graded beds are deposited from waning flows. However, grain and clast collisions induce clast dispersive pressures within grain flows, and can produce inversely graded beds, with larger clasts located sporadically within the beds. These "floating" clasts suggest high sediment concentration flows in which clasts are not able to move freely, and deposition by "freezing" is rapid (Carter, 1975; Hiscott and Middleton, 1979; Postma, 1986). Some of these beds were definitely dominated by turbulent flow, as imbricate lenses of pebbles at the base of some beds and alignment of clasts along otherwise undetectable cross-beds suggests deposition from traction currents.

In sections S2 to S4, these massive to vaguely bedded deposits grade laterally into a thick (a few metres) sequence of thinly bedded and laminated sand and silt. Similar sequences have been documented by a number of workers from various depositional environments, including distal margins of turbidity currents in front of glaciolacustrine deltas (e.g., Shaw, 1975) and within lacustrine basins (Lambert and Hsü, 1979), and as levée/overbank deposits from glacial outwash (e.g., Krzyszkowski, 1994) and non-glacial deltas (Elliot, 1974; Fielding, 1984; Farrell, 1987; van Gelder *et al.*, 1994). The obvious lateral relationship between the vaguely bedded pebbly sand and the laminated sand and silt precludes the conclusion that the latter are glaciolacustrine sediments of facies 7.

A lack of strong evidence for channelization suggests these laminated sediments were deposited at the distal margins of underflows or turbidity currents. Pulsating turbidity currents would have deposited graded beds, and even local inverse grading (Lambert and Hsü, 1979). Similar cycles have been interpreted as annual deposits (Østrem and Olsen, 1987), but other workers believe that the turbidity currents or underflows are related to meteorological events (diurnal and/or seasonal cycles; Gustavson *et al.*, 1975; Lambert and Hsü, 1979), or related to retrogressive slope failure (Postma *et al.*, 1983; Postma, 1984). However, the laminated fine-grained sediments were deposited at the margins of the flows that deposited the vaguely bedded pebbly sand. In fact, the rapidly alternating coarse and fine beds with a general coarsening-upward sequence are typical of levée deposits (Elliot, 1974; Farrell, 1987). Minor coarsening-upward and fining-upward sequences within this section may indicate minor splays followed by abandonment of subaqueous crevasse channels (Elliot, 1974; Bridge, 1984; Fielding, 1984). Some of the thicker sand beds record exceptional floods. Periodic high-energy flows would have transported coarser sediment beyond channel breaches, and into interchannel areas. These flows were normally erosive, and deposited gravel from traction transport, causing them to have strong a(t) b(i) fabrics.

## 2.5 FACIES 5 DISTAL CHANNEL-INTERCHANNEL

### 2.5.1 Descriptions

Facies 5 is dominated by horizontal to low-angle dipping bedded sand, ripple cross-laminated sand, and laminated sand and silt. These deposits exhibit both cyclic, well-defined, fining-upward sequences of horizontally bedded to rippled sand, and thick ungraded ripple cross-laminated and horizontally laminated sand. Both types of sequences contain local or rare units of laminated silt and clay. Because the transition from facies 4 to facies 5 is gradual in some sections, this facies also includes local cross-bedded sand and discontinuous gravel lenses.

Fining-upward sequences in proximal locations of this facies (S7) are mainly composed of ripple cross-laminated sand and silt, and rarely include basal horizontal beds and thin, discontinuous, cross-bedded sand lenses (Fig. 2.22). The ripple sequences begin with subcritically (type A) trough and tabular ripple cross-laminae in fine to medium sand, overlain by subcritically to supercritically climbing ripple cross-laminae (types A and B) and sinusoidal ripple cross-laminae in fine to very fine sand. Such sequences are normally capped by units of horizontally laminated silt and clayey silt up to several centimetres thick.

In distal positions of the deposit, gently dipping beds of horizontally laminated and rippled sand occurs. Horizontal laminae are defined by heavy mineral sheets (Cheel and Middleton, 1986). Section L1B displays a sequence of nested channel scours in the lower half of the section which display minimal lateral migration (Fig. 2.23). These scours are filled with trough-cross bedded sand, truncate adjacent horizontal beds, and decrease in size upsection from 3 metres wide and 1 metre deep, to 0.5 metres wide, and 0.2 metres deep. Because of the somewhat arbitrary delineation of the gradational contact with facies 4, facies 5 displays a few isolated gravel beds, which vary from imbricate lenses within shallow channel





Fig. 2.22. Fining-upward sequence, from rippled sand, to silt, to clay laminae (S7). Shovel blade approximately 15 cm long.



Fig. 2.23. Small, nested scoured channels filled with trough cross-beds, truncating adjacent gently inclined beds. Note how the channels become smaller upsection (L1B). Person is 1.85 m tall.



scours to lenses displaying inclined gravel beds.

Relatively small-scale soft-sediment deformation structures are abundant in this facies. A variety of structures occur where massive to slightly normally graded medium sand beds overlie laminated silt and clay. These include flames, recumbent folds, pillars and ball and pillow structures (e.g., Fig. 2.24).

### 2.5.2 Interpretations

The fining-upward sequences from horizontally and rare cross-bedded sand up into climbing ripple sequences are deposited from density underflows, or quasi-continuous turbidity currents (Gorrell and Shaw, 1991) which spilled out of the main channel. Coarse basal beds record only minor, shallow scour events and most beds are laterally extensive, deposited from unconfined sheetflows. Strong density underflows move across these zones, initially over upper flow regime plane beds, and less commonly dunes, across a surface with shallow localized scours. As these flows wane, climbing ripple sequences are deposited. Type A to sinusoidal ripple sequences represent the transition from predominantly traction to suspension sedimentation associated with waning flows (e.g., Jopling and Walker, 1968), and are overlain by silt and occasional clay laminae deposited from suspension. Experimental results indicate that these sequences can be deposited in a matter of hours (Allen, 1970; Ashley *et al.*, 1982).

Rapid deposition of sediment with variable grain sizes cause ideal conditions for porewater overpressure and for the formation of soft-sediment deformation structures in response to post- or syn-depositional pore-water expulsion. Deposition of sand on finer grained silt and very fine sand produces density inversions. These conditions help to initiate liquefaction and fluidization (e.g., Lowe, 1975, 1976b; Mills, 1983). As a result, a variety of flames, ball and pillows and convolute laminae were formed in these deposits.

a



b

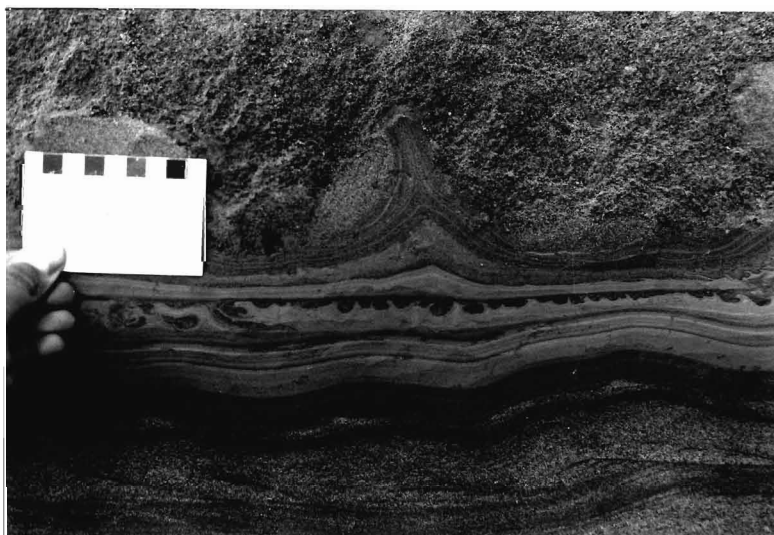


Fig. 2.24 a) and b) Soft-sediment deformation structures, including flames, balls and convolute laminae (S3.2). Knife handle is 10 cm long.

## 2.6 FACIES 6 MASSIVE SAND CHANNELS

### 2.6.1 Descriptions

This facies includes steep-walled channels filled with massive to vaguely bedded sand which apparently overlie and truncate nested shallow scours filled with rippled sand sequences, and horizontally laminated sand and silt of facies 5. This facies occurs in limited exposures at the base of S16 and in sections slightly downflow (tens of metres), at S16B which were revealed after initial field work was complete.

The original exposure exhibited four to five metres of massive to vaguely bedded fine to medium sand. Three or four nested, steep-walled scours were present, defined weakly by heavy mineral concentrations. These deposits seem to grade up-unit into increasingly defined horizontal beds (S16).

Subsequent exposures revealed more nested scours at several metres lower elevation and downflow. However, these were filled with rippled sand sequences, oriented parallel to the original scour surfaces (Fig. 2.25). Most sequences contain horizontally laminated fine sand at their base, and grade upwards into type A and type B climbing ripples (Fig. 2.25b). Multiple sequences occur within each nested scour. The shallow scours grade downflow into horizontally laminated very fine sand and silt.

Exposures another ten metres towards the south display more of the steep-walled channels, filled with massive to vaguely horizontally bedded sand. Channels are up to four or five metres across, several metres deep, and are filled with vaguely bedded fine to medium sand (Fig. 2.26a). Near the channel margins, laminae are parallel to the scour surface, but flatten upwards into increasingly horizontal beds near the centre of the channels. These channels truncate rippled and horizontally

a



b



Fig. 2.25. a) Scours filled with rippled sand sequences which seem to parallel to the original scour surfaces in which they are located (S16B); b) Ripple sequences; horizontal laminae, grading into type A ripples with slight variations in angle of climb (S16B).

laminated sand (Fig. 2.26b). The massive sand channels at S16 are truncated abruptly by cross-stratified gravel within shallow scours (Fig. 2.27).

## 2.6.2 Interpretations

Steep-walled, well defined channels filled with vaguely bedded to massive sand are produced by powerful (high discharge), sediment-laden meltwater flows that move over the fan as density underflow currents, or originate from sediment gravity flows initiated by slumping of the oversteepened channel walls upfan (Rust and Romanelli, 1975; Rust, 1977; Cheel, 1982; Thomas, 1984; Shaw, 1985; Smith and Ashley, 1985). Bedform development within the channels is inhibited by high sediment concentrations and rapid rates of deposition. The steep channel margins exceed the angle of repose which were maintained due to dispersive pressure, and were preserved when sandy sediment gravity flows stopped, and effectively plugged the channels (Postma *et al.*, 1983).

Diffuse bedding parallel to the channel margins is formed by frictional resistance along the boundary of the channels. Plastic flow mechanisms (cohesive debris flows and grain flows) of a more or less rigid plug are inferred to produce such shear zones along channel margins (Postma *et al.*, 1983). However, a study by Lowe (1976a) showed that pure grain flows generally cannot be thicker than approximately 5 centimetres, although buoyancy and turbulence of the matrix may produce thicker flows (Hampton, 1979). Therefore, the depositional mechanisms are termed non-cohesive debris flows after Postma *et al.* (1983). Diffuse horizontal banding towards the centre of the channels is produced by rapid deposition and vertical accretion of layers of sediment from the base of high concentration sediment flows (Carter, 1975). These massive sand-filled channels represent the proximal to mid portions of sediment gravity-flow deposits (Fig. 2.28; Postma *et al.*, 1983).



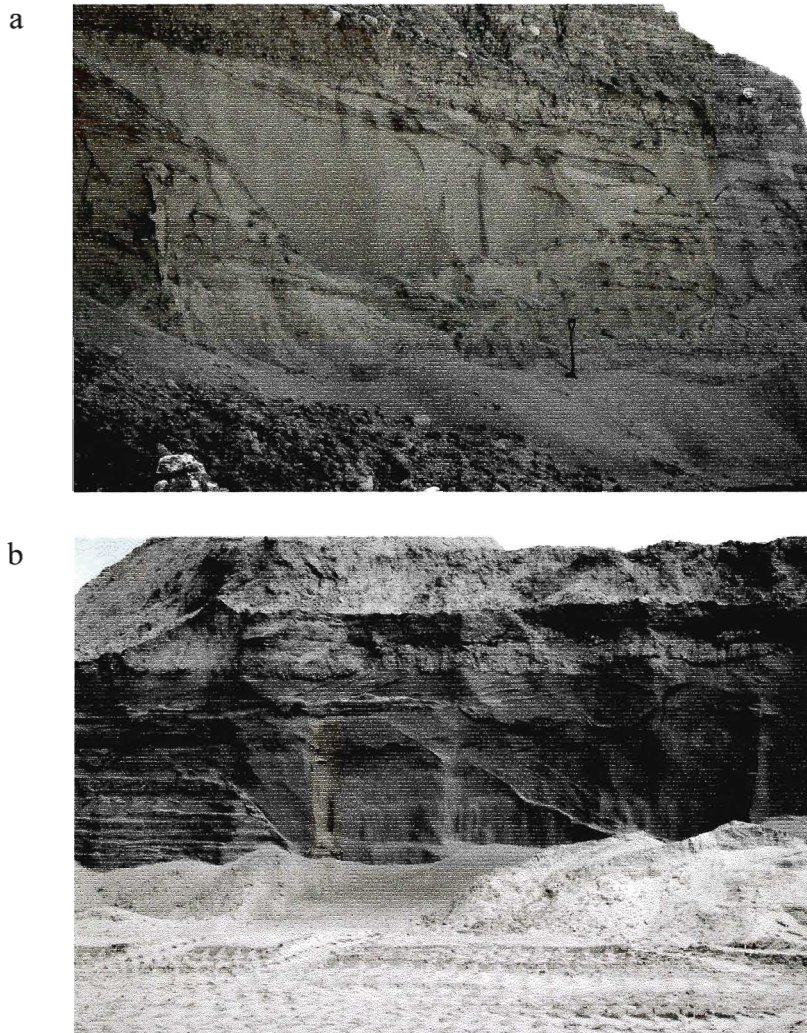


Fig. 2.26. a) large massive channel. Shovel shaft is 1 m long;  
b) nested channels cutting into rippled and laminated silt and sand.  
Exposure is 3 m high.



Fig. 2.27. Massive sand channels truncated by stratified gravels.  
Face is 2.5 m high.

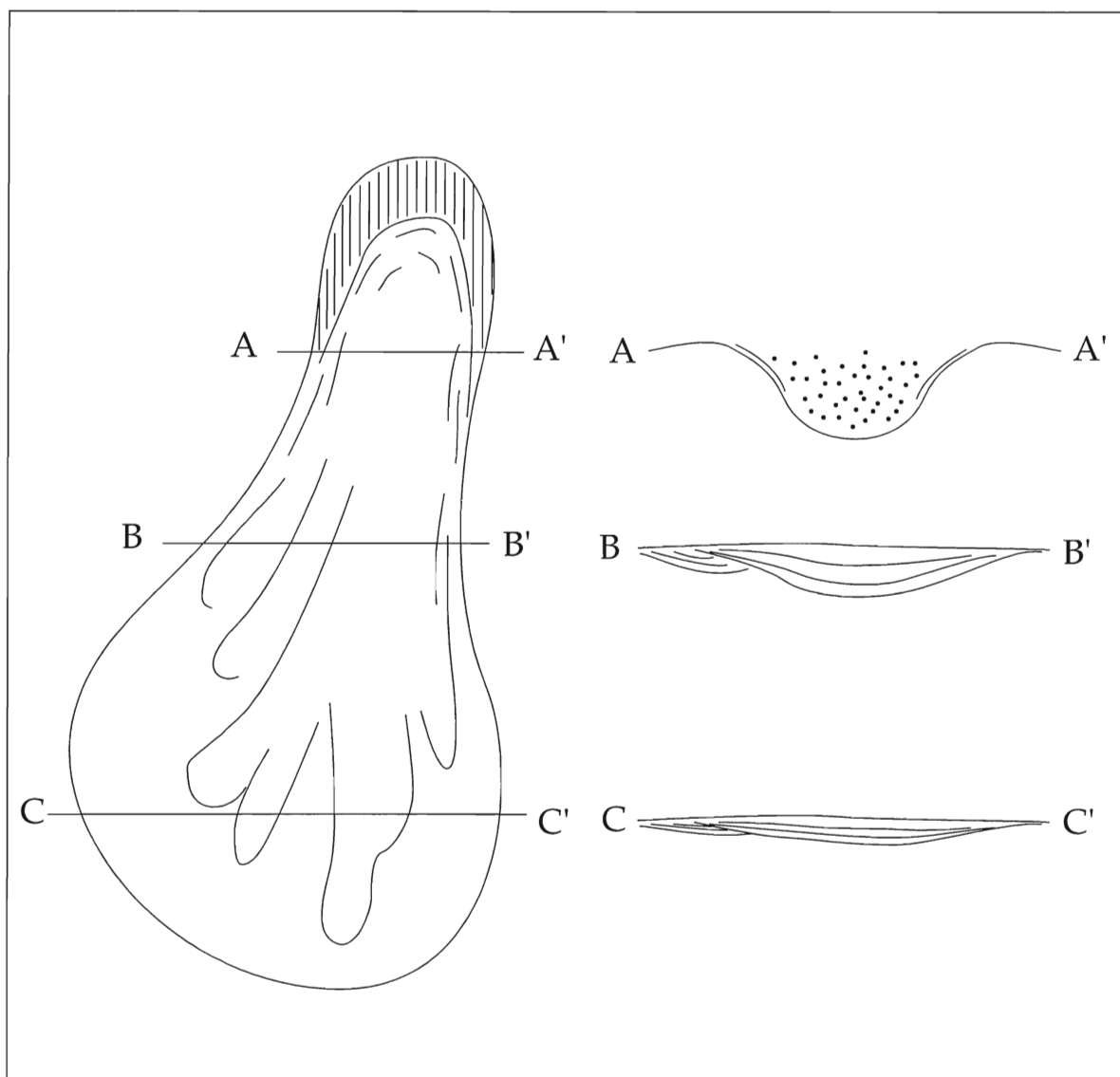


Fig. 2.28. Downflow transition from steep-walled channels filled with massive sediment, into progressively shallower channels filled with subhorizontally laminated sediment. After Postma *et al.* (1983).

Nested scours filled with climbing ripple sequences overlain and truncated by massive sand channels were deposited in distal portions of sediment-gravity flows (Postma *et al.*, 1983). Erosion is limited to shallow scours, produced by density underflows which have diminished in strength over time or across the fan. As a result, multiple climbing ripple sequence are deposited within each weakly defined scour, reflecting variable (or pulsating) flows, lateral migration of flows, or retrogressive flow slides upslope (Pickering, 1979; Postma *et al.*, 1983). These cycles may also represent fluctuations of discharge into the lake basin due to meteorological cycles, or other cycles controlling the generation of flows (cf. Gustavson *et al.*, 1975). Therefore the massive channels truncating shallow rippled channels indicates fan lobe progradation or lateral migration.

## **2.7 FACIES 7 GLACIOLACUSTRINE DEPOSITS**

### **2.7.1 Descriptions**

Facies 7 is characterized by horizontally laminated sand, silt and clay, and is normally found as laterally continuous units near the top of sections. Facies 7 also occurs as thick, (10 m) laterally discontinuous units which maintain their location and lateral relationships with adjacent coarser facies vertically within a section. Facies 7 includes rhythmically laminated silt and clay; these deposits were rarely documented, in part due to a lack of direct access which prevented close inspection of some exposures.

Most exposures of this facies contain horizontally laminated fine sand to silt with occasional clay laminae. Massive fine sand and silt occurs in thin beds up to 15 centimetres thick and amalgamated clay laminae are present up to a thickness of 5 millimetres (Fig. 2.29). Rippled sand beds within these units are thin, and normally exhibit rapid transitions from type A to type B climbing ripples, overlain by draping silt layers.



Rhythmically laminated silt and clay is also included in this facies, and attain a maximum unit thickness of 0.7 metres (L7). Rhythmites generally decrease in thickness upsection and display multiple laminae within each couplet; individual silt laminae are normally graded (Fig. 2.29). Units of apparently rhythmically laminated silt and clay, greater than one metre thick, were documented in Sections L9 and L11. However, direct access was limited, and sediments were observed only from the pit floor.

The thickness of laterally continuous exposures of facies 7 ranges from less than a metre to several metres. Both upper and lower contacts of facies 7 are generally sharp; in some sections this facies overlies glaciofluvial gravels of facies 9 (Fig. 2.30), while in others it is directly overlain by diamict of facies 10. Facies 7 also occurs as a laterally discontinuous unit (Fig. 2.31) where laminated sand and silt are interdigitated with, and sharply grade laterally into, cross-bedded sand and gravel of facies 3. However, they are persistent throughout almost the entire vertical section, unconformably overlain by coarser sand and gravel at the top of the exposure.

Various forms of soft-sediment deformation structures occur within this facies. The large-scale deformed sequences (L10-L12 and west of S18), incorporate facies 7 deposits within the deformed package. Facies 7 overlies the large thrust sequences and appears to be attenuated and somewhat convoluted (Fig. 2.32). Other evidence of deformation includes boudinage structures directly underlying facies 7 in these sections (further details of this deformed package will be discussed in section 2.11). Other types of smaller scale soft-sediment deformation structures also include convolute laminae, flames, and ball and pillow structures; all formed by a combination of loading and de-watering. Most of the deformed laminae are overlain by thin beds of massive fine to very fine sand. Faulting also occurs in this facies in various forms, including large scale normal faults which penetrate through

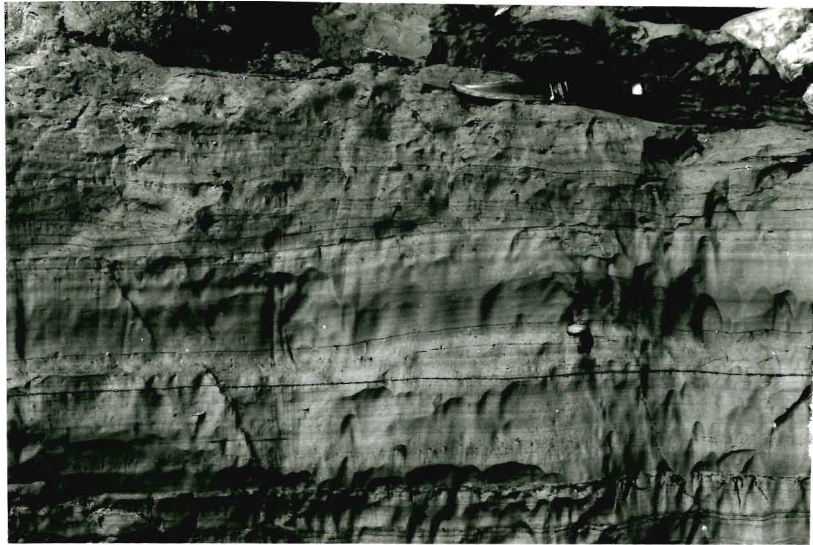


Fig. 2.29. Laminated silt and clay, containing dropstones. Knife handle is 10 cm long.

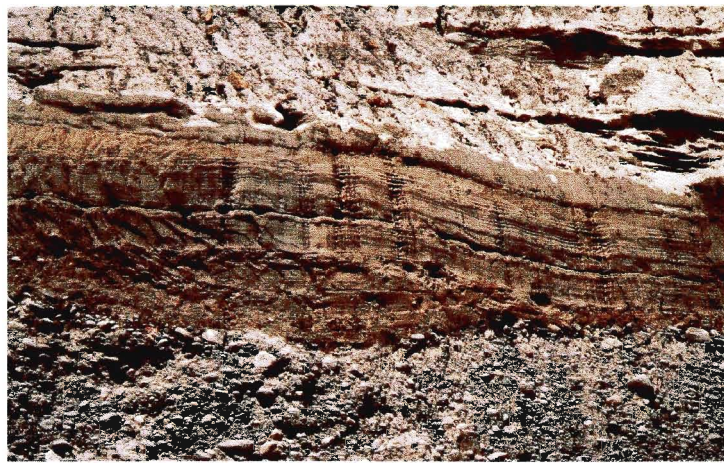


Fig. 2.30. Basal contact of facies 7, where it overlies glaciofluvial gravels of facies 9. Facies 7 is 1 m thick in this photograph.

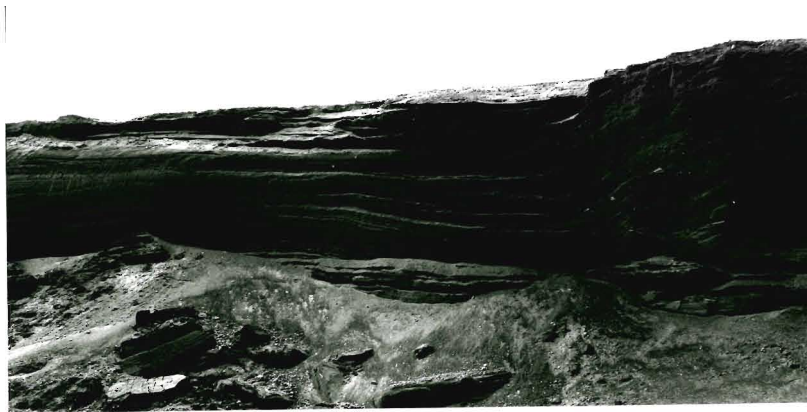


Fig. 2.31. Laterally discontinuous, yet persistent upsection, exposure of facies 7. Section is approximately 9 m high.

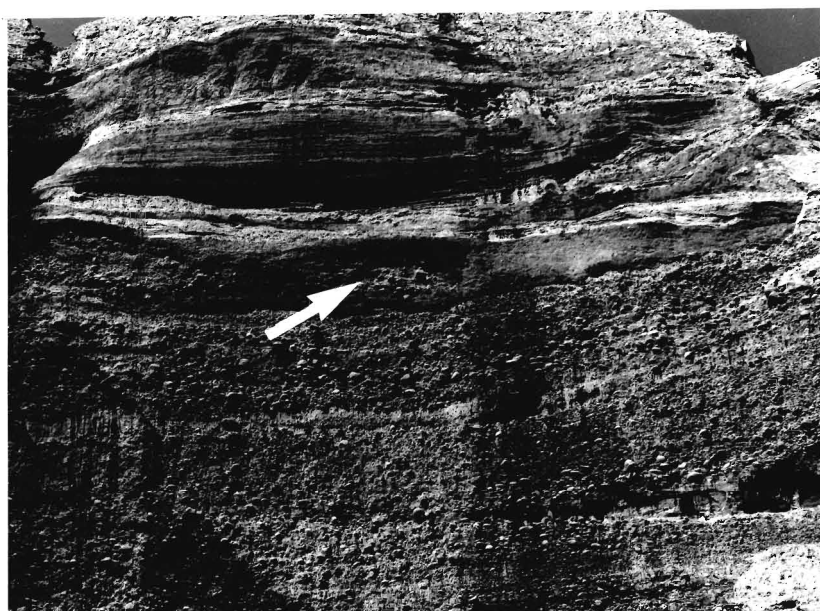


Fig. 2.32. Deformation of Facies 7 and 9 at L11 includes boudins of gravel (arrow), a convoluted unit of laminated silt and clay, and a massive, folded unit which increases in thickness to the north (right). Massive unit is approximately 1 m thick.

numerous facies (S10, S21), to smaller scale reverse and high angle normal faults near the top of sections.

### 2.7.2 Interpretations

Fine-grained glaciolacustrine sediments are deposited at distal margins of underflows, and out of suspension from overflows and interflows (Gustavson *et al.*, 1975; Smith and Ashley, 1985). These deposits may indicate both annual and non-annual cycles; probable annual cycles (varves) are marked by thicker clay laminae, deposited out of suspension in quiet-water conditions during winter months when meltwater discharge and sediment input is minimal (Smith and Ashley, 1985). Periodic (non-annual) sedimentation results from seasonal and diurnal discharge variations, and may be due to surges in flow strength at distal margins of underflows or quasi-continuous turbidity currents (Theakstone, 1976; Lambert and Hsü, 1979; Leeder, 1983; Smith and Ashley, 1985). Quasi-continuous turbidity currents can occur if the loss of turbulence by mixing is compensated by continuous supply of fluid (Middleton and Hampton, 1976; Lambert and Hsü, 1979). These inherently pulsating flows deposit numerous laminae within individual couplets (Lambert and Hsü, 1979). Thin beds of massive fine sand, beds of type A to sinusoidal climbing ripple cross-laminae sequences, overlain normally graded silt, are deposited from waning flows.

These sediments were deposited in distal zones, during decreases in discharge, possibly related to ice margin retreat. Laminae which tend to thin upwards may indicate source (ice margin?) retreat, or be related to increasing water depths.

## 2.8 FACIES 8 ICE-MARGINAL COMPLEX

### 2.8.1 Descriptions

This facies is similar to facies 7, but is differentiated on the basis of the greater variety of glaciofluvial and glaciolacustrine sediments, and the presence of weakly stratified diamicts. This facies is also defined by its relationship with the overlying massive diamicts, and the occurrence of paleocurrent indicators towards the northwest. This facies includes a wide range of grain sizes, from laminated sand, silt and clay, to rippled sand, thin beds of weakly stratified gravel, and massive to weakly laminated sandy silt diamicts with occasional clasts.

Individual layers of fine-grained laminated sediments are thicker than those in facies 7, up to 10 cm thick in some normally graded very fine sand and silt. Small clay and silt balls are common in these thicker strata. Facies 8 is marked by an increased number of massive, pebbly fine to medium sand beds (Fig. 2.33) and faintly bedded and rippled fine to medium sand. Normal grading was visible in some sequences and rhythmic bedding was rare (e.g., S19).

Interbedded diamicts are moderately compact to loose silt to very fine sand, and exhibit thin, discontinuous sand stringers. Beds ranged from 20 cm to 80 cm thick with little or no grading of the matrix. Up to a maximum of three diamict beds were documented from within a single exposure (e.g., S3.2, S7). In some exposures, laminated silt and sand in contact with the diamicts are folded and sheared into complex flame structures (Fig. 2.34). Clast content is variable (up to ten percent by volume), although local concentrations of clasts also occur in some beds. Pebble counts were taken from two beds (S3-D2; S5.2-B1); the lithologies of these samples are summarized below in Table 2.2 (p. 90). Stratification in some diamict beds is represented by massive and rippled sand lenses. Intraclasts of glaciolacustrine silt and clay occur near the base of diamicts. Upper contacts are generally sharp,

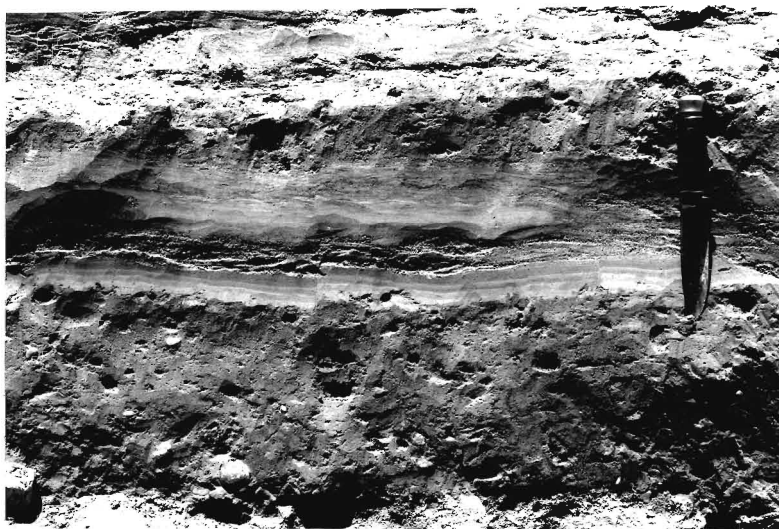


Fig. 2.33. Massive, pebbly sand diamict beds, interbedded with laminated sands (S3). Knife handle is 10 cm long.

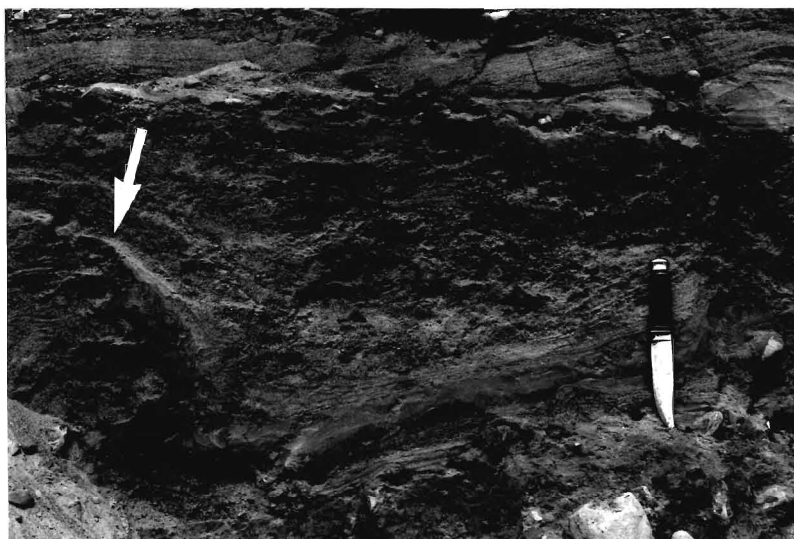


Fig. 2.34. Complex flame of silts (arrow) within flow diamicts at S3.2. Knife handle is 10 cm long.

commonly with clasts from within the diamict protruding into overlying sediments. Other beds exhibit gradational contacts with overlying massive diamicts. Some beds have blocks of diamict bounded by normal faults protruding into overlying units (Fig. 2.35).

Basal contacts of this facies are also quite variable. Weakly stratified diamicts tended to have both erosional and gradational basal contacts. Where sandy diamicts mark the base of this facies, the contact is mantled with a lag of pebbles and cobbles (Fig. 2.36).

In some sections, facies 8 exhibits trough-like depressions which are bounded by closely spaced, high-angle reverse faults (Fig. 2.37). In this particular example, sediment directly outside the central trough appears to be above the surrounding stratified sediment.

Deformation is prominent in this facies. Convolute sand and silt laminae are common. Ripple cross-laminae and horizontal laminae show evidence of post-depositional shearing towards the north (Fig. 2.38a) and deformation around dropstones (Fig. 2.38b). In sections where facies 8 is interbedded with glaciofluvial sand and gravel, extensive deformation occurs along the contacts.

### 2.8.2 Interpretations

The similarities between facies 7 and facies 8 suggests that they had a similar origin. The stratified sands and silts of facies 8 are attributed to deposition from suspended sediment plumes, from glaciogenic sediment gravity flows, and episodic downslope slumping. Glaciolacustrine sand, silt and clay is deposited from distal density underflows, and by deposition from suspension. Thicker, ripple cross-laminated and massive beds and thin, poorly sorted, weakly stratified gravel suggests higher energy flows, and probably a proximal ice margin. Massive to



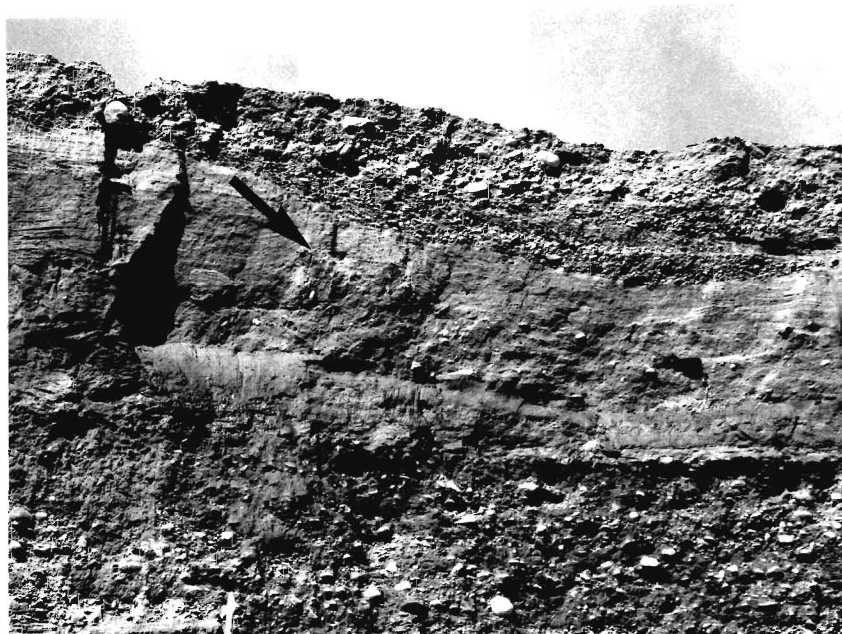


Fig. 2.35. Fault-bounded block of diamict protruding into overlying sediments (arrow) at S4. Scale bar has 10 cm increments.



Fig. 2.36. Facies 8; diamicts and basal stratified sandy gravels, truncating underlying sediments (S4). Note erosional surface mantled by pebble and cobble lag (arrow). Face is 7 m high.



Fig. 2.37. Trough-like isolated depression bounded by high-angle reverse faults (S4). Note "upthrown" sediment at margins of central depression. Scale bar has 10 cm increments.

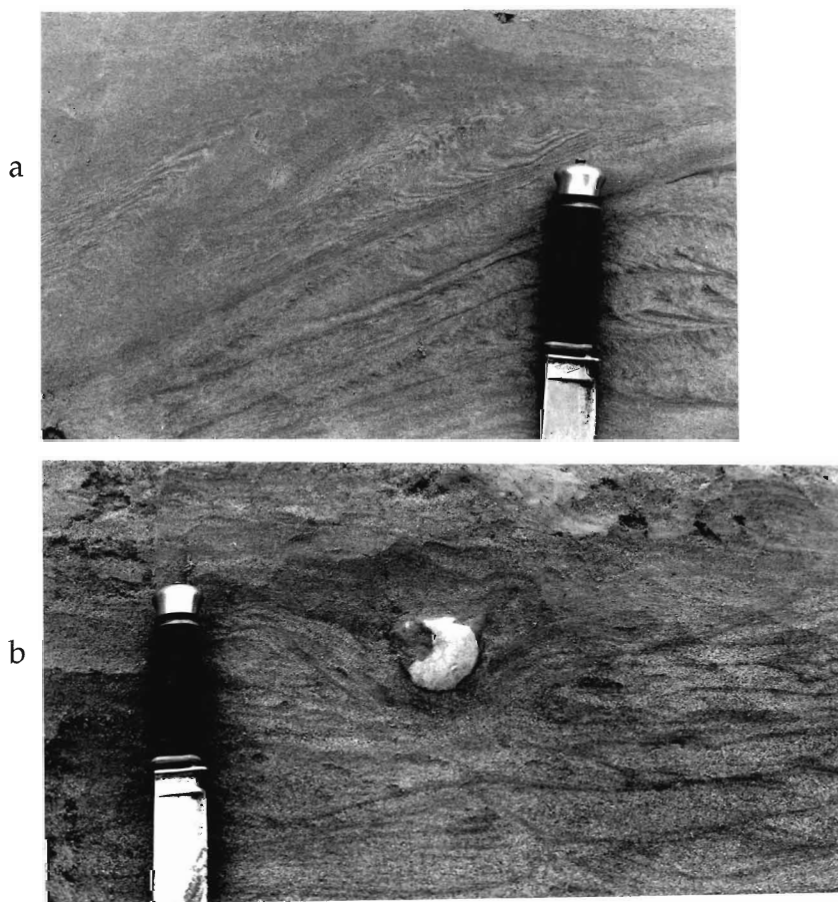


Fig. 2.38. Deformed sediments at S7: a) sheared ripples and laminae; b) deformation around dropstone. Knife handle is 10 cm long.

weakly stratified diamicts may have also originated from an ice source.

Normal grading in the thicker massive beds, from fine sand to silt, is more prevalent than in facies 7. This is because they were deposited at slightly more ice-proximal locations, adjacent to topographic highs. Because of this, slightly erosive events are indicated by the presence of silt and clay balls within overlying massive very fine sand.

The weakly stratified diamicts were either formed by glacially derived sediment gravity flows or by passive melt-out, and are interbedded with glaciofluvial sand and gravel. The lack of detailed textural and fabric analyses of the massive diamicts makes it difficult to determine a subglacial or proglacial origin. However, structures normally associated with melt-out tills, including clasts of unlithified sediments within the diamict, and sub till boulder scours (Haldorsen and Shaw, 1982; Shaw, 1982), were not documented. The presence of rafted clasts at the top of some beds, crude stratification, and internal flow folds (L11, L12) suggests a debris-flow origin, specifically as glacially derived sediment gravity flows (Evenson *et al.*, 1977; Hicock *et al.*, 1981; Broster and Hicock, 1985; Eyles, 1987; Lawson, 1988).

Deformed contacts between the diamict beds and subjacent and suprajacent stratified sediments suggest at least periodic grounding ice conditions (e.g., Talbot and von Brunn, 1987; Benn, 1989). Cyclic detachment of the glacier bed would allow subglacial flows to wash through between the substrate and the base of the glacier, depositing stratified sand and gravel and rippled sand with northerly flow indicators. The lithological counts of pebble samples from two diamict beds exhibit similar results as those taken from the overlying Halton Till (Table 2.2, p. 90). From this, a shared provenance can be inferred.

Isolated, narrow trough-like depressions bounded by high-angle reverse faults are similar to grounding structures documented by Thomas (1984) and

Thomas and Connell (1985). Although the structure is not filled with diamict (as in those documented by Thomas and Connell, 1985), this does not negate grounding ice, as diamict is found in section directly above the poorly sorted gravel in which the structure is formed. Grounding followed by lifting of the glacier bed may have not resulted in deposition of diamict, or, alternatively, diamict could have been eroded by subsequent releases of subglacial meltwater, and produce the erosional surfaces. Periodic lifting and re-grounding is also supported by the complex formation of the deformed sequences, which will be discussed in section 2.11.

Deformation in this particular example (Fig. 2.37) appears to be dominated by vertical displacement. This probably negates formation of extensional tension joints associated with glaciotectonic deformation, followed by slumping of sediment into the resultant cavity. Alternatively, this steep-sided depression could have been formed by melting of small buried ice blocks (McDonald and Shilts, 1975, their Fig. 2; Eyles, 1977). High-angle reverse faults form during sediment collapse into the void left by the melting ice. However, it seems unlikely that melting of an ice block could have produced sufficient fluid movement to upwardly mobilize sediment adjacent to the main depression. Therefore, there is support, however weak, for an ice margin that may have become detached and re-grounded on multiple occasions.

## **2.9 FACIES 9 STRATIFIED SAND AND GRAVEL**

### **2.9.1 Descriptions**

Facies 9 includes a variety of sediment types which are located stratigraphically above an extensive erosional contact in the upper portions of exposures. Facies 9 is differentiated on the basis of well stratified sand and gravel. Horizontal beds of gravel are defined by continuous large cobble and boulder concentrations. Pebbly trough and planar cross-beds are commonly interbedded with the coarser gravel. This facies is exposed in relatively continuous faces in the

western and eastern portion of the Standard Pit (Appendix IV.1,2 and S21-S24, respectively) and the northwestern portion of the Lee Pit (Appendix IV.5).

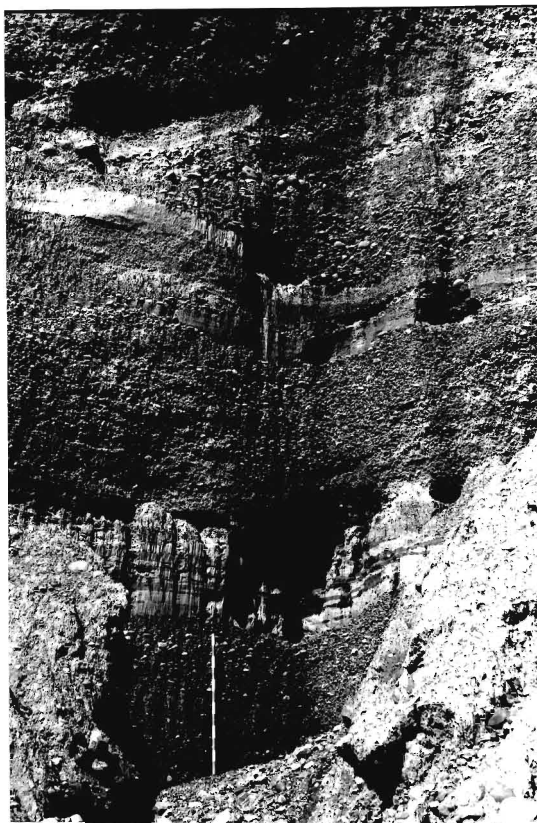
Overall, this facies is moderately to well sorted, and primarily clast-supported with both open and closed framework. Clasts range in size from pebbles to boulders, up to 0.8 m in diameter. The matrix is moderately sorted medium to very coarse sand.

Planar tabular cross-bedded gravel, in sets up to two metres thick, is composed mainly of pebble to cobble sized clasts. Cross-beds dip at low-to steep angles (Fig. 2.39) and are normally interbedded with discontinuous sand lenses which drape some of the cross-beds. Most exposures have multiple cross-bed sets which vary in orientation (Fig. 2.39b). Clasts are normally aligned along bedding planes, with a-axes parallel to the strike of the cross-beds. Normal grading is common within each bed, from open framework pebble to cobble gravel fining upward into granular sand (Fig. 2.40a). Some cross-bed sets are very well sorted, so that the entire set seems to be predominantly open framework pebble gravel, alternating with cross-strata of pebbly sand (Fig. 2.40b).

Large-scale sets of dipping gravel beds also occur, with individual set thicknesses up to five metres (Fig. 2.41). These gravels differ from those discussed above simply by scale, and their location above large scours. Horizontally bedded topset gravel overlies large-scale steeply-dipping gravel beds in some sections (Fig. 2.41b). These gravel foresets are common as a single unit interbedded with horizontally bedded and smaller-scale cross-bedded gravel.

Horizontally bedded cobble to boulder gravel is the most common style of bedding in this facies. Definition of the subhorizontal bedding planes is not as distinct as with the cross-bedded gravels, and is defined by cobble and boulder concentrations (Fig. 2.42). Stratification is further defined in some exposures by

a



b

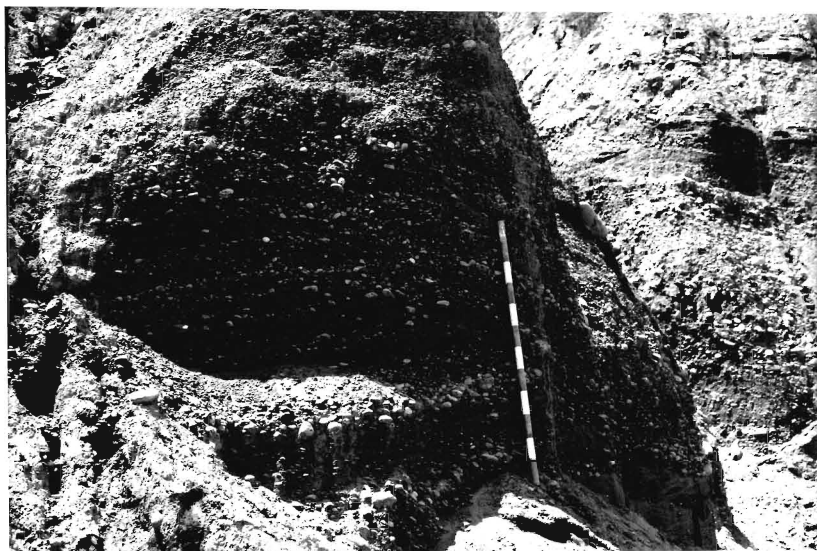


Fig. 2.39. Large-scale cross-bedded gravels, cosets up to 2 metres thick; a) tangential gravel cross-beds, with rare drapes of laminated sand (L12); b) planar tabular cross-beds, with some cross-strata showing normal grading (S21). Scale bar has 10 cm increments.

a



b

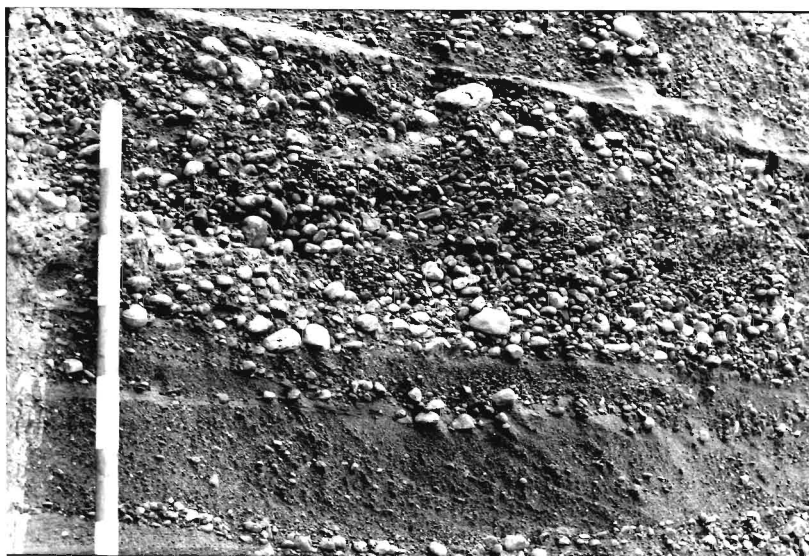


Fig. 2.40. Sorting in gravels: a) Normal grading within gravelly cross-beds (S21). Knife blade is 13 cm long. b) Bimodal cross-beds of open framework and sandy pebble gravel (S24). Scale bar has 10 cm increments.



a



b



Fig. 2.41. Large scale gravel cross-beds: a) Large foresets gravels, with silt lenses (arrow) at S23N-S. Person is 1.85 m high; b) Steeply dipping cross-beds truncated by horizontal topsets (arrow) at L11. Horizontally bedded gravel unit is 1.5 m thick.

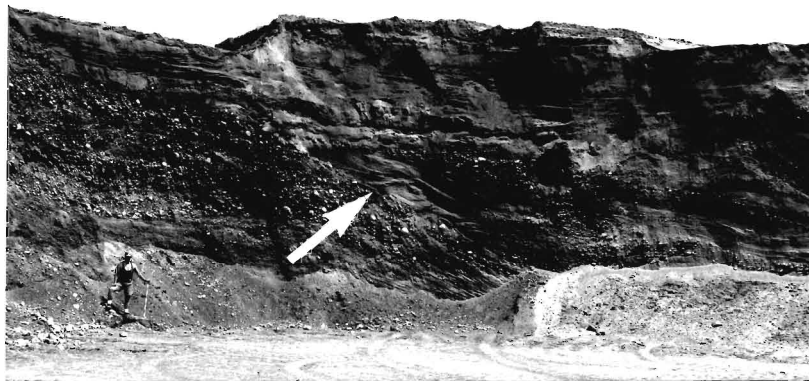


Fig. 2.42. Weakly horizontally bedded gravel defined by basal cobble and boulder concentrations (S23N-S). Scale bar has 10 cm increments.



Fig. 2.43. Pebbly medium to coarse sand planar cross-bedded sand (S24). Scale bar has 10 cm increments.

a



b



c



Fig. 2.44. Characteristics of well-defined channels of facies 9: a) Large, shallow erosional channels (arrow) at S22. Person is 1.85 m tall. b) Fining towards channel margin (S22). Scale bar has 10 cm increments. c) rip-up clast along channel scour (S21). Knife handle is 10 cm long.

### 2.9.2 Interpretations

Crudely horizontally bedded gravel are produced by aggradation and migration of longitudinal bars during flood stages of braided gravelly rivers, and are typical of subaerial proximal proglacial outwash deposits (Williams and Rust, 1969; Boothroyd, 1972; Gustavson, 1974; Eynon and Walker, 1974; Boothroyd and Ashley, 1975; Church and Gilbert, 1975; Gustavson *et al.*, 1975; Rust, 1975; Hein and Walker, 1977; Hein, 1984; Smith, 1985), and commonly documented in coarse-grained glaciodeltaic topsets (Clemmensen and Houmark-Nielsen, 1981). Movement of sediment occurred as "diffuse gravel sheets" (Hein and Walker, 1977) during flood stages. Rare normal grading in horizontal beds is produced by accretion during waning flood flows (Smith, 1974).

Clast orientations are dominantly a(t) b(i), indicative of deposition from traction currents (Johansson, 1963; Boothroyd and Ashley, 1975; Rust, 1972, 1975; Hein, 1984). However, fabrics are variable, as occasional a(p) a(i) fabrics also occur. The differences in a-axis orientation may reflect variations in clast size and concentrations (Johansson, 1963; Sedimentary Petrology Seminar, 1965; Rust, 1972, 1975). During high water flood levels, proglacial meltwater would not be confined to discrete channels, but would flood most of the proglacial zone, depositing stacked sequences of longitudinal bars (Fraser, 1993). Interbedded with these bars are discontinuous lenses of cross-bedded sand and pebbly sand deposited in channels between bars, and on top of bars during waning flows (Bluck, 1974; Gustavson, 1974; Gustavson *et al.*, 1975; Boothroyd and Ashley, 1975; Dawson and Bryant, 1987; Fraser, 1993). Deposition of fine sand and silt lenses occurs from overbank flows during high water levels into adjacent lows during the waning flow stages (Costello and Walker, 1972; Boothroyd and Ashley, 1975; Theakstone, 1976).

Pebbly trough and planar cross-beds are formed by bedform migration in the channels between bars during low flow, and on top of bars during flood levels (Costello and Walker, 1972; Gustavson *et al.*, 1975; Fraser, 1993) or as wedges at the margins of longitudinal bars during periods of relatively low flow following floods. Cross-beds with variable orientations are indicative of the complexity of the braided channel patterns.

Rhythmic textural changes within horizontal and cross-stratified gravels, defined by open framework pebble gravel and pebbly sand, have been attributed to a variety of processes. These include avalanche processes at flood stages, changing conditions during falling-stages (Rust, 1975; Steel and Thompson, 1983), rapid deposition downstream of a bar-front, or particle over-passing bars and planar gravel sheets (Carling and Glaister, 1987; Carling, 1990), and longitudinal sorting mechanisms (Iseya and Ikeda, 1987; Kuhnle and Southard, 1988; Whiting *et al.*, 1988).

Large scale gravel cross-beds (foresets) occur within distinct channels at L12 and S23. Channel incision and the evidence of large bedforms suggest sporadic, powerful flows eroded large scours in proximal location on the northwestern and northern margins of the deposit (S21, L12). The incision of the larger channel at L12 is probably related to successive flow events, as a single flood could probably not incise a channel this deep (11 m); (see calculations in Maizels, 1987). Some of the large foresets are truncated by horizontal beds; probably analogous to topsets prograding over underlying foresets. These gravels are believed to have been deposited between the ice margin to the north, and the fan as ice retreated slightly. Similar "high" bars with foresets are found in narrow bedrock channels by Baker (1984).

## 2.10 FACIES 10 DIAMICT

### 2.10.1 Descriptions

The deposits of both the Lee and Standard pits are overlain by a sheet of diamict of varying thickness, characterized by a sandy silt to clay silt matrix and a low clast content. A detailed investigation of these glacial sediments was not performed, and as a result only limited interpretations are made. The diamicts truncate underlying sediment near the top of most of the northern sections in both the Standard and Lee Pits. Diamict is absent in the southern exposures of both pits, where it has been stripped off to gain access to the aggregate materials below.

The diamict in the study pits is olive-grey to grey in colour, but is commonly lighter in the basal portions near the contact with underlying stratified sediments due to higher proportions of fine to very fine sand. The diamict is generally dense and compact, ranging from blocky to fissile, with rare lenses of silt-rich diamict defining weak internal stratification (Fig. 2.45). The concentration of clasts ranges from five to ten percent (Fig. 2.45). In some exposures, portions of the diamict just above the contact with underlying stratified sediments had higher concentrations of clasts, and exhibited weak internal stratification.

Nine clast fabric measurements and four clast lithology samples were taken from the massive diamict, in an attempt to deduce general ice-flow direction, and to allow comparison with diamicts described by other workers from the study area. The clast fabrics generally exhibit a-axes oriented in a south-southeast to north-northwest direction, dipping gently towards the south (Fig. 2.46). Although all of the clast fabric measurements were taken from the massive diamict, five of the fabrics exhibited slightly stronger preferential orientations (Fig. 2.46a).



Fig. 2.45. Diamict exhibiting weak internal stratification and low clast content (S3.2). Knife handle is 10 cm long.



## TILL CLAST FABRICS

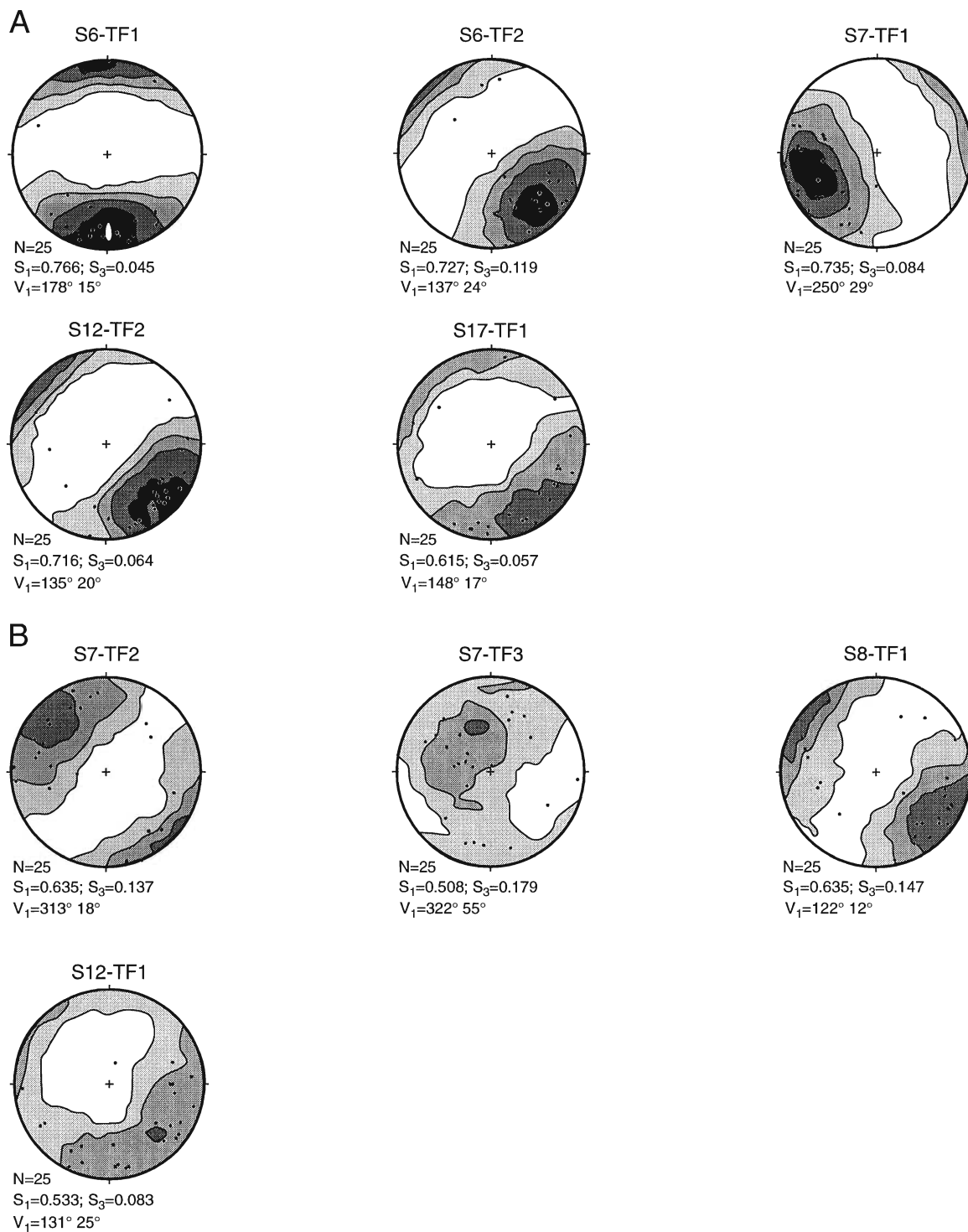


Figure 2.46. Contoured lower hemispheric projections of clast orientations, Halton Till: a) lodgement till; b) sediment gravity flows. Statistical calculations using eigenvector method of Mark (1973, 1974). Contour interval  $2\sigma$ .

The thickness of the diamict varied greatly, from 2.5 metres (S17) to over ten metres (S21) in sections where the existence buried pedogenic horizons suggest that the original thicknesses of the diamict had been preserved. This variability of thickness may have been due in part to the irregular topography of the underlying fan surface, causing diverging ice flow paths. Some of the thickest accumulations of diamict occur in sections where large-scale normal faults penetrate through the diamict as well as underlying stratified sediments (Appendix IV.2).

The lower contact of the diamict ranges from sharp and planar where it overlies stratified sand and silt (Fig. 2.47), to gradational where there is an upsection transition from interbedded stratified diamicts and glaciolacustrine sediments of facies 8, into the slightly sandier diamict at the base of facies 10, and finally overlain by the very dense and compact silt to clayey silt diamict of facies 10. Basal contacts of the diamicts displayed deformation structures at a few sections, including large scale roll-up and shear structures incorporating underlying sediment (discussed in following section 2.11), and small scale injection structures (Fig. 2.48). Both types of structures show similar orientations; the small injections and roll-up structure are oriented towards the north, and fault axes in the larger deformation structures strike approximately  $110^{\circ}$  and dip towards the south. Deformed rippled units underlying the diamict are also sheared towards the north (Fig. 2.38a).

### 2.10.2 Interpretations

The texture of the massive diamict is similar to that described by other workers from the Halton Till Plain south of the Oak Ridge Moraine and regions around Lake Ontario (Karrow, 1967, 1991; Gwyn and Dilabio, 1973; White, 1975; Cowan *et al.*, 1978; Feenstra, 1981; Duckworth, 1982). The stratigraphic position of the diamict on the crest of the Oak Ridges Moraine suggests that the massive diamict at the top of many sections in the study pits is the Halton Till. Textures are notably

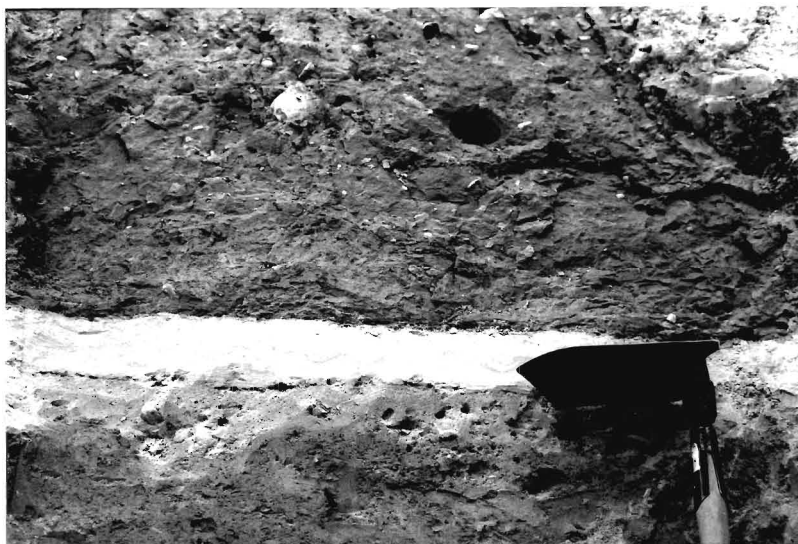


Fig. 2.47. Sharp, planar contact between diamict and thin, underlying rippled sand bed, with possible sediment gravity flow below (S21). Shovel blade is 15 cm long.



Fig. 2.48. Small scale injection structures where sand is sheared up into overlying diamict of facies 10 (S12). Knife handle is 10 cm long.

variable because of the variety of depositional processes associated with deposition of the Halton Till (Sharpe, 1988b). The fine-grained nature of the Halton Till may be a result of the ice advancing out of the lake basin to the south (Ontario ice lobe), overriding and incorporating fine-grained glaciolacustrine sediments (e.g., Feenstra, 1981).

The diamict fabrics were analyzed, recognizing that not only that a variety of subglacial and proglacial processes may have deposited the diamicts and imparted primary fabrics, but numerous processes may have also caused post-depositional removal or enhancement of primary fabric orientation patterns (Boulton, 1971; Dowdeswell and Sharp, 1986). As a result, interpretations of ice-flow directions and depositional mechanisms based on these fabrics are made with caution. However, the literature generally suggests that till clast fabrics measured in lodgement facies are generally parallel to ice-flow direction, and may range from horizontal to plunging as much as 20° in the up-ice direction (Lindsay *et al.*, 1970; Boulton, 1971; Mark, 1973, 1974; Mills, 1977; Dowdeswell *et al.*, 1985).

Most of the fabrics indicate that the Ontario ice lobe that deposited the Halton Till flowed generally towards the north and northwest (Fig. 2.46), as described by many workers; (e.g., Karrow, 1967, 1991; Gwyn and Dilabio, 1973; White, 1975; Cowan *et al.*, 1978; Feenstra, 1981; Duckworth, 1975, 1979, 1982; Sharpe, 1988b). All samples show statistically non-random orientations (for 25 clasts,  $S_1 > 0.46$ ,  $S_3 < 0.21$  at the 95% level of confidence; Woodcock and Naylor, 1983). The fabrics shown in Fig. 2.46a have mean  $S_1$  eigenvalues, standard deviations (grand mean  $S_1=0.712$ ; grand s.d.= $\pm 0.057$ ) and  $S_1$  vs.  $S_3$  eigenvalue plots (Fig. 2.49) similar to those documented by others for lodgement tills (Sharp, 1982; Dowdeswell *et al.*, 1985; Dowdeswell and Sharp, 1986). In addition, the fissility and dense exposures of diamict in the study site may suggest that the Halton Till was deposited in some sections by lodgement processes. However, it is certain that the lack of detailed

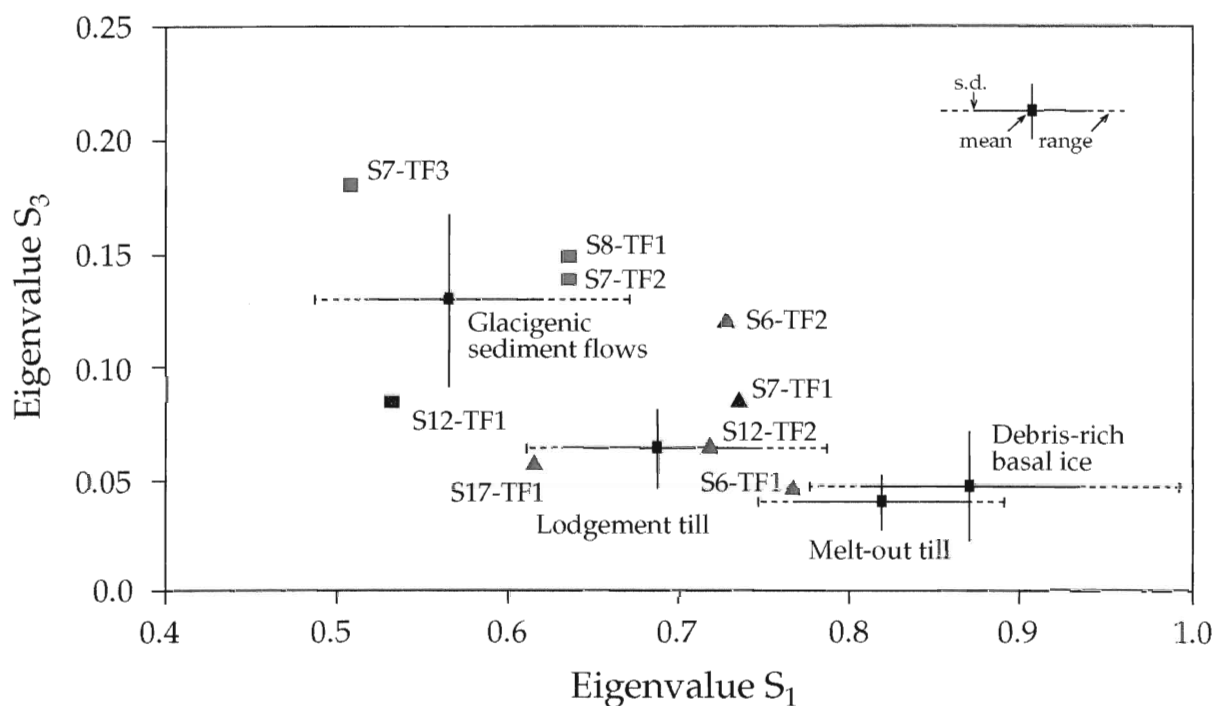


Figure 2.49. Plot of  $S_1$  against  $S_3$  eigenvalues for clast fabrics measured in this study, compared to those measured in four environments of modern glacial transport and deposition (Lawson, 1979; Sharp, 1982). The variability of fabric strength in modern environments is shown as standard deviation and range about the mean eigenvalue. After Dowdeswell and Sharp (1986).

analysis of the diamicts precludes precise interpretation of the depositional processes.

The texture and the clast fabric orientations of the less compact, weakly laminated diamict with higher sand content suggest deposition by glacial sediment gravity flows (flow tills). Although a-axis alignments are similar to those that are tentatively suggested to be deposited by lodgement processes (Figs. 2.46b, 2.49), the weaker cluster in these samples (grand mean  $S_1=0.578$ ) is indicative of the increasingly random orientation of clasts normally produced by deposition from glacial sediment gravity flows (Boulton, 1971; Evenson *et al.*, 1977; Lawson, 1979, 1988; Hicock *et al.*, 1981; De Jong and Rappol, 1983; Dowdeswell *et al.*, 1985; Gravenor, 1985, 1986).

Based on the limited evidence documented in this study, it is suggested that more than one diamict facies may be recognized from the fabrics and textures. Without a detailed study, it is impossible to determine the exact range of subglacial and/or proglacial deposited processes, and the spatial distribution of the various diamict facies of the Halton Till at the study site. The analysis of the clast lithologies is summarized below (Table 2.2); samples S7-T3 to S17-T1 are from the Halton Till (facies 10), from both the weakly interpreted lodgement and sediment gravity flow facies. Samples S3-D2 and S5.2-B1 are from sediment gravity flows of facies 8.

Table 2.2: Summary of Diamict Pebble Lithologies

Sample	Facies	Depositional Mode (?)	Sample size	% limest.	% dolost.	% sandst.	% siltst.	% shale	% igneous/meta
S7-T3	10	s. grav. flow	130	85.38	1.54	0.77	3.08	2.31	6.92
S8-T1	10	s. grav. flow	110	91.82	2.73	1.82	-	-	3.64
S12-T1	10	s. grav. flow	172	83.14	1.74	2.91	2.91	2.33	6.98
S17-T1	10	lodgement	90	77.78	1.11	2.22	-	2.22	16.67
S3-D2	8	s. grav. flow	220	72.73	3.18	1.82	2.73	0.91	17.27
S5.2-B1	8	s. grav. flow	157	75.80	1.27	2.55	4.46	4.46	11.46

Although there appear to be two weakly defined populations, without a detailed analysis the results are inconclusive. However, the results of pebble counts are comparable to the Halton Till described by White (1975) and Karrow (1967; his Upper Leaside Till).

## **2.11 LARGE-SCALE DEFORMATION STRUCTURES**

Several sections in the study site (L10, S5 and S11) were characterized by thick (up to eight metres) sequences of deformed sediment. Each of these sites will be described and interpreted separately, followed by a brief discussion of possible implications of the presence of these structures.

### **2.11.1 Sections L10a and L10b**

#### **2.11.1.1 Description**

Deformation in these sections is dominated by large, metre-scale imbricate sediment blocks, defined by reverse and thrust faults, with subsidiary folds and faults affecting interbedded gravel, sand, silt and clay. The sequences are exposed near the top of the deposit, in sections where the uppermost stratigraphy has been removed by excavation. However, the deformed unit is overlain by deposits associated with the Halton ice in adjacent sections (sections L11, L12).

Deformed units in these sections are bounded by sharp basal contacts, which occur within beds of glaciolacustrine silt and clay. Horizontally bedded, sandy pebble to cobble gravel underlying this contact are largely undisturbed, although gravel incorporated into the deformed unit form distinct marker beds within the sediment slices (Fig. 2.50).

The imbricate, listric sediment blocks dominate a deformed unit seven to eight metres thick in section L10b (Fig. 2.50), with individual blocks up to two metres thick. Thrust faults are generally concave-up, but are locally convex-up near



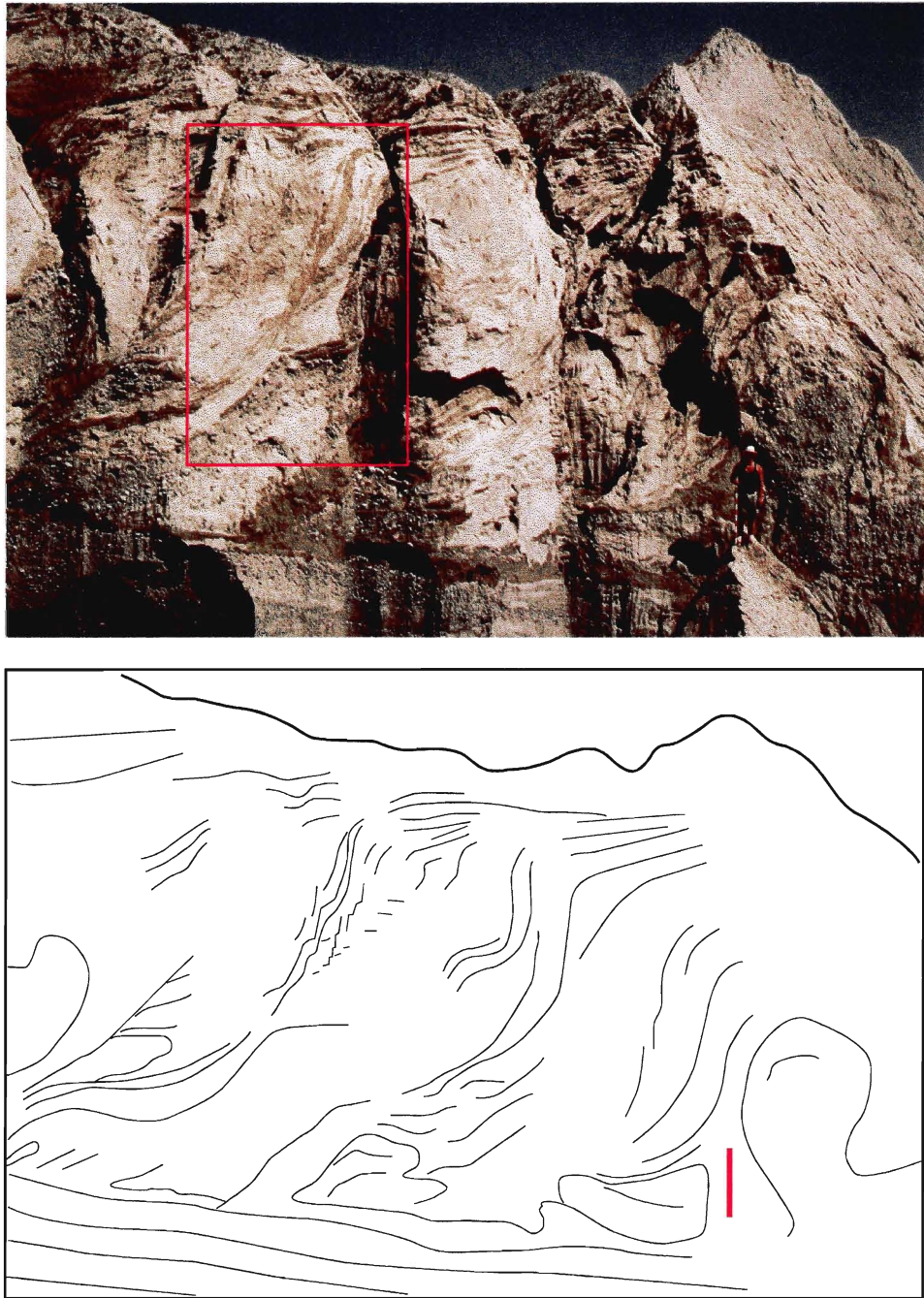


Fig. 2.50. Imbricate sediment slices at L10b. Ice flow was from left to right; thrust and reverse faults strike  $110^{\circ}$ . Scale stick is 1.2 m long. Red Box in photograph indicates location of Fig. 2.51.

the base of the faults, and have subhorizontal lower and upper contacts. This produces the characteristic sigmoidal form of the thrust slices. The faults strike  $110^\circ$ , and dip towards the south, at angles up to  $80^\circ$  at the steepest portions of the thrust faults, near the top of the deformed sequences. Rare high-angle normal faults occur in these steeply dipping zones (Fig. 2.51). Bulbous noses of complexly folded gravel occur at the base of some sediment blocks where high angle normal faults are present (Fig. 2.52). The deformed gravel bedding seems to parallel the fold noses, which are overlain by thrust and chaotically folded units of sand, silt and clay.

Section L10a is located to the south of L10b, and exhibits smaller thrust units, up to 0.8 m thick and one metre in length (Fig. 2.53). Deformation in this zone includes lower angle ( $30^\circ$  dip) thrust faults, indicated by foliations within the glaciolacustrine silt and clay. An intraclast of oxidized glaciolacustrine sediment is dips towards the north. Small isoclinal folds opening towards the south and southwest are defined by some of the thicker silt/clay laminae.

The basal contact of the deformed unit dips to the south and occurs at progressively higher elevations in exposures towards the northeast (Fig. 2.54). Deformation in the sections to the north (L11-L12) is different from the deformed sequences at L10a,b. Towards the north, there are no signs of thrusting, and deformation is largely limited to sediment above the bedded gravel. At L11, apparently massive, fine-grained sediments contain numerous boudins of the underlying bedded gravel (Fig. 2.32). These massive deposits are overlain by a gently undulating unit of laminated silt and clay, and a thin deformed unit which pinches out towards the south (Fig. 2.32). A similar deformed sequence is exposed at L12, where a massive bed displays a sharp basal contact with underlying bedded gravel. Fold anticlines along the upper contact of the massive bed are overturned towards the north and northwest (Fig. 2.55) and overlain by undulating glaciolacustrine sediments which parallel the folds.



Fig. 2.51. High angle normal faults in upper portions of sediment slices. Red scale bar is 1 m long.



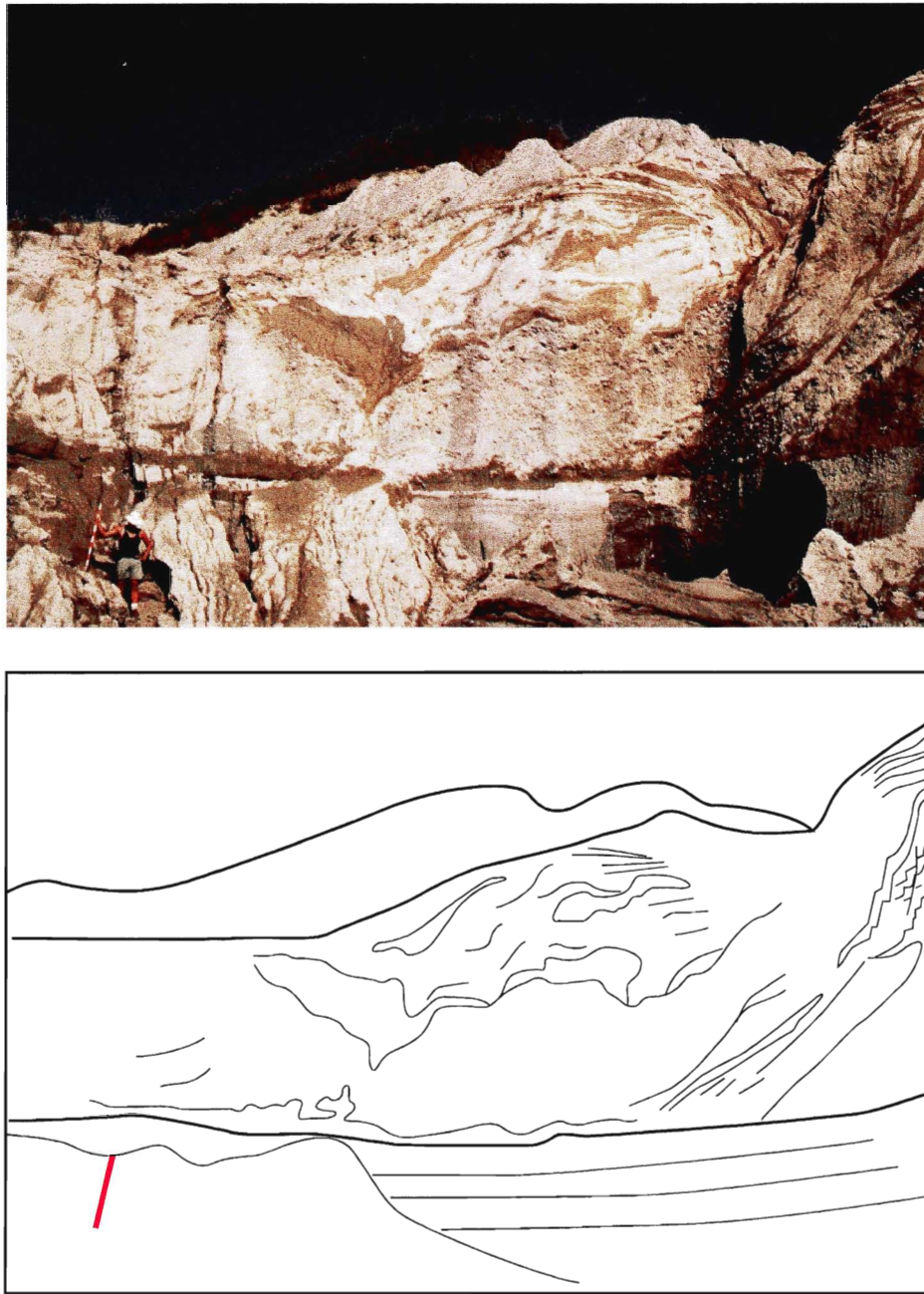


Fig. 2.52. Bulbous noses of gravel at base of sediment slices where normal faults occur. Scale bar 1.2 m long.



Fig. 2.53. Deformed unit, L10a. Red scale bar is 1 m long.





Fig. 2.54. Deformed unit is attenuated towards the north (L11). Figure is 1.85 m high. Arrows show base of deformation, which increases in elevation towards the north. Direction of ice thrust was from left to right.



Fig. 2.55. Massive unit which appears to contain clasts from underlying gravel bed. The lower contact with the gravel is sharp. The upper contact is marked by folds which are overturned towards the northwest, and is overlain by undulating glaciolacustrine sediment. The massive unit is 1-2 metres thick.

### 2.11.1.2 Interpretation

These structures are interpreted as glaciotectonic deformation structures, based on the arguments presented below. For the purposes of this study, glaciotectonic deformation is subdivided into two types. Dynamic glaciotectonic deformation includes subglacial deformation, characterized by simple shear and extensional deformation (i.e., attenuated folds, boudinage), and proglacial deformation, characterized by pure shear and compressional deformation (i.e., folds, thrusts and nappes; van der Wateren, 1987; Hart *et al.*, 1990; Hart and Boulton, 1991; Hart and Roberts, 1994). Secondly, static glaciotectonic deformation is produced by loss of ice support associated with melting ice blocks and walls (Moran, 1971; Banham, 1975).

Most of the factors that affect dynamic glaciotectonism are directly related to local topography, the characteristics of underlying sediments, subglacial pore-water content and ice dynamics (Aber *et al.*, 1989). However, only topographic variations produce lateral pressure gradients which operate ubiquitously beneath a glacier, and can therefore be considered one of the fundamental causes of glaciotectonic deformation (van der Wateren, 1985; Aber *et al.*, 1989). Advancing ice also causes tremendous lateral pressure gradients, due to push and drag forces exerted by the ice, and differential loading (as ice thickness increase up-ice from the margin).

One of the primary conditions for deformation is excessive pore-water pressures within the substrate (Aber *et al.*, 1989). As ice advances, it can cause increased pore-water pressures in subglacial and immediately proglacial sediments, within stratigraphically confined units or beneath permafrost layers (Banham, 1975; Berthelsen, 1979; Hart and Boulton, 1991). Increased pore-water pressures cause a reduction in the shear strength of sediment (Menzies, 1979; Boulton, 1987). As a result, décollement surfaces commonly occur within glaciolacustrine/glaciomarine silt and clay, facilitated by over-pressured pore-waters within underlying gravel



(Hansen *et al.*, 1961; Banham, 1975; Hicock and Dreimanis, 1985; Aber *et al.*, 1989).

At the study site, ice advancing across the proglacial lake basin to the south may have moved at a relatively rapid rate, a condition which is favourable for the formation of dynamic glaciotectionic deformation (Banham, 1975). When the ice encountered the topographic highs of the Bloomington fan complex, increased compressional ice flow would have occurred, which may have contributed to the lateral and vertical stresses necessary to invoke deformation.

For reasons noted above, lateral shear stresses caused movement to take place within failed clays. The thrusting and lifting of each block over its toe caused increased loading, and added to the vertical and lateral pressure gradients. This helped to initiate subsequent, more distal thrust faults. The accumulated weight of uplifted portions of thrust blocks may then have caused collapse once the lateral ice support was lost (Aber *et al.*, 1989). Normal faults occurred in the upper portions of the listric thrust faulted sequences, and initiated slumps at the toes of these thrust blocks. Slumps moved short distances back towards the ice margin towards the south, allowed gravel to collect as bulbous masses at the foot of some of the thrust blocks, and caused further deformation of overlying sand and silt.

Thrusting eventually ceased when the weight of the thrust blocks and internal resistance exceeded glaciotectionic stresses (Aber *et al.*, 1989). Continued ice advance may have caused the sediments to be overridden, and subglacial deformation to proceed by means of viscous folding and/or pervasive shear (Berthelsen, 1979). This produced the attenuated glaciolacustrine sediments, boudinage structures and overturned anticlines at the top of the deformed unit.

The thrust faults and folds within this sequence indicate ice flow from the south, associated with the Halton re-advance. The ice movement out of the Lake Ontario Basin to the south may have been rapid, as it advanced across the proglacial

lake, and over fine-grained glaciolacustrine sediment.

## 2.11.2 Section S5

### 2.11.2.1 Description

The deformed sequence in section S5 is similar to the one described above, as it displays numerous thrust and reverse faults that dip towards the south (Fig. 2.56). The deformed package has a sharp lower contact with underlying, undeformed sediment (Figs. 2.56, 2.57). Deformed beds with convex-up orientations commonly occur between reverse faults. However, deformation is not as systematic as at L10, and some of the deformed slices display synclines with fold axes dipping towards the south (Fig. 2.57). One particular example exhibits both normal faults, along the lower right boundary and within the interior of the deformed unit, and reverse faults along its uppermost boundary.

### 2.11.2.2 Interpretation

The deformation occurred in a similar manner to that at L10. As the ice advanced over this position, lateral shear stresses induced failure along a basal plane of décollement within fine-grained rippled sediments. Convex-up deformed beds between reverse faults, were formed as drag folds. Normal faults were formed when deformed blocks were thrust above surrounding sediments, and slumping occurred back towards the ice margin. Subsequent deformation events, or continuous deformation may have re-oriented down-ice limbs of the thrust blocks, producing complexly faulted and folded deformed units which are concave up, and dipping in an up-ice direction (Fig. 2.57).

The curved, convex-up attitudes of beds in this deformed package might suggest post- and/or syn-depositional slumping. However, it is believed that the laterally continuous, basal erosional surface that occurs in this deformed unit



Fig. 2.56. Deformed sequence at S5. Note the sharp basal plane of décollement, reverse and thrust faults which dip to the left (towards the south), and the convex-up form of some beds between faults. The photograph shows approximately 3 m of vertical exposure



Fig. 2.57. Complex deformation at S5 exhibiting both normal and reverse (thrust) faults. Note the sharp basal plane of décollement, and the concave-up fold with its axial plane dipping to the south. The photograph shows approximately 6 m of vertical section.

precludes slump deformation, as it indicates detachment and lateral movement along the contact, rather than tangential, concave-up contacts associated with slump-generated faulting. The style of faulting is also important to note, as the deformed unit at S5 is dominated by reverse and thrust faulting (Fig. 2.56). Although downflow portions of slumps are characterized by compressional faults (Collinson and Thompson, 1989), the faulting sequence at S5 cannot easily be explained by multiple slump events.

### 2.11.3 Section S11

#### 2.11.3.1 Description

Faces exposed previous to this study exhibited deformed glaciolacustrine sediments at section S11. The deformed unit appears as a large diapir, which is folded and overturned towards the north (Fig. 2.58). Several of these structures were observed along the length of this face (P.J. Barnett, pers. comm., 1994). This deformed unit is directly overlain by Halton Till.

#### 2.11.3.2 Interpretation

This structure was initially deformed by glacier loading, which caused the upward injection of a sand diapir. Continued movement of the ice towards the north overturned the diapir in this direction.

#### 2.11.4 Summary

The orientation of large-scale thrust sequences, and faults below the basal contact of the diamict can be compared to inferred ice flow directions from diamict clast fabrics. The large-scale deformed sequences described in this chapter are composed of stacked sediment slices, defined by thrust and reverse faults which strike  $110^\circ$  and dip towards the south. Normal and reverse faults measured from S2



Fig. 2.58. Overturned sand beds re-oriented towards the north. Ice flow was from right to left. Shovel for scale. Photo courtesy P.J. Barnett, Ontario Geological Survey.

located above the deformed sequence at S5 strike towards the north, and dip towards both the east and west (Fig. 2.21c). Clast fabrics measured from the diamicts indicate ice flow directions generally towards the northwest (Fig. 2.46). Therefore, since the principal stress direction (orientation of the inferred ice flow direction) lies between fault sets, ice movement may have been responsible for the formation of both fault sequences (Hatcher, 1995).

The glaciotectonic structures are believed to have a complex origin, possibly related to a continuous deformation sequence, or related to multiple deformation events. Previous work has suggested that lobes moving out of the lake basin to the south would have formed floating shelves (e.g. Eyles and Eyles, 1983). However, recent work has suggested that floating ice shelves cannot exist in temperate zones (J. Menzies, pers. comm., 1994). Therefore, it is thought that the ice margin would have been grounded, with perhaps a limited floating portion extending for a few tens to hundred metres. As a result, grounded ice conditions would have occurred at the topographically highest points on the Bloomington fan complex.

A relatively small interlobate lake basin, as documented this study, would be especially susceptible to water level changes resulting from seasonal and/or annual meltwater influx variations from surrounding ice margins. These minor water level fluctuations could have caused the ice margin to periodically detach from its base, and then subsequently re-ground, in cycles similar to documented from tidewater glaciers (e.g., Powell, 1981). This up and down movement of the ice could produce multiple phases of glaciotectonic deformation. Each interval of ice marginal detachment would also reduce basal friction, and allow the margin to surge forward incrementally, adding to the cyclicity of glaciotectonic deformation events.



### 3.0 FACIES DISTRIBUTIONS AND ASSOCIATIONS

The purpose of this section is to describe and interpret the spatial distribution, geometries and associations of facies. The first six facies described in the previous chapter compose the Bloomington fan (facies 1 to 6). This is based on initial interpretations of Barnett (1992a), and a comparison of the facies described in this study (table 2.1, p. 23) with subaqueous outwash fan facies described by other workers (table 1.1, p. 14). However, this study describes a deposit which is relatively complex. Facies 7 to 10 are not part of the subaqueous fan, but are related to changes in the depositional environment which occurred in response to fluctuations of the Ontario and Simcoe ice lobes, and consequent changes in water level in the interlobate lake basin. The facies associations will aid in the interpretations of the relatively complex subaqueous fan and of the changes in the depositional environment which occurred following the deposition of the fan.

Most of the descriptions in this section are documented in the fence diagrams (Appendix IV). This section also summarizes and discusses paleocurrent data from each facies (Figs. 3.1 to 3.8). Paleocurrent data on these maps are reproduced in a simplified form, often with multiple measurements combined; the original paleocurrent plots, and directional statistics are included in Appendix I. Detailed stereonet plots of gravel fabrics indicate both orientation of a/b planes, and trends of a-axes of clasts (Appendix II).

Before each individual facies is discussed, it is important to note the overall geometry of the deposit. The Standard and Lee pits expose sediments of an elongate, complex fan, extending from a main apex to the northeast (S11) towards the southwest, approximately parallel to the grand mean paleocurrent direction (Fig. 3.1). This reflects either the actual configuration of the interlobate lake basin (P.J. Barnett, pers. comm., 1994; Fig. 1.6a), or may be a result of dominant westerly



paleoflows that existed in the lake basin, in response to westerly drainage. As a result, most of the inflow into the lake was deflected towards the southwest.

### **3.1 FACIES 1 COARSE PROXIMAL GRAVEL**

#### **3.1.1 Description**

The dominant exposure of this facies near the main apex (Appendix IV.1) is approximately 20 metres high. Paleoflow directions inferred from both gravel fabrics and cross-strata from interbedded sands indicate south-southwesterly paleoflows (Fig. 3.1). Beds change downflow from subhorizontal to gently inclined. In this exposure, facies 1 grades rapidly laterally and obliquely downflow into facies 2 (Appendix IV.1,2). Although laterally continuous exposure is limited, this facies does seem to be elongated in the downflow direction. Lateral transitions from facies 1 (S12) into facies 2, 4 and 5 (S7, S9, S10) are relatively abrupt, and occur over 150 to 200 metres (from S12 to S7; see Fig. 2.1 for scale). These lateral relationships are maintained through the vertical extent of the facies 1 gravels (Appendix IV.1,2). The top of facies 1 is truncated sharply by a shallow, broad erosional surface at the base of facies 9, and extends from S7 to S14.

Increasingly distal exposures of facies 1 are limited to the base of the sections (L5; L14, Appendix IV.3). At section L14, these gravels are not as extensive as near the main fan apex, and are composed of thinner, somewhat lenticular beds that pinch out towards the margins of the unit where facies 1 becomes interdigitated with facies 4. Facies 1 gravels exposed at L5 are also different, with a margin marked by a sharp erosional surface of the gravel "core" with facies 2.

#### **3.1.2 Interpretation**

Deposition into a standing body of water could explain the rapid lateral and downflow transitions, and the dipping beds of the proglacial gravels. Rapid

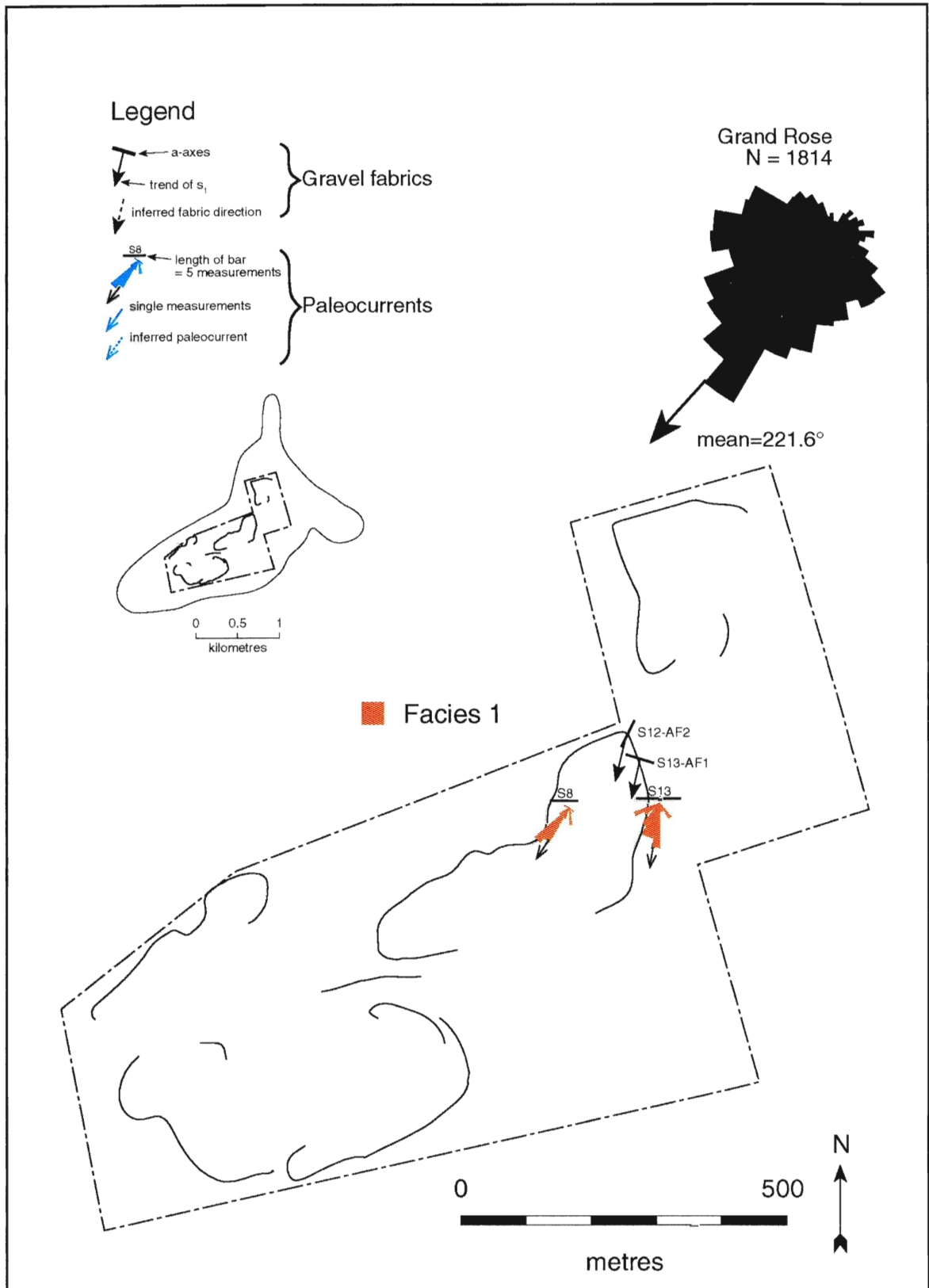


Fig. 3.1. Facies 1 paleocurrent map.

sedimentation with low lateral spreading directly in front of the conduit caused aggradation near the apex (S11), depositing horizontal to subhorizontal beds. Progradation, contemporaneous with aggradation, caused deposition of beds which decrease in dip angle in a downflow direction, and upsection (S12-S14, Appendix IV.1). Continuous aggradation at the apex suggests a source (conduit entrance) which could have been increasing in elevation, or the deposit aggraded to the level of the conduit. The former could have been accomplished with development of an R-channel (Röthlisberger, 1972).

Paleoflow, inferred from bed dip directions, clast fabrics and paleocurrents measured in interbedded sands, was to the south and southwest (Fig. 3.1). Limited exposure suggests an elongate geometry of this facies, with limited lateral spreading. A lack of lateral spreading could simply be due to deposition immediately in front of a conduit, or within a re-entrant into the ice front. Elongate geometries of proglacial gravels suggest a strong inertial influence of the effluent water (Martinsen, 1990) which could occur with a dominantly hyperpycnal mixing mode. Hyperpycnal flows occur when inflowing water is denser than ambient water. Flow lobes are successively stacked, with their positions controlled by the location of the source.

The gravel cores in distal zones of the deposit indicate the probable location of smaller, secondary conduits, although the only direct evidence for englacial or subglacial conduit sedimentation is the presence of longitudinal ridges which feed into the deposit at these distal locations (Fig. 1.3). Some of these are definitely gravel-cored eskers, but others may be till-cored (P.J. Barnett, pers. comm., 1994), and therefore do not indicate subglacial drainage conduits. Thin to medium bedded gravels within a laterally constrained "core", marked by a margin of interdigitated facies 4, suggest sedimentation within a proximal deposition of proglacial gravels (Fig. 2.3). Periodic flows deposited the gravels within the channel, and carried suspended sediment over the channel banks, deposited as the adjacent facies 4.

The gravels in L5 are enigmatic; the sharp contact (erosional?) between the gravel and the adjacent exposure of facies 2 indicates that facies 1 was deposited prior to deposition of facies 2. Moreover, flow directions interpreted from gravel clast orientations in facies 2 suggest flow was towards facies 1. This exposure of facies 1 exhibits oversteepened beds, and numerous internal faults. Two hypothesis are developed to explain this occurrence of facies 1. First, these sediments may have actually been deposited within a conduit. This notion is supported by the internal deformation of this unit, the surficial expression of a possible esker (Fig. 1.3) and the seemingly erosional surface on the eastern margin of this exposure which dips towards the east. This surface could have been produced during exposure of the esker deposits; sedimentation from the northeast, with aggradation, would have caused the main fan lobe to prograde over and re-work the eastern margin of the esker.

Alternatively, this unit may simply represent proglacial sedimentation directly in front of a secondary conduit. This could explain the presence of facies 2 sediments at the base of the western side of this unit (L7, L13) which indicate southwesterly flow directions (L7). The surficial expression of the buried esker could mark the location of the conduit which would have fed this early stage proximal lobe. Burial and re-working of these gravels would still have occurred with the progradation of the main fan from the northwest.

Smaller proximal gravel channels were deposited in front of the secondary distributary conduits. The eventual abandonment and progressive eastward migration of active fan deposition resulted when the main conduit (R-channel) captured subglacial meltwater from the smaller conduits (Röthlisberger, 1972; Shreve, 1972, 1985).

## 3.2 FACIES 2 PROXIMAL INTERCHANNEL

### 3.2.1 Description

Facies 2 is marked by laterally continuous, sub-horizontal sheets of interbedded sand and gravel. Gravel beds near the apex (S11) are up to one metre thick, and decrease in thickness to S9, towards the southwest. Beds exposed on the northern flanks of the deposit generally dip gently towards the northwest, while sediments immediately downflow of the apex dip towards the southwest.

This facies is exposed most commonly adjacent to facies 1, either in an oblique downflow (S13-S14) or lateral direction (S12-S10). Lateral transitions from facies 1 at the main fan apex are abrupt (Appendix IV.1, 2), and exhibit paleoflow directions which diverge from facies 1 (e.g., S9-BF1, paleocurrent S10; Fig. 3.2). Facies 2 shows limited lateral and downflow relationships, although downflow gradation into facies 4 occurs from S10 to S9. Facies 2 is found in two different vertical sequences. Some sections are marked by the presence of facies 2 overlying facies 4 (S9), defining a coarsening-upward sequence. This sequence is also marked by an increase in the number of gravel beds upsection, but these gravel beds tend to become thinner towards the top of this unit. Other exposures of facies 2 exhibit a fining upwards trend from sandy pebble gravels up into pebble sands, concurrent with a decrease in bed thickness. Proximal exposure of facies 2 are truncated by a broad erosional surface at the base of facies 9.

Other exposures of facies 2 are not related to proximal deposits. In section L5, facies 1 gravels are extensively faulted and deformed, and seem to be laterally truncated by facies 2 (Fig. 3.3). At S17-S19, L6 and L13 facies 2 is not adjacent to facies 1, but exhibit paleocurrent trends similar to those of this facies elsewhere in the deposit (Fig. 3.2). Notable exceptions are the gravel fabric S1-AF2, which has an a(p) a(i) fabric, with clasts dipping towards the southeast, and at L13, where

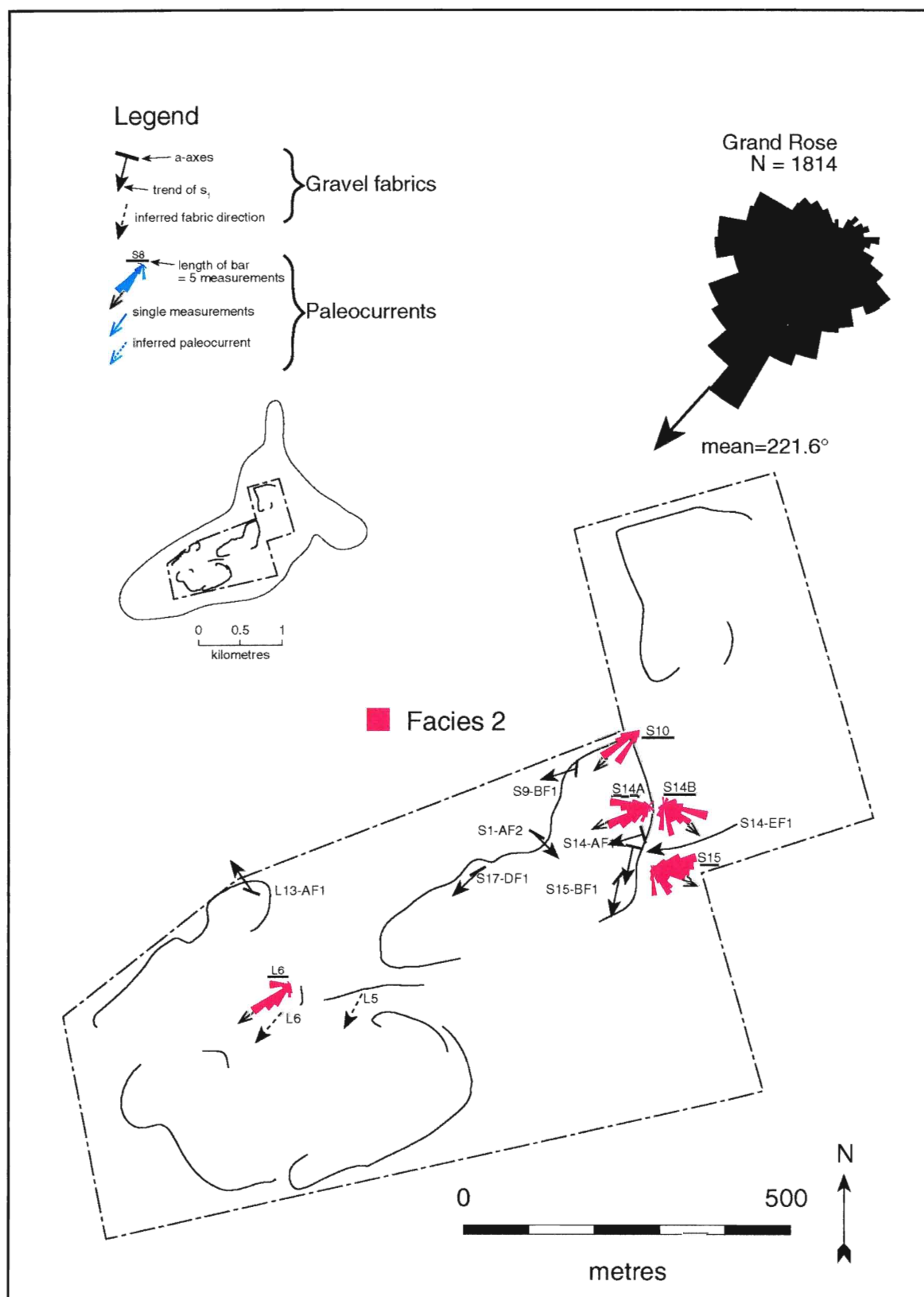


Fig. 3.2. Facies 2 paleocurrent map.

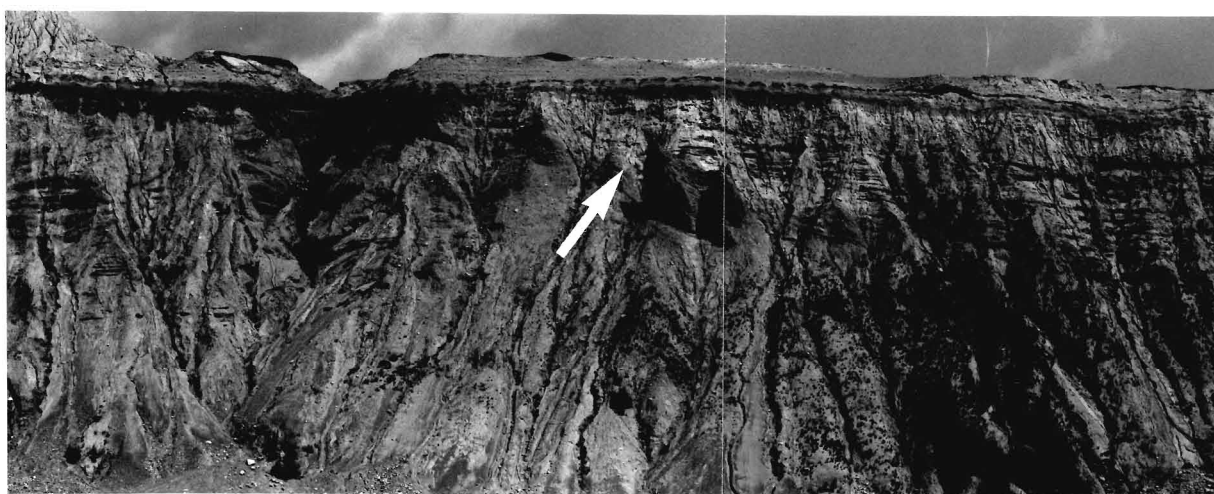


Fig. 3.3. Contact between facies 1 and facies 2, section L5 (arrow). Near-vertical sediment mounds are approximately three metres in height.



apparent paleoflow was towards the northwest.

The thick exposure of facies 2 at S14 is also peculiar, and exhibits paleocurrents that differ markedly from the surrounding deposits (Fig. 3.2). Oversteepened thin beds of poorly sorted sediment, faults and notably variable paleocurrents are documented from this exposure.

### 3.2.2 Interpretation

It is interpreted that the deposition of facies 2 occurred from unconfined sheet flows that passed over proximal interchannel portions of the fans. As a result, undeformed beds of facies 2 dip gently along the flanks of fan lobes.

Upward coarsening sequences that contain facies 2 are limited to proximal locations, near the main fan apex (Appendix IV.2). Coarsening-upward sequences probably resulted from progradation and lateral migration of individual lobes. Sections with fining-upward sequences indicate lobe migration. Decreasing bed thicknesses upsection, locally in conjunction with a coarsening upwards sequence (e.g., S9), may indicate increasingly shallow-water upsection, rather than source retreat. The vertical continuity of proximal gravels is further evidence against source retreat. The observed increased deflection of proximal gravels would have been caused by gravel aggradation directly in front of the source (similar to formation of bifurcation channels at the river mouth on friction-dominated deltas; Wright, 1977).

Paleocurrent patterns from cross-bedded and cross-laminated sand, along with gravel fabrics, trend to the southwest, similar to the dominant paleoflow across the deposit (Fig. 3.2), although those in proximal zones are divergent from this trend, and suggest paleoflows away from the main channel (S10, S9-BF1). Multiple conduits (point sources) each introduced sediment in a southerly direction, but

would have proglacial flow directions deflected by the dominant westerly flow within the interlobate lake. The two anomalous fabrics at S1 and L13 indicate deposition from sediment-gravity flows down the proximal interchannel slopes of two secondary conduits. The fabric at S1 suggests a proximity to a secondary conduit at this location (Fig. 3.2).

### **3.3 FACIES 3 PROXIMAL TO MID-FAN CHANNELS**

#### **3.3.1 Description**

Exposures of the well-defined channels (S1, L15) are laterally discontinuous, but the weakly defined, shallow "channel" zones can be exposed for several hundred metres in direction both parallel and transverse to paleoflow (Appendix IV.3, 4). Facies 3 cuts into a variety of mid to distal sediments, including facies 4, 5 and 6. Limited exposures indicate that only facies 4 occurs above, below, and downflow of the broad channel deposits of facies 3 (Appendix IV.3,4). Paleocurrents based primarily on gravel fabrics, and a few large scale tabular cross-beds (L6), show directions roughly similar to the grand mean (Fig. 3.4).

The exposure in S1 is problematic, as the facies relationships along the contact zone show interdigitation of facies 3 and the adjacent facies 4 (Fig. 2.21; Appendix IV.2). However, the paleocurrents within the gravel are dominantly to the southwest, and those within the adjacent facies 4 sediments indicate flows to the west-southwest, obliquely into the gravel channel (Figs. 3.4 and 3.5).

#### **3.3.2 Interpretation**

Facies 3 was deposited from periodic, high energy flows which caused coarse sediment to bypass proximal zones, and become channeled into mid-fan sediments. Episodic influx of higher energy flow is probably related to fluctuations in subglacial discharge. Autocyclic controls on paleoflow directions would also have been

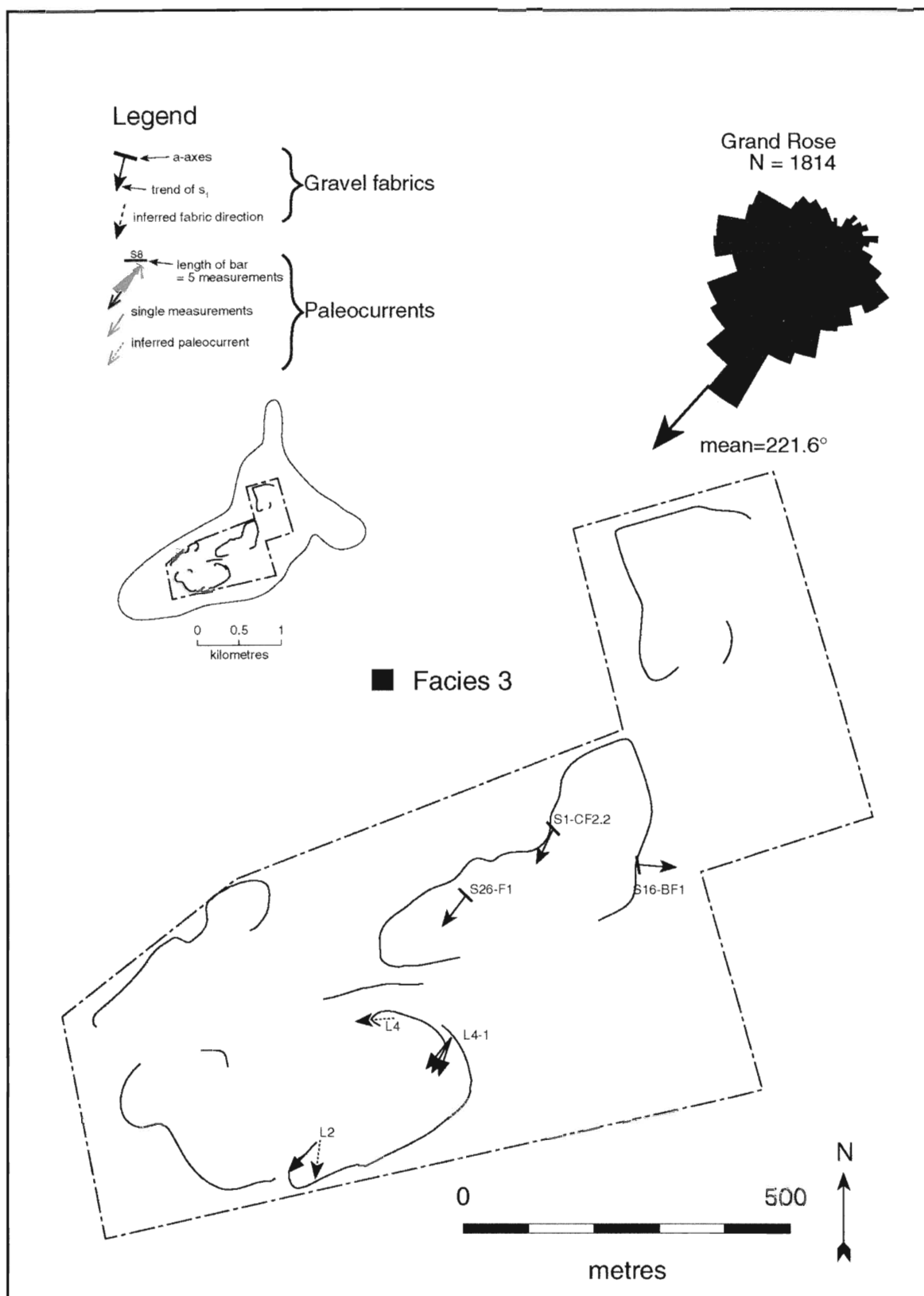


Fig. 3.4. Facies 3 paleocurrent map.

important, and may be related to sudden proximal lobe re-direction due to aggradation at the conduit entrance, deflection away from existing lobes, or increased sediment bypassing caused by a relative decrease in depth of water. This latter control is autocyclic if the decrease in the thickness of the water column available for sedimentation is produced by continued aggradation of the deposit; however, it could also be induced by the allocyclic control of an actual water level drop within the basin. However, the occurrence of facies 3 above finer grained, more distal deposits suggests that both progradation and lobe migration were occurring.

At S1 the interdigitation along the contact between facies 3 and facies 4 suggests contemporaneous deposition of both units, albeit from different sources, as inferred from the paleocurrents. The deposition of interchannel facies resulted from westerly flows which splayed from flows which deposited proximal gravels to the east. Contemporaneous development of a gravel channel originating at the apex may have flowed in a southwesterly direction. The intersection of these two depositional sub-environments produced the differing paleocurrent directions. Deformation within facies 3 is explained by faulting associated with gradual removal of support by melting of an ice block.

Flow directions from cross-bedded sand are reasonably uniform, indicating strong unidirectional (perhaps somewhat confined) flows (e.g., L4-1). This strong southerly paleoflow may provide further evidence of a secondary conduit to the north of this measurement site.

### 3.4 FACIES 4 MID-FAN INTERCHANNEL

#### 3.4.1 Description

This facies is dominated by laterally continuous, subhorizontal to gently inclined beds. Facies 4, like other interchannel facies, displays beds which dip in various directions, depending on location within the deposit. Beds on the west side of the fan apex dip to the west-southwest, away from the fan apex. In the laterally continuous exposures in the Lee Pit (L4-1 to L2), facies 4 included laterally continuous beds that dipped at 10° towards the southwest. In northern portions of the deposit, facies 4 beds dipped gently towards the northwest (L11). Beds in the western portion of the deposit dipped gently towards the west (L14).

Downflow gradations from facies 2 are common (e.g., Appendix IV.2.5); in these exposures facies 4 normally grades further downflow into distal, fine-grained sediments of facies 5. Facies 4 is also located downflow and above the broad "channels" of facies 3. In proximal sections facies 4 displays a coarsening-upwards sequence, defined by an increase in the number of gravel beds, but is accompanied by a general decrease in bed thickness upsection (e.g., S9, S10). Slightly more distal sections exhibit general fining-upward sequences, defined by an increasing number of fine-grained beds and a decreasing thickness of cross-bedded and horizontally-bedded units (e.g., S4-S2; L11).

Paleocurrents show a variety of paleoflow directions (Fig. 3.5), although those in proximal and distal zones are similar, while in mid-fan regions, paleocurrents tend to be more divergent. Paleocurrent directions measured from the sand beds and from gravel fabrics are normally similar at any one location and/or stratigraphic position (e.g., S9-AF1; S9-AP1, AP2; Fig. 3.5).

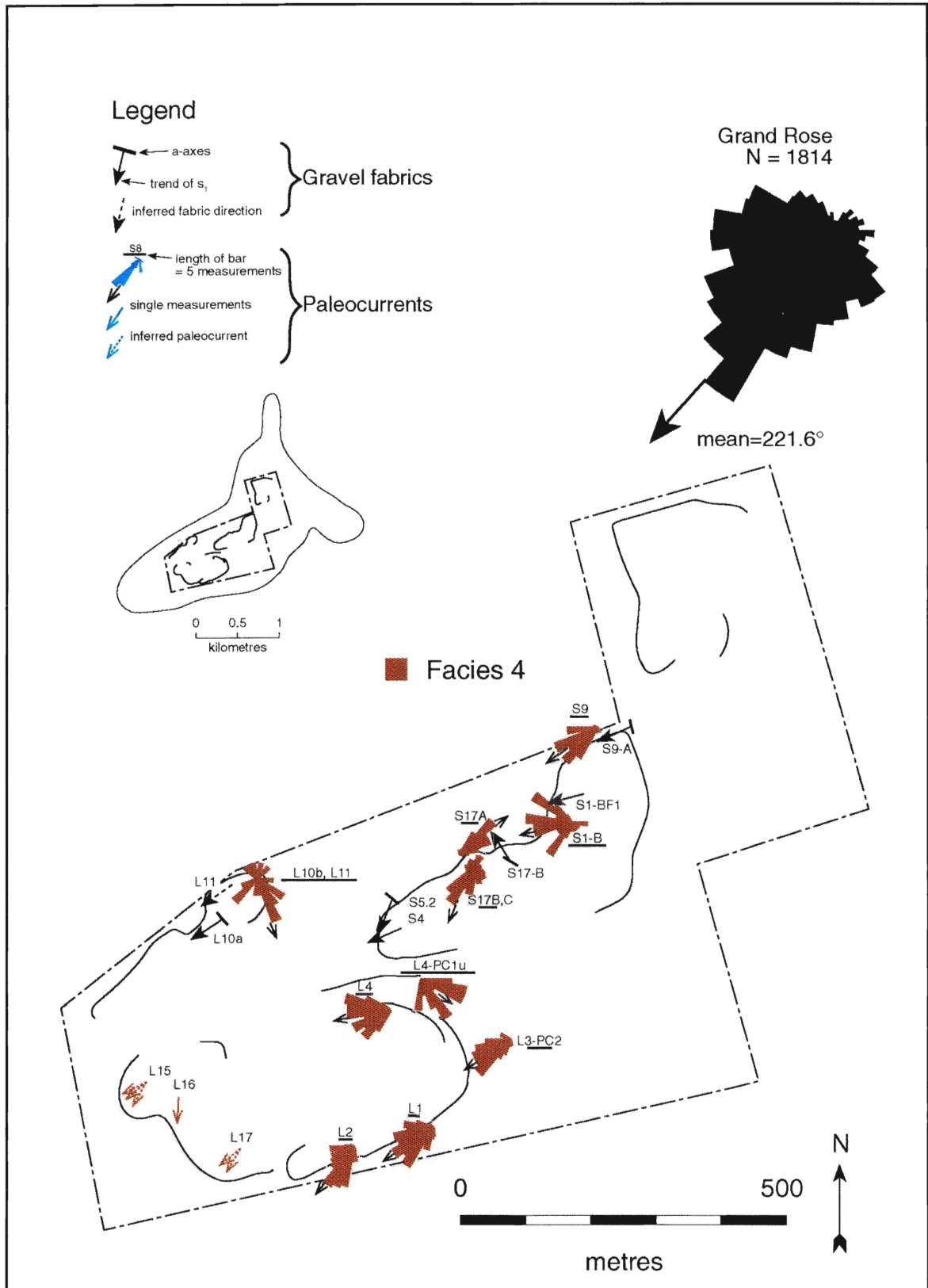


Fig. 3.5. Facies 4 paleocurrent map.

### 3.4.2 Interpretation

Paleocurrents that diverge from the proximal gravels, near the main apex (S9), suggest laterally unconfined flows which spread out from the conduit entrance, and also flows passing from the proximal gravel margins in a slightly downflow location (S1). Paleocurrents that vary strongly from the grand mean may indicate flows derived from secondary conduits (e.g., L4-PC1u; L10b). Paleocurrent data from rippled beds in mid to distal zones show consistent unidirectional trends (e.g., L1, L2). This suggests that distal zones of the fan were influenced by sheet flows which did not exhibit radiating flow patterns, but were rather controlled by the geometry of the interlobate basin, or by dominant westerly flows which occurred within this basin. As with facies 2, changes in bed dip directions indicate the surficial expression of fan lobes. Coarsening-upward sequences including facies 4 suggest proximal lobe progradation/migration (Appendix IV.2).

## 3.5 FACIES 5 DISTAL CHANNEL-INTERCHANNEL

### 3.5.1 Description

This facies generally grades downflow (towards the southwest) from facies 4 (Appendix IV.2), and includes both general fining-upwards and coarsening-upwards sequences (Appendix IV.1, 5). Exposures near the main fan apex display rapid lateral changes from the thick accumulation of facies 1 gravels into facies 5 over 150 to 175 metres (Fig. 2.1). At S15, facies 5 grades and thickens rapidly downflow (towards the southwest) from facies 2. However, the paleocurrents do not exhibit radiating patterns from the fan apex (Fig. 3.6, S7). Instead, the lower portion of facies 5 (S7) indicate southerly flow, which changes sharply upsection into a dominantly westerly paleoflow. This thick exposure of facies 5 also exhibits a notable fining-upward and bed thinning-upward sequence, similar those documented from other exposures near the main apex. Some notable variations



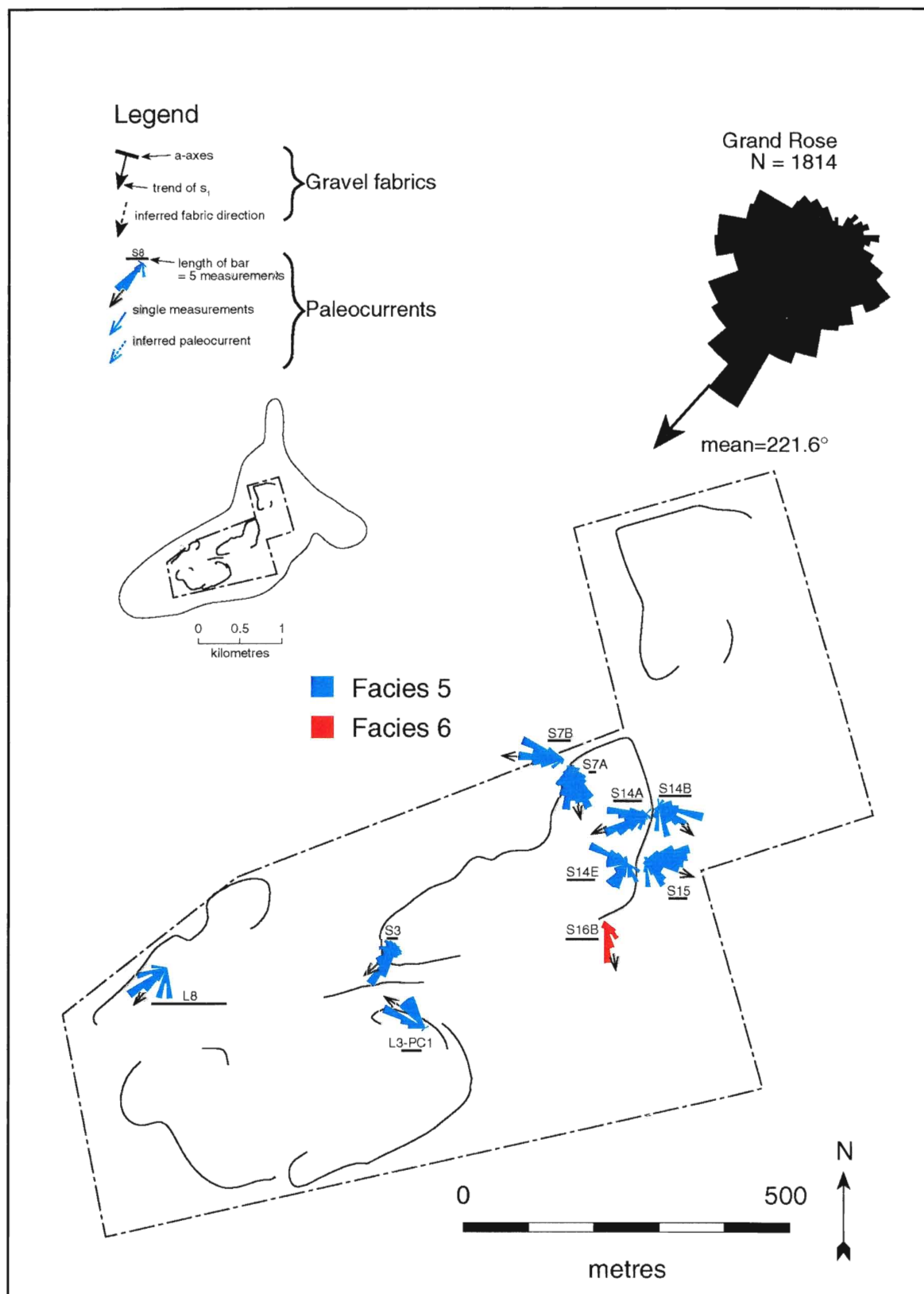


Fig. 3.6. Facies 5 and 6 paleocurrent map.

from the mean paleocurrent direction indicate northerly and northwesterly paleocurrents (L7, S21C, S22.2), and are therefore included in facies 8.

### 3.5.2 Interpretation

The upward fining and thinning suggests lateral migration of depositional lobes, perhaps in conjunction with shallower water conditions upsection. The hypothesis of changes in lobe position is further supported by changes in bed dip directions (S7), deformation southwest of S7 (Appendix IV.2), and abrupt changes in paleocurrent trends between S7A and S7B (Fig. 3.6) which resulted from increased deflection away from main sediment source, in conjunction with lobe migration. Similar transitions occur in sections directly upflow. Basal paleocurrents in S7 suggest flows parallel to the trend of proximal gravels. Therefore, early stages of fan deposition must have been laterally confined, or these basal sediments may have been deposited from a secondary lobe. Gradual deflection upsection towards the southwest would have occurred in either case; with increasing deposition on the main lobe, or with gradual expansion of a re-entrant into the ice-margin.

## 3.6 FACIES 6 MASSIVE SAND CHANNELS

### 3.6.1 Description

Exposure of this facies is limited to the base of S16, where it is overlain by facies 3 (Appendix IV.1). Paleocurrents from rippled sand in shallow channel scours indicate southerly paleoflows (Fig. 3.6). This facies exhibits downflow transitions from steep-walled, massive sand channels, into shallow channels filled with climbing ripple sequences, and finally into horizontally laminated sands and silts. Vertical sequences exhibit the massive sand channels incised into horizontally laminated sediments.

### 3.6.2 Interpretation

This is the only exposure of massive, steep-walled channelled sands in the deposit. Documented downflow transitions from the steep-walled channels into shallow channelled, rippled sands and horizontally laminated sands and silts is similar to downflow sequences from sandy sediment-gravity flows (Fig. 2.40; Postma *et al.*, 1983). Paleocurrents indicate flow to the south-southeast, similar to paleocurrents at the base of S7 (Fig. 3.6). This gives further support to the notion of deposition at distal margins of a secondary conduit in that proximity, or early stages of main lobe deposition when ice-margin configurations may have prevented lateral flow expansion. Truncation by facies 3 suggests either progradation of the same lobe, or, more likely, from the main gravel channel at the main fan apex.

## 3.7 FACIES 7 GLACIOLACUSTRINE DEPOSITS

### 3.7.1 Description

Facies 7 occurs at elevations ranging from 332 to 352 metres, notably lower than those of facies 8. Facies 7 occurs on the flanks of the fan complex, away from the crest and the highest topographic regions of the fan. A second exposure of facies 7 occurs at L16 as a laterally discontinuous unit which is interbedded with facies 3 and 4 at both margins (Appendix IV.3). Although exposure is limited, this unit exhibits minimal lateral extent, maintains lateral facies relationships vertically upsection with minimal lateral migration, and is truncated above by facies 3. A weak fining-upwards sequence occurs within this unit, defined by the increase in horizontally laminated silts.

### 3.7.2 Interpretation

The relationship between the elevation and the spatial distribution of facies 7 and 8 suggests one of two possible depositional scenarios. The most obvious

interpretation of facies 7 is that of glaciolacustrine sedimentation, draping the entire deposit. Subsequent erosion during the deposition of facies 8 on topographic high regions of the fan complex then produced the spatial distribution that exists between these two facies; facies 7 in the low regions of the deposit, and facies 8 in higher regions. In fact, many sections are marked by an erosional surface at the base of facies 8, and there are several sections where facies 7 may have been removed.

However, some sections do not display such an erosional surface, suggesting that facies 7 and facies 8 may have been deposited contemporaneously, but on different regions of the fan complex. Because facies 8 is interpreted as ice-proximal deposits, and related to periodic ice-grounding conditions, the adjacent, low-lying facies 7 was probably deposited beneath limited, floating portions of the ice margin which allowed the deposition of undeformed laminated sands, silts and clays with dropstones. Glacigenic sediment gravity flows of facies 8 were deposited in small subglacial cavities, between knobs on the high regions of the fan complex.

The laterally discontinuous exposure of facies 7 (Appendix IV.3) that is interbedded with facies 4 sediments suggests spatially restricted quiet-water sedimentation. The fining-upward sequence suggests deposition in a topographic low between two lobes, one constructed by southward flow near L14, and the distal margin of the main lobe that was constructed by flows to the southwest. These deposits must have maintained these lateral facies relationships during vertical aggradation of this zone, indicated by the vertical continuity of this contact for almost ten metres. Slight dipping of the beds along the contact may suggest deposition in a topographic low, or post-depositional subsidence.

### 3.8 FACIES 8 ICE-MARGINAL COMPLEX

#### 3.8.1 Description

This facies occurs at higher elevations than facies 7 (353-372m), but at the same stratigraphic position as facies 7, above facies 9, and directly below the Halton Till (facies 10). Paleocurrents measured from thin interbeds of rippled sands indicate flow towards the north and northwest (Fig. 3.7).

#### 3.8.2 Interpretation

The presence of gradational contacts in some sections between the massive diamicts of facies 8 and the overlying Halton Till, combined with paleocurrent data suggests that the glacial sediment gravity flows were deposited as the Ontario lobe readvanced from the south. Because the ice would have moved up and over the pre-existing Oak Ridges Moraine (of which this fan would have been one of the highest topographic points) compressive flow may have caused sufficient up-shearing at the ice margin to provide debris that would feed the glacial sediment gravity flows.

The multiple-lobate deposit would have produced a complex system of pinning points and subglacial cavities as the Halton ice advanced. Where the ice moved over topographic lows and formed subglacial cavities, glacial sediment gravity flows and periodic subglacial releases of meltwater directed toward the north would have deposited the weakly stratified diamicts, and stratified sands and gravels. During low meltwater, discharges ripple cross-laminated and horizontally laminated sand and silt were deposited, also fed from a southerly source. Periodic grounding deformed some of these low areas, but would have more drastically affected topographic highs, perhaps depositing massive diamicts and glaciotectonically deforming underlying sediments in areas where dynamic strain

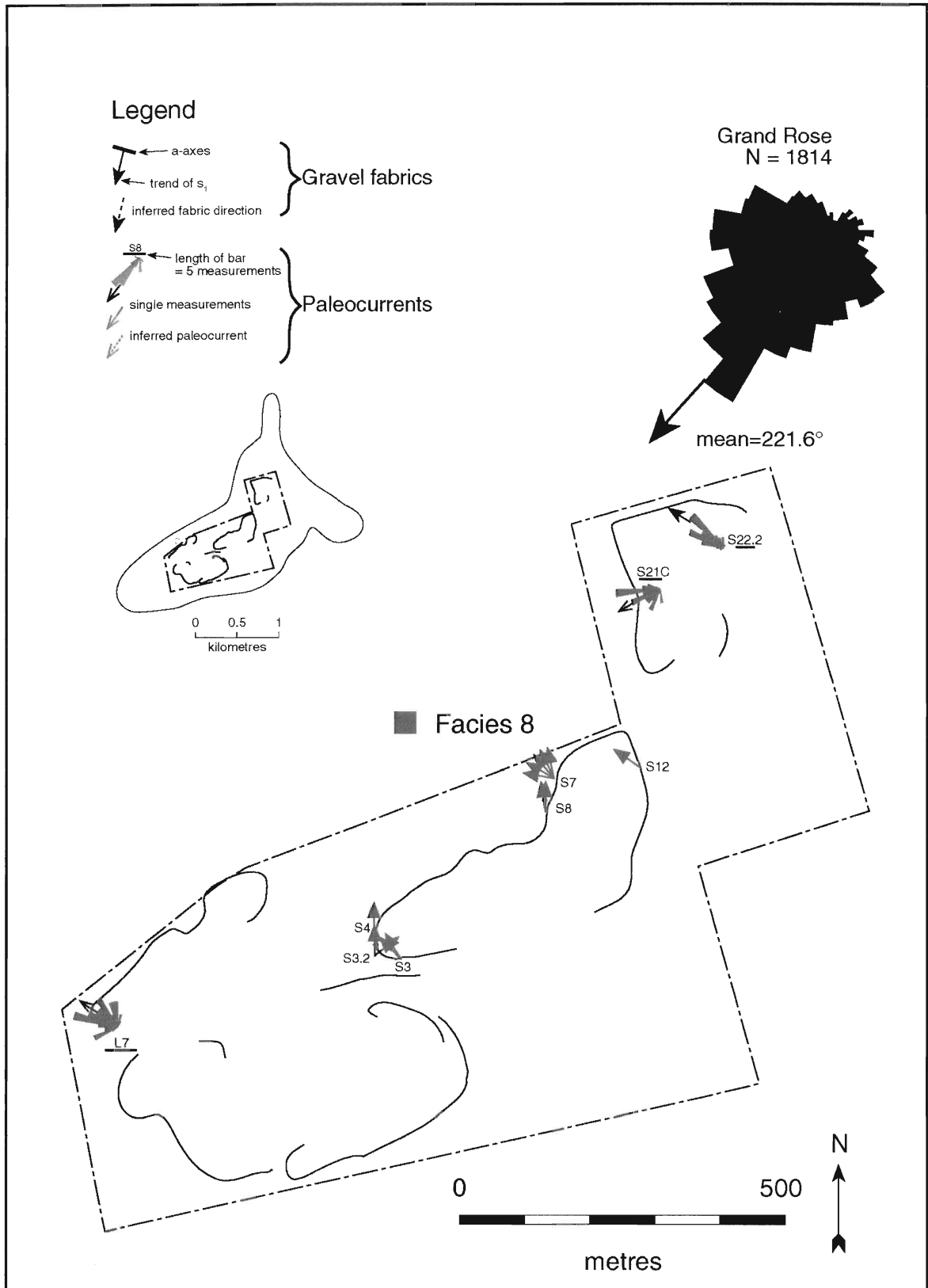


Fig. 3.7. Facies 8 paleocurrent map.

rates were substantial. Periodic groundings and glacier detachment would produce deformed contacts and large glaciotectionic structures. Similar cycles of grounded-floating ice have been documented by numerous workers, including Benn (1989).

### **3.9 FACIES 9 STRATIFIED SAND AND GRAVEL**

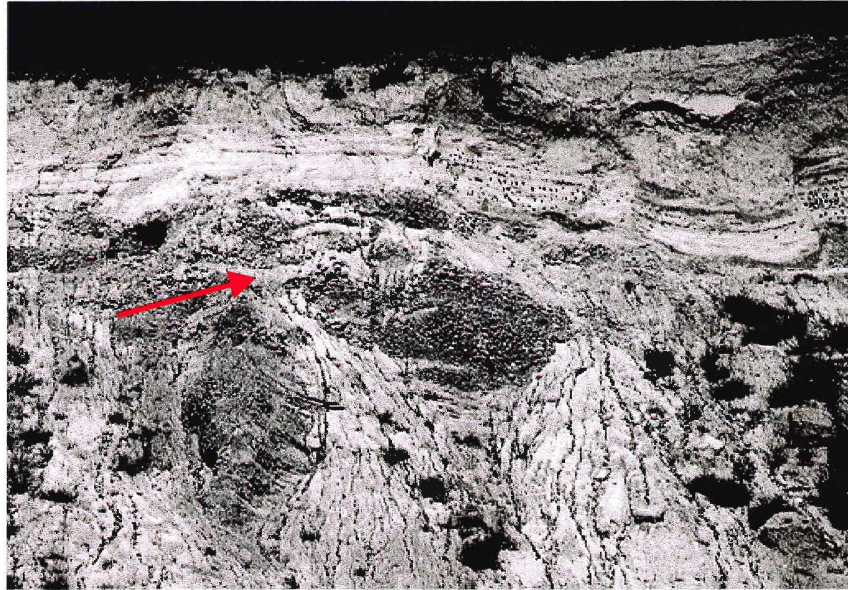
#### **3.9.1 Description**

Exposures of this facies occur in zones near the main fan apex (Appendix IV.1, 2), in sections in the eastern side of the Standard Pit (S21-S24), and at slightly lower elevations within a probable confined zone along the northwestern margin of the deposit (Appendix IV.5). This facies varies in thickness from less than a metre, where it appears to pinch out near S7, to approximately ten to twelve metres near S21. Facies 9 overlies most facies in these exposures and basal contacts are sharp and normally erosional. A particularly abrupt contact is visible where facies 9 overlies finer grained facies 7 sediments (L9). In sections where this facies overlies proximal gravels of facies 1, the contact is less discernible, defined only by slight differences in bedding dip directions. The exposures of facies 9 are marked by two distinct styles of channels; broad, shallow channels (Fig. 3.8a; Appendix IV.1, 2), and steep-walled incised channels (L12; Fig. 3.8b). The unusually steep-walled, almost overhanging contact may be partially related to post-depositional glaciotectionic deformation, as large thrust sequences are located nearby (see section 2.11). The broad channel margin is marked by underlying sediment injected into the fluvial gravels (Fig. 3.8a).

The elevation of this contact ranges from approximately 337 m at the base of the steep-walled channel at L12, to 360 m at the base of the broad channel which has its mid-point at S11. Exposures in the eastern side of the Standard Pit which are directly upflow of this broad channel are at a lower elevation (S21), and are marked by large scale normal faults along the length of the exposure (S21-S24).



a



b



Fig. 3.8. Geometry of facies 9 basal erosional channels: a) sediment diapir at base of shallow, broad erosional surface, and injected into overlying glaciofluvial sediment. Exposure approximately 20 m high. b) steep-walled channel margin at L12. The photograph shows approximately 9 m of vertical exposure.

Paleocurrents based on cross-bedding indicate paleoflow generally towards the south (Fig. 3.9). Gravel fabrics are more divergent, ranging from west-southwest to southeasterly flow directions. Paleoflows in the western portion of the Lee Pit are consistently towards the southwest (Fig. 3.9).

### 3.9.2 Interpretation

The sedimentology of this facies suggests deposition on a proximal braided fluvial environment. The erosional basal contact suggests incision (e.g., L12), caused by decreases in base level within the interlobate basin. The lower elevations of this contact in the eastern portion of the Standard Pit may be due to post-depositional subsidence in association with melting buried ice blocks.

Glaciofluvial sediments that occur at a lower elevation in the Lee Pit were deposited in a confined zone between the slightly retreated northern ice margin, and the fan complex body. These sediments may have initially been deposited subaqueously, and laterally confined flows caused the steep-walled channel incision. Subsequent continued decreases in water level eventually allowed the deposition of subaerial glaciofluvial sediments (Fig. 2.41b). The presence of facies 7 and facies 8 overlying facies 9 indicates a subsequent rise in water levels, and a return to glaciolacustrine sedimentation.

## 3.10 FACIES 10 DIAMICT

### 3.10.1 Description

The Halton Till overlies a subhorizontal surface across the deposit. The elevation of the basal contact is highest towards the main fan apex, and lowest along the westerly flanks of the Bloomington fan complex.

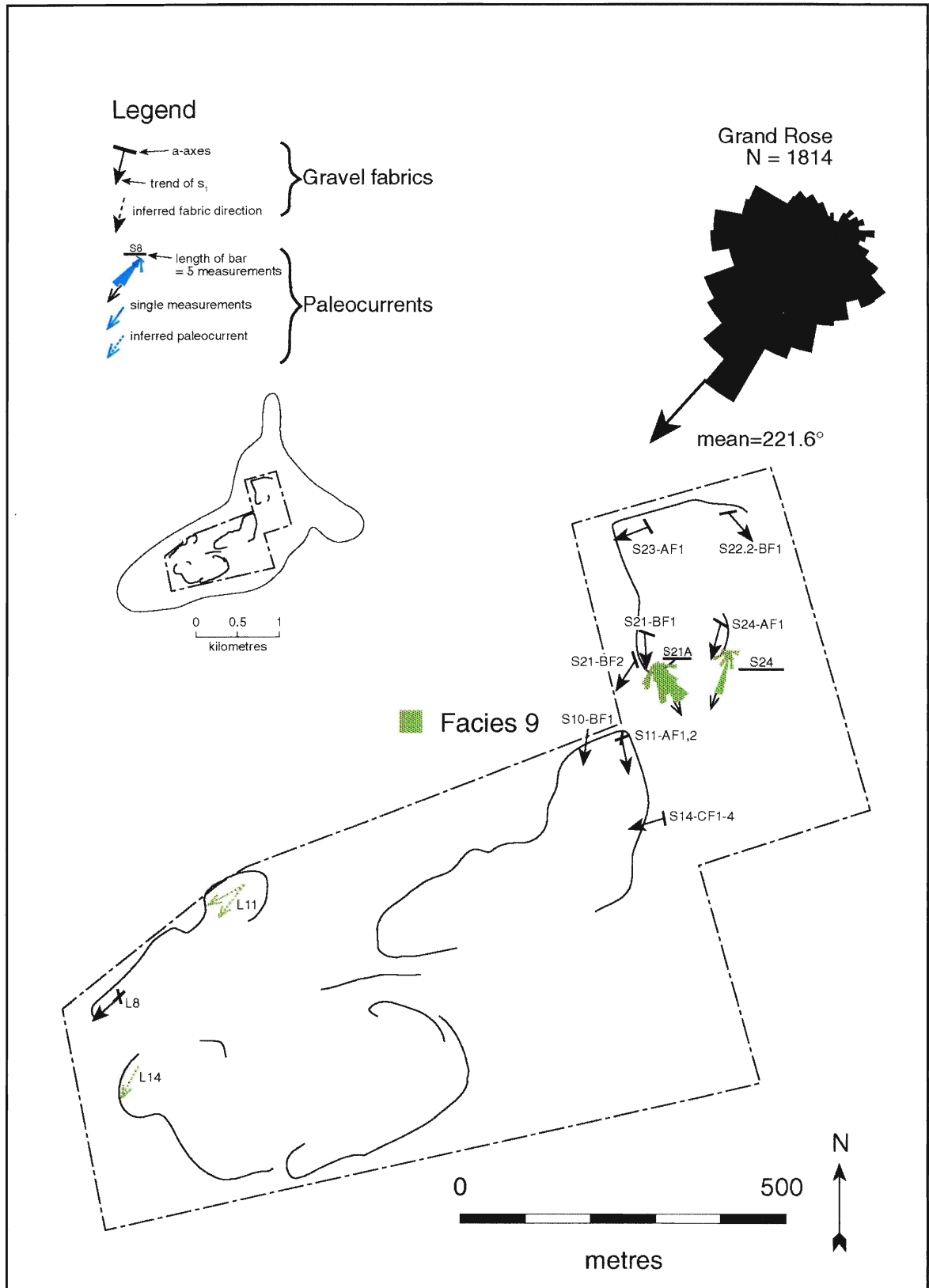


Fig. 3.9. Facies 9 paleocurrent map.

### 3.10.2 Interpretation

A late-stage re-advance of the Ontario ice lobe moved over the deposit from the south and deposited the Halton Till.

## 3.11 SUMMARY OF FACIES DISTRIBUTIONS

The previous sections have described facies associations of the Bloomington fan complex and have referred to the fence diagrams in Appendix IV to illustrate the lateral and vertical associations that provide the basis for the depositional model described in chapter 4 of the thesis. However, each fence diagram represents only a limited lateral extent, and therefore they do not depict the overall distribution of facies across the entire deposit.

Figure 3.10 is a schematic cross-section through the deposits of the Bloomington fan complex, extending from the northeast to the southwest (see Fig. 2.1 for location). This cross-section shows the overall distribution of facies and is based on the fence diagrams. The distinct occurrences of proximal sediments (facies 1 and 2 combined in Fig. 3.10) provides the initial framework for the depositional model, as they indicate the approximate location of several point sources (conduits) that are thought to have fed the fan complex. Note, particularly, the progradation of the main fan apex; mid-fan facies (facies 3 and 4) grade from the northeastern, proximal, location near the main apex, but also dominate the southwestern portion of the deposit (Fig. 3.10). Facies 5 grades from mid-fan facies near the main apex at S11, and from the fans at L5 and S17 (although the facies 5 sediments at S3 may have been deposited at the distal margin of the main fan as well; Fig. 3.10).

The fan complex is truncated in at least two locations by glaciofluvial deposits of facies 9, which clearly occur at two different elevations, and overlie shallow and broad (S11-S7; Fig. 3.10), or steep-walled, incised erosional surfaces (L12; Fig. 3.10).

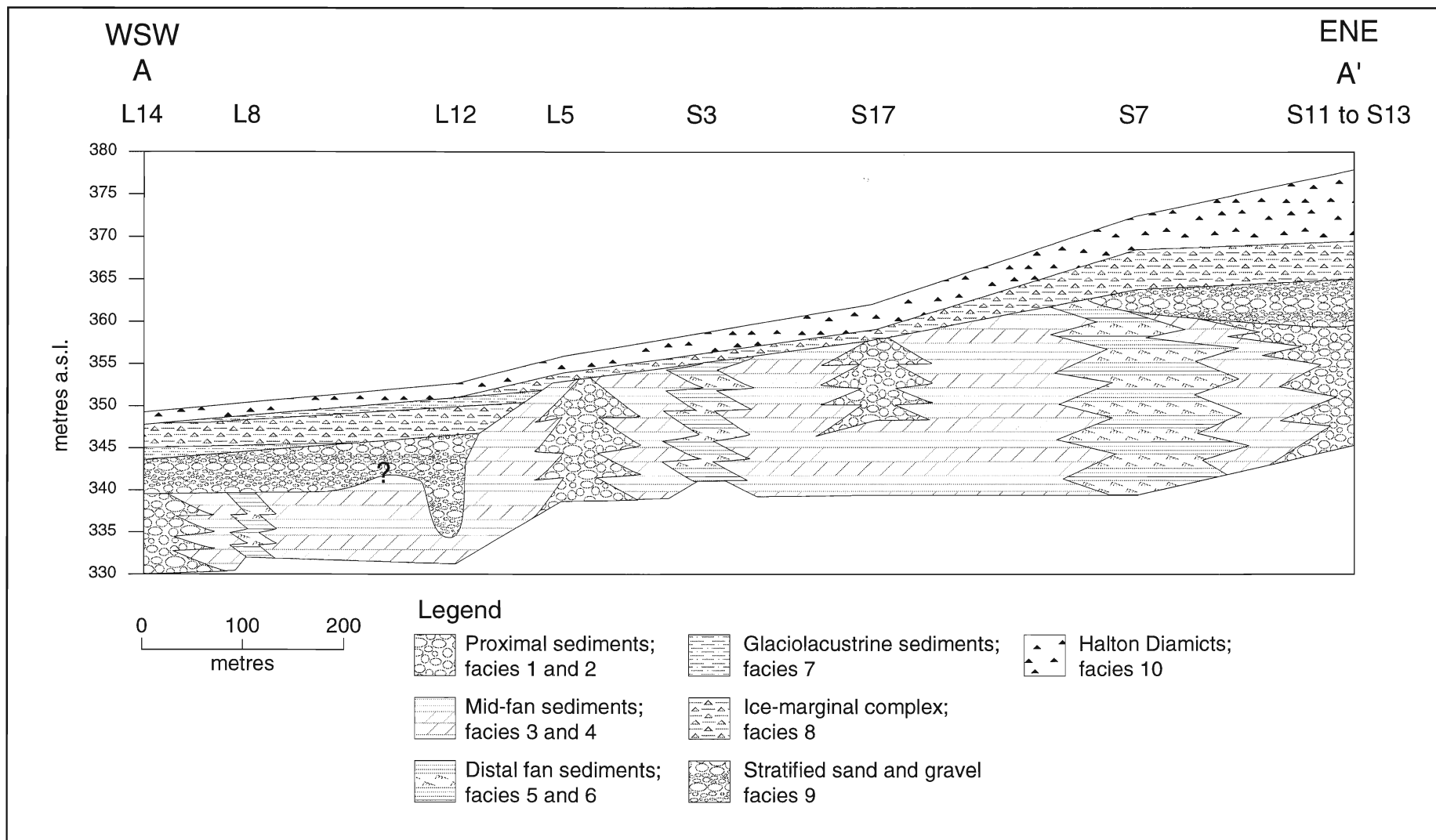


Fig. 3.10. Schematic cross-section of Bloomington Fan complex. Location of cross-section A-A' marked in Fig. 2.1. Note the multiple exposures of proximal sediment.

Facies 7 generally drapes the topographically lowest portion of the deposit, while facies 8 tends to occur on topographic highs (Fig. 3.10). Halton Till caps the entire deposit and is thickest on the topographic high near the main apex (Fig. 3.10).

## 4.0 DEPOSITIONAL MODEL

Given the sedimentology, spatial distribution and associations of each of the facies, this chapter summarizes the depositional model for the Bloomington fan complex. The depositional model for the sediments exposed in the Standard and Lee pits is subdivided into four separate phases (Figs. 4.2 to 4.4):

Phase 1) deposition of subaqueous fan complex

Phase 2) deposition of glaciofluvial sediment

Phase 3) deposition of glaciolacustrine sediment and  
Halton ice-marginal complex

Phase 4) deposition of Halton Till

Phase 1 constitutes the bulk of the deposit; a subsequent decrease in water levels in the interlobate lake basin then resulted in phase two. Phases three and four represent an increase in water level over the deposit and deposition associated with the northward advance of Halton ice.

### 4.1 PHASE 1

Phase 1 is the deposition of a fan complex within an interlobate lake basin that was fed from the northern ice lobe. Growth of the fan complex involved proglacial sedimentation from several conduits (Fig. 4.1). The timing of the influence of each of these sources is difficult to establish, but may be interpreted as subphases of fan growth, phases 1a to 1c (Fig. 4.2). Exposures throughout the deposit rarely reveal interdigitated facies with radiating paleocurrent patterns, and are instead dominated by southwesterly paleocurrent and facies trends. The deposits of distal portions of the fans are relatively uniform, and equivocal in delineating separate source areas. The position and distribution of facies 1 gravels remains the primary indicator of multiple conduit sources (Fig. 4.1). The depositional model suggests temporal relationships where possible.



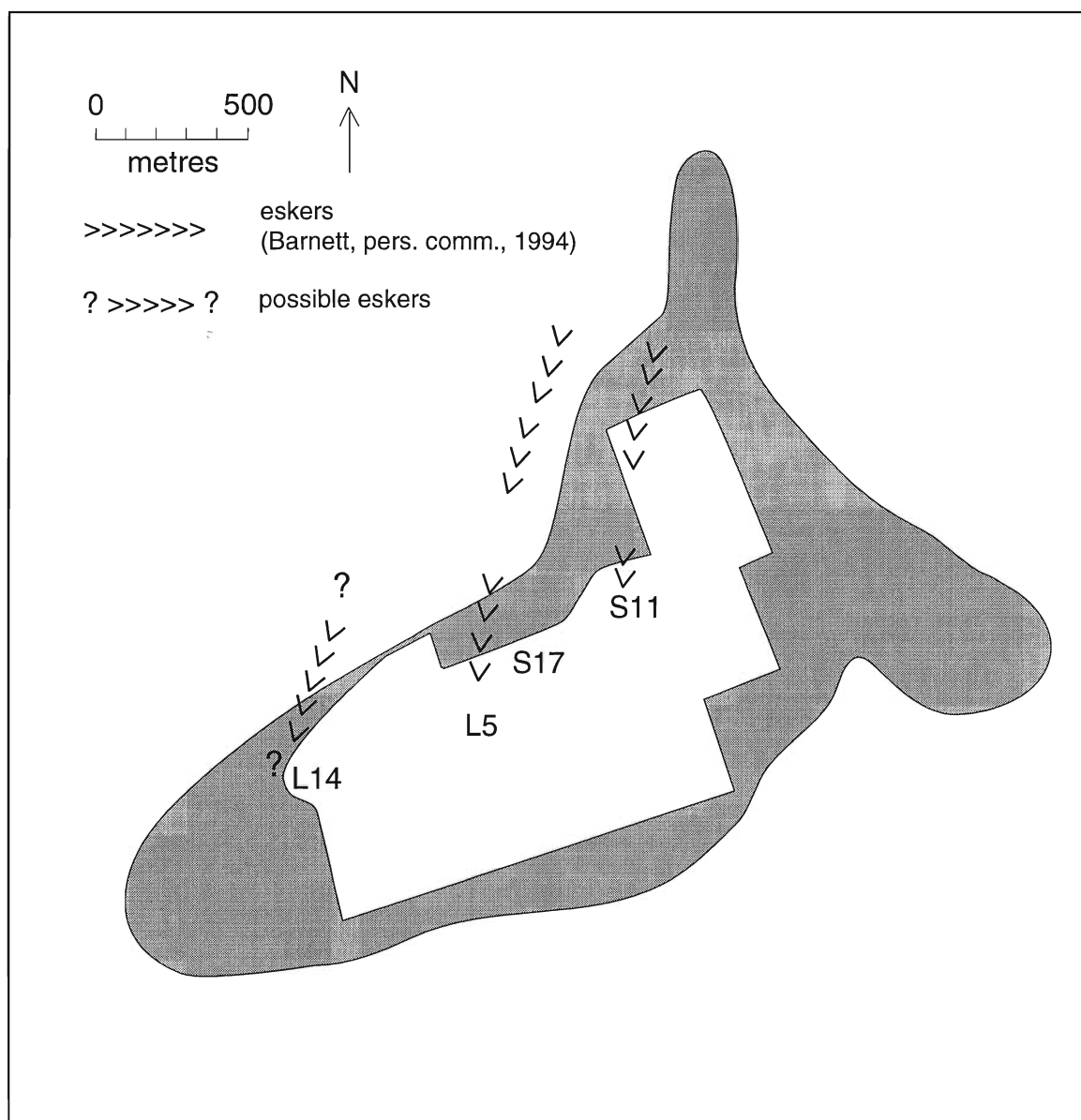


Fig. 4.1. Location of eskers feeding the western portion of the Bloomington Fan complex, in relation to sections which exhibit proximal sediments.

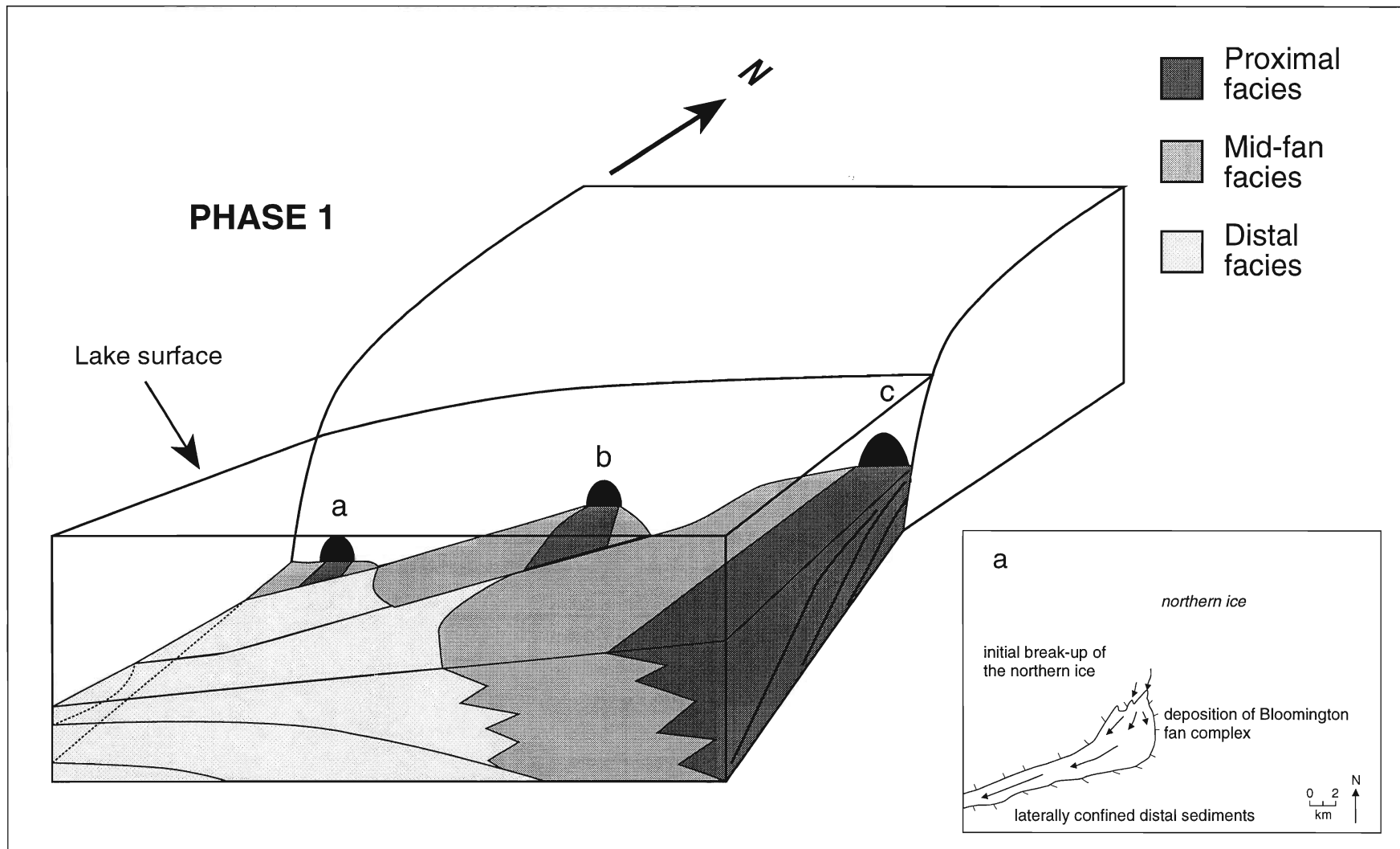


Fig. 4.2. Depositional model, phase 1. Note westerly fans are generally buried by subsequent easterly fans. Inset shows regional depositional setting (inset after Barnett, 1994).

Sub-phases are thought to have produced a time-transgressive sequence with the earliest fan growth generally at the western margin of the deposit with subsequent fans progressively eastward due ice retreat and subglacial meltwater capture by easterly conduits.

#### 4.1.1 Subphase 1a

The early subphase 1a is suggested by the exposure of facies 1 at L14 (Fig. 4.1), the occurrence of mid-fan channel gravels at L15, and mid to distal sediments at the base of sections L16 and L17. This early stage of fan growth was dominated by southerly to south-southwesterly paleocurrents from a conduit located at L14.

#### 4.1.2 Subphase 1b

Subsequent phases of fan growth are suggested by proximal gravels at L5 and S17 (Fig. 4.1). Further evidence of the lobe originating at L5 are the distal sediments which show southeasterly paleocurrents at L4. Deposition from the lobe at S17 laid down proximal to mid-fan (S17-S19) to distal sediments (L4, L6). Gravel (L4b) and sand channels (L4-1) locally cut across mid-fan zones. At some point during the accumulation of the lobe near S17, proximal gravels were deposited at the lobe near L5. Although these gravels are somewhat deformed (e.g., convoluted beds, normal faulting, oversteepened beds), the presence of sediments at the base of this exposure with both southwesterly (L4a, L6) and southeasterly (L4a) paleocurrents suggests proglacial sedimentation, and progradation of facies 1 gravels, rather than confined subglacial deposition. Continued sedimentation from the lobe at S17 produced the sharp contact between facies 1 and facies 2 in L5.

#### 4.1.3 Subphase 1c

Proximal gravels were deposited in a laterally limited zone, with mid to distal sediments spreading out from the main apex at S11 (Fig. 4.1). South-southeasterly

paleocurrents at the base of S7 and S16B may indicate the influence of another small distributary conduit that was active prior to the main lobe (the distal portion of the lobe near S17?; Fig. 4.1). Alternatively, these sediments may have been deposited during early stages of the main lobe, when ice margin configurations could have laterally confined paleoflows in a southerly direction during initial stages of formation of the interlobate lake basin.

Subsequent growth and aggradation of the main fan caused mid to distal flows to be deflected away from depocentre of proximal sediments (e.g., paleocurrents S7A and S7B). Lobe migration near the main fan apex is suggested by the coarsening-upwards sequence near the top of sections S9 and S10, and perhaps by convoluted beds at the same elevation at S7 associated with changes in bed dip direction (Appendix IV.2). Continued sedimentation near the apex caused progradation of the proximal gravels at S12-S13. Distal zones of the Bloomington fan complex (e.g., L1 and L2) were dominated by sediment input from the main fan, but were perhaps still fed by secondary conduits. Because ice margins were probably coalescing towards the west (Fig. 4.2, inset), flows in distal zones were increasingly confined downflow and caused slightly coarser, and less variable sediments to be deposited than those near the main apex.

During late stage deposition of the fan ice blocks were partially buried; subsequent melting caused overlying sediments to deform (e.g., S14-S15). The production of ice blocks was probably enhanced at late stages of the deposition of the fan complex, as the main conduit feeding S11 may have melted upwards (R-channel), decreasing the stability of marginal ice directly around the conduit.

Large supercritically climbing gravel dunes and other gravel macroforms exposed at the base of S21 and S23 after field work was complete may have been deposited in either a subglacial or proximal proglacial environment. A lack of other stratigraphic evidence prevents further speculation. In either case, deposition could

have occurred contemporaneously with the main apex gravels.

## 4.2 PHASE 2

Following deposition of the subaqueous fan complex, the northern ice remained relatively stable at the study site, but the southern (and perhaps northern) ice margin(s) would have retreated in areas west of this deposit. This caused water levels to drop in the interlobate lake basin as westerly drainage outlets were opened, and exposed the fan to subaerial processes. As a result, phase 2 is marked by the deposition of glaciofluvial sand and gravel, which truncate underlying sediments with both steep-walled incised channels (L12) and broad, shallow channels (S10-S13). Deposition of these gravels appears to be restricted to two main regions (Fig. 4.3), which may in fact be partially due to a lack of exposure of the uppermost stratigraphic units along southern margins of the deposit. The first of these was deposited in a narrow re-entrant which may have formed by progressive upward melting of the conduit at S11 and caused tunnel collapse. The glaciofluvial sediments in S21 to S23 are at a slightly lower elevation than those at S11; this may have been due to burial, and subsequent melting of a large ice block or ice sheet (formed during tunnel collapse?). A loss of support through melting ice is also suggested by the large-scale normal faults in this section.

As the northern ice lobe began to retreat, water levels in the lake basin decreased further, and gravels were deposited along the northwestern margin of the deposit (L12-L7), between the sediment body of the fan and the retreating ice. Periodic high flow discharges from any of the conduits to the east (e.g., L5) eroded steeply incised channels in this confined zone. Otherwise, it would be difficult to deposit such a confined gravel unit at a location that would have been topographically the lowest across the surface of this region of the deposit.

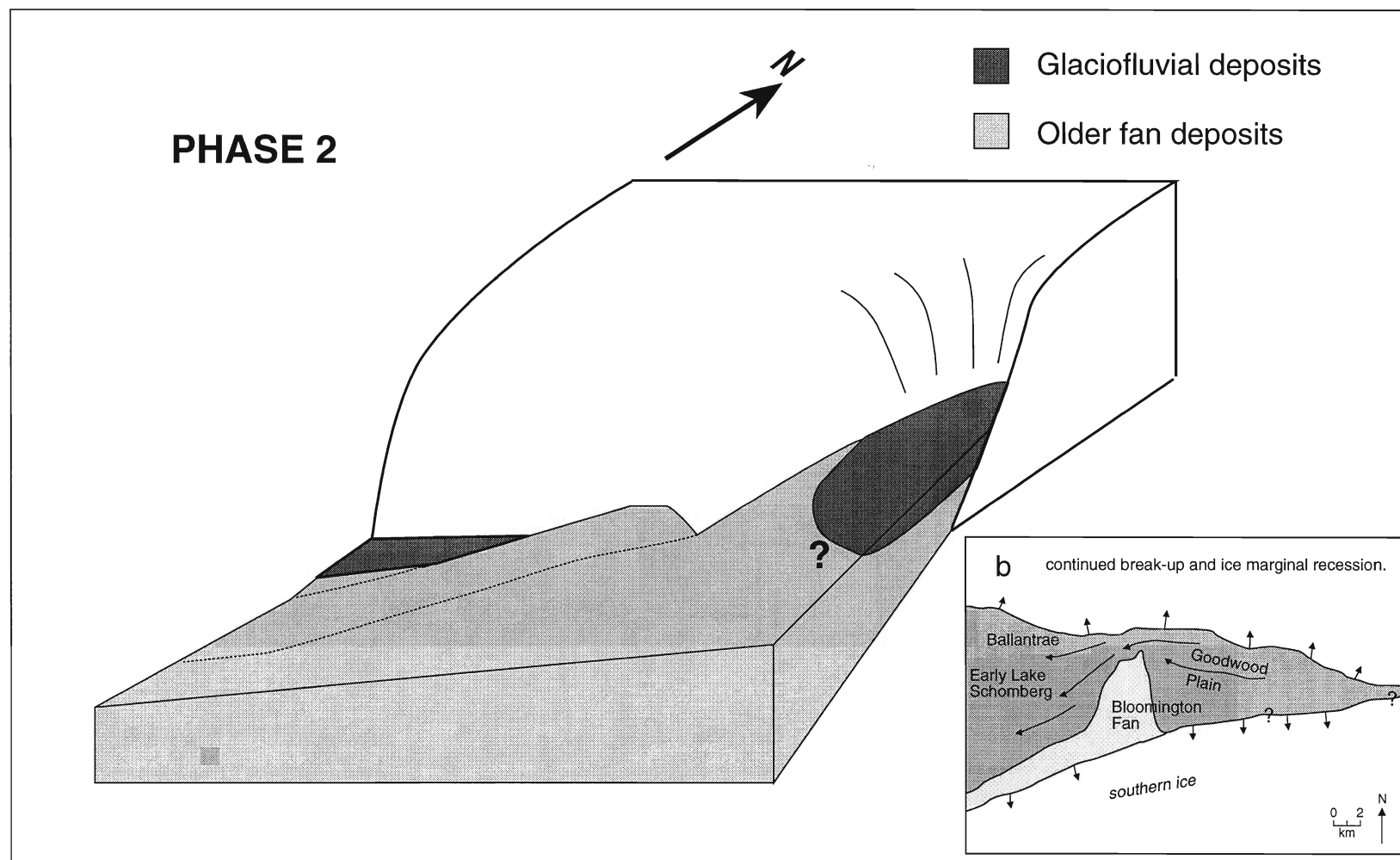


Fig. 4.3. Depositional model, phase 2. Note two zones of glaciofluvial sedimentation. Inset indicates regional setting following deposition of these sediments, and continued ice marginal retreat (inset after Barnett, 1994).

### 4.3 PHASE 3

It is thought that the next stage was initiated by a surge of the Simcoe ice lobe in the Aurora-Newmarket basin to the west (P.J. Barnett, pers. comm., 1994); (Fig. 4.4, inset). This surge would have blocked westward drainage outlets, and caused water levels in the interlobate basin to the east to rise. Fine-grained glaciolacustrine rhythmites were deposited as a drape overlying the Bloomington fan complex (Fig. 4.4). Rising water levels may have also helped to trigger the re-advance of the to the site of the Bloomington fan (P.J. Barnett, pers. comm., 1994). As the Ontario ice lobe approached the deposit, distal low-density turbidity currents deposited ripple sequences with northwesterly to westerly paleocurrents. Fine-grained glacial sediment gravity flows originated at the ice margin and flowed into topographic lows on the surface, and may have eroded underlying fine-grained glaciolacustrine sediments on the highs. Periodic subglacial discharges deposited weakly stratified sands and gravels which also indicate northerly flow directions. Where grounded ice occurred, glaciotectionic structures were formed. Periodic detachments and re-groundings of the ice caused complex glaciotectionic structures to form, and allowed the deposition of cycles of interstratified diamicts, glaciofluvial and glaciolacustrine sediments.

### 4.4 PHASE 4

The Ontario ice lobe eventually overrode the study site, and deposited the cap of Halton Till. This advance halted just north of the study area, marked by a terminal position characterized by the line of kettle depressions and kettle lakes, and termed the Palgrave Moraine (Figs. 1.2, 1.6d).



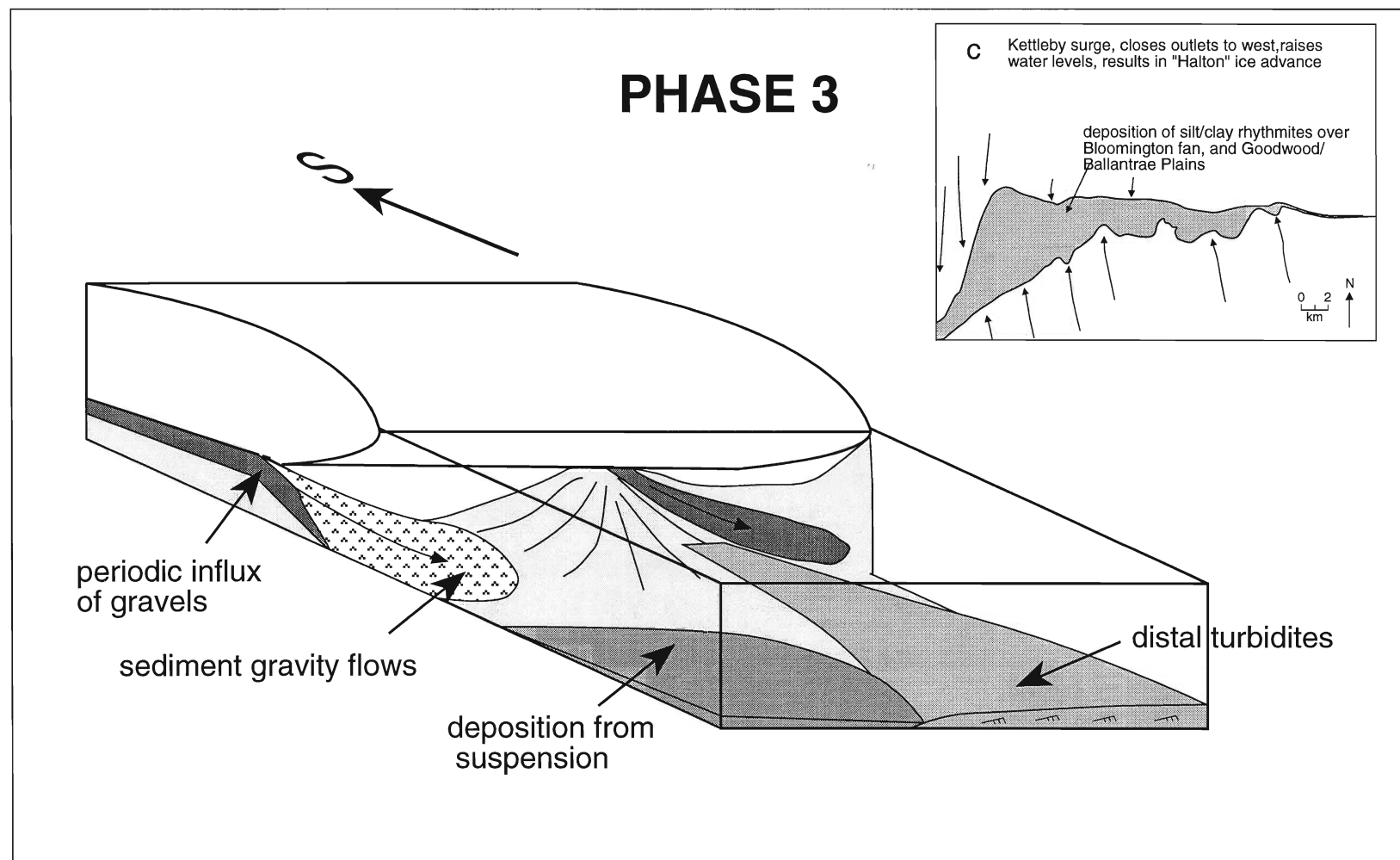


Fig. 4.4. Depositional model, phase 3; ice-marginal complex. Note re-orientation of block now pointing southwards. Inset shows Kettleby surge to the west of the study area, which triggered the Halton advance (inset after Barnett, 1994).

## 5.0 DISCUSSION

The purpose of this section is to compare the depositional model developed in the previous chapter with published models of subaqueous fans. Marked deviations from known models will be noted, followed by possible reasons for these differences. This will be followed a discussion of the controls on and effects of fluctuating water levels in the interlobate lake basin.

### 5.1 COMPARISON WITH OTHER SUBAQUEOUS FAN MODELS

Depositional models based on subaqueous fans from proglacial marine (e.g., Rust and Romanelli, 1975; Rust, 1977; Cheel, 1982; Shaw, 1985; Cheel and Rust, 1986; Burbidge and Rust, 1988; Rust, 1988), proglacial lacustrine (e.g., Gorrel, 1986; Kaszycki, 1987; Spooner, 1988; Delorme, 1989) and deep marine environments (e.g., Stow, 1986; Walker, 1992) provided an initial generalized framework to analyze this fan complex. However, while there are many similarities, there are also several notable differences between the established models and the Bloomington fan complex.

A variety of features in the Bloomington fan complex are similar to those documented from proglacial subaqueous outwash fans (e.g. Rust and Romanelli, 1975; Rust, 1977; Cheel, 1982; Shaw, 1985). One of the most obvious similarities are the rapid lateral facies changes that occur in the Bloomington deposit, near the main fan apex. Transitions from proximal gravels to distal sandy deposits occur over 100 to 150 metres, from S11 to S7 near the main apex of the Bloomington fan complex. These lateral transitions indicate rapid dissipation of flows as they enter the proglacial lake basin. Extremely variable sedimentation, due to periodic and episodic sediment influxes resulting from annual, seasonal and daily fluctuations in meltwater flow characterizes the Bloomington fan complex as well as previously documented subaqueous outwash fans. Another similarity is the steep-walled,

massive sand channels that were documented from one section in the study pits. Such channels are considered diagnostic of subaqueous outwash fans (e.g., Rust, 1977).

There are also some similarities to the deposits of submarine fans. Southwestern portions of the Bloomington fan complex are relatively uniform, lack evidence of channelization, and exhibit laterally continuous beds which dip to the southwest. The morphology of these deposits is similar to distal, non-channelized portions of submarine fans (e.g. Stow, 1986; Walker, 1992).

This thesis has also documented some noteworthy differences which contribute to the development and distillation of depositional models of subaqueous fans. Although massive sand channels were documented from one section, this facies was not as common as it is in similar fans described by other workers (e.g., Rust and Romanelli, 1975; Rust, 1977; Cheel, 1982). However, a lack of channels has also been described from other studies of subaqueous outwash fans (e.g., Gorrell and Shaw, 1991). This suggests that there may have been an overemphasis on the presence of channels in earlier subaqueous fan models (e.g., Rust and Romanelli, 1975; Rust, 1977; Cheel, 1982).

This difference may be due to differing controls on channel migration in areas where proglacial drainage is laterally unrestricted, compared to laterally confined fans. Deposition of the Bloomington fan complex occurred in a proglacial lacustrine environment which allowed rapid lateral expansion from the conduit entrance. Similar conditions of flow expansion were documented by Gorrell and Shaw (1991) in a subglacial setting. Most of the work that documented numerous massive sand channels was from deposits located in bedrock dominated terrain, where bedrock knobs tend to funnel subglacial and proglacial drainage paths (e.g., Kaszycki, 1987). Other work by Rust and Romanelli (1975), Rust (1977) and Cheel and Rust (1982, 1986) described a depositional setting laterally confined within a re-entrant. These

confined flow zones tend to be characterized by a higher frequency of density underflows, which may lead to the generation of elevated numbers of massive sand channels (e.g., Paterson, 1991). In addition, deposition on a confined fan would limit the extent of channel switching and lead to a higher concentration of channels in the resulting deposit.

Many documented subaqueous outwash fans are characterized by a ubiquitous gravel cap (e.g., Rust, 1977; Diemer, 1988; Spooner, 1988). It is thought that these gravels represent wave reworking of underlying sediments as water level drop in proglacial lake basins (e.g., Rust, 1977; Spooner, 1988), generally in response to isostatic rebound. The Bloomington fan complex does not exhibit this gravel facies, because water levels dropped rapidly, as a result of retreating ice margins which opened westward drainage outlets. Instead, the subaqueous fan was incised by glaciofluvial deposits in two isolated zones when water levels dropped.

Subaqueous outwash fans generally exhibit overall fining-upward sequences resulting from source (glacier) retreat (e.g., Rust and Romanelli, 1975; Rust, 1977). Although subaqueous outwash fans are characterized by lobe migration, progradational sequences are not commonly preserved. The Bloomington fan complex exhibits a coarsening-upwards sequence near the main fan apex which suggests a combination of lobe migration and fan apex progradation. It is thought that a relatively stable northern ice margin during the deposition of the Bloomington fan complex provided sufficient time for progradation to occur. In this respect, submarine fans provide a good analogy for the Bloomington fan complex, in that they are also subject to lobe migration, but can undergo progradation near the feeder channels (Walker, 1992).

The Bloomington fan is further complicated by the presence of laterally overlapping fans which seem to originate from multiple conduit sources. Most of the existing literature on subaqueous outwash fans document single feeder conduits

(e.g. Rust, 1977; Cheel and Rust, 1982), although a few studies have described multiple, laterally-overlapping fans (e.g. Rust and Romanelli, 1975).

Multiple, closely spaced conduit sources can occur when a retreating ice margin transects an anastomosing network of subglacial conduits. Some workers believe that laterally overlapping fans can form with increasing proglacial water levels, which causes transitions from tunnel channel to linked cavity subglacial drainage patterns (Benn, 1989). However, the Bloomington fan complex appears to have been characterized by falling, or at least stable water levels during the deposition of the fan body. The location of multiple conduits may also be controlled by the tunnel channel which exists due north of the deposit (Fig. 1.4). Tunnel channels are commonly marked by anastomosing, discontinuous eskers, and quite often themselves form interconnecting, anastomosing networks (e.g., Wright, 1973; Grube, 1983; Shaw, 1985; Boyd *et al.*, 1988; Mooers, 1989a,b; Gorrell and Shaw, 1991; Brennand and Sharpe, 1993; Brennand and Shaw, 1994). Although the tunnel channels probably existed prior to the formation of the Bloomington fan complex (Barnett, 1990, 1992a; Sharpe *et al.*, 1994), subglacial drainage systems could have re-occupied previously existing tunnel channels during the subsequent advance (P.J. Barnett, pers. comm., 1994).

The complexity of the deposit due to multiple, overlapping fans is enhanced by the configuration of the interlobate basin during the initial stages of deposition of the Bloomington fan complex. Near the fan apices, flows expanded laterally into a broadening ice-margin embayment (Fig. 1.6a). However, this basin narrowed towards the southwest, which probably constricted flows in this zone (Fig. 1.6a). This could have allowed variable types of sediment to be deposited near the main fan apex, but may have caused the sediments to be slightly coarser, and less variable towards the distal southwestern exposures in the Lee Pit.

Beyond the deposition of the original fan body, the depositional model is further complicated because it is influenced by two ice margins that advanced and retreated in opposite directions. Other studies of the influence of two ice margins have normally documented ice lobes moving in the same direction (e.g., Fraser, 1993). This deposit is also notable because of the influence of fluctuating water levels in this interlobate basin. The small size of the basin, combined with fluctuating northern and southern ice margins and the proximity of a major relief feature transverse to these ice margin movements (the Niagara Escarpment) probably induced rapid and drastic water level changes.

## **5.2 CONTROLS OF WATER LEVEL CHANGES ON THE CREST OF THE OAK RIDGES MORaine**

One of the most striking stratigraphic features of this deposit is the fan complex (glaciolacustrine)-glaciofluvial-glaciolacustrine sequence that cannot be attributed solely to autocyclic controls. Therefore, these transitions in major depositional processes result from allocyclic control on water level changes in the interlobate lake basin.

### **5.2.1 Elevations Of Depositional Model Phases 1 to 3**

Fine grained glaciolacustrine sediments on the crest of the Oak Ridges Moraine documented in this study, and by other workers (Duckworth, 1975, 1979; Chapman, 1985), indicate elevated water levels that occurred within the interlobate lake basin. These lake levels are notably higher than elevations of major glacial lakes in southern Ontario (Fig. 5.1; Chapman and Putnam, 1984; Karrow and Calkin, 1985; Barnett, 1992b) and give further proof of an ice-walled, or at least ice-dammed basin. Changes in major depositional environments recorded in the Bloomington fan complex (depositional model phases 1 to 3) reflect allocyclic control of water levels in this interlobate lake basin.

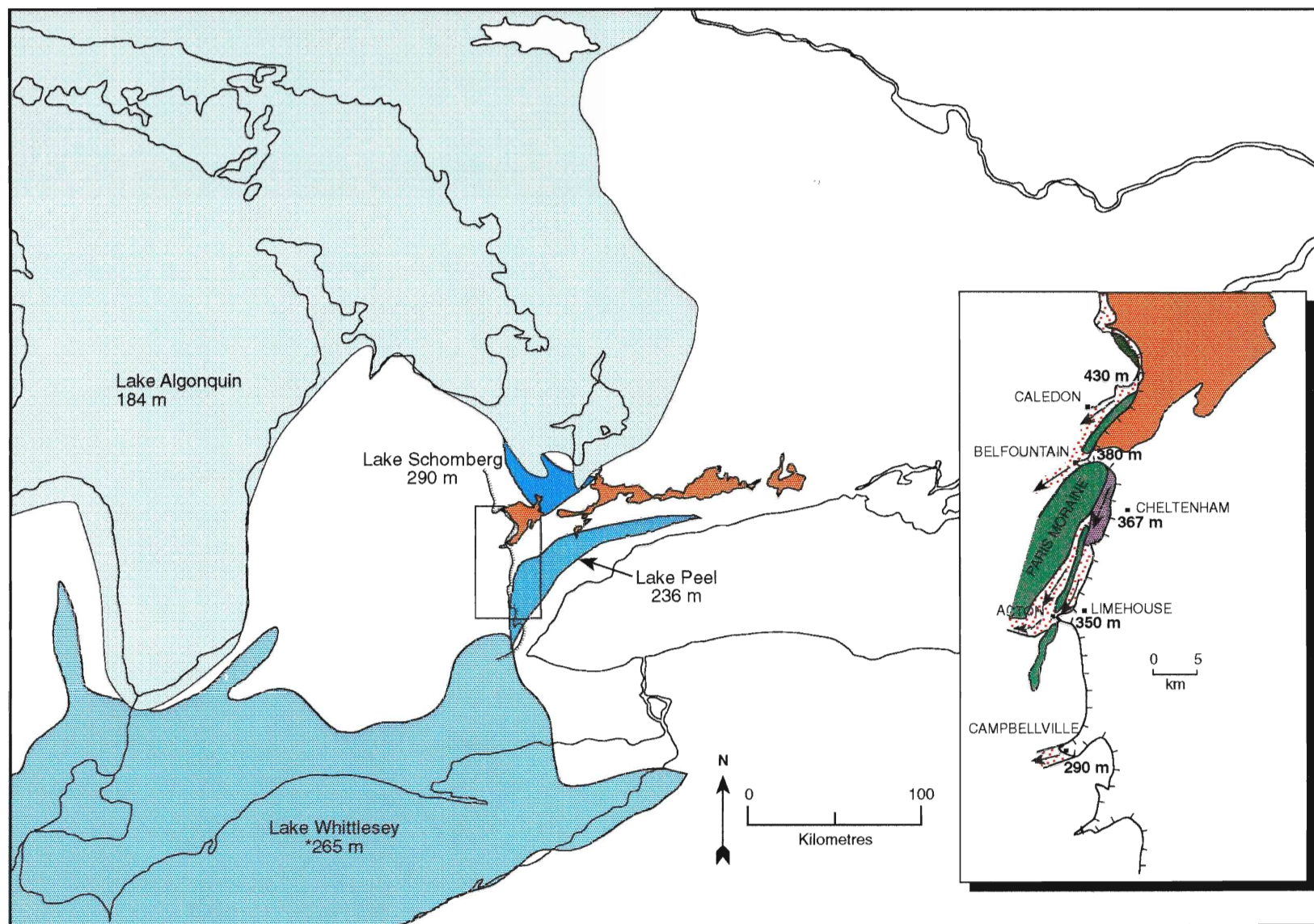


Fig. 5.1. Locations and elevations of relatively contemporaneous glacial lakes in Southern Ontario, relation to outlet levels along the Niagara Escarpment and morainic systems near the western margin of the Oak Ridges Moraine. Lake levels compiled from Chapman and Putnam (1984), Karrow and Calkin (1985), and Barnett (1992b). Inset after Chapman (1985).



During the formation of this deposit it is believed the margins of the Simcoe and Ontario ice lobes were fluctuating, and controlled westward drainage out of the interlobate lake basin. This control was achieved either by the coalescence of these two lobes east of the Niagara Escarpment to form a completely ice-bounded basin, and/or by ice margin fluctuations across the Niagara Escarpment. Even given the former condition, it is thought that water levels in the interlobate lake basin would ultimately be controlled by the Niagara Escarpment (P.J. Barnett, pers. comm., 1994). To discuss the possible controls on water levels it is first necessary to document the elevations of deposits associated with each of the depositional phases.

The phase 1 fan complex was deposited in an interlobate lake basin confined by the Simcoe and Ontario ice Lobes. The sediment package attains a maximum elevation of approximately 370 metres, which can be construed as a minimum lake level during this stage.

Phase 2 glaciofluvial sediments truncate the underlying fan complex, in response to decreasing water levels in the interlobate lake basin. These sediments occur in two separate zones and at different elevations. Zone 1 glaciofluvial sediments (broad, shallow scour at S7-S14) eroded to a base level of 361 m, and aggraded up to an elevation of 368 m. This unit is at noticeably lower elevations in sections S21-S23 because of post-depositional subsidence that resulted from the melting of a large, buried lens of ice. The second zone of glaciofluvial deposition (L12) cut a steep-walled channel to an approximate basal elevation of 333 m. Maximum water elevations of this second stage are reasonably well constrained by the horizontally bedded gravels which truncate gravel foresets at an elevation of 347 m (Fig. 3.9.5b).

Phase 3 sediments include the Halton ice-marginal complex, and contemporaneous glaciolacustrine units. These occur at elevations ranging from 344

m in the Lee Pit, up to 372 m in the Standard Pit. This difference in elevation is mainly due to the slope of the fan complex surface on which they were deposited.

Other workers have documented glaciolacustrine sediments on the crest of the Oak Ridges Moraine. Duckworth (1975, 1979) noted a 6 m thick exposure of 131 glaciolacustrine rhythmite couplets southeast of Goodwood. These were documented at elevations from 343 m to 351 m, and were overlain by subaerial outwash. Chapman (1985) documented glaciolacustrine sediments on the crest of the moraine at elevations ranging from 312 to 377 m.

### 5.2.2 Late Wisconsinan Glacial History Along the Niagara Escarpment, and Outlet Control

This section summarizes the literature concerning the glacial history along the Niagara Escarpment and across the central portion of the Oak Ridges Moraine. The assumption for this section is that water levels in the interlobate basin were ultimately controlled by ice margin positions along the Niagara Escarpment.

#### Port Bruce Stade

The Simcoe ice lobe advanced over the Niagara Escarpment near the western margin of the Oak Ridges Moraine, depositing the Newmarket Till and the Singhampton Moraine at its terminal position (White, 1975). Recent work suggests that this advance extended at least as far as the present Lake Ontario shoreline, as Newmarket Till underlies the entire central portion of Oak Ridges Moraine (Sharpe *et al.*, 1994). A period of slight retreat brought the Simcoe ice lobe to the position marked by the Gibraltar Moraine (White, 1975). The Ontario ice lobe then advanced over the Niagara Escarpment to the area near Credit Forks. North of the Credit Forks, the ice remained at the base of the Escarpment (White, 1975). This advance deposited the Wentworth Till, and reached a terminal position marked by the Paris Moraine, which truncates the Singhampton Moraine (White, 1975). Early Lake

Schomberg may have occurred at this time (Chapman and Putnam, 1951; Karrow, 1974; Duckworth 1975, 1979), as the Ontario ice lobe crossed the Niagara Escarpment and blocked southward drainage. The Ontario ice lobe then retreated slightly to the Galt Moraine.

#### Mackinaw Interstade

The retreat of the ice lobes signaled the initiation of the Mackinaw Interstade. It is generally accepted that the Oak Ridges Moraine started to accumulate at this time (approximately 13.5 ka to 12.5 ka; Sharpe *et al.*, 1994), as the Ontario ice lobe separated from the Simcoe ice lobe near the central portion of the Oak Ridges Moraine, and sediments were deposited into the interlobate basin.

The upper outwash outlets associated with the Paris and Galt Moraines (i.e., Caledon and Belfountain Outlets; Fig. 5.1) were utilized during the maximum extent of the Ontario ice lobe. The Caledon Outlet is located between the Singhampton and Paris Moraines (Fig. 5.1; Chapman, 1985) and numerous erosional terraces associated with the Caledon outwash have been documented along the Paris Moraine (White, 1975). The Caledon outwash plain is approximately one mile wide near Caledon, traverses the rim of the Niagara Escarpment, and reaches a basal elevation of approximately 430 m. It is thought that this would have been the controlling outlet at the time of deposition of the Bloomington fan complex.

As the ice retreated to the escarpment, glaciofluvial outwash was deposited between the moraine systems and the edge of the Niagara Escarpment, with possible drainage into an early phase of Lake Whittlesey (White, 1975). Progressively lower outlets would have become active drainage channels as the Ontario ice lobe retreated. These include the Belfountain Outlet (Fig. 5.1; Chapman, 1985), with a basal elevation of 380 m, and the Cheltenham Outlet, which has basal elevations ranging from 367 m (scoured bare rock on top of the Niagara Escarpment, with a

boulder lag) to 350 m (where it breaks through the Galt Moraine; Fig. 5.1; Chapman, 1985). Once both of these outlets were opened, water levels in the interlobate lake basin would drop, initiating the glaciofluvial incision of phase 2. Progressive and then complete retreat from the Niagara Escarpment would have eventually dropped water levels below the phase 2 elevations, and caused the Bloomington fan complex to become completely abandoned.

#### Port Huron Stade

The Port Huron Stade was initiated by rapid ice advances out of the lake basins. The Simcoe ice lobe may have been the first to advance (P.J. Barnett, pers. comm., 1994), from the north, blocking westward drainage, and causing lake levels to rise in the interlobate lake basin. This may have triggered the Ontario ice lobe advance from the south, deposited the Halton Till, and reach a terminal position marked either by the Acton Moraine (Straw, 1968, Karrow, 1991) and/or the Palgrave Moraine (White, 1975).

The Acton Moraine is comprised of hummocky ridges of glaciofluvial sand and gravel (White, 1975; Straw, 1968; Karrow, 1991). Previous work did not differentiate the Acton from the Galt Moraines (e.g. Chapman and Putnam, 1984) and Paris Moraines (White, 1975). However, Straw (1968) and Karrow (1991) believed the Acton Moraine to be separate, and consider it to represent the furthest extent of the Halton advance (Karrow, 1991). The Acton Moraine reaches a maximum elevation of approximately 370 m, marked by an ice-contact slope at 350 m, and is entirely located above the crest of the Niagara Escarpment. Therefore, phase 3 sediments were deposited during late stages of the Halton advance, with lake levels controlled by the Acton outlet.

It is thought the inception of Lake Whittlesey took place during this stade, at approximately 13 ka (e.g., Barnett, 1979; Karrow and Calkin, 1985). Barnett (1979)

noted shorebluffs associated with Lake Whittlesey on the Galt Moraine (Barnett, 1979). As a result, Whittlesey probably existed after the formation of the Galt Moraine, contrary to the belief of White (1975) that Whittlesey existed early in the Port Huron Stade during the formation of the Paris and Singhampton Moraines. Based on this evidence, Barnett (1979) suggested that Lake Whittlesey levels rose during the Halton advance, and may have been fed by meltwater draining the interlobate lake basin during phase 3. Most workers believe water levels rose to 226 m in the south Huron basin (Barnett, 1979, 1985; Eschman and Karrow, 1985). High levels of Lake Whittlesey (Barnett, 1979) marked by higher strandlines in the northern portion of the lake, and the Summit delta at Ancaster, range from 241 to 265 m (Fig. 5.1).

As the ice margins retreated from the area, water ponded between the ice and the crest of the Oak Ridges Moraine, and deposited Lake Schomberg sediments on the north flank, and Lake Peel sediments on the south flank of the Oak Ridges Moraine.

### 5.2.3 Summary

The preceding section describes a possible scenario in which water levels in the interlobate basin are controlled by ice margin positions along the Niagara Escarpment. Similar suggestions have been made by other workers for central portions of the Oak Ridges Moraine (Straw, 1968; Chapman, 1985), including the Bloomington fan complex. However, recent work has been inconclusive as to whether the interlobate lake basin would have existed as far west as the Niagara Escarpment. The Simcoe and Ontario ice lobes may have coalesced east of the Niagara Escarpment to form a completely ice-enclosed lake basin during the relatively deep water phases of deposition of the Bloomington fan (i.e., phases 1 and 3). However, given coalescing lobes, the ultimate control on water levels may still have been the escarpment, as low-profile ice margins may not have effectively

dammed drainage westward (P.J. Barnett, pers. comm., 1994).

During the initial phase, water levels may have been controlled by the Caledon outlet (Fig. 5.1; elevation 430 m). As the southern ice retreated from the Niagara Escarpment, water levels dropped in the lake basin. Water levels then subsequently rose in response to the Ontario ice lobe re-advance which closed westward outlets, and phase 3 was deposited.

## 6.0 CONCLUSIONS

During the initial stages of retreat in the Mackinaw Interstade, the ice divided into two lobes, one to the north and another to the south of the study area, and formed a confined, interlobate lake basin. Meltwater from the northern (Simcoe) ice lobe deposited the main sediment body of the Bloomington fan complex, one of the earliest elements of the Oak Ridges Moraine. Sediments comprising the main sediment body were deposited from multiple conduits, and produced a fan complex characterized by multiple, laterally overlapping, fans.

Subglacial drainage of the Simcoe ice lobe included an anastomosing network of subglacial conduits. Early stages of growth of the Bloomington fan complex occurred at the most westerly conduits. As the northern ice retreated, conduits to the north and east fed the fan complex. Progressive capture of subglacial meltwater by increasingly easterly conduits ultimately resulted in the main conduit at the northeastern margin of the deposit dominating the formation of the fan complex.

Continued retreat of both the Simcoe and southern (Ontario) ice lobes opened westward drainage outlets, possibly along the Niagara Escarpment, and caused water level to fall in the lake basin. Initially, subaerial glaciofluvial sand and gravel was deposited in a re-entrant which formed as the main conduit collapsed. The glaciofluvial system eroded a broad, shallow channel into the underlying fan. Retreat of the northern ice also allowed glaciofluvial sediments to be deposited in a confined zone between the fan body and the retreating ice margin, and eroded an incised, 11 m deep channel.

Subsequent readvance of the northern ice closed the westerly outlets of the lake basin and caused water levels to rise, and probably initiated the readvance of the southern ice (P.J. Barnett, pers. comm., 1994). Glaciolacustrine rhythmites were deposited on top of the fan and glaciofluvial sediment. As the Ontario ice lobe



approached the Bloomington fan complex it deposited an ice-marginal complex consisting of glacial sediment gravity flows, and glaciolacustrine and glaciofluvial sediments that preserve north and northwesterly paleocurrent indicators. Continued advance of the Ontario ice lobe produced large-scale glaciotectonic deformation structures, and deposited the Halton Till as it overrode the Bloomington fan complex.

Very few previous models of subaqueous fans document similarly complex facies associations produced by multiple conduit sources of sediment. The dynamic proglacial lacustrine environment is made more complicated by this multiple feeder system, and by the configuration of the small ice-bound lake which narrowed towards the distal margin of the deposit. This acted to confine flows on the fan, particularly to the southwest where uniform units of generally higher energy facies were deposited, contemporaneous with deposition of distal facies in the broader, central portion of the fan.

The Bloomington fan complex was further complicated by major changes in depositional environments due to changes in water level in the interlobate lake. This was initiated by the influence of two separate ice lobes which moved across the study area in opposite directions. Not only did these moving lobes cause changes in water level in the interlobate basin, but also caused deposition from two distinct source directions. Finally, erosion, deposition, and deformation of the deposit with the readvance of the southern ice contributed to the complexity of the Bloomington fan complex.

## 7.0 REFERENCES

- Aber, J.S., Croot, D.G., and Fenton, M. 1989. Glaciotectonic landforms and structures. Kluwer Academic Publishers, Boston, Ma, 200 p.
- Allen, J.R.L. 1970. A quantitative model of climbing ripples and their cross-laminated deposits. *Sedimentology*, **18**: 5-26.
- Allen, J.R.L. 1982. Sedimentary Structures. Their character and physical basis, volume 1. Development in Sedimentology 30A. Elsevier Scientific Publishing Company, New York, 593 p.
- Allen, J.R.L. 1983. Gravel overpassing on humpback bars supplied with mixed sediment: examples from the Lower Old Red Sandstone, southern Britain. *Sedimentology*, **30**: 285-294.
- Ashley, G.M., Southard, J.B., and Boothroyd, J.C. 1982. Deposition of climbing-ripple beds: a flume simulation. *Sedimentology*, **29**: 67-79.
- Ashley, G.M., Shaw, J., and Smith, N.D. 1985. Glacial Sedimentary Environments. Society of Economic Paleontologists and Mineralogists, Short Course No. 16, 246 p.
- Baker, V.R. 1984. Flood sedimentation in bedrock fluvial systems. *In* Sedimentology of Gravels and Conglomerates. *Edited by* E.H. Koster and R.J. Steel. Canadian Society of Petroleum Geologists, Memoir 10, p. 87-98.
- Banerjee, I., and McDonald, B.C. 1975. Nature of Esker Sedimentation. *In* Glaciofluvial and Glaciolacustrine Sedimentation. *Edited by* A.V. Jopling and B.C. McDonald. Society of Economic Paleontologists and Mineralogists, Special Publication 23, pp. 132-154.
- Banham, P.H. 1975. Glaciotectonic structures: a general discussion with particular reference to the Contorted drift of Norfolk. *In* Ice Ages, Ancient and Modern. *Edited by* A.E. Wright and F. Moseley. Seel House Press, Liverpool, pp. 69-94.
- Barnett, P.J. 1979. Glacial Lake Whittlesey: the probable ice frontal position in the Eastern end of the Erie Basin. *Canadian Journal of Earth Sciences*, **16**: 568-574.
- Barnett, P.J. 1985. Glacial retreat and lake levels, north-central Lake Erie basin, Ontario. *In* Quaternary Evolution of the Great Lakes. *Edited by* P.F. Karrow and P.E. Calkin. Geological Association of Canada, Special Paper 30, pp. 185-194.
- Barnett, P.J. 1990. Tunnel valleys: evidence of catastrophic release of subglacial meltwater, central-southern Ontario, Canada. Geological Society of America, Northeastern Section, Program with Abstracts, **22**: 3.

- Barnett, P.J. 1992a Geological investigations in the Oak Ridges Moraine Area, Whitchurch-Stouffville and Uxbridge Township Municipalities, Ontario. *In* Summary of Field Work and Other Activities 1992, Ontario Geological Survey, Miscellaneous Paper 160, pp. 144-146.
- Barnett, P.J. 1992b. Quaternary Geology of Ontario. *In* Geology of Ontario, Ontario Geological Survey, Special Volume 4, Part 2, pp. 1011-1088.
- Barnett, P.J. 1993. Geological investigations in the Oak Ridges Moraine Area, parts of Scugog, Manvers and Newcastle Township Municipalities and Oshawa City Municipality, Ontario. *In* Summary of Field Work and Other Activities 1993, Ontario Geological Survey, Miscellaneous Paper 162, pp. 158-159.
- Benn, D.I. 1989. Controls on sedimentation in a late Devensian ice-dammed lake, Achnasheen, Scotland. *Boreas*, **18**: 31-42.
- Berthelsen, A. 1979. Recumbent folds and boudinage structures formed by subglacial shear: an example of gravity tectonics. *Geologie En Mijnbouw*, **58**: 253-260.
- Bigsby, J.J. 1829. A sketch of the topography and geology of Lake Ontario. *Philosophical Magazine*, **5**, 1-5, 81-87, 263-274, 339-347, 424-431.
- Bluck, B.J. 1974. Structure and directional properties of some sandur deposits in southern Iceland. *Sedimentology*, **21**, 533-554.
- Boothroyd, J.C. 1972. Coarse-grained sedimentation on a braided outwash fan, northeast Gulf of Alaska. Technical Report No 6-CRD, Coastal Research Division, University of South Carolina, 127 p.
- Boothroyd, J. C., and Ashley, G. M. 1975. Processes, bar morphology, and sedimentary structures on braided outwash fans, Northeastern Gulf of Alaska. *In* Glaciofluvial and Glaciolacustrine Sedimentation. *Edited by* A. V. Jopling and B. C. McDonald. Society of Economic Paleontologists and Mineralogists, Special Publication 23, pp. 193-222.
- Boulton, G.S. 1971. Till genesis and fabric in Svalbard, Spitsbergen. *In* Till, a Symposium. *Edited by* R.P. Goldthwait. Ohio State University Press, Columbus, pp. 41-72.
- Boulton, G.S. 1986. Push-moraines and glacier-contact fans in marine and terrestrial environments. *Sedimentology*, **33**: 677-698.
- Boulton, G.S. 1987. A theory of drumlin formation by subglacial deformation. *In* Drumlin Symposium. *Edited by* J. Menzies and J. Rose. Balkema, Rotterdam, pp. 25-80.
- Boyd, R., Scott, D.B., and Douma, M. 1988. Glacial tunnel valleys and Quaternary history of the outer Scotian Shelf. *Nature*, **333**: 61-64.

- Brennand, T.A., and Sharpe, D.R. 1993. Ice-sheet dynamics and subglacial meltwater regime inferred from form and sedimentology of glaciofluvial systems: Victoria Island, District of Franklin, Northwest Territories. *Canadian Journal of Earth Sciences*, **30**: 928-944.
- Brennand, T.A., and Shaw, J. 1994. Tunnel channels and associated landforms, south-central Ontario: their implications for ice-sheet hydrology. *Canadian Journal of Earth Sciences*, **31**: 505-522.
- Bridge, J.S. 1984. Large-scale facies sequences in alluvial overbank environments. *Journal of Sedimentary Petrology*, **54**: 583-588.
- Brookfield, M.E., Gwyn, Q.H.J., and Martini, I.P. 1982. Quaternary sequences along the north shore of Lake Ontario: Oshawa-Port Hope. *Canadian Journal of Earth Sciences*, **22**: 33-41.
- Broster, B.E., and Hicock, S.R. 1985. Multiple flow and support mechanisms and the development of inverse grading in a subaquatic glacial debris flow. *Sedimentology*, **32**: 645-657.
- Burbidge, G.H., and Rust, B.R. 1988. A Champlain Sea subwash fan at St. Lazare, Quebec. *Geological Association of Canada, Special Paper 35*, pp. 47-61.
- Carling, P.A. 1990. Particle over-passing on depth-limited gravel bars. *Sedimentology*, **37**: 345-355.
- Carling, P.A., and Glaister, M.S. 1987. Rapid deposition of sand and gravel mixtures downstream of a negative step: the role of matrix-infilling and particle-overpassing in the process of bar-front accretion. *Journal of the Geological Society of London*, **144**: 543-551.
- Carter, R.M. 1975. A discussion and classification of subaqueous mass-transport, with particular application to grain-flow, slurry-flow and fluxoturbidites. *Earth Science Reviews*, **11**, 145-177.
- Chapman, L.J. 1985. On the origin of the Oak Ridges Moraine, southern Ontario. *Canadian Journal of Earth Sciences*, **22**: 300-303.
- Chapman, L.J., and Putnam, D.F. 1943. The moraines of Southern Ontario. *Transactions of the Royal Society of Canada, 3rd Series, Volume 37, Section 4*: 33-41.
- Chapman, L.J., and Putnam, D.F. 1951. *The physiography of southern Ontario*. University of Toronto Press, Toronto, Ontario, 284 p.
- Chapman, L.J., and Putnam, D.F. 1966. *The physiography of southern Ontario*. University of Toronto Press, 2nd edition, Toronto, Ontario, 386 p.
- Chapman, L.J., and Putnam, D.F. 1984. *The physiography of southern Ontario*. Ontario Geological Survey, Special Volume 2, 270 p.

- Cheel, R.J. 1982. The depositional history of an esker near Ottawa, Canada. *Canadian Journal of Earth Sciences*, **19**: 1417-1427.
- Cheel, R.J., and Middleton, G.V. 1986. Horizontal lamination formed under upper flow regime plane bed conditions. *Journal of Geology*, **94**: 489-504.
- Cheel, R.J., and Rust, B.R. 1982. Coarse-grained facies of glaciomarine deposits near Ottawa, Canada. *In* Research in Glacial, Glacio-fluvial, and Glacio-lacustrine Systems. *Edited by* R. Davidson-Arnott, W. Nickling and B.D. Fahey. 6th Guelph Symposium on Geomorphology, GeoBooks, Norwich, pp. 279-295.
- Cheel, R.J., and Rust, B.R. 1986. A sequence of soft-sediment deformation (dewatering) structures in Late Quaternary outwash near Ottawa, Canada. *Sedimentary Geology*, **47**: 77-93.
- Church, M., and Gilbert, R. 1975. Proglacial and lacustrine environments. *In* Glaciofluvial and Glaciolacustrine Sedimentation. *Edited by* A.V. Jopling and B.C. McDonald. Society of Economic Paleontologists and Mineralogists, Special Publication 23, pp. 22-100.
- Clemmensen, L.B., and Houmark-Nielsen, M. 1981. Sedimentary features of a Weichselian glaciolacustrine delta. *Boreas*, **10**: 229-245.
- Coleman, A.P. 1899. Lake Iroquois and its predecessors at Toronto. *Geological Society of America Bulletin*, **10**: 165-176.
- Collinson, J.D., and Thompson, D.B. 1989. *Sedimentary Structures*, second edition. Chapman & Hall, London, 207 p.
- Costello, W.R., and Walker, R.G. 1972. Pleistocene sedimentology, Credit River, Southern Ontario: A new component of the braided river model. *Journal of Sedimentary Petrology*, **42**: 389-400.
- Cowan, W.R. 1976. Quaternary Geology of the Orangeville area, southern Ontario. Ontario Division of Mines, Geological Report 119, 91 p.
- Cowan, W.R., Sharpe, D.R., Feenstra, B.H. and Gwyn, Q.H.J. 1978. Glacial geology of the Toronto-Owen Sound area. *In* Toronto '78 Field Trips Guidebook for a Joint Meeting of the Geological Society of America, The Geological Association of Canada and The Mineralogical Association of Canada, pp. 1-16.
- Dawson, M.R., and Bryant, I.D. 1987. Three-dimensional facies geometry in Pleistocene outwash sediments, Worcestershire, U.K. *In* Recent Developments in Fluvial Sedimentology. *Edited by* F.G. Ethridge, R.M. Flores, and M.D. Harvey. Society of Economic Paleontologists and Mineralogists, Special Publication 39, pp. 191-196.
- De Jong, M.G.G., and Rappol, M. 1983. Ice-marginal debris-flow deposits in western Allgäu, southern West Germany. *Boreas*, **12**: 57-70.

- Delorme, R.J. 1989. A sedimentological study of subaquatic outwash fans, in bedrock controlled terrain, near Ullswater, Ontario. Unpublished M. Sc. Thesis, University of Waterloo, Waterloo, Ontario, 181 p.
- Diemer, J.A. 1988. Subaqueous outwash deposits in the Ingraham ridge, Chazy, New York. *Canadian Journal of Earth Sciences*, **25**: 1384-1396.
- Dowdeswell, J.A., and Sharp, M.J. 1986. Characterization of pebble fabrics in modern terrestrial glacial sediments. *Sedimentology*, **33**: 699-710.
- Dowdeswell, J.A., Hambrey, M.J., and Wu, R. 1985. A comparison of clast fabric and shape in Late Precambrian and modern glacial sediments. *Journal of Sedimentary Petrology*, **55**: 691-704.
- Dreimanis, A., and Goldthwait, R.P. 1973. Wisconsin glaciation in the Huron, Erie and Ontario lobes. *Geological Society of America Memoir* 136, p. 71-106.
- Duckworth, P.B. 1975. Paleocurrent trends in the latest outwash at the western end of the Oak Ridges Moraine, southern Ontario. Unpublished Ph.D. thesis, University of Toronto, Toronto, Ontario, 259 p.
- Duckworth, P.B. 1979. The late depositional history of the western end of the Oak Ridges Moraine, Ontario. *Canadian Journal of Earth Sciences*, **16**: 1094-1107.
- Duckworth, P.B. 1982. The Oak Ridges Moraine in Whitchurch and Uxbridge Townships. In *Excursion 11A: Late Quaternary sedimentary environments of a glaciated area: Southern Ontario*. Edited by P.F. Karrow, A.V. Jopling, and I.P. Martini. International Association of Sedimentologists, Eleventh International Congress on Sedimentology, pp. 23-30.
- Elliot, T. 1974. Interdistributary bay sequences and their genesis. *Sedimentology*, **21**: 611-622.
- Eschman, D.F., and Karrow, P.F. 1985. Huron basin glacial lakes: a review. In *Quaternary Evolution of the Great Lakes*. Edited by P. F. Karrow and P. E. Calkin. Geological Association of Canada, Special Paper 30, pp. 79-93.
- Evenson, E.B., Dreimanis, A., and Newsome, J.W. 1977. Subaquatic flow tills: a new interpretation for the genesis of some laminated till deposits. *Boreas*, **6**: 114-133.
- Eyles, C.H. and Eyles, N. 1983. Sedimentation in a large lake: a reinterpretation of the late Pleistocene stratigraphy at Scarborough Bluffs, Ontario, Canada. *Geology*, **11**: 146-152.
- Eyles, N. 1977. Late Wisconsinan glacial tectonic structures and evidence of postglacial permafrost in north-central Newfoundland. *Canadian Journal of Earth Sciences*, **14**: 2797-2806.
- Eyles, N. 1987. Late Pleistocene debris-flow deposits in large glacial lakes in British Columbia and Alaska. *Sedimentary Geology*, **53**: 33-71.

- Eyles, N., and Kocsis, S. 1988. Sedimentology and clast fabric of subaerial debris flow facies in a glacially-influenced alluvial fan. *Sedimentary Geology*, **59**: 15-28.
- Eyles, N., Clark, B.M., Kaye, B.G., Howard, K.W.F., and Eyles, C.H. 1985. The application of basin analysis techniques to glaciated terrains: An example from the Lake Ontario basin, Canada. *Geoscience*, **12**: 22-32.
- Fahnestock, R.K., and Haushild, W.L. 1962. Flume studies of transport of pebbles and cobbles on a sand bed. *Geological Society of America Bulletin*, **73**: 1431-1436.
- Farrell, K.M. 1987. Sedimentology and facies architecture of overbank deposits of the Mississippi River, False River Region, Louisiana. *In* Recent Developments in Fluvial Sedimentology. *Edited by* F.G. Ethridge, R.M. Flores, and M.D. Harvey. Society of Economic Paleontologists and Mineralogists, Special Publication 39, pp. 111-120.
- Feenstra, B.H. 1981. Quaternary geology and industrial minerals of the Niagara-Welland area, southern Ontario. Ontario Geological Survey, Open File Report 5361, 260 p.
- Fielding, C.R. 1984. Upper delta plain lacustrine and fluviolacustrine facies from the Westphalian of the Durham coalfield, NE England. *Sedimentology*, **31**: 547-567.
- Flint, J.J., and Lolcama, J. 1985. Buried ancestral drainage between Lakes Erie and Ontario. *Geological Society of America Bulletin*, **97**: 75-84.
- Fraser, G.S. 1993. Sedimentation in an interlobate outwash stream. *Sedimentary Geology*, **83**: 53-70.
- Gorrell, G. 1986. Development of a subaqueous outwash fan, an example from the County of Lanark, Ontario, Canada. Unpublished M.Sc. thesis, Queen's University, Kingston, Ontario, 239 p.
- Gorrell, G., and Shaw, J. 1991. Deposition in an esker, bead and fan complex, Lanark, Ontario, Canada. *Sedimentary Geology*, **72**: 285-314.
- Gravenor, C.P. 1957. Surficial geology of the Lindsay-Peterborough area, Ontario. Geological Survey of Canada, Memoir 288, 68 p.
- Gravenor, C.P. 1985. Magnetic and pebble fabrics of glaciomarine diamictons in the Champlain Sea, Ontario, Canada. *Canadian Journal of Earth Sciences*, **22**: 422-434.
- Gravenor, C.P. 1986. Magnetic and pebble fabrics in subaquatic debris-flow deposits. *Journal of Geology*, **94**: 683-698.
- Grube, F. 1983. Tunnel valleys. *In* Glacial deposits in north-west Europe. *Edited by* J. Ehlers. A.A. Balkema, Rotterdam, pp. 257-258.

- Gustavson, T.C. 1974. Sedimentation on gravel outwash fans, Malaspina Glacier Foreland, Alaska. *Journal of Sedimentary Petrology*, **44**: 374-389.
- Gustavson, T.C., Ashley, G.M., and Boothroyd, J.C. 1975. Depositional sequences in glaciolacustrine deltas. *In* *Glaciofluvial and Glaciolacustrine Sedimentation*. Edited by A. V. Jopling and B. C. McDonald. Society of Economic Paleontologists and Mineralogists, Special Publication 23, pp. 264-280.
- Gwyn, Q.H.J. 1972. Quaternary geology of the Alliston-Newmarket area, southern Ontario. Ontario Division of Mines, Miscellaneous Paper 53, pp. 144-147.
- Gwyn, Q.H.J., and Cowan, W.R. 1978. The origin of the Oak Ridges and Orangeville Moraines of southern Ontario. *Canadian Geographer*, **22**: 345-352.
- Gwyn, Q.H.J., and DiLabio, R.N.W. 1973. Quaternary geology of the Newmarket area, southern Ontario. Ontario Division of Mines, Preliminary Map P. 836.
- Haldorsen, S., and Shaw, J. 1982. The problem of recognizing melt-out till. *Boreas*, **11**: 261-277.
- Hampton, M.A. 1979. Buoyancy in debris flows. *Journal of Sedimentary Petrology*, **49**: 753-793.
- Hansen, E., Porter, S.C., Hall, B.A., and Hills, A. 1961. Décollement structures in glacial-lake sediments. *Geological Society of America Bulletin*, **72**: 1415-1418.
- Hart, J.K. 1994. Proglacial glaciotectonic deformation at Melabakkar-Asbakkar, west Iceland. *Boreas*, **23**: 112-121.
- Hart, J.K., and Boulton, G.S. 1991. The interrelation of glaciotectonic and glaciodepositional processes within the glacial environment. *Quaternary Science Reviews*, **10**: 335-350.
- Hart, J.K., and Roberts, D.H. 1994. Criteria to distinguish between subglacial glaciotectonic and glaciomarine sedimentation, I. Deformation styles and sedimentology. *Sedimentary Geology*, **91**: 191-213.
- Hart, J.K., Hindmarsh, R.C.A., and Boulton, G.S. 1990. Styles of subglacial glaciotectonic deformation within the context of the Anglian ice-sheet. *Earth Surface Processes and Landforms*, **15**: 227-241.
- Hatcher, R.D., Jr. 1995. *Structural Geology: principles, concepts and problems*. Second Edition. Prentice-Hall, Englewood Cliffs, 525 p.
- Hayward, M., and French, H.M. 1980. Pleistocene marine kettle-fill deposits near Ottawa, Canada. *Canadian Journal of Earth Sciences*, **17**: 1236-1245.



- Hein, F.J. 1984. Deep-sea and fluvial braided channel conglomerates: a comparison of two case studies. *In* Sedimentology of Gravels and Conglomerates. *Edited by* E.H. Koster and R.J. Steel. Canadian Society of Petroleum Geologists, Memoir 10, p. 33-49.
- Hein, F.J., and Walker, R.G. 1977. Bar evolution and development of stratification in the gravelly, braided, Kicking Horse River, British Columbia. *Canadian Journal of Earth Sciences*, **14**: 562-570.
- Henderson, P.J. 1988. Sedimentation in an esker system influenced by bedrock topography near Kingston, Ontario. *Canadian Journal of Earth Sciences*, **25**: 987-999.
- Hewitt, D.F. 1969. Industrial Mineral Resources of the Markham-Newmarket Area. Ontario Department of Mines, Industrial Mineral Report No. 29, 105 p.
- Hewitt, D.F., and Karrow, 1963. Sand and gravel in Southern Ontario. Ontario Department of Mines, Industrial Minerals Report No. 11, 151 p.
- Hicock, S.R., and Dreimanis, A. 1985. Glaciotectonic structures as useful ice-movement indicators in glacial deposits: four Canadian case studies. *Canadian Journal of Earth Sciences*, **22**: 339-346.
- Hicock, S.R., Dreimanis, A., and Broster, B.E. 1981. Submarine flow tills at Victoria, British Columbia. *Canadian Journal of Earth Sciences*, **18**: 71-80.
- Hiscott, R.W., and Middleton, G.V. 1979. Depositional mechanics of thick-bedded sandstones at the base of a sub-marine slope, Tourella Formation (Lower Ordovician), Quebec, Canada. *In* Geology of Continental Slopes. *Edited by* L.J. Doyle and O.H. Pilkey Jr. Society of Economic Paleontologists and Mineralogists, Special Publication 27, pp. 307-326.
- Iseya, F., and Ikeda, H. 1987. Pulsations in bedload transport rates induced by a longitudinal sediment sorting: A flume study using sand and gravel mixtures. *Geografiska Annaler*, **69A**: 15-27.
- Johansson, C.E. 1963. Orientation of pebbles in running water. A laboratory study. *Geografiska Annaler*, **45A**: 85-112.
- Johnson, M.D., Armstrong, D.K., Sanford, B.V., Telford, B.V., and Rutka, M.A. 1992. Paleozoic and Mesozoic Geology of Ontario. *In* Geology of Ontario, Ontario Geological Survey, Special Volume 4, Part 2, pp. 907-1008.
- Jopling, A.V. 1965. Hydraulic factors controlling the shape of laminae in laboratory deltas. *Journal of Sedimentary Petrology*, **35**: 777-791.
- Jopling, A.V., and Walker, R.G. 1968. Morphology and origin of ripple-drift cross-laminations, with examples from the Pleistocene of Massachusetts. *Journal of Sedimentary Petrology*, **38**: 971-984.

- Kamb, B. 1987. Glacier surge mechanism based on linked cavity configuration of the basal water conduit system. *Journal of Geophysical Research*, **92B**: 9083-9100.
- Kamb, B., Raymond, C.F., Harrison, W.D., Engelhardt, H., Echelmeyer, K.A., Humphrey, N., Brugman, M. M., and Pfeffer, T. 1985. Glacier surge mechanism: 1982-1983 surge of Variegated Glacier, Alaska. *Science*, **227**: 469-479.
- Kanter, R. 1990. Space for all - options for a Greater Toronto area greenlands strategy. Ontario Government, 164 p.
- Karrow, P.F. 1963. Pleistocene geology of the Hamilton-Galt area, Ontario Department of Mines, Geological Report 16, 68 p.
- Karrow, P.F. 1967. Pleistocene geology of the Scarborough area. Ontario Department of Mines, Geological Report 46, 108 p.
- Karrow, P.F. 1974. Till stratigraphy in parts of Southwestern Ontario. *Geological Society of America Bulletin*, **85**: 761-768.
- Karrow, P.F. 1984. Quaternary stratigraphy and history, Great Lakes-St. Lawrence region. *In* Quaternary Stratigraphy of Canada-A Canadian Contribution to IGCP Project 25. Geological Survey of Canada, Paper 84-10, pp. 137-153.
- Karrow, P.F. 1989. Quaternary geology of the Great Lakes subregion. *In* Chapter 4, Quaternary Geology of Canada and Greenland, Geological Survey of Canada, Geology of Canada, no 1, pp. 326-350.
- Karrow, P.F. 1991. Quaternary geology of the Brampton area, Ontario Geological Survey Open File Report 5819, 136 p.
- Karrow, P.F., and Calkin, P.E. 1985. Quaternary evolution of the Great Lakes. Geological Association of Canada, Special Paper 30, 258 p.
- Kaszycki, C.A. 1987. A model for glacial and proglacial sedimentation in the shield terrane of southern Ontario. *Canadian Journal of Earth Sciences*, **24**: 2373-2391.
- Krzyszowski, D. 1994. Sedimentology of Wartanian outwash near Belchatów, central Poland. *Boreas*, **23**: 149-163.
- Kuhnle, R.A., and Southard, J.B. 1988. Bedload transport fluctuation in a gravel bed laboratory channel. *Water Resources Research*, **24**: 247-260.
- Lambert, A., and Hsü, K.J. 1979. Non-annual cycles of varve-like sedimentation in Walensee, Switzerland. *Sedimentology*, **26**: 453-461.
- Lash, G.G. 1984. Density-modified grain-flow deposits from an Early Paleozoic passive margin. *Journal of Sedimentary Petrology*, **54**: 557-562.
- Lawson, D.E. 1979. A comparison of the pebble orientations in ice and deposits of the Matanuska glacier, Alaska. *Journal of Geology*, **87**: 629-645.

- Lawson, D.E. 1988. Glacigenic resedimentation: Classification concepts and application to mass-movement processes and deposits. *In Genetic Classification of Glacigenic Deposits. Edited by R.P. Goldthwait and C.L. Matsch. Final Report of the INQUA Commission on Genesis and Lithology of Glacial Quaternary Deposits, Balkema, Rotterdam, pp. 147-172.*
- Leeder, 1983. On the interactions between turbulent flow, sediment transport and bedform mechanics in channelised flows. *In Modern and ancient fluvial systems. Edited by J.D. Collinson and J. Lewin. International Association of Sedimentologists, Special Publication 6, pp. 5-18.*
- Liberty, B.A. 1969. Paleozoic geology of the Lake Simcoe area, Ontario. Geological Survey of Canada Memoir 355, 201 p.
- Lindsay, J.F. 1968. The development of clast fabric in mudflows. *Journal of Sedimentary Petrology*, **38**: 1242-1253.
- Lindsay, J.F., Summerson, C.H., and Barrett, P.J. 1970. A long-axis clast fabric comparison of the squantum "Tillite", Massachusetts and the Gowganda Formation, Ontario. *Journal of Sedimentary Petrology*, **40**: 475-479.
- Logan, Sir W. 1863. Geology of Canada, Canada Geological Survey Summary Report, p. 983.
- Lowe, D.R. 1975. Water escape structures in coarse-grained sediments. *Sedimentology*, **22**: 157-204.
- Lowe, D.R. 1976a. Grain flow and grain flow deposits. *Journal of Sedimentary Petrology*, **46**: 188-199.
- Lowe, D.R. 1976b. Subaqueous liquefied and fluidized sediment flows and their deposits. *Sedimentology*, **23**: 285-308.
- Maizels, J.K. 1987. Large-scale flood deposits associated with the formation of coarse-grained, braided terrace sequences. *In Recent Developments in Fluvial Sedimentology. Edited by F. G. Ethridge, R. M. Flores and M. D. Harvey. Society of Economic Paleontologists and Mineralogists Special Publication No. 39, pp. 135-148.*
- Maizels, J.K. 1989. Sedimentology, paleoflow dynamics and flood history of jökulhlaup deposits: paleohydrology of Holocene sediment sequences in Southern Iceland sandur deposits. *Journal of Sedimentary Petrology*, **59**: 204-223.
- Maizels, J.K. 1991. The origin and evolution of Holocene sandur deposits in areas of jökulhlaup drainage, Iceland. *In Environmental Change in Iceland: Past and Present. Edited by J. K. Maizels and C. Caseldine. pp. 267-302.*
- Mark, D.M. 1973. Analysis of axial orientation data, including till fabrics. *Geological Society of America Bulletin*, **84**: 1369-1374.

- Mark, D.M. 1974. On the interpretation of till fabrics. *Geology*, **2**: 101-104.
- Martinsen, O.J. 1990. Fluvial, inertia-dominated deltaic deposition in the Namurian (Carboniferous) of northern England. *Sedimentology*, **37**: 1099-1113.
- McCabe, A.M., and Ó Cofaigh, C. 1994. Sedimentation in a subglacial lake, Enniskerry, eastern Ireland. *Sedimentary Geology*, **91**: 57-95.
- McDonald, B.C., and Shilts, W.W., 1975. Interpretation of faults in glaciofluvial systems. *In* Glaciofluvial and Glaciolacustrine Sedimentation. *Edited by* A.V. Jopling and B.C. McDonald. Society of Economic Paleontologists and Mineralogists, Special Publication 23, pp. 123-131.
- Menzies, J. 1979. Mechanics of drumlin formation. *Journal of Glaciology*, **27**: 372-384.
- Middleton, G.V., and Hampton, M.A. 1976. Subaqueous sediment transport and deposition by sediment gravity flows. *In* Marine Sediment Transport and Environmental Management. *Edited by* D.J. Stanley and D.J.P. Swift. John Wiley, New York, pp. 197-218.
- Mills, H.H. 1977. Basal till fabrics of modern alpine glaciers. *Geological Society of America Bulletin*, **88**: 824-828.
- Mills, P.C. 1983. Genesis and diagnostic value of soft-sediment deformation structures a review. *Sedimentary Geology*, **35**: 83-104.
- Mooers, H.D. 1989a. Drumlin formation: a time transgressive model. *Boreas*, **18**: 99-107.
- Mooers, H.D. 1989b. On the formation of the tunnel valleys of the Superior Lobe, central Minnesota. *Quaternary Research*, **32**: 24-35.
- Moran, S.R. 1971. Glaciotectonic structures in drift. *In* Till/ a symposium. *Edited by* R.P. Goldthwait. Ohio State University Press, pp. 127-148.
- Nye, J.F. 1976. Water flow in glaciers: Jökulhlaups, tunnels and veins. *Journal of Glaciology*, **17**: 181-207.
- Østrem, G. and Olsen, H.C. 1987. Sedimentation in a glacier lake. *Geografiska Annaler*, **69A**: 123-138.
- Paterson, J.T. 1991. Soft-sediment deformation structures found in subaqueous outwash deposits in bedrock-dominated terrain near Bracebridge, Ontario. Unpublished B.Sc. thesis, Queen's University, Kingston, Ontario, 173 p.
- Pharo, C.H., and Carmack, E.C. 1979. Sedimentation processes in a short residence-time intermontane lake, Kamloops Lake, British Columbia. *Sedimentology*, **26**: 523-541.

- Pickering, K.T. 1979. Possible retrogressive flow-slide deposits from the Kjongsfjord Formation. A Precambrian submarine fan, Finnmark, N. Norway. *Sedimentology*, **26**, 295-306.
- Postma, G. 1984. Slumps and their deposits in fan delta front and slope. *Geology*, **12**: 27-30.
- Postma, G. 1986. Classification for sediment gravity-flow deposits based on flow conditions during sedimentation. *Geology*, **14**: 291-294.
- Postma, G., Roep, T.B., and Ruegg, G.J.J. 1983. Sandy-gravelly mass-flow deposits in an ice-marginal lake (Saalian, Leuvenumsche Beek Valley, Veluwe, The Netherlands), with emphasis on plug-flow deposits. *Sedimentary Geology*, **34**: 59-82.
- Powell, R.D. 1981. A model for sedimentation by tidewater glaciers. *Annals of Glaciology*, **2**: 129-134.
- Ringrose, S. 1982. Depositional processes in the development of eskers in Manitoba. *In Research in Glacial, Glacio-fluvial, and Glacio-lacustrine Systems. Edited by R. Davidson-Arnott, W. Nickling and B.D. Fahey. 6th Guelph Symposium on Geomorphology, GeoBooks, Norwich, pp. 117-138.*
- Röthlisberger, H. 1972. Water pressure in intra- and subglacial channels. *Journal of Glaciology*, **11**: 177-203.
- Rubin, D.M., and Hunter, R.E. 1982. Bedform climbing in theory and nature. *Sedimentology*, **29**: 121-138.
- Russell, D.J., and Telford, P.G. 1983. Revisions to the stratigraphy of the Upper Ordovician Collingwood Beds of Ontario-A potential oil shale. *Canadian Journal of Earth Sciences*, **20**: 1780-1790.
- Rust, B.R. 1972. Pebble orientation in fluvial sediments. *Journal of Sedimentary Petrology*, **42**: 384-388.
- Rust, B.R. 1975. Fabric and structure in glaciofluvial gravels. *In Glaciofluvial and Glaciolacustrine Sedimentation. Edited by A.V. Jopling and B.C. McDonald. Society of Economic Paleontologists and Mineralogists, Special Publication 23, pp. 238-248.*
- Rust, B.R. 1977. Mass flow deposits in a Quaternary succession near Ottawa, Canada: diagnostic criteria for subaqueous outwash. *Canadian Journal of Earth Sciences*, **14**: 175-184.
- Rust, B.R. 1988. Ice-proximal deposits of the Champlain Sea at South Gloucester, near Ottawa, Canada. *In The Late Quaternary Development of the Champlain Sea Basin. Edited by N.R. Gadd. Geological Association of Canada, Special Paper 35, pp. 37-45.*

- Rust, B.R., and Romanelli, R. 1975. Late Quaternary subaqueous outwash deposits near Ottawa, Canada. *In* Glaciofluvial and Glaciolacustrine Sedimentation. *Edited by* A.V. Jopling and B.C. McDonald. Society of Economic Paleontologists and Mineralogists, Special Publication 23, pp. 177-192.
- Saunderson, H.C. 1977. The sliding bed facies in esker sands and gravels: a criterion for full-pipe (tunnel) flow? *Sedimentology*, **24**: 623-638.
- Sedimentary Petrology Seminar. 1965. Gravel fabric in Wolf Run. *Sedimentology*, **4**: 273-283.
- Sharp, M.J. 1982. Modification of clasts in lodgement tills by glacial erosion. *Journal of Glaciology*, **28**: 475-481.
- Sharpe, D.R. 1988a. Glaciomarine fan deposition in the Champlain Sea. *In* The Late Quaternary Development of the Champlain Sea Basin. *Edited by* N.R. Gadd. Geological Association of Canada, Special Paper 35, pp. 63-82.
- Sharpe, D.R. 1988b. The internal structure of glacial landforms: an example from the Halton till plain, Scarborough Bluffs, Ontario. *Boreas*, **17**: 15-26.
- Sharpe, D.R., Barnett, P.J., Dyke, L.D., Howard, K.W.F., Hunter, G.T., Gerber, R.E., Paterson, J., and Pullan, S.E. 1994. Quaternary geology and hydrogeology of the Oak Ridges Moraine Area. Geological Association of Canada, Mineralogical Association of Canada, Joint Annual Meeting, Waterloo, 1994. Field Trip A7: Guidebook, 32 p.
- Shaw, J. 1975. Sedimentary Successions in Pleistocene ice-marginal lakes. *In* Glaciofluvial and Glaciolacustrine Sedimentation. *Edited by* A. V. Jopling B. C. McDonald. Society of Economic Paleontologists and Mineralogists, Special Publication 23, pp. 28-303.
- Shaw, J. 1982. Melt-out till in the Edmonton area, Alberta, Canada. *Canadian Journal of Earth Sciences*, **19**: 1548-1569.
- Shaw, J. 1985. Subglacial and ice marginal environments. *In* Glacial Sedimentary Environments. *Edited by* G.M. Ashley, J. Shaw and N.D. Smith. Society of Economic Paleontologists and Mineralogists, Short Course No. 16, pp. 7-84.
- Shreve, R.L. 1972. Movement of water in glaciers. *Journal of Glaciology*, **11**: 205-214.
- Shreve, R.L. 1985. Esker characteristics in terms of glacier physics, Katahdin esker system, Maine. *Geological Society of America Bulletin*, **96**: 639-646.
- Smith, N.D. 1974. Sedimentology and bar formation in the Upper Kicking Horse River, a braided outwash stream. *Journal of Geology*, **82**: 205-225.
- Smith, N.D. 1985. Proglacial fluvial environment. *In* Glacial Sedimentary Environments. *Edited by* G.M. Ashley, J. Shaw and N.D. Smith. Society of Economic Paleontologists and Mineralogists, Short Course No. 16, pp. 85-134.

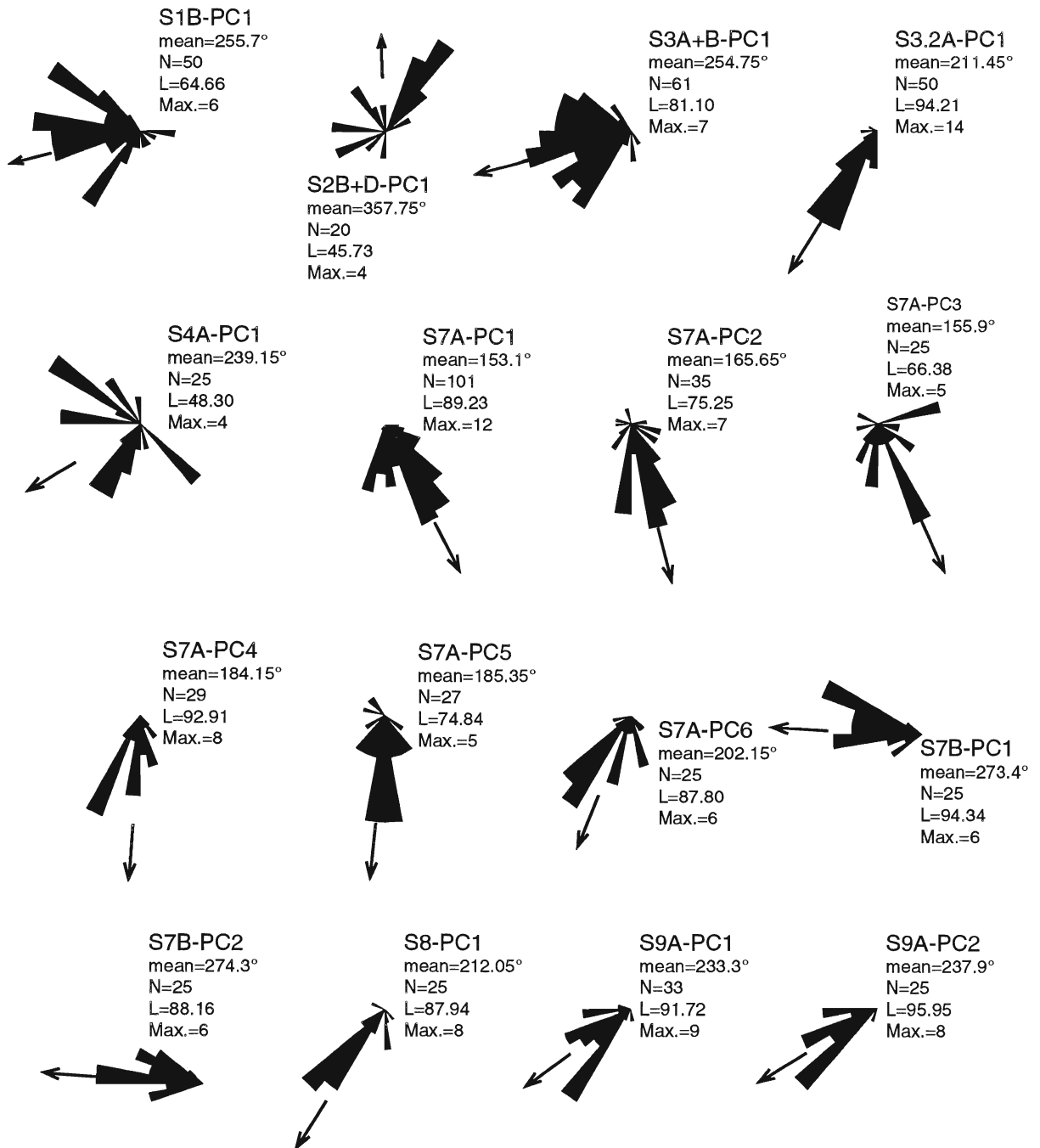
- Smith, N.D., and Ashley, G.M. 1985. Proglacial lacustrine environment. *In* Glacial Sedimentary Environments. *Edited by* G.M. Ashley, J. Shaw and N.D. Smith. Society of Economic Paleontologists and Mineralogists, Short Course No. 16, pp. 135-216.
- Spencer, J.W. 1890. Origin of the basins of the Great Lakes of America. *American Geologist*, 7:86-97.
- Spencer, J.W. 1907. The falls of Niagara, their evolution and varying relations to the Great Lakes, characteristics of the power and the effect of its diversion. Geological Survey of Canada, Report 970, 490 p.
- Spooner, I.S. 1988. Applied sedimentological evaluation of a glacial deposit, Joyceville, Ontario. Unpublished M. Sc. Thesis, Queen's University, Kingston, Ontario, 221 p.
- Steel, R.J., and Thompson, D.B. 1983. Structures and textures in Triassic braided stream conglomerates ('Bunter' Pebble Beds) in the Sherwood Sandstone Group, North Staffordshire, England. *Sedimentology*, 30: 341-367.
- Stow, D.A.V. 1986. Deep clastic seas. *In* Sedimentary Environments and Facies. Edited by H.G. Reading. Blackwell Scientific Publications, Oxford, pp. 399-444.
- Straw, A. 1968. Late Pleistocene glacial erosion along the Niagara Escarpment of Southern Ontario. *Geological Society of America Bulletin*, 79: 889-910.
- Talbot, C.J. Von Brunn, V. 1987. Intrusive and extrusive (micro)mélange couplets as distal effects of tidal pumping by a marine ice sheet. *Geological Magazine*, 124: 513-525.
- Taylor, F.B. 1913a. Moraines north of Toronto. Ontario Bureau of Mines, Annual Report 22, p. 256-260.
- Taylor, F.B. 1913b. The Moraine Systems of Southwestern Ontario. *Transactions of the Royal Canadian Institute*, 10: 57-79.
- Theakstone, W.H. 1976. Glacial lake sedimentation, Austerdalsisen, Norway. *Sedimentology*, 23: 671-688.
- Thomas, G.S.P. 1984. Sedimentation of a sub-aqueous esker-delta at Strabathie, Aberdeenshire. *Scottish Journal of Geology*, 20: 9-20.
- Thomas, G.S.P., and Connell, R.J. 1985. Iceberg drop, dump, and grounding structures from Pleistocene glacio-lacustrine sediments, Scotland. *Journal of Sedimentary Petrology*, 55: 243-249.
- van Gelder, A., van den Berg, J.H., Cheng, G., and Xue, C. 1994. Overbank and channelfill deposits of the modern Yellow River delta. *Sedimentary Geology*, 90: 293-305.

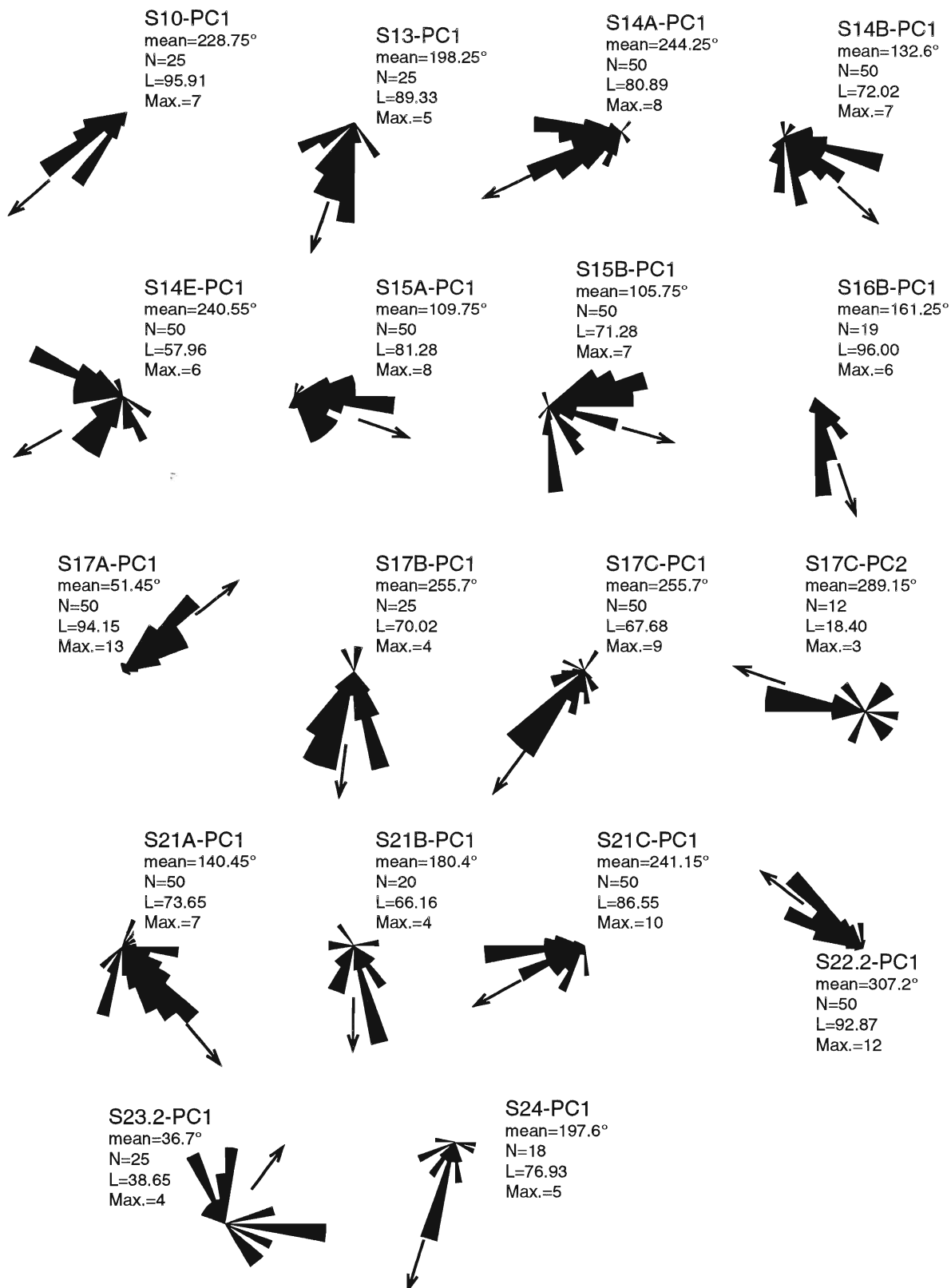
- Walker, R.G. 1975. Generalized facies models for resedimented conglomerates of turbidite association. *Geological Society of America Bulletin*, **86**: 737-748
- Walker, R.G. 1992. Turbidites and submarine fans. *In Facies Models: Response to Sea Level Change. Edited by R.G. Walker and N.P. James. Geological Association of Canada*, pp. 239-263.
- Wateren, D.F.M. van der, 1987. Structural geology and sedimentology of the Dammer Berge push moraine, FRG. *In Tills and Glaciotectonics. Edited by J.J.M. van der Meer. A.A. Balkema, Rotterdam*, pp. 157-182.
- White, O.L. 1975. Quaternary Geology of the Bolton Area, Southern Ontario. Ontario Division of Mines GR 117, 119 p. Accompanied by Maps 2275 and 2276, scale 1 inch to 1 mile.
- White, O.L., and Karrow, P.F. 1971. New evidence for Spencer's Laurentian River. *Proceedings of the 14th Conference on Great Lakes Research*, pp. 394-400.
- Whiting, P.J., Deitrich, W.E., Leopold, L.B., Drake, T.G., and Shreve, R.L. 1988. Bedload sheets in heterogeneous sediment. *Geology*, **16**: 105-108.
- Williams, P.F., and Rust, B.R. 1969. The sedimentology of a braided river. *Journal of Sedimentary Petrology*, **39**: 649-679.
- Woodcock, N.H. and Naylor, M.A. 1983. Randomness testing in three-dimensional orientation data. *Journal of Structural Geology*, **4**: 539-548.
- Wright, H.E., Jr. 1973. Tunnel valleys, Glacial surges, and subglacial hydrology of the Superior lobe, Minnesota. *In The Wisconsinan Stage. Edited by R.F. Black, R.P. Goldthwait, and H.B. Willman, Geological Society of America, Memoir 136*, pp. 251-276.
- Wright, L.D. 1977. Sediment transport and deposition at river mouths: a synthesis. *Geological Society of America Bulletin*, **88**: 857-868.



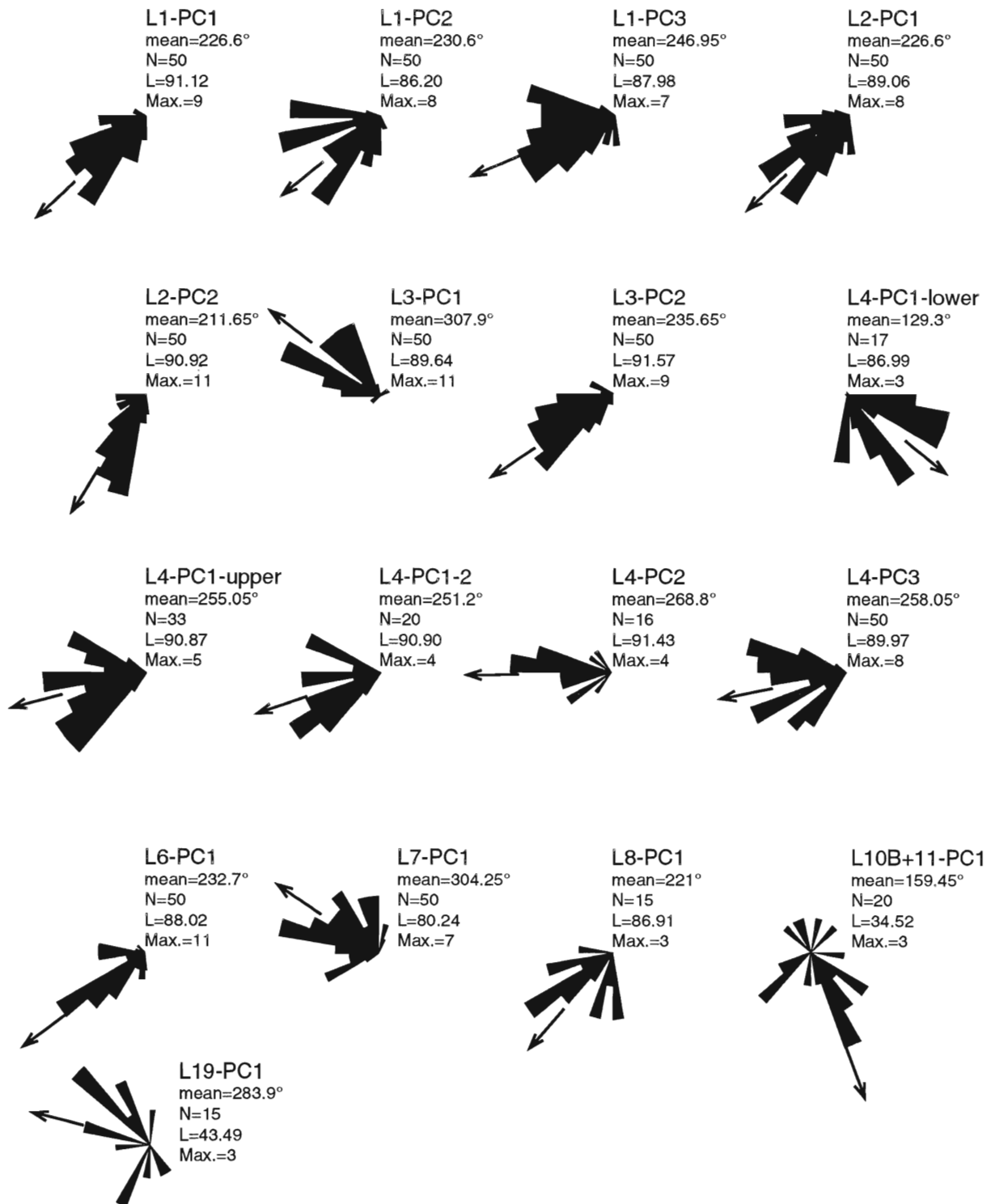
**APPENDIX I**  
**PALEOCURRENT DATA**

## STANDARD AGGREGATES PIT





## LEE SAND AND GRAVEL PIT



## APPENDIX II

### GRAVEL FABRICS

Stereonet plots of poles to a/b planes of clasts

contour interval  $2\sigma$

N=number of clasts

$V_1$ =direction of  $E_1$  eigenvector

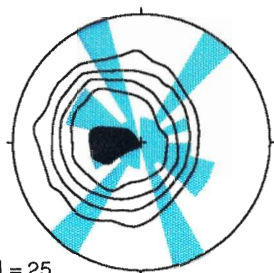
$S_1$ =strength of clustering around  $V_1$

Rose diagrams of a-axes of clasts

M.R.=maximum rose; number of observations at  
outside edge of stereonet

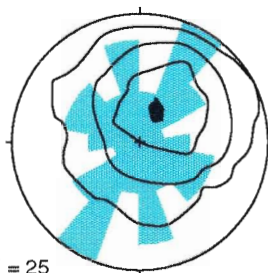
## FACIES 1

S12-AF1



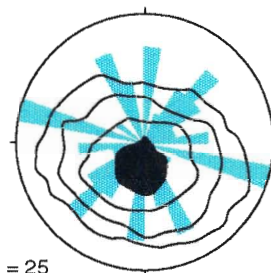
N = 25  
 $V_1=275^\circ, 74^\circ$   
 $S_1=0.849$   
 M.R.=5

S12-AF2



N = 25  
 $V_1=39^\circ, 66^\circ$   
 $S_1=0.663$   
 M.R.=5

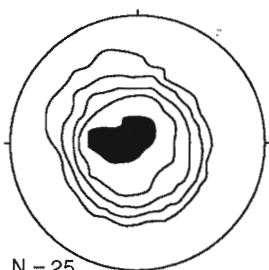
S13-AF1



N = 25  
 $V_1=190^\circ, 74^\circ$   
 $S_1=0.718$   
 M.R.=4

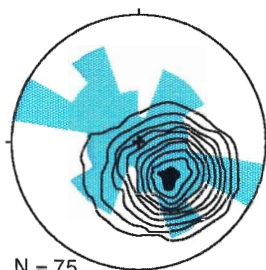
## FACIES 2

S1-AF1



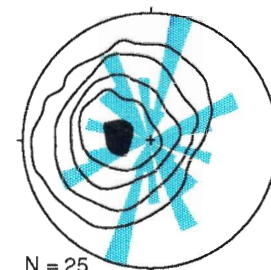
N = 25  
 $S_1=0.851$

S1-AF2, 2.2



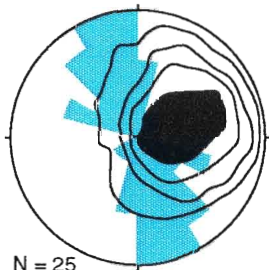
N = 75  
 $V_1=140^\circ, 63^\circ$   
 $S_1=0.832$   
 M.R.=5

S9-BF1.2



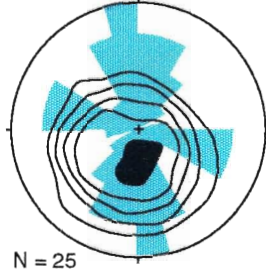
N = 25  
 $V_1=283^\circ, 70^\circ$   
 $S_1=0.787$   
 M.R.=4

S14-AF1



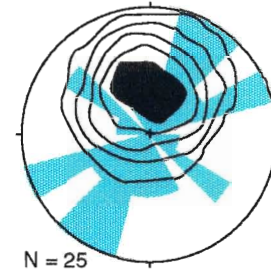
N = 25  
 $V_1=73^\circ, 60^\circ$   
 $S_1=0.775$   
 M.R.=5

S14-EF1



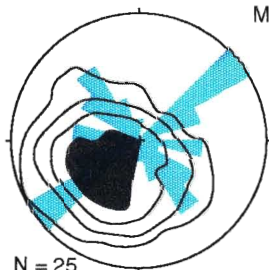
N = 25  
 $V_1=197^\circ, 70^\circ$   
 $S_1=0.857$   
 M.R.=4

S15-BF1



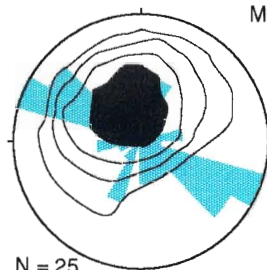
N = 25  
 $V_1=357^\circ, 62^\circ$   
 $S_1=0.860$   
 M.R.=4

S17-DF1



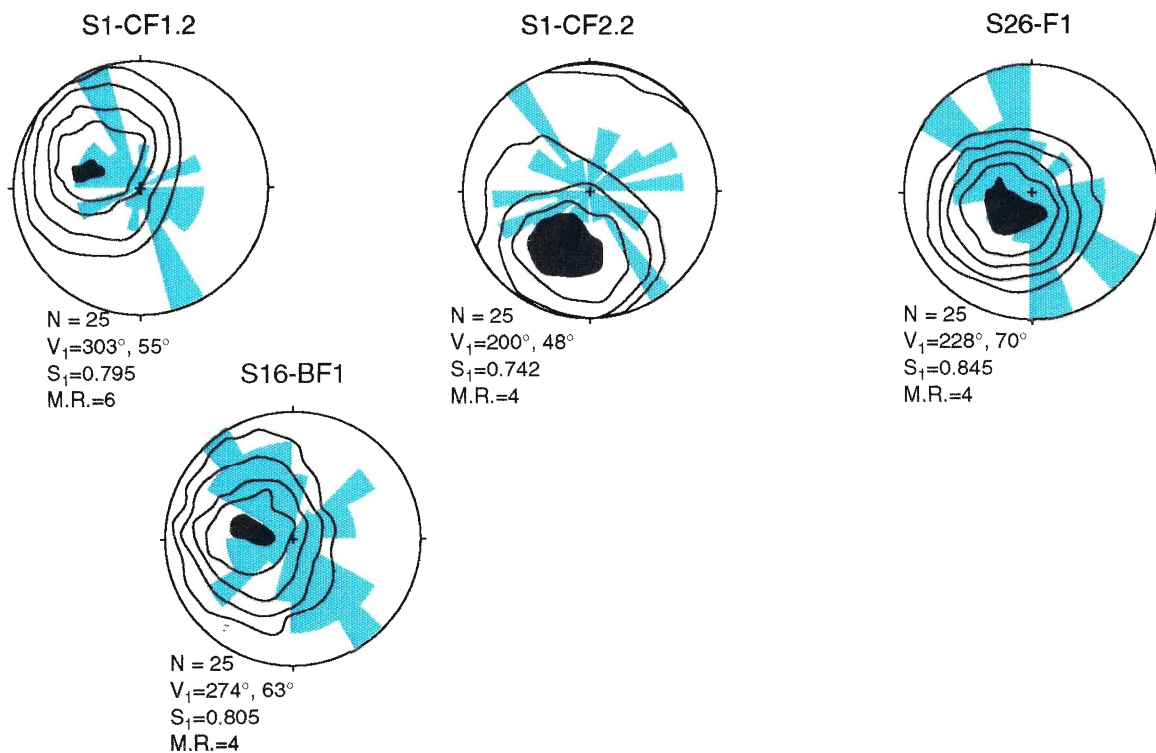
N = 25  
 $V_1=226^\circ, 64^\circ$   
 $S_1=0.765$   
 M.R.=6

L13-AF1

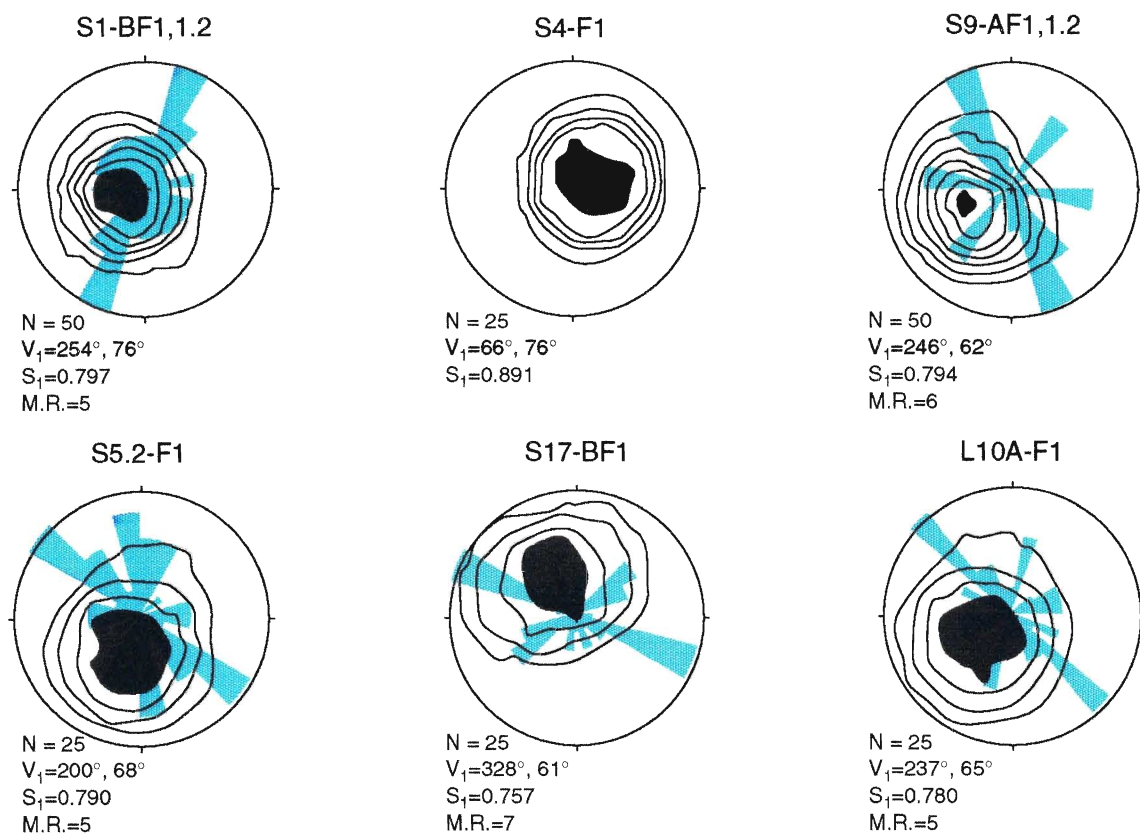


N = 25  
 $V_1=337^\circ, 68^\circ$   
 $S_1=0.786$   
 M.R.=6

## FACIES 3

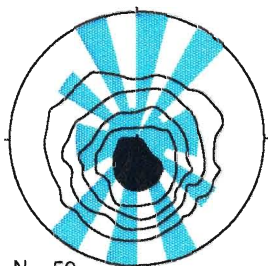


## FACIES 4



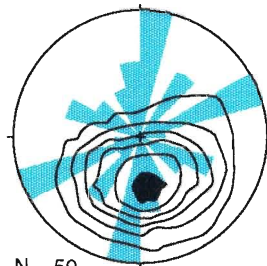
## FACIES 9

S10-BF1,1.2



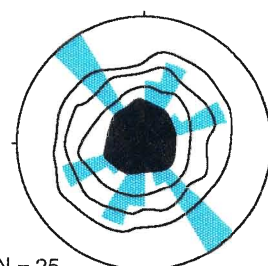
$N = 50$   
 $V_1 = 188^\circ, 76^\circ$   
 $S_1 = 0.721$   
 $M.R. = 4$

S11-AF1,2



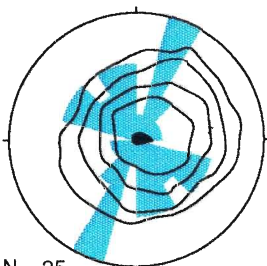
$N = 50$   
 $V_1 = 186^\circ, 52^\circ$   
 $S_1 = 0.739$   
 $M.R. = 5$

S14-CF1



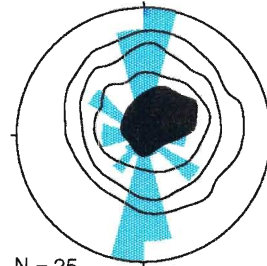
$N = 25$   
 $V_1 = 295^\circ, 88^\circ$   
 $S_1 = 0.772$   
 $M.R. = 6$

S14-CF2



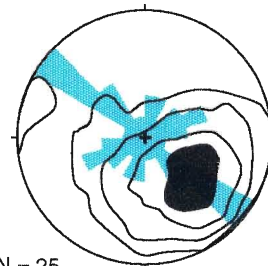
$N = 25$   
 $V_1 = 78^\circ, 78^\circ$   
 $S_1 = 0.795$   
 $M.R. = 5$

S14-CF3



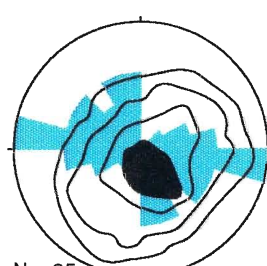
$N = 25$   
 $V_1 = 33^\circ, 80^\circ$   
 $S_1 = 0.755$   
 $M.R. = 6$

S14-CF4



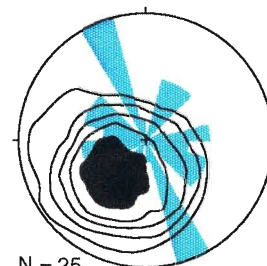
$N = 25$   
 $V_1 = 134^\circ, 51^\circ$   
 $S_1 = 0.709$   
 $M.R. = 6$

S21-BF1



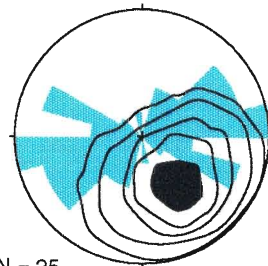
$N = 25$   
 $V_1 = 145^\circ, 77^\circ$   
 $S_1 = 0.719$   
 $M.R. = 4$

S21-BF2



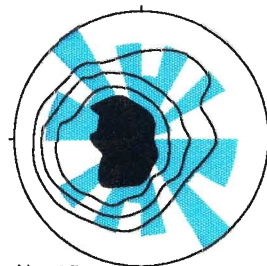
$N = 25$   
 $V_1 = 218^\circ, 61^\circ$   
 $S_1 = 0.873$   
 $M.R. = 6$

S22.2-BF1



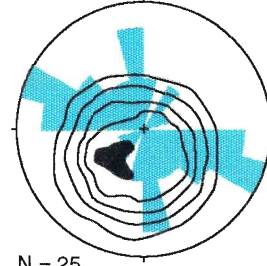
$N = 25$   
 $V_1 = 295^\circ, 88^\circ$   
 $S_1 = 0.772$   
 $M.R. = 6$

S23-AF1



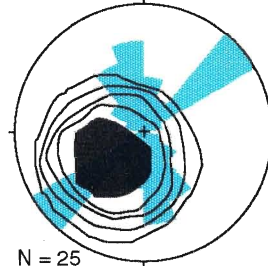
$N = 25$   
 $V_1 = 261^\circ, 75^\circ$   
 $S_1 = 0.772$   
 $M.R. = 4$

S24-AF1



$N = 25$   
 $V_1 = 195^\circ, 69^\circ$   
 $S_1 = 0.819$   
 $M.R. = 5$

L8-F1

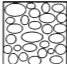


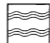


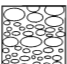



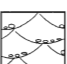
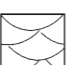
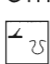
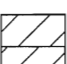



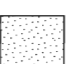
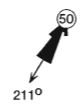

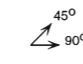





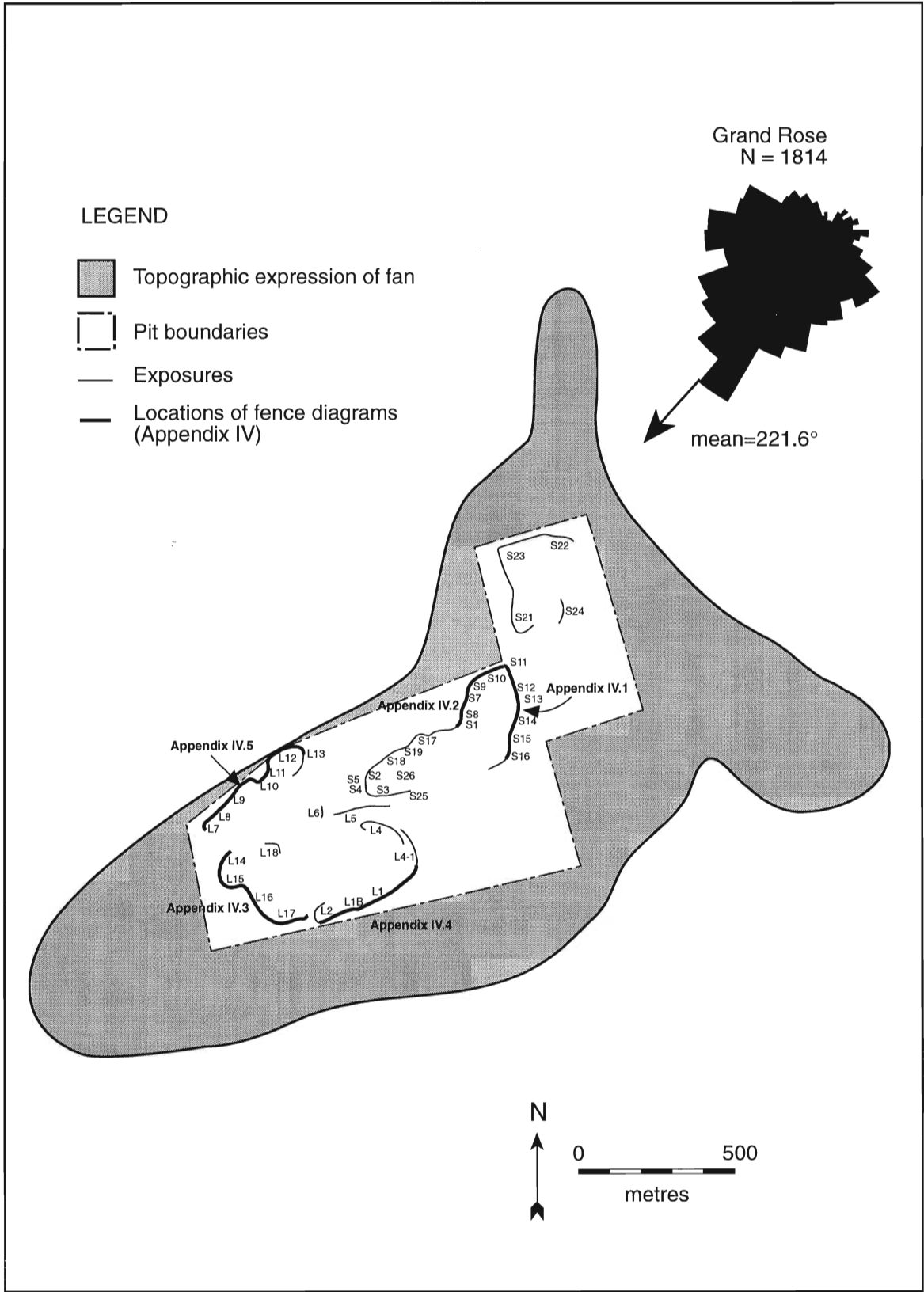
$N = 25$   
 $V_1 = 228^\circ, 63^\circ$   
 $S_1 = 0.795$   
 $M.R. = 7$



# APPENDIX III SECTION LOGS

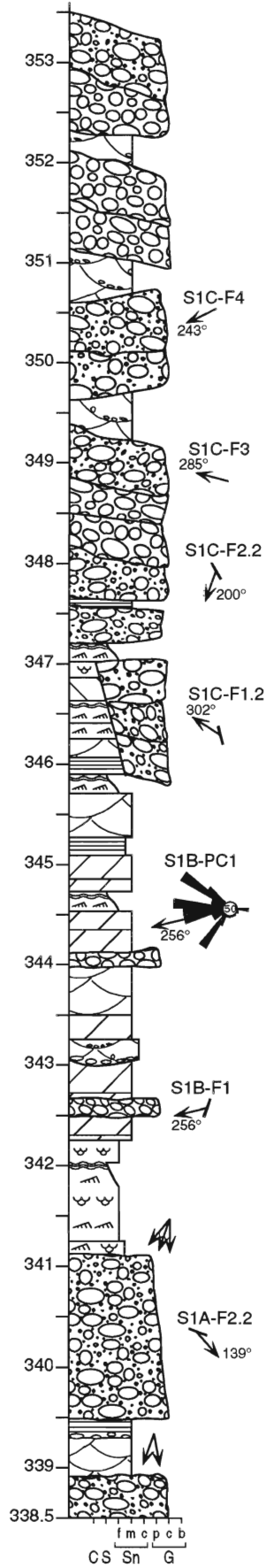
## LEGEND

	GRAVEL-WELL SORTED, MASSIVE		HORIZONTAL LAMINAE
	GRAVEL-IMBRICATE		SINUSOIDAL OR DRAPE LAMINAE
	GRAVEL-POORLY SORTED		TYPE A CLIMBING RIPPLES
	GRAVEL-WEAKLY BEDDED		CLIMBING RIPPLES TYPES A→B
	PEBBLY PLANAR TABULAR CROSS-BEDS		TROUGH CROSS-LAMINAE
	PEBBLY TROUGH CROSS-BEDS	OTHER STRUCTURES	
	TROUGH CROSS-BEDS		DEFORMATION STRUCTURES: FLAMES; BALL AND PILLOW
	PLANAR TABULAR CROSS-BEDS		CARBONATE CONCRETIONS
	HORIZONTAL TO GENTLY DIPPING BEDS		FAULTING
	MASSIVE SAND		PALEOCURRENT MEASUREMENTS; MULTIPLE
	WEAKLY STRATIFIED DIAMICT		PALEOCURRENT MEASUREMENTS; INDIVIDUAL
	DIAMICT		INFERRED PALEOCURRENT
			DROPSTONES

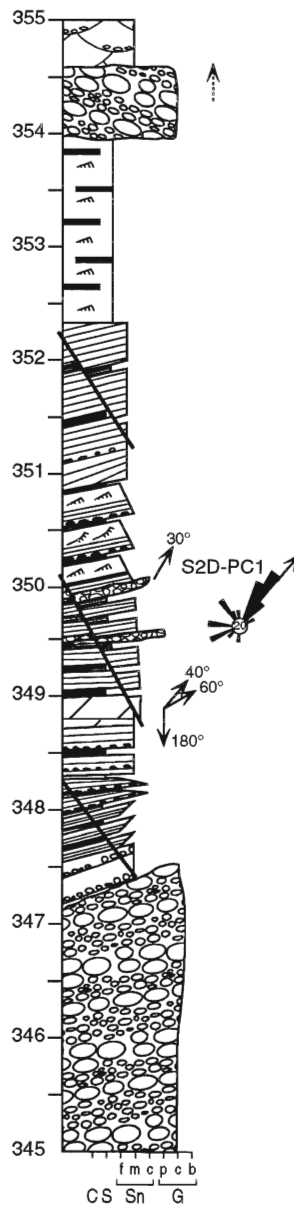


Reproduction of Fig. 2.1 to locate the section logs and fence diagrams located in Appendices III and IV.

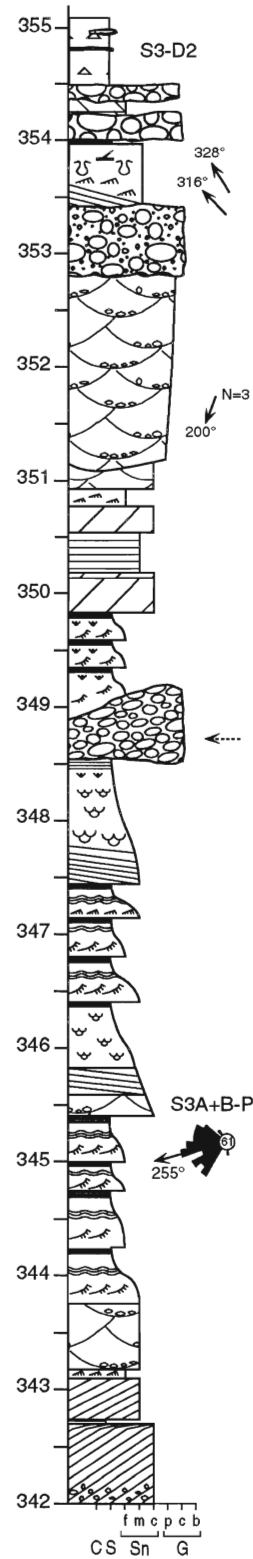
S1



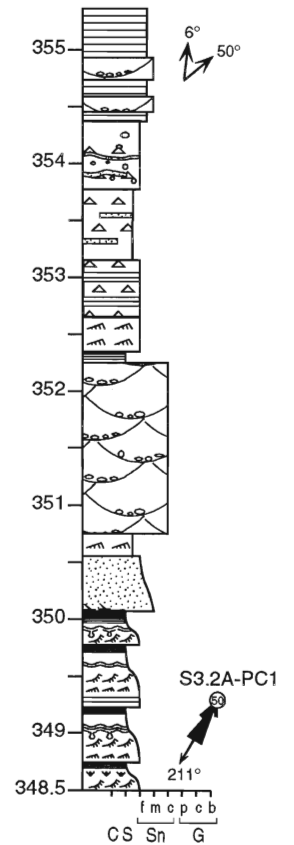
S2

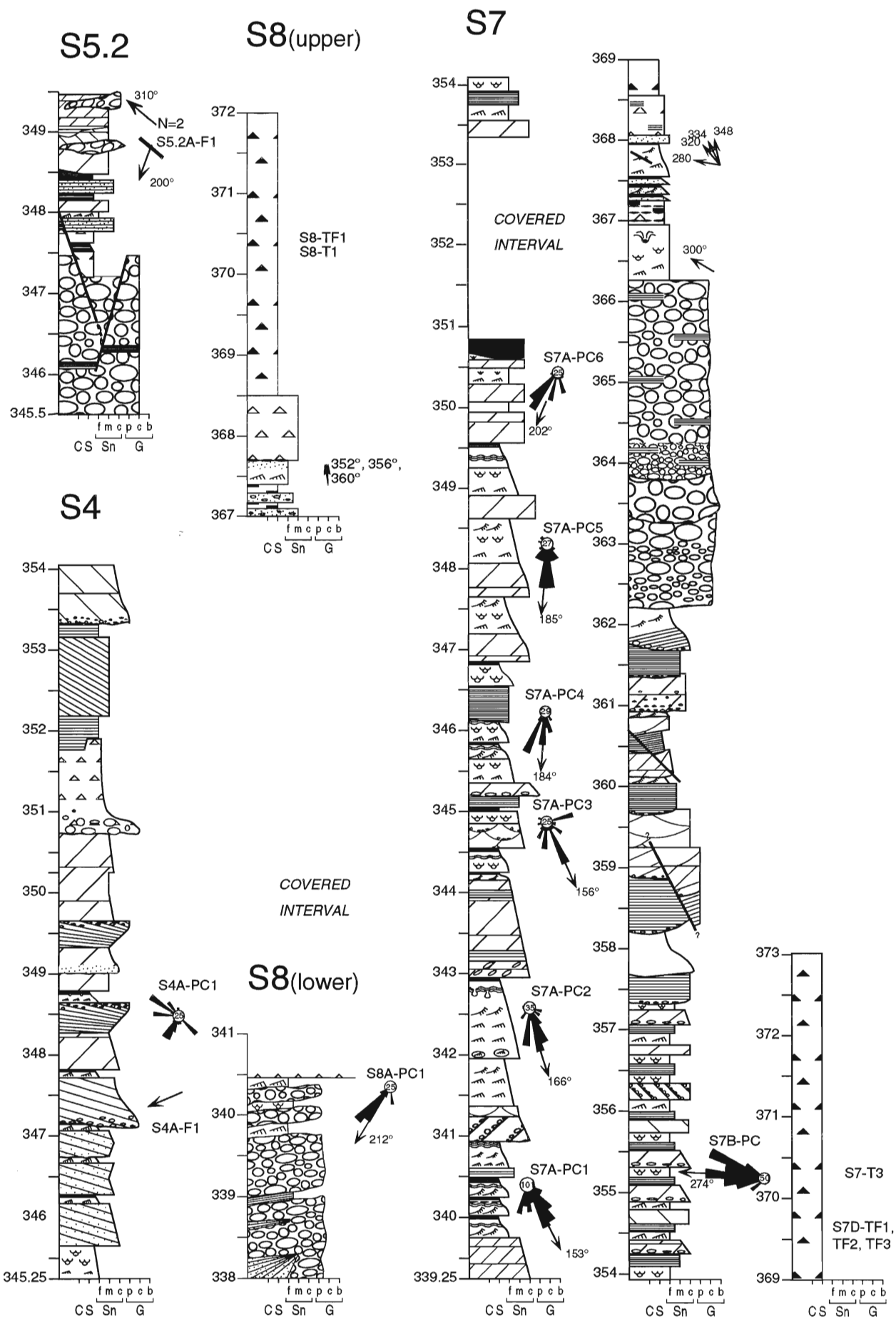


S3

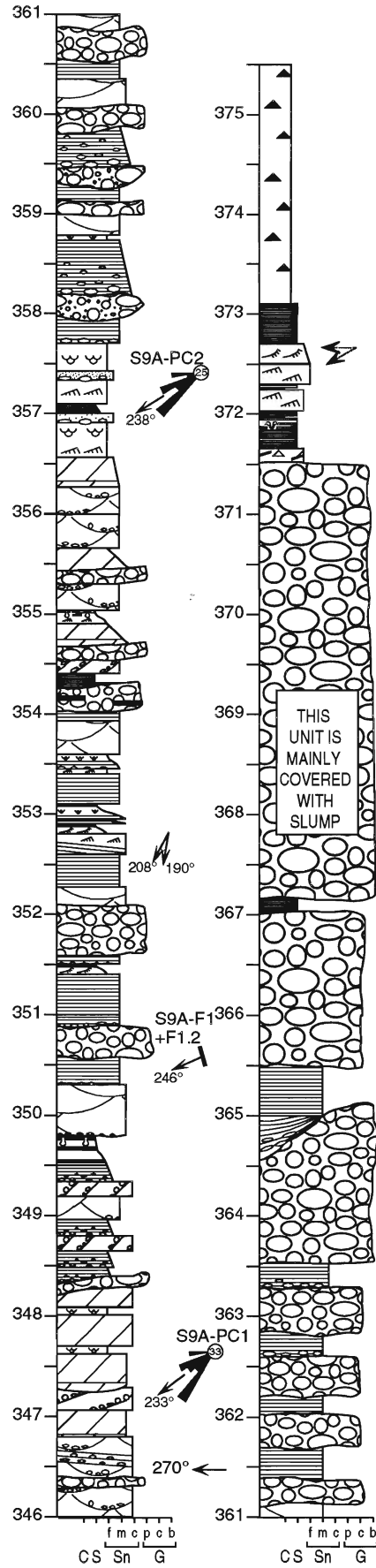


S3.2

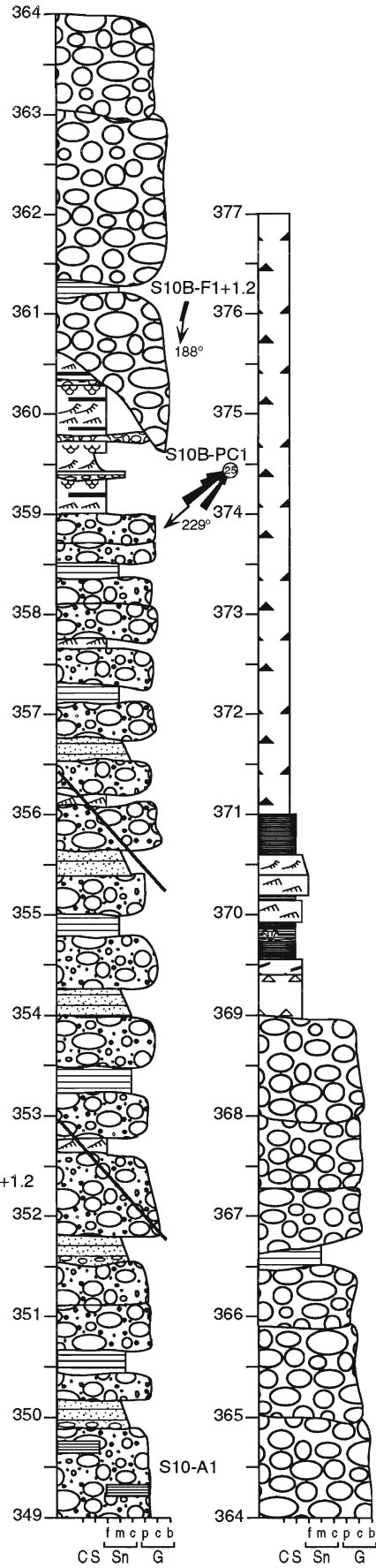




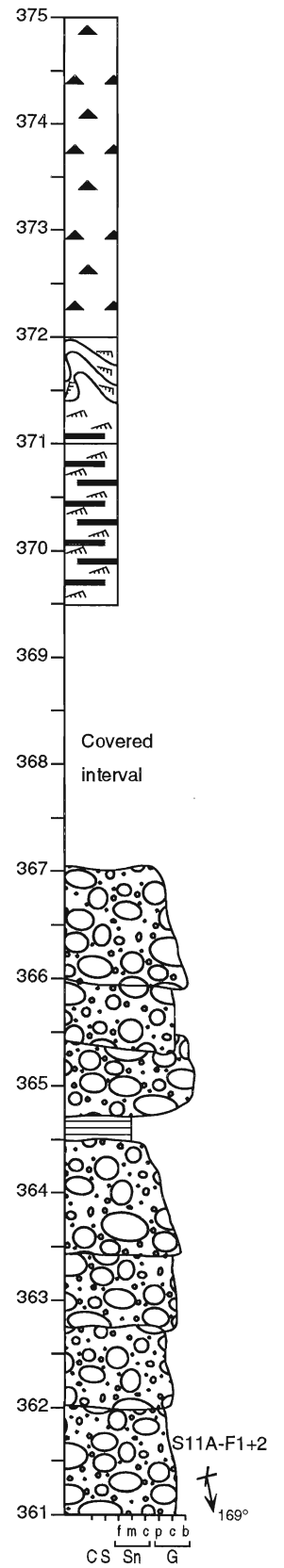
# S9

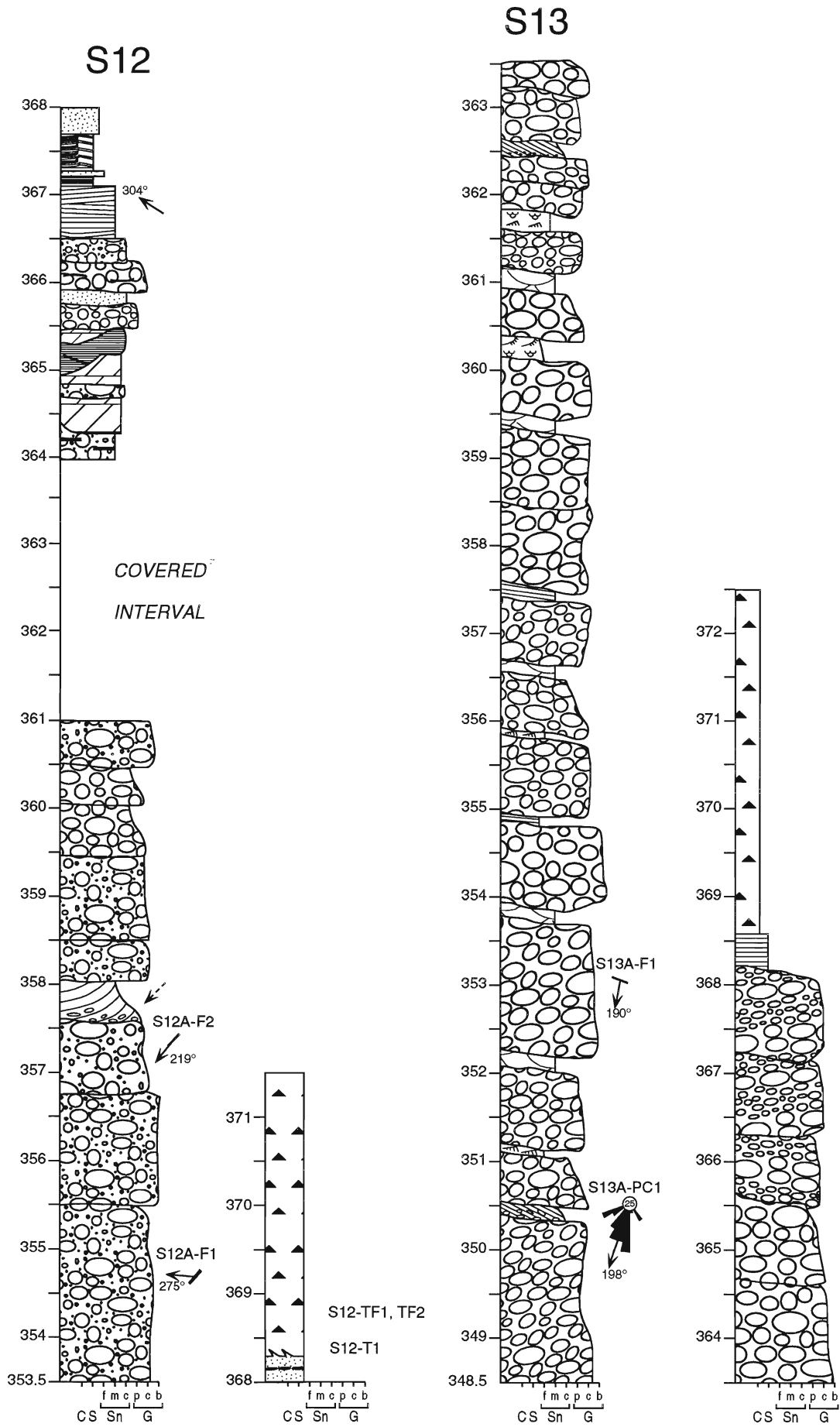


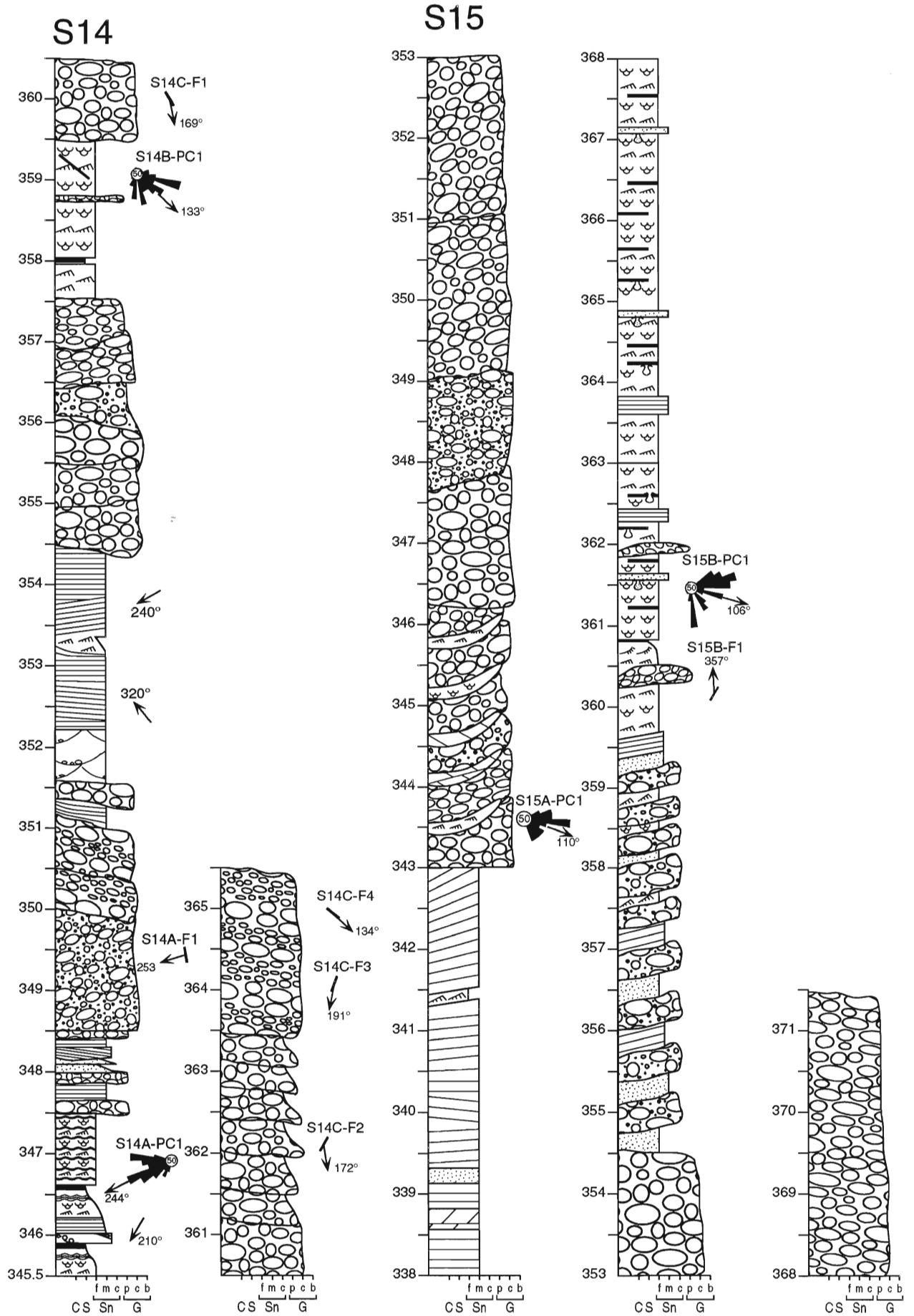
# S10

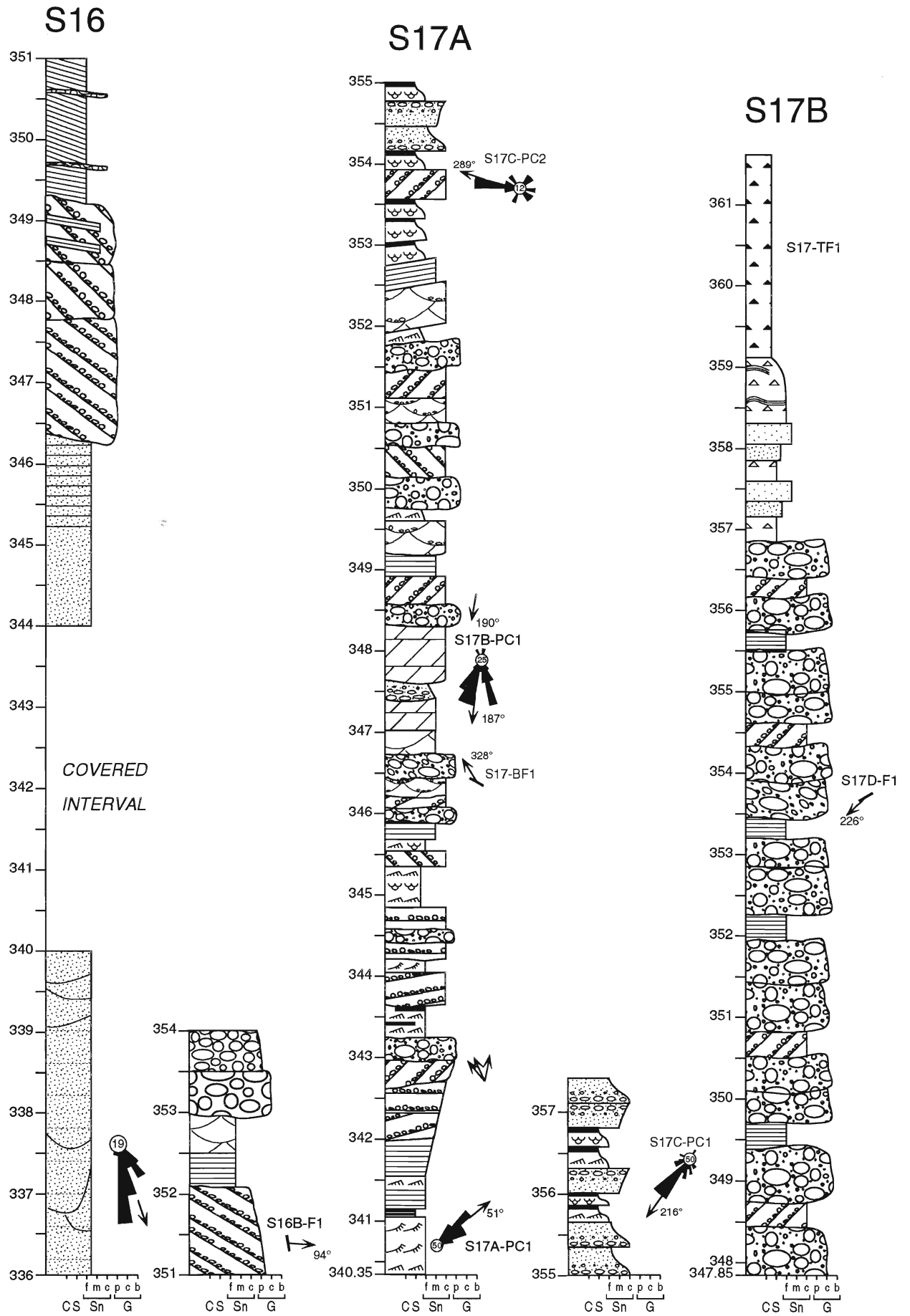


# S11

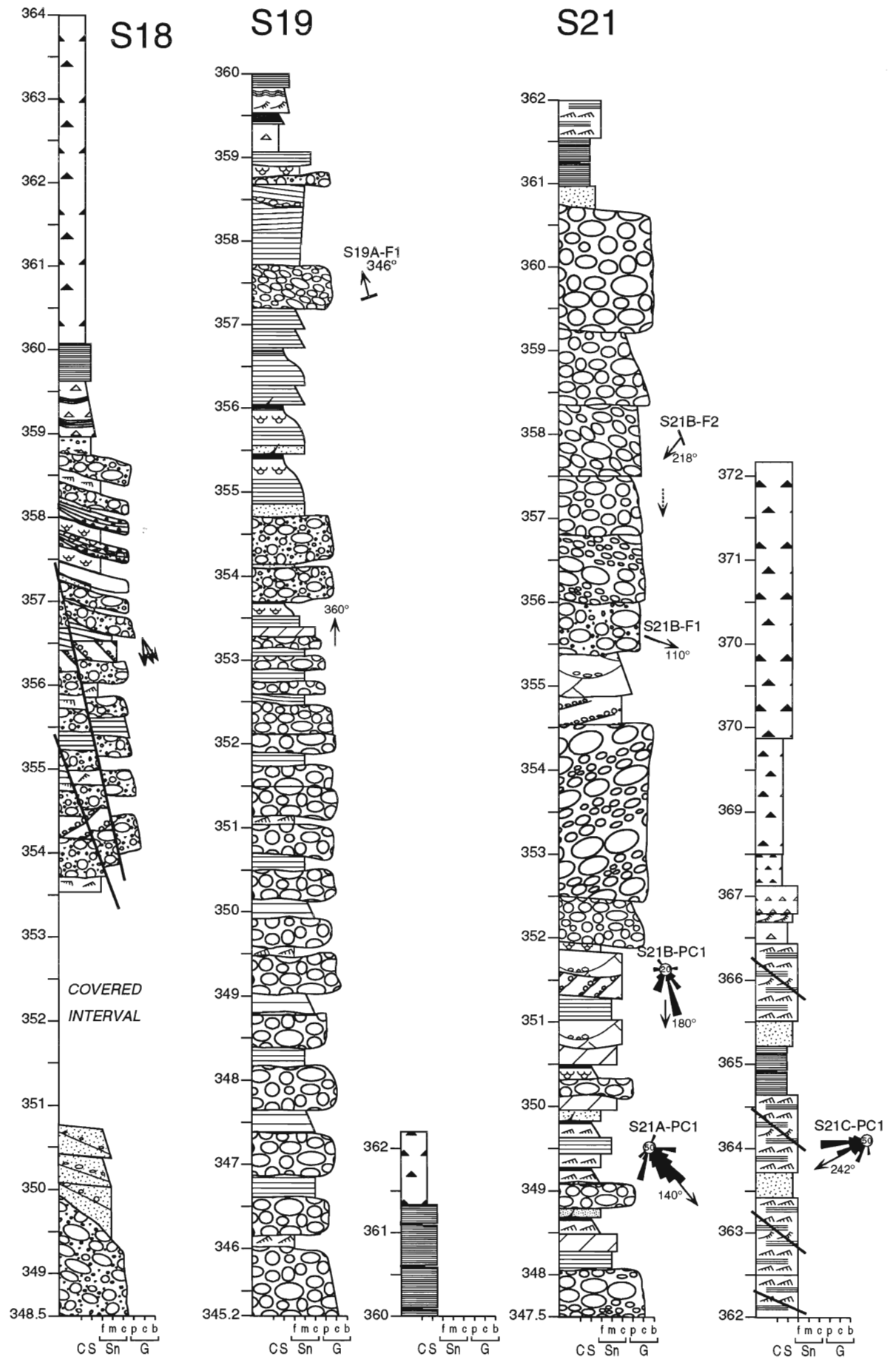


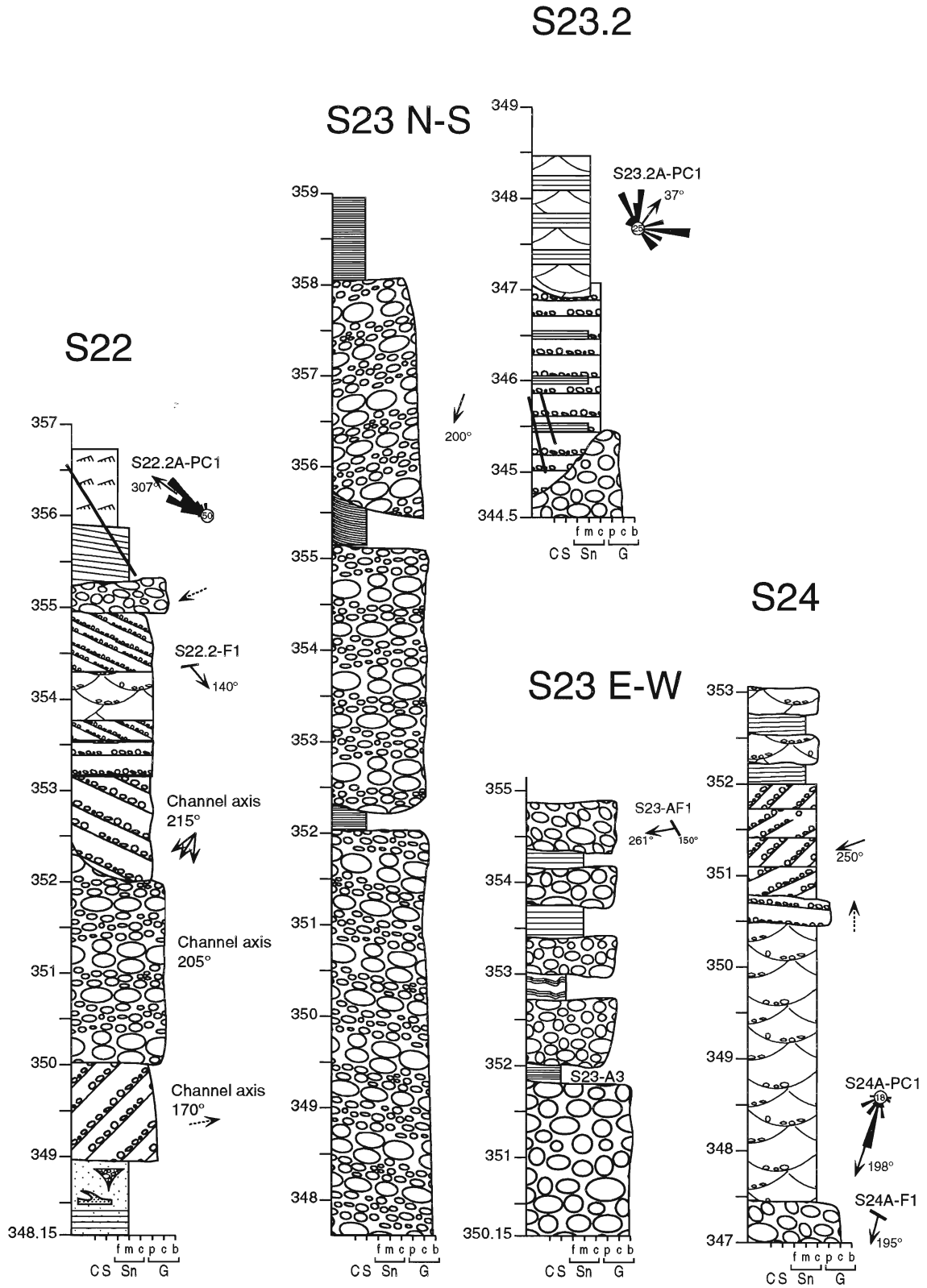


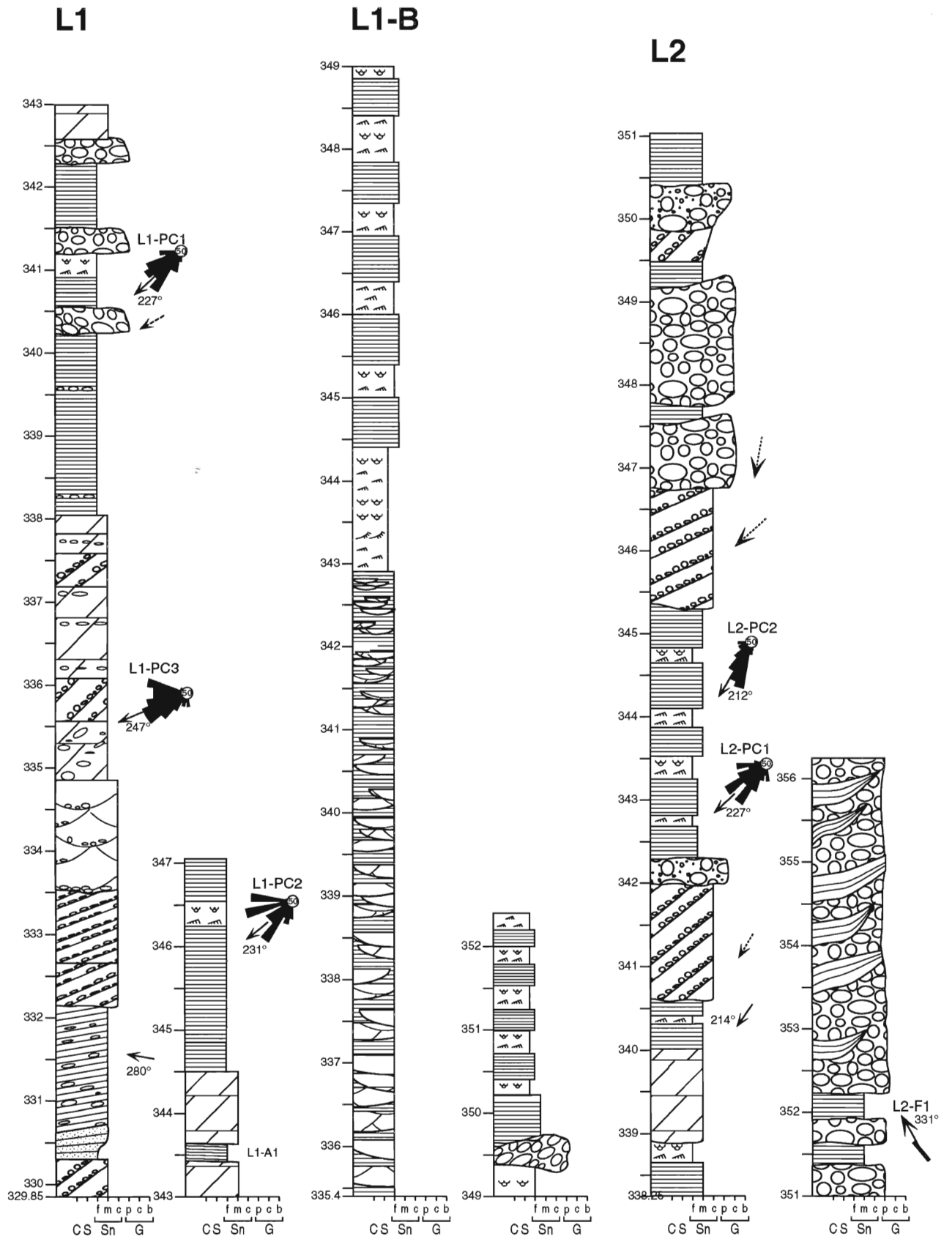


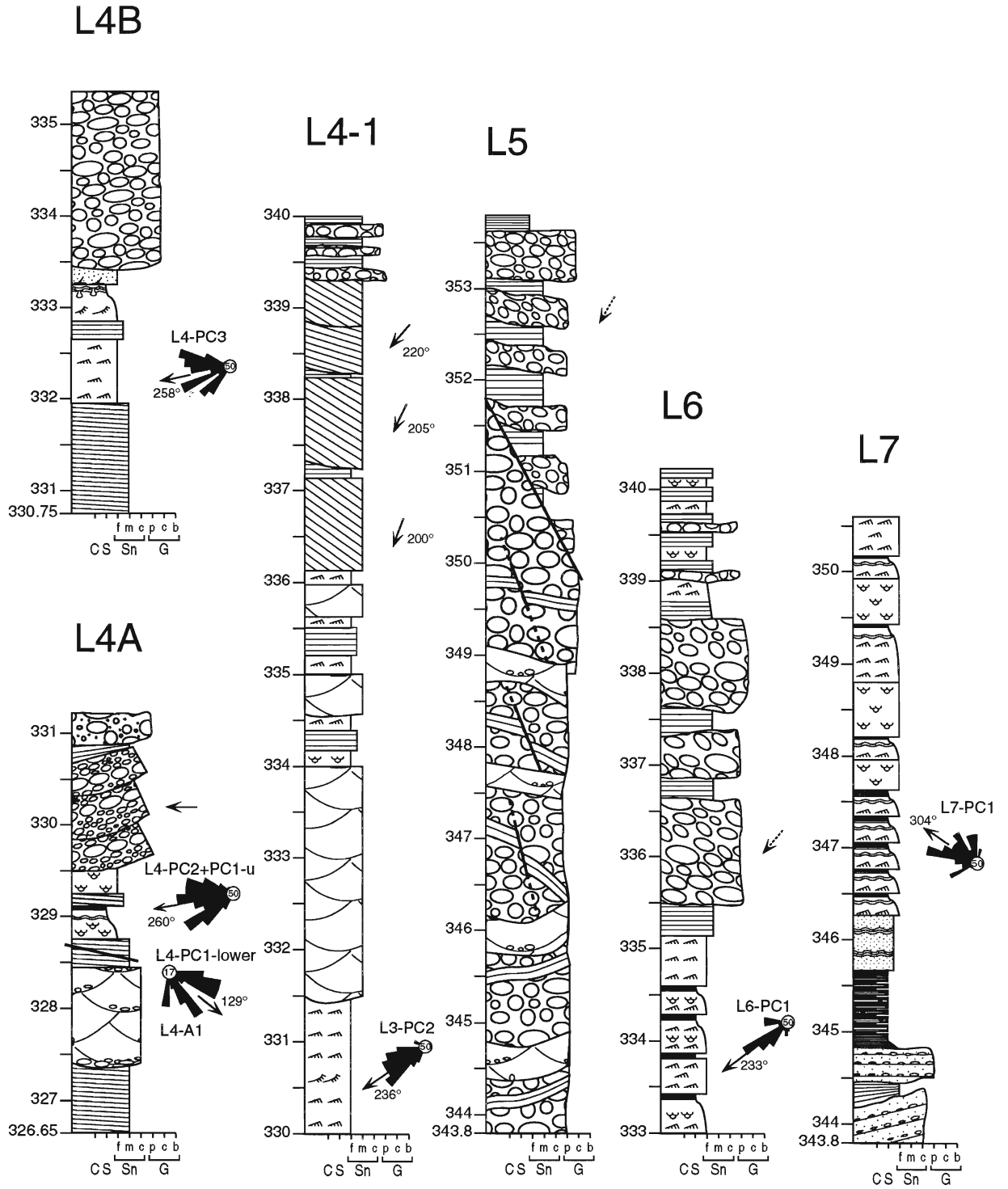


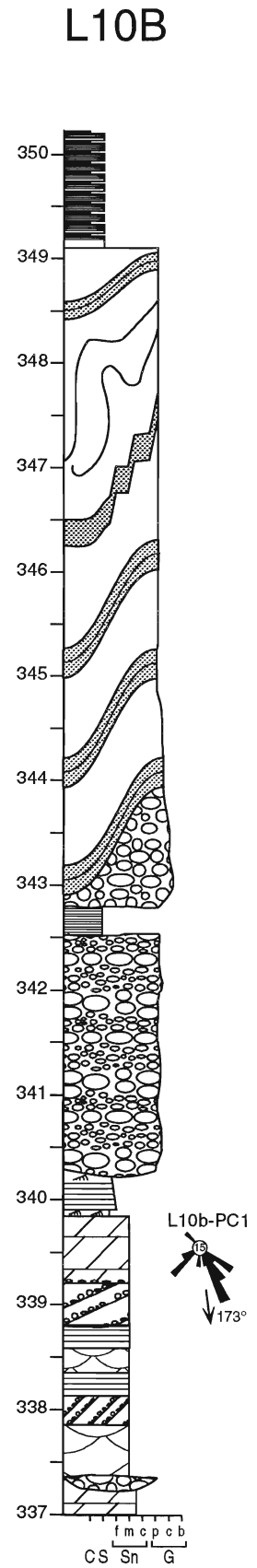
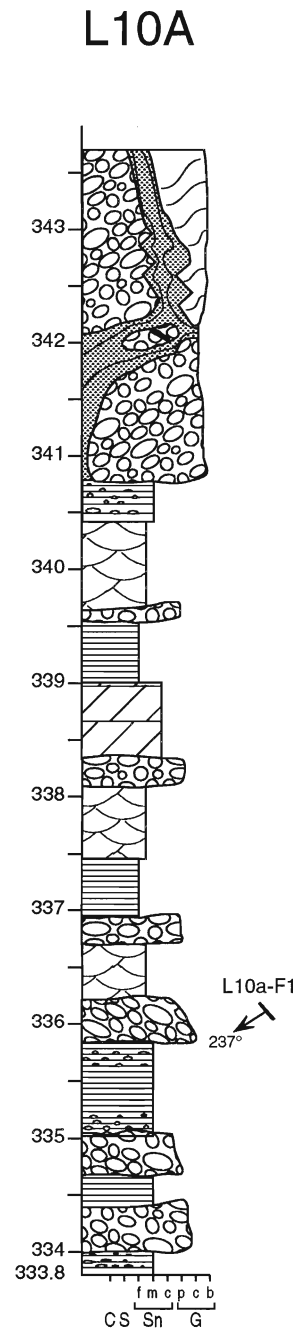
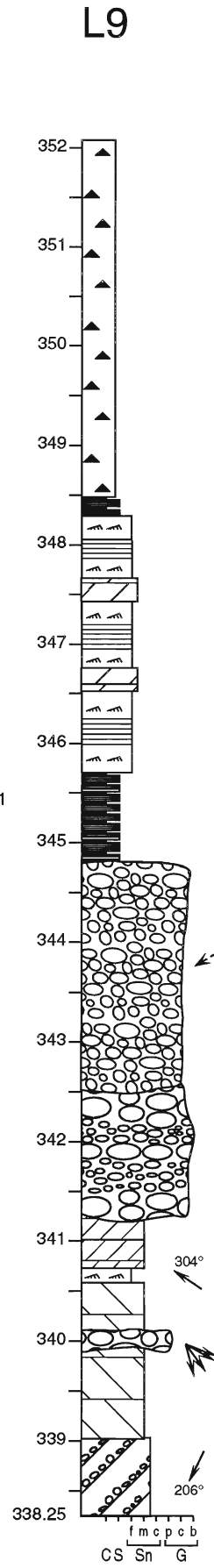
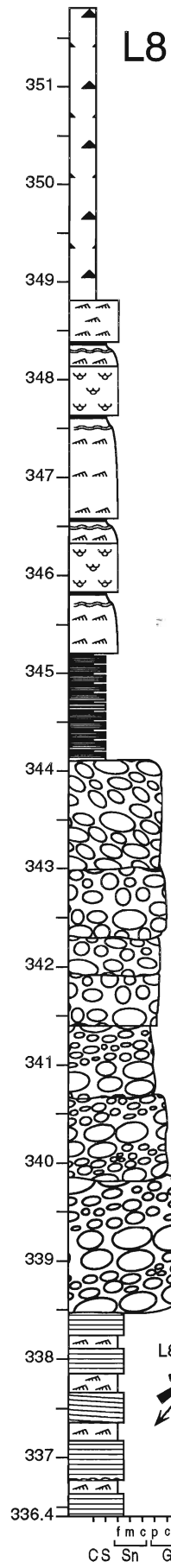




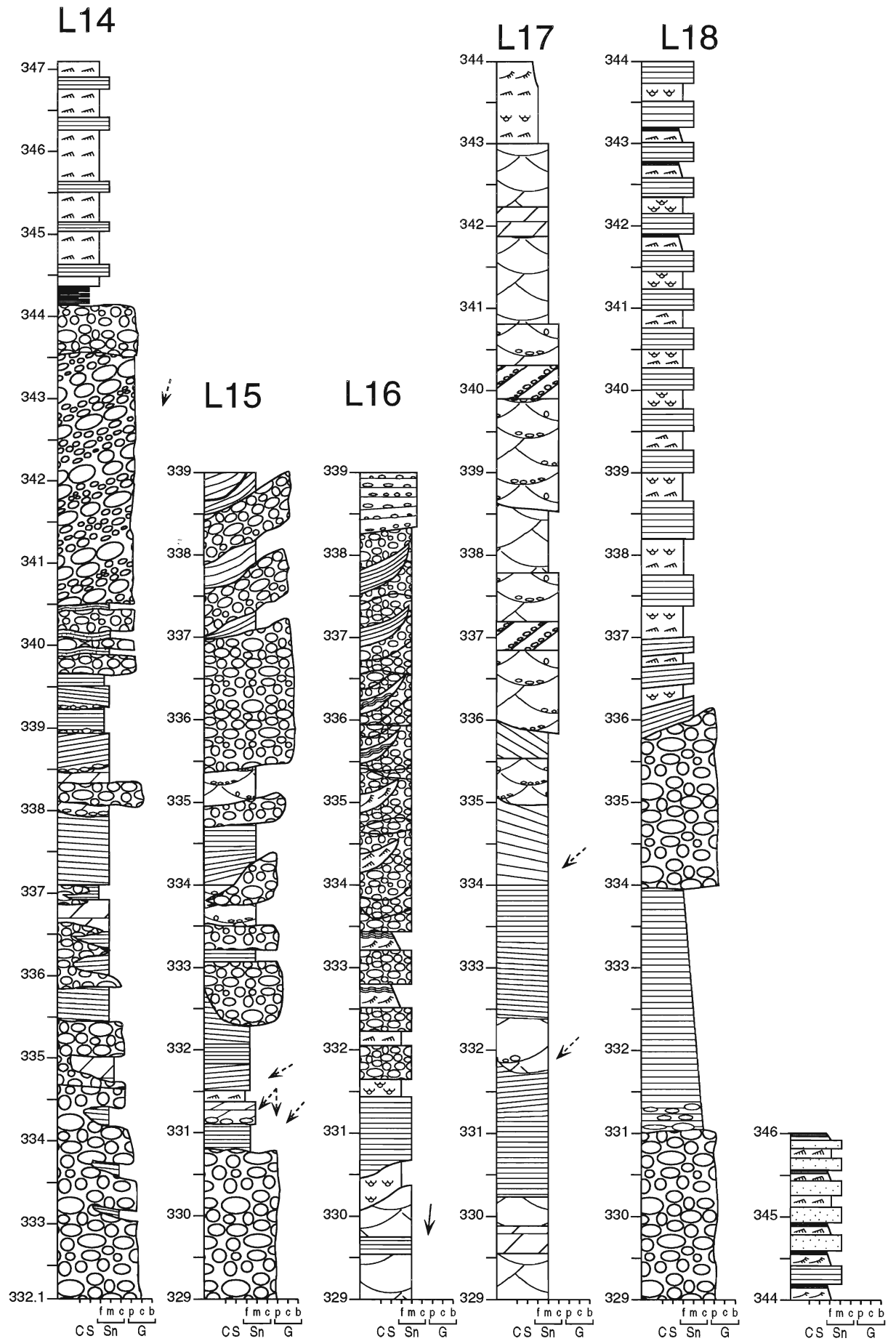








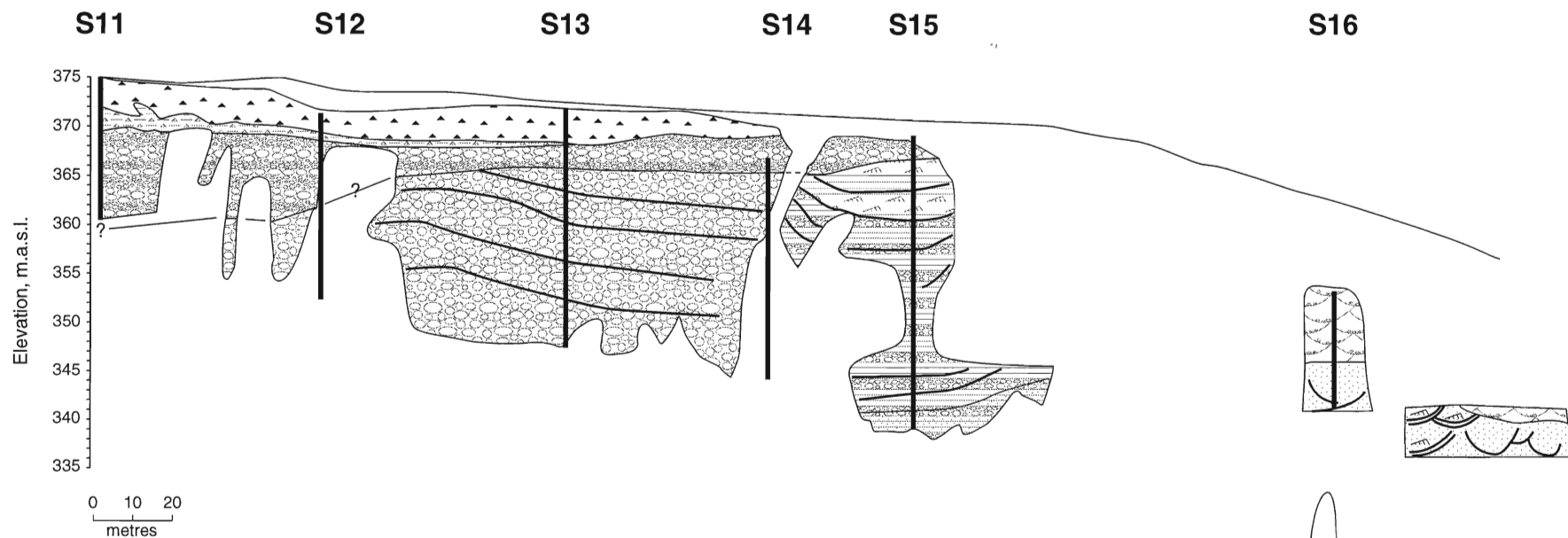




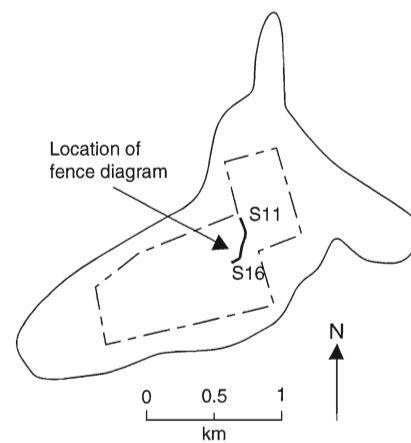
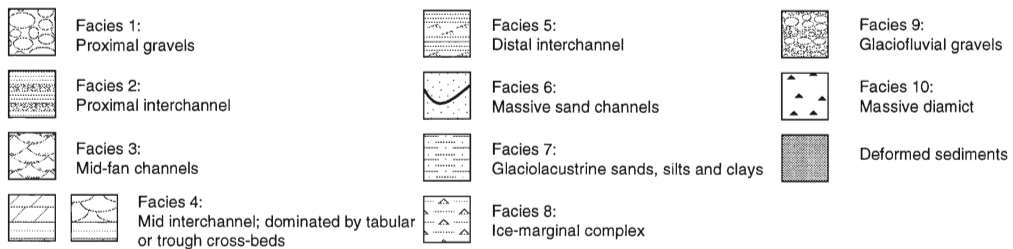
**APPENDIX IV**  
**FENCE DIAGRAMS**



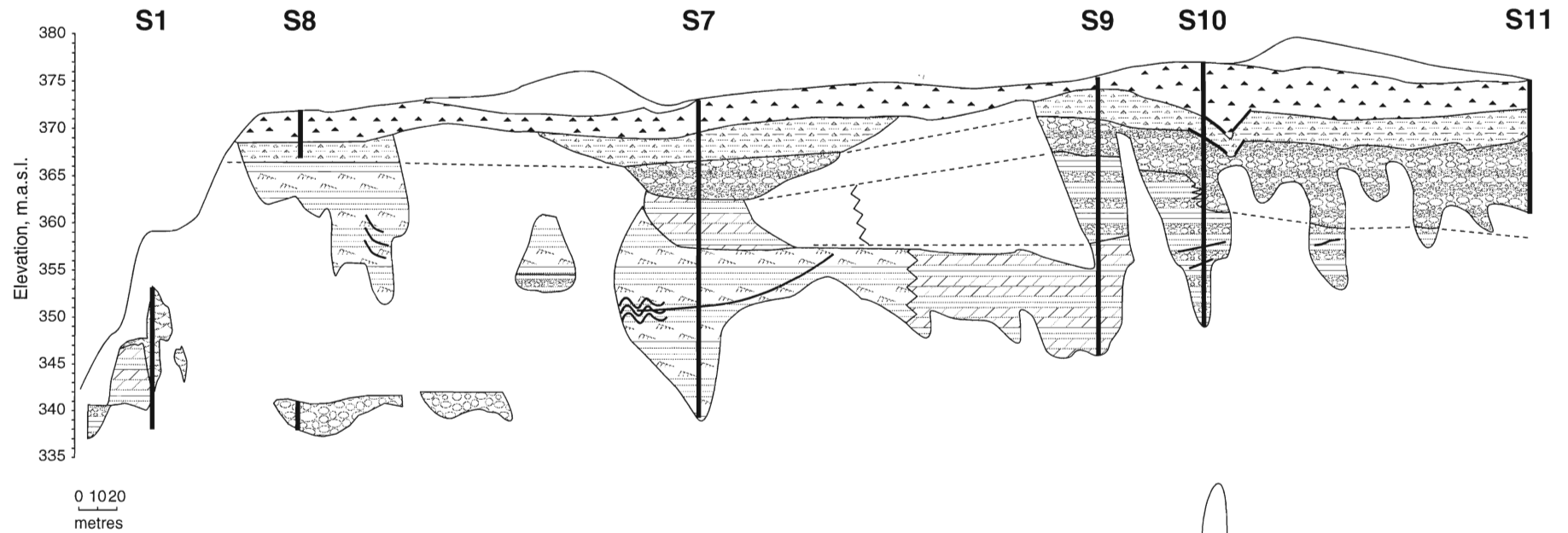
# FENCE DIAGRAM #1



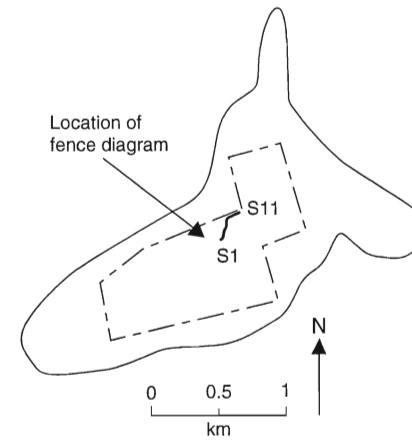
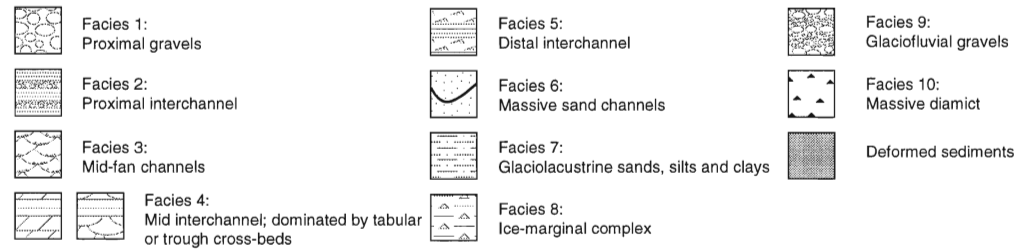
## LEGEND



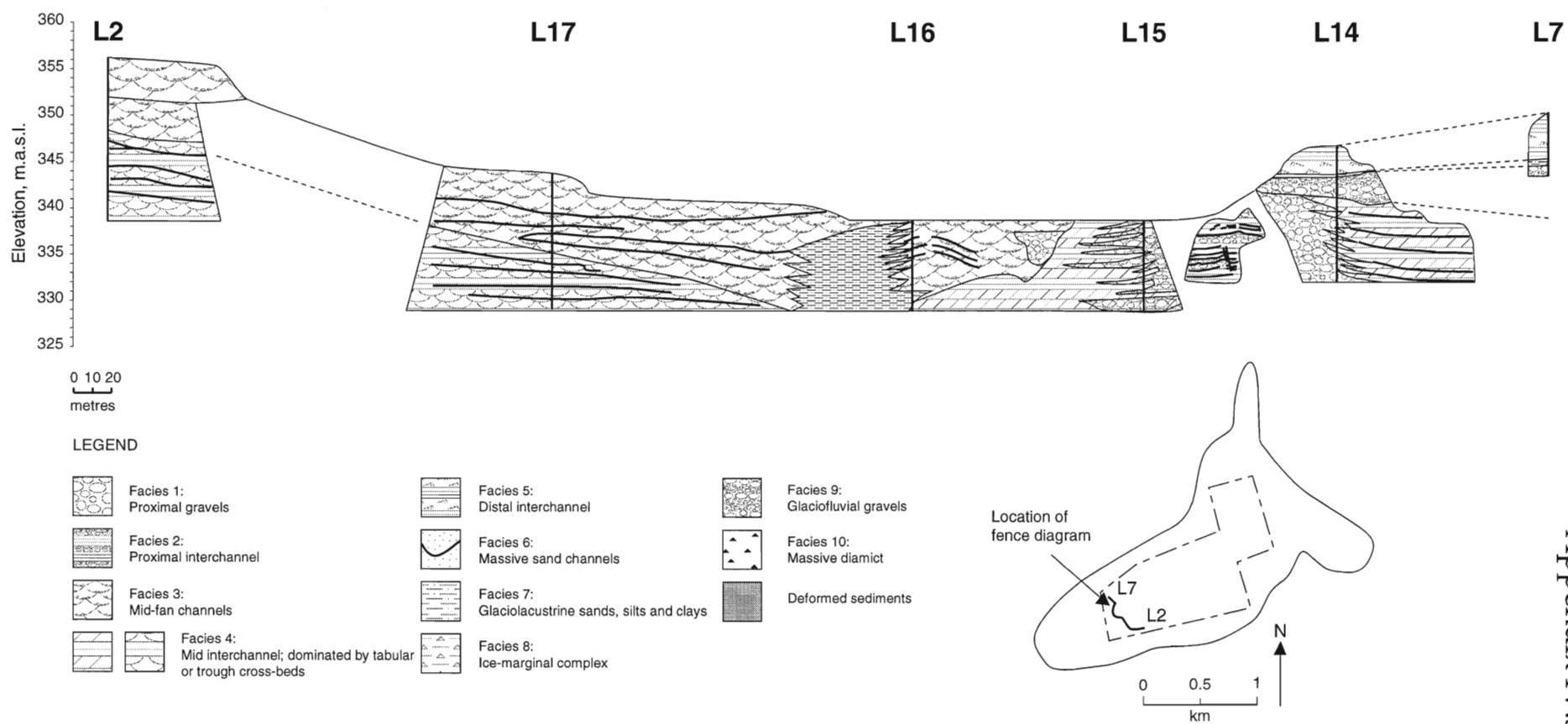
## FENCE DIAGRAM #2



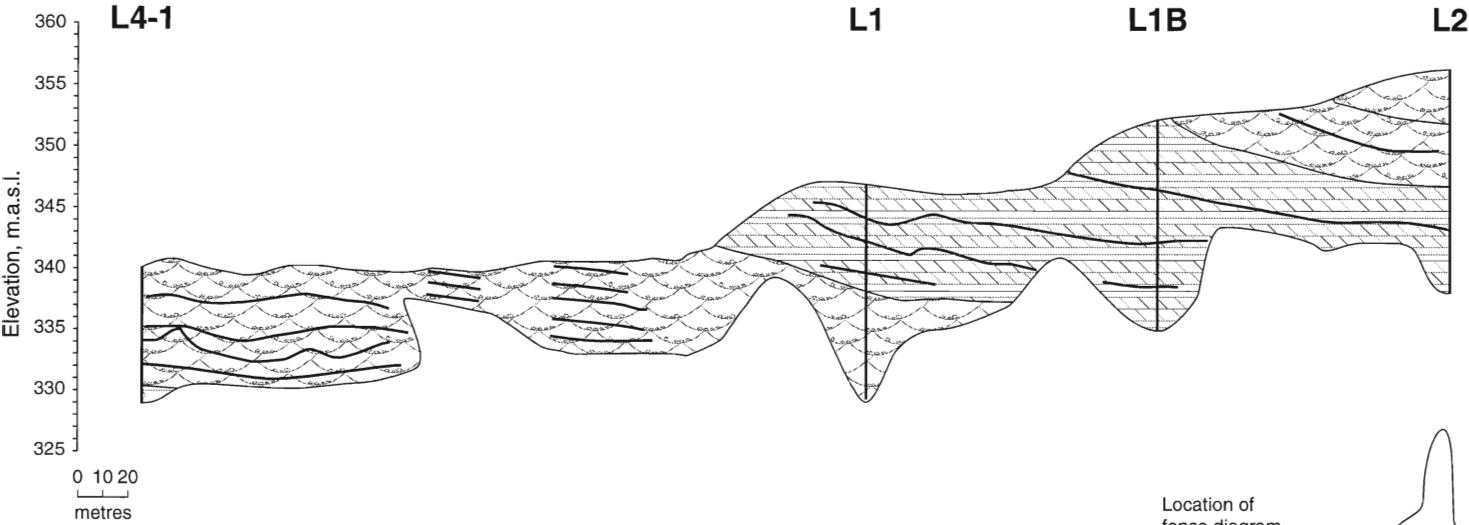
### LEGEND



## FENCE DIAGRAM #3

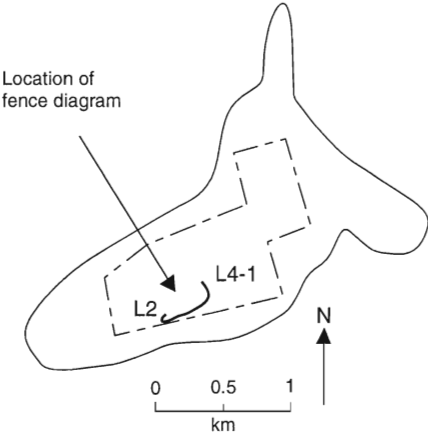


# FENCE DIAGRAM #4



## LEGEND

	Facies 1: Proximal gravels		Facies 5: Distal interchannel		Facies 9: Glaciofluvial gravels
	Facies 2: Proximal interchannel		Facies 6: Massive sand channels		Facies 10: Massive diamict
	Facies 3: Mid-fan channels		Facies 7: Glaciolacustrine sands, silts and clays		Deformed sediments
	Facies 4: Mid interchannel; dominated by tabular or trough cross-beds		Facies 8: Ice-marginal complex		



## FENCE DIAGRAM #5

